2018

The Potential of CRL4-DCAF1 and KSR1 as Therapeutic Targets in Low-grade Merlin-Deficient Tumours

Lyons Rimmer, Jade

UNIVERSITY OF
PLYMOUTH

The potential of CRL4-DCAF1 and KSR1 as therapeutic targets in low-grade Merlin-deficient tumours

By

JADE LYONS RIMMER

A thesis submitted to the University of Plymouth

in partial fulfilment for the degree of

DOCTOR OF PHILOSOPHY

Peninsula Medical School

April 2018

Acknowledgements

First and foremost I would like to thank the University of Plymouth and Brain Tumour Research for the opportunity to undertake this project, whose financial support was greatly appreciated. This thesis would also not have been possible without the invaluable support and guidance from my supervisors, past and present. I would like to thank Dr Lu Zhou for teaching me the necessary skills, for his enthusiasm when I was discouraged and for believing in me. I would also like to thank Dr Daniele Baiz for his words of encouragement throughout my PhD and for agreeing to supervise me in an established project, I know that couldn't have been easy! I would also like to thank Professor Oliver Hanemann for the opportunity to be a part of his research group, for teaching me to question my assumptions and for giving me the self-confidence to believe in myself and most importantly to believe in my work.

I would like to show my gratitude to my research group and fellow PhD students; I am grateful to be part of such a wonderful group of people. A big thank you to Sheri, Lauren, Foram, Bora, Liyam and Jemma for keeping me sane! I would not be about to submit this thesis without Jemma Dunn's support from the beginning of this journey as a colleague and as a friend. I also owe her my thanks for the summer she spent digesting tumours! I would like to thank Dr Emanuela Ercolano for her technical support, her help and guidance with the drug project and for being enthusiastic, friendly and approachable every day.

I owe my deepest gratitude to my family for their ongoing love and support in everything I do. I am truly grateful to be blessed with such a great support network. I would not be where I am today without my mum and dad who always have time to talk about anything and have helped me to make the right decisions in life, my grandparents who always show me how proud they are of my achievements, and my fiancée Dr Kayleigh Bassiri who reassures me that I can do anything I set my mind to and encourages me to always strive for more. I would also like to thank my best friends Chelsea and Dee who have never doubted me, even when I doubt myself. Last but not least I would like to thank my siblings; Rosie, Zak, Molly, Thomas and Harry for their unconditional love. You motivate me to achieve and succeed so that you can see that anything you want is possible.

Author's Declaration

At no time during the registration for the degree of Doctor of Philosophy has the author been registered for any other University award without prior agreement of the Doctoral College Quality Sub-Committee.

Work submitted for this research degree at the University of Plymouth has not formed part of any other degree either at the University of Plymouth or at another establishment.

This study was financed with the aid of a studentship from Plymouth University and funded by Brain Tumour Research.

The following external institutions were visited for consultation purposes: None

Publications (or public presentation of creative research outputs): None

Presentations at conferences:

- RASopathies in Asia: Advances in RASopathies and Neurofibromatoses; Identification of New Therapeutic Targets 2017 – Poster and oral presentation.
- Brain Tumor Meeting 2017 Berlin – Poster presentation.
- The British Neuro-Oncology Society (BNOS) 2017: Engaging Science Enhancing Survival meeting – Poster presentation.

Word count of main body of thesis: 59737

Signed_____

Date_____

Jade Lyons Rimmer

Title: The potential of CRL4-DCAF1 and KSR1 as potential therapeutic targets for low-grade Merlin-deficient tumours

Merlin is a tumour suppressor protein that is frequently mutated or downregulated in cancer. Biallelic Merlin inactivation is causative of tumour formation, including schwannoma, meningioma and ependymoma. These tumours can occur sporadically or as part of the genetic condition Neurofibromatosis type 2 (NF2) and cause significant morbidity. The current treatment options are restricted to surgery and radiotherapy, which are invasive and may cause further tumour development.

The activity of both the E3 ubiquitin ligase complex Cullin 4 really interesting new gene (RING) E3 ubiquitin ligase- DNA damage binding protein (DDB1) and Cullin 4 associated factor 1 (CRL4-DCAF1) and Kinase suppressor of RAS 1 (KSR1) have been shown to be upregulated in schwannoma to drive tumour growth. KSR1 has also been shown to interact with components of the CRL4-DCAF1 complex. We investigated the expression, interaction and therapeutic potential of targeting these proteins in Merlin-deficient schwannoma and meningioma using a primary human cell model and relevant cell lines.

We found that DCAF1 and KSR1 protein were overexpressed in schwannoma and meningioma and confirmed that targeting both DCAF1 and KSR1 in meningioma had additive effects on proliferation. We also identified that CRL4-DCAF1 facilitates KSR1-dependent RAF/Mitogen-activated protein kinase (MAPK)/ Extracellular signal-regulated kinase (ERK) kinase (MEK)/ERK pathway activity. We showed MLN3651, a neddylation inhibitor that targets ubiquitin ligase activity, reduced proliferation and activated apoptosis in Merlin-deficient tumours. We also showed that Merlin-positive tumours were less sensitive to MLN3651 than Merlin-deficient tumours; therefore, MLN3651 sensitivity may be CRL4-DCAF1-dependent. Finally, combination of MLN3651 and the MEK1/2 inhibitor AZD6244 had additive effects, particularly in meningioma. Combinatorial therapy activated the Hippo pathway, inhibited RAF/MEK/ERK pathway activity and proliferation demonstrating that targeting the activity and downstream pathways of both DCAF1 and KSR1 represents an attractive novel therapeutic strategy in Merlin-deficient tumours.

List of contents

Abbreviations	17
Chapter 1 - Introduction	21
1.1 Background	22
1.2 The *Nf2* gene and Merlin signalling	23
1.2.1 Merlin regulation	23
1.2.2 Downstream Merlin signalling	25
1.3 Merlin-deficient tumours	31
1.3.1 Merlin loss in cancer	31
1.3.2 Schwannoma	32
1.3.3 Meningioma	35
1.3.4 Ependymoma	37
1.4 Neurofibromatoses	38
1.4.1 Neurofibromatosis type 1 (NF1)	38
1.4.2 Neurofibromatosis type 2 (NF2)	40
1.4.3 Schwannomatosis	46
1.5 Treatment and clinical trials for Merlin-deficient tumours	46
1.5.1 Lapatinib	49
1.5.2 Everolimus	50
1.5.3 PDGFR inhibitors	50
1.5.4 Bevacizumab	52
1.5.5 Selumetinib (AZD6244)	53
1.5.6 Combination therapy	53
1.6 CRL4-DCAF1	54

1.6.1 CRL4-DCAF1 roles and regulation 57

1.6.2 CRL4-DCAF1 in cancer 58

1.6.3 Targeting CRL4-DCAF1 and DCAF1 kinase activity 59

1.7 KSR1 61

1.7.1 KSR1 roles and regulation 62

1.7.2 Roles in cancer 65

1.7.3 Targeting KSR1 67

1.8 Aims 68

Chapter 2 - Materials and Methods 70

2.1 Buffers and reagents 71

2.2 Cell culture 73

2.2.1 Sample collection 73

2.2.2 Tumour digestion 73

2.2.3 Normal nerve digestion 76

2.2.4 Cell splitting and storage 76

2.2.5 Cells and medium 77

2.3 Co-immunoprecipitation 78

2.3.1 Endogenous DCAF1 IP 78

2.3.2 FLAG IP 79

2.3.3 Myc IP 79

2.4 Cytoplasmic and nuclear fractionation 82

2.5 Drug treatments 82

2.5.1 Drugs used 82

2.5.2 ATP viability assay 83

2.5.3 Caspase 3/7 assay 84

2.6 Immunocytochemistry 84

2.6.1 Ki-67 84

2.6.2 FLAG 85

2.6.3 S100 86

2.7 Immunocytochemistry 88

2.8 Lentivirus production and infection 91

2.8.1 Lentivirus production 91

2.8.2 Lentivirus infection 91

2.8.3 Lentiviral information 92

2.9 Plasmids 95

2.9.1 Plasmid information 95

2.9.2 Plasmid amplification 95

2.9.3 Restriction enzyme plasmid digestion 96

2.9.4 Plasmid transfection 99

2.10 Western blotting 99

2.10.1 Cell lysis/tissue homogenisation 99

2.10.2 Protein estimation 99

2.10.3 Gels 101

2.10.4 Protein separation and transfer 103

2.10.5 Membrane probing 103

2.10.6 Stripping and storing membranes 106

2.10.7 Western blot analysis 106

Chapter 3 - DCAF1 and KSR1 expression and regulation of KSR1 by DCAF1 in Merlin-deficient tumours 107

3.1 Introduction 108

3.2 DCAF1 is overexpressed in schwannoma 108

3.3 DCAF1 and KSR1 are overexpressed in meningioma 113

3.4 The higher molecular weight KSR1 band 118

3.5 DCAF1 does not regulate KSR1 expression or localization 119

3.6 DCAF1 regulates RAF/MEK/ERK activity in schwannoma and reduces proliferation of schwannoma and meningioma 127

3.7 Targeting DCAF1 and KSR1 together reduces proliferation in BenMen-1 similar to schwannoma 132

3.8 Discussion 139

3.9 Conclusion 144

Chapter 4 - Characterising the DCAF1/KSR1 interaction 146

4.1 Introduction 147

4.2 Endogenous DCAF1 and KSR1 interact in Merlin-deficient meningioma 147

4.3 The C-terminus of DCAF1 interacts with the N-terminus of KSR1 in the cytoplasm and nucleus 150

4.4 C-terminal KSR1 ubiquitination is not dependent on DCAF1 159

4.5 DCAF1 facilitates the association of KSR1 with MEK1/2 and ERK1/2 161

4.6 Discussion 165

4.7 Conclusion 167

Chapter 5 - Targeting DCAF1 in Merlin-deficient tumours 169

5.1 Introduction 170

5.2 MLN3651 treatment reduces NEDD8-conjugates and activates the Hippo pathway in Merlin-deficient cells 170

5.3 MLN3651 treatment leads to enhanced RAF/MEK/ERK activity in Merlin-deficient cells 177

5.4 MLN3651 reduces cell viability and proliferation of Merlin-deficient schwannoma 180

5.5 MLN3651 reduces cell viability and proliferation of Merlin-deficient meningioma 184

5.6 Merlin-positive schwannoma and meningioma cells are less sensitive to MLN3651 than Merlin-negative cells 193

5.7 Control cells are less sensitive to MLN3651 than Merlin-deficient tumour cells 195

5.8 B32B3 reduces viability and proliferation of Merlin-deficient cells 199

5.9 Discussion 204

5.10 Conclusion 211

Chapter 6 - Targeting DCAF1 and KSR1 in Merlin-deficient tumours 213

6.1 Introduction 214

6.2 APS_2_79 has no effect on RAF/MEK/ERK activity or proliferation of Merlin-deficient schwannoma and meningioma 214

6.3 MLN3651 and AZD6244 treatment inhibits RAF/MEK/ERK activity and activates the Hippo pathway 215

6.4 Discussion 225

6.5 Conclusion 227

Chapter 7 - Discussion 229

7.1 Introduction 230

7.2 DCAF1 and KSR1 expression is increased in schwannoma and meningioma 232

7.3 CRL4-DCAF1 does not regulate KSR1 expression or localization 233

7.4 CRL4-DCAF1 regulates KSR1-dependent RAF/MEK/ERK activity 234

7.5 DCAF1 and KSR1 as therapeutic targets 237

7.6 MLN3651 inhibits CRL4-DCAF1 activity in Merlin-deficient cells and has potential as a therapeutic 238

7.7 MLN3651 increases RAF/MEK/ERK activity in Merlin-deficient cells 241

7.8 Combination of MLN3651 and AZD6244 242

7.9 Experimental limitations 244

7.10 Translational potential 246

7.11 Conclusions 246

Appendix - Supplementary Figures 250

References 257

List of figures

Figure 1.1 - Merlin-deficient signalling.	30
Figure 1.2 - Roles of ubiquitination.	56
Figure 1.3 - KSR1 regulation.	64
Figure 2.1 - Determining schwannoma and meningioma Merlin status.	75
Figure 2.2 - Proportion of S100-positive cells in Schwann cell cultures.	87
Figure 2.3 - Control and human KSR1 overexpression plasmid maps used for lentiviral production.	94
Figure 2.4 - DCAF1 plasmid digests	97
Figure 2.5 - KSR1 plasmid digests	98
Figure 3.1 - DCAF1 is overexpressed in schwannoma tissue.	110
Figure 3.2 - DCAF1 expression is highly variable in schwannoma cells.	112
Figure 3.3 - DCAF1 and KSR1 are overexpressed in meningioma tissue.	114
Figure 3.4 - DCAF1 and KSR1 are overexpressed in meningioma cells.	117
Figure 3.5 - DCAF1 does not regulate KSR1 degradation in meningioma.	120
Figure 3.6 - Cytoplasmic KSR1 is increased in schwannoma compared with Schwann cells.	122
Figure 3.7 - DCAF1 does not regulate KSR1 localization in schwannoma.	123
Figure 3.8 - Cytoplasmic KSR1 is not upregulated in BenMen-1 compared with HMC.	125
Figure 3.9 - DCAF1 does not regulate KSR1 localization in meningioma or BenMen-1.	126
Figure 3.10 - DCAF1 knockdown reduces pERK1/2, but not CYCLIN D1 in schwannoma.	128

Figure 3.11 - DCAF1 knockdown does not alter pERK1/2 but significantly reduces proliferation in meningioma. 130

Figure 3.12 - DCAF1 knockdown does not alter pERK1/2 but significantly reduces proliferation in BenMen-1. 131

Figure 3.13 - DCAF1 and KSR1 knockdown reduces pMEK1/2 but not pERK1/2 or CYCLIN D1 in schwannoma. 134

Figure 3.14 - DCAF1 and KSR1 knockdown does not reduce pERK1/2 in BenMen-1. 136

Figure 3.15 - DCAF1 and KSR1 knockdown reduces proliferation of BenMen-1 cells. 138

Figure 4.1 - Endogenous DCAF1 and KSR1 interact in BenMen-1. 149

Figure 4.2 - DCAF1 interacts with KSR1 via the C-terminal of DCAF1. 152

Figure 4.3 - KSR1 interacts with the CRL4-DCAF1 complex via the N-terminal of KSR1. 154

Figure 4.4 - KSR1 construct localization in HEK293T cells. 156

Figure 4.5 - The DCAF1/KSR1 interaction occurs both in the cytoplasm and nucleus of HEK293T cells. 158

Figure 4.6 - Wild type KSR1 and C-terminal KSR1 are ubiquitinated in HEK293T cells. 160

Figure 4.7 - KSR1 poly-ubiquitination is not dependent on DCAF1 in HEK293T cells. 163

Figure 4.8 - KSR1 and RAF/MEK/ERK binding is partly dependent on DCAF1 in HEK293T cells. 164

Figure 5.1 - MLN3651 reduces NEDD8-conjugates in Merlin-deficient tumours. 171

Figure 5.2 - MLN3651 activates the Hippo pathway in schwannoma. 174

Figure 5.3 - MLN3651 activates the Hippo pathway in meningioma. 175

Figure 5.4 - MLN3651 does not activate the Hippo pathway in BenMen-1. 176

Figure 5.5 - MLN3651 increases pERK1/2 in schwannoma. 178

Figure 5.6 - MLN3651 increases pERK1/2 in meningioma but not BenMen-1. 179

Figure 5.7 - MLN3651 reduces cell viability and increases apoptosis in schwannoma. 182

Figure 5.8 - MLN3651 reduces proliferation of schwannoma. 183

Figure 5.9 - MLN3651 reduces cell viability and increases apoptosis in meningioma. 186

Figure 5.10 - MLN3651 reduces proliferation of meningioma cells. 187

Figure 5.11 - MLN3651 reduces cell viability and increases apoptosis in BenMen-1 189

Figure 5.12 - MLN3651 reduces proliferation of BenMen-1 cells. 190

Figure 5.13 - Viability of WHO II and III meningioma after MLN3651 treatment. 192

Figure 5.14 - Viability of Merlin-positive schwannoma and meningioma after MLN361 treatment. 194

Figure 5.15 - Human Schwann cells and HMC are less sensitive to MLN3651 than tumour cells. 197

Figure 5.16 – Viability of meningioma in HMC or meningioma medium after MLN3651 treatment. 198

Figure 5.17 - B32B3 effect on viability and proliferation of schwannoma. 200

Figure 5.18 - B32B3 effect on viability and proliferation of meningioma. 202

Figure 5.19 - B32B3 effect on viability and proliferation of BenMen-1. 203

Figure 6.1 - MLN3651 and AZD6244 treatment activates the Hippo pathway in schwannoma. 217

Figure 6.2 - MLN3651 and AZD6244 effect on proliferation in schwannoma. 218

Figure 6.3 - MLN3651 and AZD6244 treatment activates the Hippo pathway and prevents ERK1/2 activation in meningioma. 220

Figure 6.4 - MLN3651 and AZD6244 effect on proliferation in meningioma.	221
Figure 6.5 - MLN3651 and AZD6244 activates the Hippo pathway and prevents ERK1/2 activation in BenMen-1.	223
Figure 6.6 - MLN3651 and AZD6244 reduces proliferation in BenMen-1.	224
Supplementary figure 1 - Additional HMC and BenMen-1 repeats for DCAF1 and KSR1 localization.	251
Supplementary figure 2 - Additional BenMen-1 DCAF1 knockdown repeats for KSR1 localization.	252
Supplementary figure 3 - Additional repeats for endogenous DCAF1 and KSR1 interaction in BenMen-1 and KT21-MG1-Luc5D.	253
Supplementary figure 4 - Additional overexpressed DCAF1 immunoprecipitation experiments.	254
Supplementary figure 5 - Additional overexpressed KSR1 immunoprecipitation experiments.	255
Supplementary figure 6 - Additional human KSR1 immunoprecipitation experiments showing RAF/MEK/ERK proteins after DCAF1 knockdown.	256

List of tables

Table 1.1 – Manchester criteria for the diagnosis of NF2.	42
Table 1.2 - Baser criteria [2011] used for diagnosis of NF2.	43
Table 1.3 - Ongoing clinical trials for the treatment of NF2-related and sporadic tumours.	48
Table 2.1- Cells and medium used	77
Table 2.2 - Antibodies used for co-immunoprecipitation experiments.	81
Table 2.3 - Antibodies used for immunohistochemistry experiments.	90
Table 2.4 - Western blot resolving gel recipe.	101
Table 2.5 - Western blot stacking gel recipe.	102
Table 2.6 - Antibodies used for Western blotting.	105

Abbreviations

Aa	Amino acids
ABL	Abelson murine leukemia viral oncogene homolog 1
AKT1	v-akt murine thymoma viral oncogene homolog 1
AKT3	v-akt murine thymoma viral oncogene homolog 3
AMPK	Adenosine monophosphate-activated protein kinase
ANOVA	Analysis of Variance
APS	Ammonium persulphate
ATP	Adenosine triphosphate
BAER	brainstem auditory evoked responses
BARD1	BRCA1-associated RING domain protein 1
BCA	bicinchoninic acid
BCR	Breakpoint cluster region
BenMen-1	Benign meningioma cell line 1
B-KSR1	Brain isoform - Kinase suppressor of RAS-1
BRCA1	Breast cancer 1
BSA	Bovine serum albumin
cAMP	Cyclic Adenosine Monophosphate
CD44	Cluster of Differentiation 44
CDC27	Cell division cycle protein 27 homolog
CDC42	Cell division cycle protein 42 homolog
CDT1	Chromatin Licensing And DNA Replication Factor 1
CER I	Cytoplasmic Extraction Reagent I
CER II	Cytoplasmic Extraction Reagent II
CK2	Casein kinase 2
CRL	Cullin-RING ligase
CRL4-DCAF1	Cullin4-RING E3 ubiquitin ligase- DDB1 and Cullin 4 associated factor 1
C-TAK1	Cdc25C-associated kinase 1
CUL4A	Cullin 4A
D1	pRK5-Myc-DCAF1
D2	pRK5-Myc-DCAF1 (1-744)
D3	pRK5-Myc-DCAF1 (745-1507)
DAB	3’3 diaminobenzidine
DAL-1	Differentially expressed in adenocarcinoma of the lung 1
DAPI	4',6-diamidino-2-phenylindole
DBC1	Deleted in bladder cancer protein 1
DCAF1	DDB1 and Cullin 4 associated factor 1
DCNL1	Defective in Cullin Neddylation 1
DDB1	DNA damage binding protein
DMEM	Dulbecco's modified eagle medium
DMSO	Dimethyl sulphoxide
DNA	Deoxyribonucleic acid
DPBS	Dulbecco's phophate buffered saline

DPX	Distyrene, plasticizer, and xylene
DTT	Dithiothreitol
ECL	Enhanced chemiluminescent substrate
EDTA	Ethylenediaminetetraacetic acid
EGFP	Enhanced green fluorescent protein
EGFR	Epidermal growth factor receptor
EGTA	ethylene glycol-bis(β-aminoethyl ether)-N,N,N',N'-tetraacetic acid
ERBB2	Erythroblastic oncogene B homolog 2
ERBB3	Erythroblastic oncogene B homolog 3
ERK	Extracellular signal-regulated kinase
ERM	ezrin/radixin/moesin
FAK	Focal adhesion kinase
FBS	Foetal bovine serum
FDA	Food and Drug Administration
FERM	4.1 protein ERM
FOXM1	Forkhead Box M1
GAPDH	Glyceraldehyde 3-phosphate dehydrogenase
GRB2	Growth factor receptor bound protein 2
H2A	Histone 2A
HCL	Hydrochloric acid
HDAC1	Histone Deacetylase 1
HIF1α	Hypoxia-inducible factor 1-alpha
hK1	Human KSR1
HMC	human meningeal cells
HRS	Hepatocyte growth factor-regulate tyrosine kinase substrate
HSP70	Heat shock protein 70
HSP90	Heat shock protein 90
IBMX	3-isobutyl-1-methylxanthine
IGF-1	Insulin-like growth factor 1
IGF1R	Insulin-like growth factor 1 receptor
IQ	Intelligence quotient
JNK	c-Jun N-terminal kinase
K1	pCMV5 WT KSR1
KC	pCMV5 C540
KD	Knockdown
KIBRA	Kidney and brain expressed protein
KLF4	Krupple-like factor 4
KN	pCMV5 N539
KSR1	Kinase suppressor of RAS 1
KSR2	Kinase suppressor of RAS 2
LATS1	Large tumor suppressor kinase 1
LATS2	Large tumor suppressor kinase 2
LB	Luria Bertani
LRP6	Low-density lipoprotein receptor-related protein 6
LZTR1	Leucine zipper-like transcription regulator 1

MAPK	Mitogen-activated protein kinase
MDM2	Mouse double minute 2 homolog
MEK	MAPK/ERK kinase
MER	Membrane estrogen receptor
MOI	Multiplicity of infection
MPNST	Malignant peripheral nerve sheath tumours
MRI	Magnetic resonance imaging
MST1/2	Mammalian Ste20-like kinases 1/2
MTOR	Mammalian target of rapamycin
MTORC1	mammalian target of rapamycin complex 1
NAE	NEDD8-activating enzyme E1
NEDD4	Neural precursor cell expressed developmentally down-regulated protein 4
NEDD8	Neural precursor cell expressed developmentally down-regulated protein 8
NE-PER	Nuclear and cytoplasmic extraction reagents
NER	Nuclear extraction reagent
Nf1	Neurofibromin 1 gene
NF1	Neurofibromatosis type 1
Nf2	Neurofibromin 2 gene
NF2	Neurofibromatosis type 2
NIH	National Institutes of Health
NP-40	Nonidet p40
NSCLC	Non-small-cell lung carcinoma
OCT	Optimal cutting temperature
PAK	p21-activated kinases
PALS1	Protein-associated with Lin7
PATJ	Pals1-associated tight junction protein
PDGF	Platelet-derived growth factor
PDGFR	Platelet-derived growth factor receptor
PES	Polyethersulfone
PFA	Paraformaldehyde
PI3K	Phosphoinositide 3-kinase
PIK3CA	PI3K catalytic subunit, alpha
PIK3R1	PI3K regulatory subunit, alpha
PIKE-L	Phosphatidylinositol 3-kinase enhancer-L
PKA	Protein kinase A
PLL	Poly-L-lysine
PNGase	Peptide: N-glycosidase F
POLR2A	Polymerase (RNA) II (DNA directed) polypeptide A, 220 kDa
PP2A	Protein phosphatase 2A
PRAS40	Proline-rich AKT substrate of 40 kDa
PRKAR1A	Protein kinase, cAMP-dependent, regulatory, type I, alpha
PTCH1	Protein patched homolog 1
PTEN	Phosphatase and tensin homolog
PVDF	Polyvinylidene fluoride
RAC1	RAS related C3 botulinum toxin substrate 1

RAF	Rapidly accelerated fibrosarcoma
RAS	Rat sarcoma
RBX1	Ring-Box 1
REC	Research Ethics Committee
REiNS	Response Evaluation in Neurofibromatosis and Schwannomatosis
RELA	v-rel avian reticuloendotheliosis viral oncogene homolog A
RING	Really interesting new gene
RIPA	Radioimmunoprecipitation assay
RNA	Ribonucleic acid
RON	Recepteur d'origine nantais
R-SMAD	Receptor regulated Small worm phenotype (SMA) Mothers Against Decapentaplegic (MAD)
SAV	Salvador
SCHIP-1	Schwannomin interacting protein 1
SDS	Sodium dodecyl sulphate
shRNA	Short hairpin RNA
SEM	standard error of the mean
SMAD4	Small worm phenotype mothers against decapentaplegic homolog 4
SMARCB1	Switch/Sucrose Non-fermentable-related matrix-associated actin-dependent regulator of chromatin subfamily B member 1
SMO	smoothened, frizzled family receptor
SOS	Son of Sevenless
SP-EPN	spinal ependymoma
ST-EPN-RELA	supratentorial ependymoma chromothripsis; RELA-fusion
SUFU	suppressor of fused homolog (Drosophila)
TAM	Tyro3, Axl, and Mer
TBE	Tris/Borate/EDTA
TBST	Tris buffered saline-Tween
TEMED	Tetramethylethylenediamine
TIF1	Transcriptional intermediary factor 1
TRAF7	TNF receptor-associated factor 7
TM	Transport medium
UBE2M	Ubiquitin conjugating enzyme E2 M
UNG2	Uracil-DNA glycosylase 2
USP8	Ubiquitin carboxyl-terminal hydrolase 8
v/v	volume/volume
VEGF	Vascular endothelial growth factor
VPR	HIV1 Viral protein R
VPRBP	Viral protein R binding protein
w/v	weight/volume
WHO	World Health Organization
WNT	Wingless integration-1
YAP	Yes-associated protein
ZAP-70	Zeta-chain-associated protein kinase 70

Chapter 1 – Introduction

1.1 Background

Merlin is a tumour suppressor protein that functions at the cell membrane, cytoplasm and nucleus to prevent tumour growth (Ammoun *et al.*, 2012; Li *et al.*, 2010; Morrison *et al.*, 2007; Zhang *et al.*, 2010). Merlin-deficient tumours arise when the Neurofibromin 2 (*NF2)* gene is mutated in both alleles; this mutation can occur as a result of the genetic condition Neurofibromatosis type 2 (NF2), or sporadically (Bianchi *et al.*, 1994; Evans, 2009). NF2 is a genetic condition characterized by the growth of multiple low-grade tumours, namely schwannomas, meningiomas and ependymomas (Evans *et al.*, 1992; Hanemann, 2008). The current standard treatment for schwannomas, meningiomas and ependymomas is surgery and rarely radiotherapy. Surgery is invasive and possibly linked to further morbidities (Evans, 2009). Unfortunately, there are no approved therapeutics that are able to shrink or prevent the growth of these tumours. As such, a successful therapeutic option is urgently required.

Both Cullin 4 really interesting new gene (RING) E3 ubiquitin ligase- DNA damage binding protein (DDB1) and Cullin 4 associated factor 1 (CRL4-DCAF1) and Kinase suppressor of RAS 1 (KSR1) have been shown to be hyper-active in schwannoma (Li *et al.*, 2014; Li *et al.*, 2010; Zhou *et al.*, 2016a). This hyper-activity contributes to tumourigenesis and is dependent on the loss of Merlin. The overall aim of this project was to explore the potential of CRL4-DCAF1 and KSR1 as novel therapeutic targets in low grade Merlin-deficient tumours using primary schwannoma and meningioma cultures as a model.

1.2 The *Nf2* gene and Merlin signalling

The *Nf2* gene is located on chromosome 22q12 and encodes the tumour suppressor protein, Merlin (Trofatter *et al.*, 1993). Merlin shares sequence homology with other ezrin/radixin/moesin (ERM) proteins and includes an N-terminal 4.1 protein ERM (FERM) domain followed by an alpha-helical domain and a C-terminal domain (Petrilli & Fernández-Valle, 2016). Merlin is different from other ERM proteins in that it lacks the actin-binding site in the C-terminal domain, which instead is found in the N-terminal FERM domain (Xu & Gutmann, 1998). The functions of Merlin are varied dependent on post-translational modifications, spatial conformation, location and cell density.

There are two isoforms of Merlin; Merlin-1 and Merlin-2 which are formed as a result of alternative splicing (Golovnina *et al.*, 2005). Merlin-1 is the longest isoform and lacks exon 16 whereas Merlin-2 is slightly shorter, contains exon 16 and lacks the carboxy-terminal residues required for intra-molecular binding (Bianchi *et al.*, 1994; Sher *et al.*, 2012).

1.2.1 Merlin regulation

Merlin is regulated by post-translational modifications, predominantly by phosphorylation. Phosphorylation of S518 regulates the conformation of Merlin and therefore its activity (Bretscher, Edwards & Fehon, 2002; Shaw *et al.*, 2001). It has been proposed that phosphorylation leads to an open conformation that activates the scaffold function of Merlin and inactivates its tumour suppressor roles, whereas dephosphorylation leads to a closed conformation and activation of tumour suppressor roles (Bretscher, Edwards & Fehon, 2002; Shaw *et al.*, 2001). Conversely, Sher *et al.* demonstrated that wild type Merlin is neither fully open nor closed and

phosphorylation leads to a less-active more closed state of Merlin (Sher *et al.*, 2012). In addition, lipid binding has been shown to regulate the open conformation of Merlin leading to membrane localization critical for Merlin's tumour suppressive functions (Chinthalapudi *et al.*, 2018). This demonstrates that the regulation of Merlin conformation is more complex and may be dependent on many factors other than phosphorylation.

Both open and closed conformations can interact with binding partners and Merlin's scaffolding role remains active regardless of its conformation (Petrilli & Fernández-Valle, 2016). Expression of activated RAS related C3 botulinum toxin substrate 1 (RAC1) or Cell division cycle protein 42 homolog (CDC42) leads to Merlin phosphorylation at S518 (Shaw *et al.*, 2001; Xiao *et al.*, 2002). This phosphorylation is directly mediated by p21-activated kinases (PAK), a common downstream target of both RAC1 and CDC42 and decreases Merlin's association with the cytoskeleton (Rong *et al.*, 2004a; Shaw *et al.*, 2001; Xiao *et al.*, 2002). Protein kinase A (PKA) can also phosphorylate S518 and S10 whereby regulating Merlin's interaction with the actin cytoskeleton and leading to modification of cell morphology (Alfthan *et al.*, 2004; Laulajainen *et al.*, 2008). Morrison *et al.* reported that at high cell density Cluster of Differentiation 44 (CD44) is activated by its ligand, hyaluronate, leading to Merlin dephosphorylation and activation of tumour suppressor activities (Morrison *et al.*, 2001). In addition, Hepatocyte growth factor-regulate tyrosine kinase substrate (HRS) is also required for Merlin-mediated growth suppression (Sun *et al.*, 2002).

v-akt murine thymoma viral oncogene homolog (AKT) phosphorylates Merlin at S10, T230 and S315 resulting in decreased interdomain binding and ubiquitination (Tang *et al.*, 2007). This poly-ubiquitination leads to proteasome-mediated Merlin degradation

with a protein half-life of more than 24 hours (Cooper & Giancotti, 2014; Li *et al.*, 2010). The Merlin protein half-life is relatively long; therefore, it is unlikely to be as important as phosphorylation in the regulation of Merlin function.

1.2.2 Downstream Merlin signalling

Merlin is a tumour suppressor protein that acts as a contact-dependent inhibitor of growth by suppressing or activating cell signalling pathways and preventing normal cytoskeletal reorganization (Morrison *et al.*, 2007). Merlin inhibits growth by regulating the number of receptor tyrosine kinases on the cell membrane, particularly, Platelet-derived growth factor receptor (PDGFR), Erythroblastic oncogene B homolog 2 (ERBB2) and Erythroblastic oncogene B homolog 3 (ERBB3) (Ammoun *et al.*, 2012). Merlin promotes PDGFR degradation when overexpressed in the human schwannoma cell line HEI 193 (Fraenzer *et al.*, 2003). In addition, Merlin overexpression inhibits the delivery of receptors, such as ERBB2, ERBB3, Insulin-like growth factor 1 receptor (IGF1R)β and PDGFRβ, to the cell membrane via secretory vesicles, leading to their degradation (Lallemand *et al.*, 2009). Accordingly, Merlin knockdown led to increased PDGFRβ, IGF1Rβ, Epidermal growth factor receptor (EGFR), ERBB2 and ERBB3 protein expression in human Schwann cells (Ahmad *et al.*, 2010; Lallemand *et al.*, 2009). In an analysis of ten Merlin-deficient schwannoma samples, EGFR was strongly activated as well as ERBB2, ERBB3 and ERBB4 receptors (Ammoun *et al.*, 2010a). In addition, in some samples, PDGFRβ, AXL, SKY, Membrane estrogen receptor (MER) and Recepteur d'origine nantais (RON) phosphorylation was detected indicating receptor activation (Ammoun *et al.*, 2010a). These data show that a wide range of receptors are upregulated and hyperactivated in the absence of Merlin, leading to subsequent downstream mitogenic pathway activation.

Merlin also directly interacts with many pathway components to regulate signalling and cell growth. Merlin inhibits the RAC1/PAK pathway via multiple mechanisms, leading to inhibition of downstream c-Jun N-terminal kinase (JNK) signalling. Merlin can regulate the subcellular localization of RAC1, and directly binds to PAK to inhibit its binding to RAC1 whereby restricting PAK recruitment to focal adhesions (Kaempchen *et al.*, 2003; Kissil *et al.*, 2003; Okada, Lopez-Lago & Giancotti, 2005; Shaw *et al.*, 2001). Merlin can also inhibit RAC1/PAK signalling further upstream by forming a complex with Angiomotin, Pals1-associated tight junction protein (PATJ) and Protein-associated with Lin7 (PALS1) leading to the release of RICH1 which then inactivates Rac1 (Yi *et al.*, 2011). Finally, non-phosphorylated Merlin binds to and inhibits CD44 to mediate contact inhibition of growth at high cell density and thus prevents RAS and RAC activation via CD44 (Morrison *et al.*, 2001).

Merlin also inhibits RAS activation, independent of RAC1 inhibition, by displacing ERM proteins and RAS from the Growth factor receptor bound protein 2 (GRB2)- Son of Sevenless (SOS) complex therefore preventing RAS activation and downstream Rapidly accelerated fibrosarcoma (RAF)/Mitogen-activated protein kinase (MAPK)/ Extracellular signal-regulated kinase (ERK) kinase (MEK)/ERK signalling (Morrison *et al.*, 2007). Indeed, Merlin-deficient primary schwannoma cells displayed enhanced RAF/MEK/ERK activation that was further enhanced by PDGFRβ, supporting a role for Merlin in suppressing RAF/MEK/ERK activity (Ammoun *et al.*, 2008). Merlin re-expression in Merlin-deficient malignant mesothelioma cells led to a reduction in Focal adhesion kinase (FAK) phosphorylation at tyrosine 297 which then disrupted FAK interaction with SRC and p85 (Poulikakos *et al.*, 2006). Ammoun *et al.* identified

increased FAK activation in Merlin-deficient schwannoma and showed that this activation led to a further increase in RAF/MEK/ERK activation (Ammoun *et al.*, 2008).

Merlin suppresses the Phosphoinositide 3-kinase (PI3K)/AKT/Mammalian target of rapamycin (MTOR) pathway by binding to and inhibiting the interaction between Phosphatidylinositol 3-kinase enhancer-L (PIKE-L) and PI3K (Rong *et al.*, 2004b). Indeed, in the absence of Merlin there was an increase in AKT protein expression and phosphorylation in both schwannoma and meningioma (Hilton, Ristic & Hanemann, 2009; Jacob *et al.*, 2008; Johnson *et al.*, 2002).

In Merlin-deficient mouse embryonic fibroblasts, Mammalian target of rapamycin complex 1 (MTORC1) was elevated and the overexpression of wild-type Merlin but not a Merlin mutant was able to suppress MTORC1 signalling (James *et al.*, 2009). mTORC1 inhibition was independent of PI3K/AKT and RAF/MEK/ERK signalling as wortmannin and UO126, inhibitors of PI3K and MEK1/2 respectively, were unable to inhibit S6 activation in Merlin-deficient cells (downstream of MTORC1) (James *et al.*, 2009). MTOR signalling is an important factor in Merlin-deficient tumourigenesis as treatment of mouse and human schwannoma cells with rapamycin, an MTOR inhibitor, led to a significant decrease in proliferation at < 0.1 nM (Giovannini *et al.*, 2014).

Merlin interacts with Low-density lipoprotein receptor-related protein 6 (LRP6) to inhibit proliferation and prevents Wingless integration-1 (WNT) signalling activation, which in turn inhibits β-catenin-dependent transcription of genes such as *c-Myc* and *Cyclin D1* (Kim & Jho, 2016). Increased nuclear β-Catenin, C-MYC and CYCLIN D1 has been observed in confluent primary human schwannoma cells, indicating elevated WNT signalling (Zhou *et al.*, 2011). Using this model, WNT signalling was shown to be dependent upon PAK2 and PDGFR activation (Zhou *et al.*, 2011).

Merlin activates the Hippo pathway and therefore inhibits the transcription of key growth regulatory genes at the cell cortex and nucleus (Zhang *et al.*, 2010). Zhang *et al.* showed that Merlin, Kidney and brain expressed protein (KIBRA) and Salvador (SAV) proteins interact to stimulate Large tumor suppressor kinase 2 (LATS2) phosphorylation in HEK293T and ACHN cells (Zhang *et al.*, 2010). In addition, Yin *et al.* showed that Merlin directly binds to and directs Large tumor suppressor kinase 1/2 (LATS1/2) to the plasma membrane where it is phosphorylated by Mammalian Ste20-like kinases 1/2 (MST1/2) facilitated by SAV (Yin *et al.*, 2013). *In vivo* loss of NF2, specifically in hepatocytes and biliary mouse cells, reduced LATS1/2 and Yes-associated protein (YAP) phosphorylation, leading to hepatocellular carcinoma and bile duct hamartoma formation (Zhang *et al.*, 2010). Tumour formation was largely ameliorated by further deletion of YAP, suggesting that Merlin functions as a tumour suppressor in a YAP-dependent manner (Zhang *et al.*, 2010). In addition, using a conditional null mouse model, Merlin loss in Schwann cells inhibited nerve repair following nerve injury demonstrating that Merlin is essential for Schwann cell plasticity and nerve repair (Mindos *et al.*, 2017). Failure to initiate nerve repair in Merlin-deficient Schwann cells was associated with increased YAP expression and indeed loss of YAP in Merlin-null Schwann cells restored axonal regrowth and nerve repair following injury in this model (Mindos *et al.*, 2017).

Li *et al.* showed that Merlin suppressed CRL4-DCAF1 activity in the nucleus to regulate many signalling pathways such as the Hippo pathway (Li *et al.*, 2010; Mori *et al.*, 2014). Merlin shuttles to the nucleus at the early G1 cell cycle phase and binds to the carboxy-terminal tail of DDB1 and Cullin 4 associated factor 1 (DCAF1) directly competing with CRL4 binding to DCAF1 and preventing ubiquitin substrate recruitment

(Li *et al.*, 2010; Muranen *et al.*, 2005). Indeed, Merlin depletion in Cos7 cells led to a significant increase in CRL4-DCAF1 activity (Li *et al.*, 2010). Furthermore, DCAF1 knockdown in schwannoma cells was able to significantly inhibit growth demonstrating the importance of Merlin regulation of CRL4-DCAF1 (Li *et al.*, 2010). Li et al. also demonstrated that Merlin activates the Hippo pathway through inhibition of CRL4-DCAF1-dependent ubiquitination of LATS1/2 (Li *et al.*, 2014). Reduced LATS1/2 ubiquitination activates the Hippo kinase cascade and leads to phosphorylation of YAP; therefore, inactivation of YAP transcriptional activities (Li *et al.*, 2014).

Merlin loss leads to hyperactivation of mitogenic signalling and therefore drives tumourigenesis, summarized in figure 1.1.

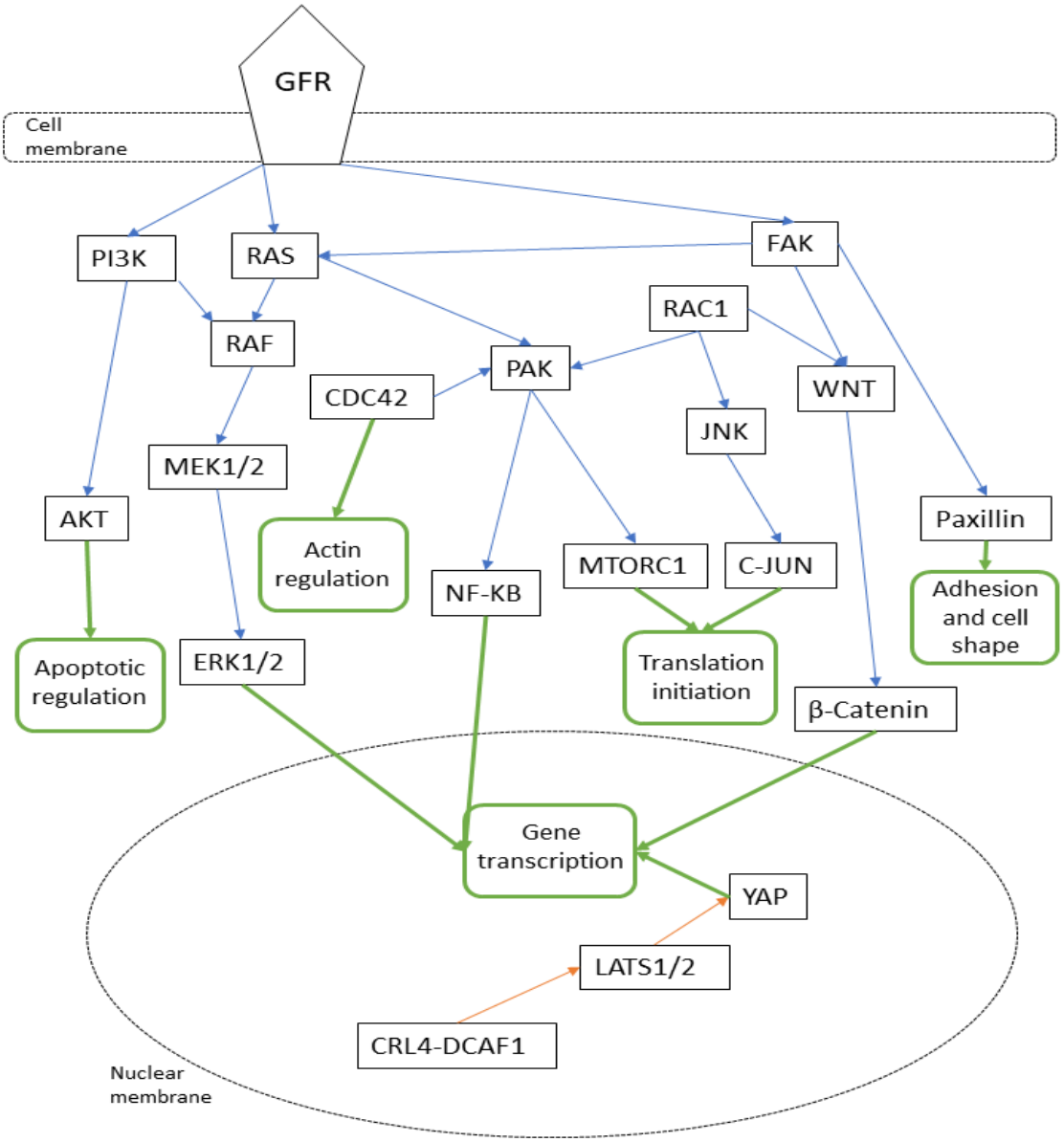

Figure 1.1 - Merlin-deficient signalling. A summary of hyperactivated signalling pathways in Merlin-deficient cells. Blue arrows represent activation of a protein and red arrows represent an inhibitory interaction whereas the green arrows represent the signalling outcome. When Merlin is lost, there is an increased accumulation of growth factor receptors (GFR) at the cell membrane leading to activation of downstream signalling (Lallemand *et al.*, 2009). These GFRs include PDGFR, IGF1R, EGFR, ERBB2, ERBB3, ERBB4 and Tyro3, Axl, and Mer (TAM) family receptors (Ahmad *et al.*, 2010; Ammoun *et al.*, 2010a; Lallemand *et al.*, 2009). Activation of the RAF/MEK/ERK, PI3K/AKT pathways by GFRs leads to increased gene transcription of genes involved in proliferation and downregulation of pro-apoptotic proteins. FAK is also hyper-activated in Merlin-deficient cells and activates the WNT/β-CATENIN pathway that modulates gene transcription as well as paxillin that forms focal adhesions to regulate cell adhesion and cell shape (Ammoun *et al.*, 2008; Zhou *et al.*, 2011). RAS, CDC42 and RAC1 activate PAK signalling and PAK activates NF-KB that regulates gene transcription (Balasenthil *et al.*, 2004) and MTORC1 that initiates RNA translation (Flaiz *et al.*, 2009; James *et al.*, 2009; Kaempchen *et al.*, 2003; Kissil *et al.*, 2003; López-Lago *et al.*, 2009; Morrison *et al.*, 2007; Okada, Lopez-Lago & Giancotti, 2005; Shaw *et al.*, 2001). In addition, RAC1 activates the JNK/c-JUN pathway that also initiates RNA translation (Cargnello *et al.*, 2012; Kaempchen *et al.*, 2003; Patel *et al.*, 2012). CRL4-DCAF1 is hyper-activated when Merlin is lost and inhibits LATS1/2, in the nucleus, therefore releasing the LATS1/2-dependent inhibition of YAP function allowing YAP to regulate gene transcription (Mori *et al.*, 2014). CRL4-DCAF1 also has other unidentified substrates that regulate the growth of Merlin-deficient tumours (Li *et al.*, 2010). Components of the pathways shown are also directly inhibited by Merlin and are more active in Merlin's absence such as RAS, RAC, CDC42, FAK, PI3K, PAK, and CRL4-DCAF1 (Flaiz *et al.*, 2009; Kissil *et al.*, 2003; Li *et al.*, 2010; Morrison *et al.*, 2007; Poulikakos *et al.*, 2006; Rong *et al.*, 2004b).

1.3 Merlin-deficient tumours

Inactivating *Nf2* mutations and a significant reduction in Merlin protein expression has been observed with high frequency in cancers including mesothelioma, glioma, and hepatocellular carcinoma demonstrating its relevance in tumourigenesis (Bott *et al.*, 2011; Lau *et al.*, 2008; Zhang *et al.*, 2017). Furthermore, *Nf2* mutations and/or inactivation has been identified at a much lower rate in; breast cancer, colorectal cancer, prostate cancer and melanoma (Petrilli & Fernández-Valle, 2016). Bi-allelic *Nf2* mutations are causative of tumour formation, especially in the case of NF2-related and sporadic schwannomas, meningiomas and ependymomas (Hanemann, 2008).

1.3.1 Merlin loss in cancer

Inactivating *Nf2* mutations have been identified in 21% (11/53) of primary mesothelioma tumour DNA samples (Bott *et al.*, 2011). Furthermore, 50% of mesothelioma cell lines have somatic *Nf2* gene mutations (Bianchi *et al.*, 1995; Sekido *et al.*, 1995). In addition, Thurneysen *et al.* found that Merlin protein expression was significantly reduced in 43% of primary mesothelioma tissue samples and inactive in the remaining samples (Thurneysen *et al.*, 2009). Low Merlin expression has been associated with reduced survival in mesothelioma patients highlighting the importance of Merlin as a tumour suppressor in these tumours (Meerang *et al.*, 2016).

Lau *et al.* identified reduced Merlin protein expression in 20/23 glioblastoma samples and decreased Merlin RNA expression in 21 out of 23 samples with significant concordance (Lau *et al.*, 2008). Moreover, overexpression of Merlin in the glioma cell lines U87MG and U251 led to inhibition of anchorage-independent growth and reduced invasiveness *in vitro* which was specific to wild-type Merlin and the constitutively active non-phosphorylated form of Merlin (S518A) (Lau *et al.*, 2008). In

addition, mice injected intracranially with U87MG cells overexpressing wild-type or S518A Merlin survived significantly longer than those injected with U87MG cells or U87MG cells overexpressing the phosphorylated form of Merlin (S518D) (Lau *et al.*, 2008). Collectively, these studies demonstrate the high rate of Merlin inactivation in glioblastoma and its critical role in tumour development.

Spontaneous development of hepatocellular carcinoma occurs in around 10% of mice with a heterozygous *Nf2* mutation suggesting that normal Merlin function is important in preventing tumour formation (Kalamarides *et al.*, 2002; McClatchey *et al.*, 1998). Zhang *et al.* showed that Merlin loss in hepatocytes and biliary cells at the perinatal stage led to the development of hepatocellular carcinomas in 100% of mutant mice demonstrating the critical role of Merlin in supressing tumour growth (Benhamouche *et al.*, 2010). Interestingly, liver overgrowth and hepatocellular carcinoma development were dependent on functional Hippo signalling (Benhamouche *et al.*, 2010; Zhang *et al.*, 2017).

1.3.2 Schwannoma

Benign schwannomas are often associated with NF2 but can occur sporadically and often harbour an *Nf2* gene mutation (Bianchi *et al.*, 1994; Evans, 2009). Schwannomas arise from Schwann cells that produce myelin and envelop nerves of the peripheral nervous system. Schwannomas can cause varying symptoms dependent on location including hearing loss, tinnitus, balance problems, headache and numbness (Petrilli & Fernández-Valle, 2016). Vestibular schwannomas are the most common and develop on the eighth cranial nerve, i.e., the vestibulocochlear nerve (Twist *et al.*, 1994).

Vestibular schwannomas are diagnosed by magnetic resonance imaging (MRI) in the general population at an incidence of around 2 per 100000 people per year (Lin *et al.*,

2005; Stangerup & Caye-Thomasen, 2012). Interestingly, the prevalence is thought to be much higher as 3–4% of patients are found to have a head or neck schwannoma at post-mortem, suggesting that a proportion of schwannomas are asymptomatic (Hanemann & Evans, 2006).

Observation, surgical resection and stereotactic radiotherapy are the main treatment options for vestibular schwannoma (Apicella *et al.*, 2016). Most tumours can be successfully resected but preserving normal nerve function and hearing remains a challenge (Battaglia, Mastrodimos & Cueva, 2006). Stereotactic radiotherapy leads to similar tumour control rates and improved hearing preservation compared with surgery for small vestibular tumours (Maniakas & Saliba, 2012; Yamakami *et al.*, 2003). However, stereotactic radiation can still lead to complications such as hearing loss, facial nerve palsy and trigeminal dysfunction (Hansasuta *et al.*, 2011). One study found that radiation dose was a significant factor in hearing preservation with doses < 13 Gy leading to a higher hearing preservation rate compared with doses > 13 Gy (Yang *et al.*, 2010). Interestingly, a study reported that patients managed by observation compared with patients treated with stereotactic radiotherapy had a comparable profile of symptoms and quality of life (Breivik *et al.*, 2013). In addition, hearing was lost in 76% of those under observation compared with 64% in stereotactic radiotherapy patients, which was not significant (Breivik *et al.*, 2013). However, the study did report that there was a significant reduction in tumour volume and a reduction in the need for additional treatment in patients treated with radiotherapy (Breivik *et al.*, 2013). Therefore, Muzevic *et al.* recommended that the treatment method should be chosen on an individual basis in the absence of substantial evidence to show that stereotactic radiotherapy is superior to observation or surgery (Muzevic *et al.*, 2014).

Hadfield *et al.* detected one *Nf2* gene mutation in 89% of NF2-associated schwannomas and two *Nf2* gene mutations in 79% of NF2-associated schwannomas (Hadfield *et al.*, 2010). However, it is well documented that all NF2-associated schwannomas have one germline *Nf2* mutation and therefore the methods used were not sensitive enough to detect all mutations. Therefore, the majority (possibly all) NF2-associated schwannoma have biallelic inactivation of the *Nf2* gene. In addition, most sporadic schwannomas harbour mutations in the *Nf2* gene. Indeed, Hadfield *et al.* detected at least one *Nf2* mutation in 66% of sporadic schwannomas tested (Hadfield *et al.*, 2010). Similarly, Havik *et al.* detected *Nf2* mutations in 35/46 (76%) of sporadic schwannomas and reported that 16/46 (35%) had two *Nf2* mutations (Håvik *et al.*, 2018). Lassaletta *et al.* also reported at least one mutation in 72% sporadic vestibular schwannoma with two mutations detected in 45% of tumours (Lassaletta *et al.*, 2013). Tumours with only one *Nf2* mutation retained Merlin protein expression and the presence of two *Nf2* mutations correlated well with Merlin protein loss (Chen *et al.*, 2017). However, some tumours with a mutation in both *Nf2* alleles had a proportion of cells that expressed Merlin suggesting that sporadic schwannomas can contain both one-hit and two-hit schwannoma cells (Chen *et al.*, 2017). In addition, Havik *et al.* identified mutations in Cell division cycle protein 27 homolog (*Cdc27*) (11%) and Ubiquitin Specific Peptidase 8 (*Usp8*) (7%) genes in sporadic schwannoma samples which were exclusive of *Nf2* mutations (Håvik *et al.*, 2018).

Merlin loss leads to schwannoma development caused by changes in Schwann cells such as increased proliferation, increased resistance to apoptosis, increased adhesion to the extracellular matrix and a change to a multipolar shape (Hilton, Ristic & Hanemann, 2009).

1.3.3 Meningioma

Meningiomas are the most common intracranial tumours and arise from the meningeal cells of the arachnoidal layer of the leptomeninges surrounding the brain and spinal cord (Ostrom *et al.*, 2015; Wiemels, Wrensch & Claus, 2010). Meningiomas most commonly occur in the elderly (> 65 years) and more frequently in females (Klaeboe *et al.*, 2005; Ostrom *et al.*, 2013). The majority of meningiomas are benign and classified as World Health Organisation (WHO) I and consist of meningothelial, fibrous, and transitional subtypes (Mawrin, Chung & Preusser, 2015). Atypical, clear cell, and chordoid meningiomas, classified as WHO II, account for up to 34% of all meningiomas whilst anaplastic meningiomas, classified as WHO III, account for 1–2% (Durand *et al.*, 2009; Pearson *et al.*, 2008).

Meningiomas often present as headaches and/or cranial nerve deficits (Wu *et al.*, 2018). Other symptoms are dependent on tumour location. The primary treatment for meningiomas is surgery, although complete resection is not always possible meaning a greater likelihood of recurrence (Gousias, Schramm & Simon, 2016). Radiotherapy is considered after resection of a recurrent tumour or WHO III meningioma but may also be useful where surgery is not possible due to tumour location (Dziuk *et al.*, 1998; Walcott *et al.*, 2013). Interestingly, the primary environmental risk factor for meningiomas is ionising radiation exposure and therefore radiotherapy may increase the risk of meningioma recurrence (Wiemels, Wrensch & Claus, 2010).

Around 60% of sporadic meningioma and 100% of meningiomas associated with NF2 have a *Nf2* gene mutation (Lomas *et al.*, 2005; Ruttledge *et al.*, 1994; Wellenreuther *et al.*, 1995). Paediatric meningiomas are rare and strongly associated with NF2 rather than occurring sporadically (Preusser, Brastianos & Mawrin, 2018). Clark et al.

detected Switch/Sucrose Non-fermentable-related matrix-associated actin-dependent regulator of chromatin subfamily B member 1 (*Smarcb1)* mutations in 6.4% of *Nf2*-mutant meningioma highlighting that *Nf2* mutations are not necessarily exclusive of other alterations (Clark *et al.*, 2016).

Several more mutations have been identified in meningioma in the TNF receptor-associated factor 7 (*Traf7*), Krupple-like factor 4 (*Klf4*), v-akt murine thymoma viral oncogene homolog 1 (*Akt1)* and smoothened, frizzled family receptor (*Smo*) genes (Clark *et al.*, 2013). Additional somatic mutations identified in meningioma include polymerase (RNA) II (DNA directed) polypeptide A, 220 kDa (*Polr2a*), PI3K catalytic subunit, alpha (*Pik3ca*), v-akt murine thymoma viral oncogene homolog 3 (*Akt3*), PI3K regulatory subunit, alpha (*Pik3r1*), protein kinase, Cyclic Adenosine Monophosphate (cAMP)-dependent, regulatory, type I, alpha (*Prkar1a*) and suppressor of fused homolog (Drosophila) (*Sufu*) (Clark *et al.*, 2016). *Akt1*, *Pik3ca* and *Smo* mutations, as well as *Smarcb1*, can co-occur with *Nf2* mutations in a small proportion of meningioma (Clark *et al.*, 2016). Differentially expressed in adenocarcinoma of the lung 1 (DAL-1) protein is normally expressed in the brain and testes (Perry *et al.*, 2000). The *Dal-1* gene is downregulated in around 75% of meningiomas leading to loss of the DAL-1 protein (Perry *et al.*, 2000). *Nf2* mutations and *Dal-1* mutations or protein downregulation can co-occur, most commonly in WHO II and III meningiomas, suggesting DAL-1 loss causes additional meningioma growth and/or invasion rather than driving meningioma development (Nunes *et al.*, 2005; Perry *et al.*, 2000; Perry *et al.*, 2001).

Nevoid basal cell carcinoma syndrome (gorlin syndrome) is a genetic disease which leads to the development of tumours including basal cell carcinomas,

medulloblastoma, meningiomas, and ovarian tumours (Santos *et al.*, 2011; Wicking *et al.*, 1997). Mutations in the Protein patched homolog 1 (*Ptch1*) gene encoding the PTCH1 protein are the most common cause of nevoid basal cell carcinoma (Boutet *et al.*, 2003; Rimkus *et al.*, 2016). Interestingly, both PTCH1 and SMO are components of the Hedgehog signalling pathway highlighting this pathway as dysregulated in a subset of meningiomas.

1.3.4 Ependymoma

Ependymomas arise from ependymal cells of the spinal cord and cranial ventricles, which are responsible for the production of cerebrospinal fluid (Gilbert, Ruda & Soffietti, 2010). Whilst two thirds of ependymomas in adults arise in the spinal cord, 90% of paediatric ependymomas occur in the cranial ventricles (Hamilton & Pollack, 1997). The main treatment for ependymomas is surgery followed by radiotherapy; however, tumour recurrence may occur even when the tumour is completely resected (Hamilton & Pollack, 1997; Kawabata *et al.*, 2005; Merchant & Fouladi, 2005).

Chromosomal abnormalities are frequently identified in ependymomas, particularly chromosome 22 and *c11orf95*-v-rel avian reticuloendotheliosis viral oncogene homolog A (*Rela*) gene fusions (Hamilton & Pollack, 1997; Pajtler *et al.*, 2015; von Haken *et al.*, 1996). Whilst NF2 patients frequently develop ependymomas, *Nf2* mutations in sporadic paediatric ependymomas are rare and *Nf2* mutations are found most commonly in adult spinal ependymomas (Buccoliero *et al.*, 2010; Ebert *et al.*, 1999; Lamszus *et al.*, 2001; Rubio *et al.*, 1994; von Haken *et al.*, 1996). Methylation profiling identified nine distinct ependymoma groups (Pajtler *et al.*, 2015). Some of these sub-groups had distinct genetic profiles; for example, 88% of ependymomas in the supratentorial ependymoma chromothripsis; *rela*-fusion (ST-EPN-RELA) sub-group

had one of the two major types of *C11orf95-Rela* gene fusions (Pajtler *et al.*, 2015). Furthermore, loss of 22q (containing the *Nf2* locus) was predominantly, but not exclusively, found in the spinal ependymoma (SP-EPN) sub-group of ependymomas as expected. Interestingly, a microarray study of 19 paediatric ependymomas identified the Schwannomin interacting protein 1 (*Schip-1*) gene, on chromosome 22, as commonly downregulated (Suarez-Merino *et al.*, 2005). SCHIP-1 protein has been shown to regulate Merlin function demonstrating that Merlin protein dysregulation may have a prominent role in ependymoma pathogenesis (Goutebroze *et al.*, 2000). Misdiagnosis can complicate genetic analysis and cell culture of ependymomas; therefore, this project focussed on schwannoma and meningioma.

1.4 Neurofibromatoses

Neurofibromatoses are a small group of genetic diseases which predispose patients to tumour formation as well as other conditions such as cataracts or scoliosis. These conditions are caused by a mutation in one allele of a tumour suppressor. A secondary somatic mutation leads to complete protein loss and therefore loss of tumour suppressor function leading to tumour formation. The neurofibromatoses include Neurofibromatosis type 1 (NF1), NF2 and schwannomatosis.

1.4.1 Neurofibromatosis type 1

NF1 is caused by a germline mutation in the Neurofibromin 1 (*Nf1*) gene and has an incidence of 1:2500 (Ferner & Gutmann, 2002). NF1 patients develop a somatic mutation in the remaining normal allele leading to loss of Neurofibromin 1 protein in cells and tumour development. These tumours include plexiform neurofibromas, cutaneous neurofibromas and malignant peripheral nerve sheath tumours (MPNST) (Ferner *et al.*, 2007). There is no evidence of malignant change of cutaneous

neurofibromas, but they can be removed by surgery if they cause cosmetic problems or excessive itching (Ferner *et al.*, 2007). However, plexiform neurofibromas cause significant morbidity as they can grow along nerves and infiltrate soft tissue and surround bone (Ferner *et al.*, 2007). Furthermore, the growth rate of plexiform neurofibromas can be unpredictable and can lead to the development of MPNSTs (Ferner *et al.*, 2007). NF1 patients also have characteristic *café au lait* macules and cutaneous neurofibromas which aid diagnosis (Ferner *et al.*, 2007; Lu-Emerson & Plotkin, 2009). In addition, NF1 patients may have a lower than average IQ, scoliosis and/or congenital heart defects (Akbarnia *et al.*, 1992; Ferner, Hughes & Weinman, 1996; Friedman *et al.*, 2002).

NF1 patients have a lifetime risk of 8–13% of developing MPNSTs which represents the main cause of mortality in these patients (Evans *et al.*, 2002). MPNSTs are aggressive malignancies associated with significant morbidity and a median survival time of just 17 months (Zehou *et al.*, 2013). Unfortunately, NF1 patients have a reduced life expectancy of around 15 years less than the general population, which is often due to MPNST formation and malignancy (Zöller *et al.*, 1995). Therefore, NF1 patients must be monitored at least every 12 months for clinical features of MPNSTs such as persistent pain, neurological symptoms and changes in the size or texture of an existing neurofibroma (Ferner *et al.*, 2007).

Neurofibromin 1, the protein product of the *Nf1* gene, mediates RAS inactivation to suppress RAF/MEK/ERK signalling and therefore inhibits cell growth (Johansson *et al.*, 2008). Mutations in *Nf1* lead to aberrant RAF/MEK/ERK activation that drives tumour formation (Jessen *et al.*, 2013). *Nf1* mutations are the only mutations identified in NF1-associated plexiform neurofibromas and is suggested to drive tumour formation

(Pemov *et al.*, 2017). Furthermore, Neurofibromin 1 protein is often lost in sporadic MPNSTs, glioblastoma, lung adenocarcinoma and ovarian cancer demonstrating its importance as a tumour suppressor (Jessen *et al.*, 2013).

1.4.2 Neurofibromatosis type 2

NF2 has an incidence rate of 1:25000 and is an autosomal dominant genetic disease caused by a mutation in the *Nf2* gene (Bianchi *et al.*, 1994; Evans *et al.*, 2005; Hanemann, 2008). NF2 is characterized by the development of multiple benign tumours including schwannomas, meningiomas and ependymomas throughout life (Hanemann, 2008). Bilateral vestibular and spinal schwannoma, intracranial and intraspinal meningioma and ependymomas are common in NF2 patients (Evans, 2009). Spinal tumours are identified in around 60% of NF2 patients including spinal schwannoma, meningiomas and ependymomas (Dow *et al.*, 2005; Egelhoff *et al.*, 1992; Mautner *et al.*, 1995). These tumours represent a significant burden to NF2 patients with multiple symptoms and are currently managed with surgery or radiosurgery (Hanemann, 2008; Petrilli & Fernández-Valle, 2016). In addition, NF2 patients may have ocular abnormalities such as early onset cataracts and skin abnormalities including subcutaneous nodular schwannomas (Mautner *et al.*, 1997; Ragge *et al.*, 1997).

NF2 leads to a shortened life expectancy and has a significant effect on quality of life (Baser *et al.*, 2002a). In 1992, Evans *et al.* reported a mean survival of 62 years in NF2 patients compared with 76.4 years in the general UK population in the same year (Evans *et al.*, 1992; Office-for-National-Statistics, 2016). Considerable morbidity is often due to pre and post-operative complications such as seizures, paralysis and wasting (Evans, Sainio & Baser, 2000). Interestingly, NF2 patient mortality has

significantly improved since 1980 and this may be attributable to the improved care received at specialist centres (Hexter *et al.*, 2015). Indeed, in 2014, 97% of NF2 patients living in the UK were managed by one of four speciality centres (Hexter *et al.*, 2015).

The presence of bilateral vestibular schwannoma is the most characteristic feature of NF2 and is primarily used for diagnosis. The original criteria for NF2 diagnosis was the National Institutes of Health (NIH) criteria [1987] which diagnosed patients with either bilateral vestibular schwannoma or a family member with NF2 as well as a unilateral vestibular schwannoma or two other NF2-associated tumours (Conference-statement, 1988). However, improved sensitivity in detecting vestibular schwannoma means that a greater proportion of patients are diagnosed with bilateral vestibular schwannoma at an older age, despite the absence of NF2 (Evans *et al.*, 2015). Conversely, bilateral vestibular schwannoma in NF2 patients may not occur until adolescence preventing early NF2 diagnosis and management (Baser *et al.*, 2002b). The Manchester criteria was created to address and improve the sensitivity and specificity of diagnosis, table 1.1 (Evans, 2009). In addition, identification of a pathogenic *Nf2* mutation also leads to a NF2 diagnosis. Alternatively, the Baser criteria for diagnosis of NF2 [2011] (table 1.2) permits earlier diagnosis in a greater proportion of patients compared with other criteria (Baser *et al.*, 2011; Baser *et al.*, 2002b).

Main criteria
Bilateral vestibular schwannoma *or*
Family history of NF2 *plus*
Unilateral vestibular schwannoma *or*
Any two of: meningioma, glioma, neurofibroma, schwannoma, posterior subcapsular lenticular opacities
Additional criteria
Unilateral vestibular schwannoma *plus*
Any two of: meningioma, glioma, neurofibroma, schwannoma, posterior subcapsular opacities, *alternatively*
Multiple meningiomas (two or more) *plus*
Unilateral vestibular schwannoma *or* any two of: glioma, neurofibroma, schwannoma, and cataract

Table 1.1 – Manchester criteria for the diagnosis of NF2. Adapted from (Evans, 2009)

A NF2 diagnosis is given if there is a score of six or more according to the below criteria:

Feature	**Score if present < 30 years**	**Score if present > 30 years**
First-degree relative with NF2	2	2
Unilateral vestibular schwannoma	2	1[a]
Second vestibular schwannoma	4	3[a]
One meningioma	2	1
Second meningioma	2	1
Cutaneous schwannoma	2	1
Cranial nerve tumour (excluding vestibular)	2	1
Mononeuropathy	2	1
Cataract	2	0

a – No points if age of vestibular schwannoma diagnosis > 70 years

- A definite NF2 diagnosis can also be given if a constitutional pathogenic *Nf2* mutation is identified
- Mosaic NF2 is diagnosed if no constitutional pathogenic *Nf2* mutation is identified but a pathogenic mutation is found in the blood **OR** if no pathogenic *Nf2* mutation is found in the blood but the same pathogenic NF2 mutation is identified in two separate tumours
- Possible NF2 is diagnosed if there is no constitutional pathogenic *Nf2* mutation identified, pending further clarification

Table 1.2 - Baser criteria [2011] used for diagnosis of NF2. Adapted from (Baser *et al.*, 2011)

Management of patients after diagnosis involves evaluation every 12 months in patients without acute problems (Ruggieri *et al.*, 2016). MRI scans of the brain, spinal cord and of symptomatic lesions outside the brain are used to monitor tumour growth as well as audiology examinations and brainstem auditory evoked responses (BAER) to assess eighth cranial nerve dysfunction associated with vestibular schwannomas (Ruggieri *et al.*, 2016). Whilst surgery and stereotactic radiotherapy are options for individual tumours, the presence of multiple tumours in NF2 patients means that each tumour must be assessed individually (Ruggieri *et al.*, 2016). Treatment decisions are based on preserving function and minimizing the effects on quality of life (Ruggieri *et al.*, 2016).

There are several additional considerations to consider when choosing a treatment for schwannoma, meningioma and ependymoma in NF2 patients compared with sporadic patients. Firstly, stereotactic radiotherapy treatment outcomes are worse for vestibular schwannomas in NF2 patients compared with sporadic vestibular schwannomas (Ruggieri *et al.*, 2016). Secondly, stereotactic radiotherapy may increase the risk of secondary malignancies more so in NF2 patients than sporadic patients (Ruggieri *et al.*, 2016). Thirdly, NF2-associated schwannomas and ependymomas are often multi-lobulated due to several distinct tumours, with different Merlin mutations, merging to form a larger tumour (Dewan *et al.*, 2015). This multi-lobulated appearance complicates surgical removal of NF2-associated tumours compared with sporadic tumours. Finally, NF2-associated ependymomas are commonly asymptomatic and surgery is often avoided in favour of monitoring growth and appearance of symptoms (Nowak *et al.*, 2016). For example, Nowak *et al.* reported that 2 out of 34 NF2 patients

underwent surgery for ependymoma excision between 1998 and 2014 (Nowak *et al.*, 2016).

The treatment and management of NF2 patients can also be influenced by the type of germline *Nf2* mutation. Frameshift and nonsense mutations that result in production of a truncated form of Merlin are associated with a more severe disease phenotype and reduced life expectancy compared with missense mutations, large deletions and in-frame mutations that result in complete loss of Merlin protein (Selvanathan *et al.*, 2010). Truncating *Nf2* gene mutations are also associated with an earlier age of onset of symptoms such as hearing loss, increased prevalence of meningiomas and spinal tumours and an earlier age of diagnosis of vestibular schwannoma (Selvanathan *et al.*, 2010). Evans *et al.* show that patients with truncating mutations have an average age at onset of symptoms of 19 years compared with 27.8 years for patients with splice-site mutations, missense mutations or large deletions (Evans *et al.*, 1998). Therefore, truncating *Nf2* gene patients should be evaluated more often than other *Nf2* gene mutation patients. Furthermore, *Nf2* mosaicism exists in up to 33% of NF2 patients (Bernards & Gusella, 1994; Evans *et al.*, 2007). Mosaicism is a mutation which occurs in the post-zygotic stage after fertilization and during development. Mosaicism leads to segmental and milder disease even in the presence of truncating mutations (Evans *et al.*, 1998; Kluwe & Mautner, 1998). Unfortunately, mosaic NF2 is often undetectable in the blood of patients, which confounds diagnosis (Ruggieri *et al.*, 2016). However, as mosaic NF2 is a milder disease, management and treatment can be more conservative than traditional NF2 patients.

1.4.3 Schwannomatosis

Schwannomatosis is caused by a mutation in the *Smarcb1* or Leucine zipper-like transcription regulator 1 (*Lztr1)* gene and leads to the formation of multiple cranial, spinal and peripheral schwannomas and, less commonly, vestibular schwannoma (Ruggieri *et al.*, 2016). Schwannoma formation in schwannomatosis is thought to follow the four-hit, three-step model of tumourigenesis (Ruggieri *et al.*, 2016). This model involves the inactivation of the *Nf2* gene as well as the *Smarcb1/Lztr1* genes and therefore re-iterates the importance of Merlin in tumour formation. The main symptom of schwannomatosis is pain and the annual incidence is 0.58 cases per million people, so the condition is extremely rare, even in comparison with the other neurofibromatoses (Merker *et al.*, 2012). NF2 diagnosis can be complicated by schwannomatosis individuals as these patients can have a unilateral vestibular schwannoma and two non-intradermal schwannomas (Smith *et al.*, 2017). Smith *et al.* reported that 5/204 patients diagnosed with NF2 had a germline *Lztr1* mutation; therefore, schwannomatosis should be considered in the absence of a germline *Nf2* mutation.

1.5 Treatment and clinical trials for Merlin-deficient tumours

Treatment options for all the forms of neurofibromatosis is still limited with no Food and Drug Administration (FDA)-approved drugs available. Most often, tumours are removed during surgery. However, there are some drugs that have been tested/are being tested in clinical trials, which are detailed below, and ongoing trials are outlined in table 1.3.

As there is no effective therapeutic regimen currently available, further investigation of the pathways associated with Merlin loss will propel the understanding of NF2-

associated tumourigenesis. This will allow the discovery of new targets for the development of effective therapies and possible combination therapies.

Reference Number	Drug	Tumours Targeted	Clinical Trial Phase	Stage of Study	Completion Date
EudraCT2011-001789-16	Sorafenib	NF2-related cutaneous schwannoma	Early phase I	Ongoing	Unknown
EudraCT2010-023508-28	Nilotinib	NF2-related cutaneous schwannoma	Early phase I	Ongoing	Unknown
NCT01880749	Everolimus	Vestibular schwannoma and meningioma	Early phase I	Active, not recruiting	December 2019
NCT02282917	AR-42	Vestibular schwannoma and meningioma	Early phase I	Recruiting	August 2018
NCT02934256	Icotinib	NF2-related	II	Recruiting	June 2018
NCT02831257	AZD2014	NF2-related Meningiomas	II	Active, not recruiting	November 2024
NCT01767792	Bevacizumab	Progressive NF2-related vestibular schwannomas	II	Active, not recruiting	December 2019
NCT01125046	Bevacizumab	Recurrent or progressive meningiomas	II	Active, not recruiting	July 2018
NCT01345136	Everolimus	NF2-related vestibular schwannoma	II	Active, not recruiting	February 2020
NCT02129647	Axtinib	NF2-related	II	Recruiting	January 2019
NCT02523014	Vismodegib or FAK inhibitor (GSK2256098)	Progressive meningiomas (visomodegib for *smo/ptch1* mutations and GSK2256098 for *nf2* mutations)	II	Recruiting	Unknown
NCT03095248	Selumetinib	NF2-related	II	Recruiting	May 2021
NCT03079999	Aspirin	Vestibular schwannoma	II	Not yet recruiting	February 2022

Table 1.3 - Ongoing clinical trials for the treatment of NF2-related and sporadic tumours. Information was derived from publicly available information from (Clinicaltrialsregister.eu[Internet]) and (ClinicalTrials.gov[Internet]) using the search term NF2 and accessed on the 26th April 2018.

1.5.1 Lapatinib

Lapatinib is an EGFR/ERBB2 inhibitor which reduces tyrosine phosphorylation of both EGFR and ERBB2 and thus their activation (Xia *et al.*, 2002). Lapatinib was able to supress ERK1/2 and AKT activation, downstream of EGFR and ERBB2 receptors, to inhibit proliferation in schwannoma (Ammoun *et al.*, 2010a; Xia *et al.*, 2002). A phase II clinical trial recruited 21 NF2 patients with progressive vestibular schwannoma (Karajannis *et al.*, 2012). The primary endpoint was a reduction in vestibular schwannoma of more than 15% (which is slightly less than the 20% recommended by the Response Evaluation in Neurofibromatosis and Schwannomatosis (REiNS) consortium) and the secondary endpoint was a hearing improvement of 10 dB pure tone average or increase in word recognition scores (Karajannis *et al.*, 2012). Only four patients reached the primary endpoint of more than a 15% volumetric reduction in vestibular schwannoma size and four met the secondary endpoint of improved hearing with acceptable toxicities (Karajannis *et al.*, 2012). Unfortunately, in this study there was no meningioma response observed by imaging (Karajannis *et al.*, 2012). In addition, a phase II clinical study of Lapatinib in paediatric patients with recurrent ependymoma showed that there was no measurable response reported in any of the 14 ependymoma patients enrolled (Fouladi *et al.*, 2013). Due to the modest responses observed in schwannoma, lack of response in meningioma or ependymoma, and side effects such as diarrhoea, rash and fatigue, Lapatinib is unlikely to be suitable as a monotherapy for NF2 patients. Paldor *et al.* implanted mouse schwannoma cells (SC4) in the mouse sciatic nerve and compared tumour growth after treatment with Lapatinib or treatment with Lapatinib and radiotherapy (Paldor *et al.*, 2017). Lapatinib in combination with radiotherapy reduced tumour growth rates significantly compared

with Lapatinib alone and these tumours did not regrow after Lapatinib treatment ended (Paldor *et al.*, 2017). This suggests that the combination of targeted therapy with conventional therapy, such as radiotherapy, may be efficacious.

1.5.2 Everolimus

Everolimus is an inhibitor of the MTORC1, which is activated in Merlin-deficient cells such as meningioma (James *et al.*, 2009). A phase II study of Everolimus treatment in ten progressive vestibular schwannoma patients reported that no patients had more than a 20% reduction in tumour volume after 12 months of treatment (Goutagny *et al.*, 2015). However, five patients experienced a decrease in the median annual growth rate during Everolimus treatment of 66.5% compared with before treatment (Goutagny *et al.*, 2015). In addition, the growth rate of six meningiomas in the same study was delayed during Everolimus treatment reflective of the cytostatic properties of the drug (Goutagny *et al.*, 2015). Similarly, another phase II study of nine NF2 patients with progressive vestibular schwannoma showed partial tumour shrinkage of < 15% in 3 out of 11 vestibular schwannomas analysed after Everolimus treatment and no hearing improvements (Karajannis *et al.*, 2014). This evidence suggests that Everolimus may have a growth-delaying effect on vestibular schwannoma that cannot be confirmed without a larger sample size, and is relatively ineffective to reduce tumour size or preserve hearing in NF2 patients.

1.5.3 PDGFR inhibitors

Imatinib is a PDGFR/C-KIT inhibitor that decreases viability, proliferation and increases apoptosis of the schwannoma cell line, HEI-193 (Altuna *et al.*, 2011; Mukherjee *et al.*, 2009). A case study of a single NF2 patient with progressive vestibular schwannoma who was treated with Imatinib experienced a decrease in schwannoma growth and

self-reported improvements in hearing (Lim & de Souza, 2013). However, Imatinib was discontinued after four months due to side effects including nausea, vomiting and abdominal pain accompanied by hearing loss (Lim & de Souza, 2013). A phase II study of Imatinib in patients with recurrent meningiomas showed no partial or full responses in any of the 22 patients treated (Wen *et al.*, 2009).

Nilotinib is an Adenosine triphosphate (ATP) competitive PDGFR inhibitor that also has activity against Breakpoint cluster region (BCR)- Abelson murine leukemia viral oncogene homolog 1 (ABL) fusion kinase protein and C-KIT receptor kinases (Deremer, Ustun & Natarajan, 2008). Nilotinib inhibits Platelet-derived growth factor (PDGF)-mediated activation of PDGFRβ, ERK1/2 and AKT leading to reduced proliferation of human primary schwannoma cells at a concentration ten-fold lower than that of Imatinib (Ammoun *et al.*, 2011). Nilotinib also decreased viability, proliferation and increased apoptosis in the schwannoma cell line, HEI-193 (Sabha *et al.*, 2012). Nilotinib also significantly reduced the growth of tumours derived from the SC4 cell line and implanted in the flank of a mouse (Paldor *et al.*, 2017). This suggests that Nilotinib may have more potential as a therapeutic for Merlin-deficient tumours than Imatinib due to increased potency. Indeed, investigation of intra-tumoural concentration and activity of Nilotinib in cutaneous schwannomas of NF2 patients is currently underway (EudraCT: 2010-023508-28).

The PDGFR and C-RAF inhibitor Sorafenib is also a potential therapeutic for Merlin-deficient tumours which has been shown to reduce ERK1/2 and AKT activity as well as proliferation of human primary schwannoma cells and was more effective than Nilotinib (Ammoun *et al.*, 2008). Investigation of *in vivo* intra-tumoural concentration and activity of Sorafenib in cutaneous schwannomas of NF2 patients is currently

ongoing (EudraCT: 2011-001789-16). Unfortunately, the outcome of this trial was negative highlighting the need for further research into potential treatment options (unpublished data).

1.5.4 Bevacizumab

Vascular endothelial growth factor (VEGF) is overexpressed in both NF2-related and sporadic schwannomas, which correlates with tumour growth rate (Cayé-Thomasen *et al.*, 2003; Cayé-Thomasen *et al.*, 2005). Bevacizumab, a VEGF inhibitor, has been tested in vestibular schwannoma where tumour regression, reductions in tumour growth rates and improved hearing have been reported (Alanin *et al.*, 2015; Hochart *et al.*, 2015; Mautner *et al.*, 2010; Plotkin *et al.*, 2012). One study showed a response of more than 20% tumour shrinkage in 50% of patients and 50% also reported subjective neurological improvements (Alanin *et al.*, 2015). A retrospective study of 15 NF2 patients treated with Bevacizumab for progressive vestibular schwannoma showed a response of more than 20% tumour volume shrinkage in 14/48 meningiomas (Nunes *et al.*, 2013). Unfortunately, in nine cases, the response was not maintained following discontinuation of Bevacizumab treatment, and the tumours increased in volume at the same rate as the non-responding tumours (Nunes *et al.*, 2013). In another study, there was a partial response in two atypical meningiomas treated with Bevacizumab for nine months and stable disease in an additional five meningiomas (Hawasli *et al.*, 2013). A retrospective study of Bevacizumab in eight patients with recurrent ependymoma (WHO II and III) reported a partial radiographic response in 75% of patients treated with Bevacizumab-containing regimens (Green *et al.*, 2009). However, 5/6 patients received Bevacizumab alongside chemotherapy such as temozolomide or carboplatin making it difficult to determine the therapeutic agent responsible for the

tumour response (Green *et al.*, 2009). There are currently two ongoing phase II clinical trials: testing Bevacizumab in children in young adults with NF2 (NCT01767792); and assessing Bevacizumab potential in treating patients with recurrent or progressive meningioma (NCT01125046).

1.5.5 Selumetinib (AZD6244)

AZD6244 is a MEK1/2 inhibitor with demonstrated anti-tumourigenic activity in a primary human schwannoma model. AZD6244 was able to completely abrogate Platelet-derived growth factor (PDGF) induced ERK1/2 activation and proliferation but had no effect on cell viability at concentrations tested (Ammoun *et al.*, 2010b). A phase I trial of Selumetinib in NF1 children with inoperable plexiform neurofibromas was carried out to determine the maximum tolerated dose (Dombi *et al.*, 2016). The study reported that 60% of the recommended adult dose of Selumetinib could be administered long-term in children. In addition, 71% of children had a partial response in their plexiform neurofibromas (tumour volume decrease > 20%) (Dombi *et al.*, 2016). Selumetinib has been shown to be safe, efficacious and suitable for long-term treatment; therefore, it has the potential to be translated into the treatment of NF2 patients. A phase II clinical trials of AZD6244 in NF2 patients with NF2-asscoiated tumours is currently recruiting patients (NCT03095248).

1.5.6 Combination therapy

Combinatorial regimens targeting different activated pathways in Merlin-deficient tumours may have a beneficial effect in reducing tumour size compared with one drug alone. A phase II clinical trial of Bevacizumab and Everolimus treatment for recurrent, progressive meningiomas showed that the majority of meningiomas treated had a stable disease pattern after treatment (15/17) (Shih *et al.*, 2016). However, there was

no reduction in tumour volume in any of the meningiomas and four patients discontinued treatment due to toxicity demonstrating the unsuitability of this drug combination to treat NF2 patients long term (Shih *et al.*, 2016). In addition, lower concentrations of Bevacizumab and Everolimus for the treatment of low grade Merlin-deficient tumours should be tested.

Unfortunately, a phase II study of Bevacizumab and Lapatinib in 24 patients with recurrent ependymoma showed no response (DeWire *et al.*, 2015). This was particularly disappointing as an earlier retrospective study in recurrent ependymoma suggested Bevacizumab was efficacious and led to reductions in tumour size (Green *et al.*, 2009). However, the combination of Bevacizumab and Lapatinib has not yet been tested in less aggressive, non-recurrent, Merlin-deficient tumours.

Nilotinib and AZD6244 were tested in human primary schwannoma cells and were shown to be more effective at reducing proliferation when delivered together (Ammoun *et al.*, 2011). However, consideration must be given to long-term toxicity of any potential therapeutic as NF2 patients would need long term treatment to be effective on multiple tumours that continue to grow throughout life. Combination of drugs leads to increased complexity when determining tolerated long-term toxicities.

1.6 CRL4-DCAF1

The CRL4-DCAF1 complex comprises Cullin 4A/B, the adaptor protein DDB1 and DCAF1 as the substrate receptor protein (Angers *et al.*, 2006; He *et al.*, 2006; Jin *et al.*, 2006). CRL4-DCAF1 is an E3 ubiquitin ligase complex that ubiquitinates lysine residues within substrates, often resulting in substrate degradation (Jin *et al.*, 2006; Kaur *et al.*, 2012; Li *et al.*, 2014; Yu *et al.*, 2015). There are around 600 E3 ubiquitin ligase complexes that are responsible for ubiquitin modification of over 20% of all intracellular proteins

(Jackson & Xiong, 2009; Soucy *et al.*, 2009). The type of ubiquitin modification determines the function of the ubiquitination. Poly-ubiquitination often directs the substrate to the proteasome or lysosome where it is degraded, whereas mono-ubiquitination can significantly alter protein function, summarized in figure 1.2 (Hershko & Ciechanover, 1998; Sugiura *et al.*, 2014). For example, mono-ubiquitination of Defective in Cullin Neddylation 1 (DCNL1) protein leads to nuclear export (Wu *et al.*, 2011).

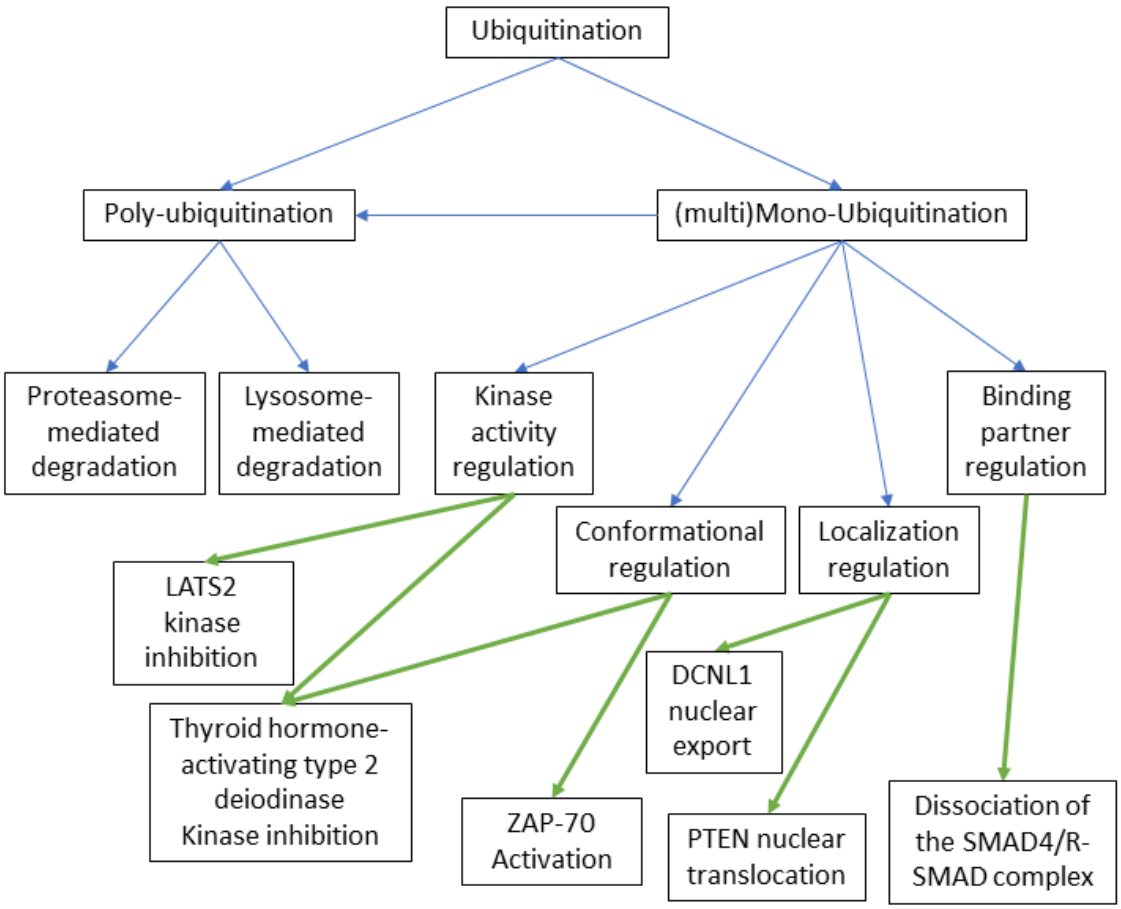

Figure 1.2 - Roles of ubiquitination. Ubiquitination regulates protein signalling predominantly through poly-ubiquitination of substrates leading to proteasome-mediated and lysosome-mediated degradation (Hershko & Ciechanover, 1998; Sugiura *et al.*, 2014). (multi)Mono-ubiquitination regulates protein signalling by altering binding partners, localization, conformation and kinase activity (Komander & Rape, 2012). Mono-ubiquitination can also be the precursor to poly-ubiquitination of substrates indicated by a blue arrow (Windheim, Peggie & Cohen, 2008). The green arrows show examples of (multi)mono-ubiquitination regulating degradation-independent protein functions. Dissociation of the Small worm phenotype (SMA) Mothers Against Decapentaplegic (MAD) (SMAD4)/Receptor regulated Small worm phenotype (SMA) Mothers Against Decapentaplegic (MAD) (R-SMAD) complex is mediated by ECTO/Transcriptional intermediary factor 1 (TIF1-γ) induced mono-ubiquitination of SMAD4 (Dupont *et al.*, 2005). Neural precursor cell expressed developmentally down-regulated protein 4 (NEDD4)-1 mono-ubiquitinates Phosphatase and tensin homolog (PTEN) leading to nuclear import (Trotman *et al.*, 2007). Conversely, NEDD4-1 mono-ubiquitination of DCNL1 mediates nuclear export (Wu *et al.*, 2011). Mono-ubiquitination of Zeta-chain-associated protein kinase 70 (ZAP-70) at K476 can stabilize an active ZAP-70 conformation (Ball *et al.*, 2016). Association of thyroid hormone-activating type 2 deiodinase with WSB01 leads to ubiquitination, a change in conformation and inhibition of catalytic activity (Sagar *et al.*, 2007). Finally, CRL4-DCAF1-mediated ubiquitination of LATS2 can inhibit its kinase activity (Li *et al.*, 2014).

1.6.1 CRL4-DCAF1 roles and regulation

Cullin-RING ligase (CRL) ubiquitin complexes are activated by neddylation, which leads to a conformational change allowing the Cullin-substrate to bind and thus be ubiquitinated (Duda *et al.*, 2008; Saha & Deshaies, 2008; Zheng *et al.*, 2002; Zhou *et al.*, 2018). The Neural precursor cell expressed developmentally down-regulated protein 8 (NEDD8) E3 ligase, Ring-Box 1 (RBX1), pairs with the E2, Ubiquitin conjugating enzyme E2 M (UBE2M) and the NEDD8-activating enzyme E1 (NAE) to catalyse the neddylation of Cullin 1, 2, 3, 4A, 4B and 5 proteins (Hochstrasser, 1998; Jones *et al.*, 2008).

DCAF1, also known as Viral protein R binding protein (VPRBP) was first discovered in 1994 as a protein of unknown function that bound to the HIV1 Viral protein R (VPR) (Hochstrasser, 1998). VPR can activate CRL4-DCAF1's ubiquitin ligase activity and has been shown to facilitate ubiquitination and subsequent degradation of Uracil-DNA glycosylase 2 (UNG2) (Ahn *et al.*, 2010). Conversely, CRL4-DCAF1 activity is inhibited by the closed, active form of Merlin which binds to the C-terminal of DCAF1 in the nucleus and prevents substrate recruitment (Li *et al.*, 2010).

DCAF1 inhibition prevents ubiquitin modification of LATS1/2 and therefore enhances YAP phosphorylation and subsequent degradation to control growth (Li *et al.*, 2014). When active, CRL4-DCAF1 targets LATS1/2 for ubiquitination in the nucleus which inhibits the Hippo pathway kinase cascade and downregulates the phosphorylation of YAP. This leads to nuclear retention of YAP and activation of Hippo-mediated gene transcription required for proliferation (Li *et al.*, 2014). CRL4-DCAF1 also poly-ubiquitinates the transcription factor Forkhead Box M1 (FOXM1) which leads to proteasomal-mediated degradation (Wang *et al.*, 2017). Interestingly, DCAF1 has an additional role in FOXM1 regulation and activates FOXM1 in an E3 ubiquitin ligase

independent manner highlighting the complexity of CRL4-DCAF1 signalling (Wang *et al.*, 2017). In addition, DCAF1 has an E3 ubiquitin ligase independent function as a kinase that phosphorylates histone 2A (H2A) in the nucleus (H2AT120p) (Kim *et al.*, 2013).

There is evidence from our group that KSR1, a scaffold protein of the RAF/MEK/ERK pathway may also interact with CRL4-DCAF1 (Zhou *et al.*, 2016a). Transfected KSR1 was immunoprecipitated from HEK293T cells and the complex was then analysed by mass spectrometry (Zhou *et al.*, 2016a). This analysis identified 225 binding partners, 30% of which were nuclear proteins including several components of the CRL4-DCAF1 ubiquitin ligase complex; Cullin 4B, DDB1 and DCAF1 (Zhou *et al.*, 2016a). Additional characterization of the DCAF1/KSR1 interaction and downstream signalling is necessary.

1.6.2 CRL4-DCAF1 in cancer

CRL4-DCAF1's most significant role in cancer is in Merlin-deficient tumourigenesis. Indeed, Li *et al.* demonstrated that DCAF1 is required for Merlin-deficient tumourigenesis and thus DCAF1 inhibition by Merlin is an essential tumour suppressor function (Li *et al.*, 2010). Increased CRL4-DCAF1 function in other cancers has also been reported. Expression of Long noncoding uc. 134 (long non-coding RNA) was reduced in hepatocellular carcinoma tissues compared with adjacent normal tissue and was shown to inhibit Cullin 4A (CUL4A)-mediated LATS1 ubiquitination suggesting that CRL4-DCAF1 is important in hepatocellular carcinoma development (Ni *et al.*, 2017). Furthermore, overexpression of p62 and DCAF1 in Non-small-cell lung carcinoma (NSCLC) patients was associated with poor prognosis (Wang *et al.*, 2013). CRL4-DCAF1 is also essential for cell cycle progression into S phase. However, it is still unclear

whether the role of DCAF1 in cell cycle progression is crucial for cancer growth (Hrecka *et al.*, 2007).

Interestingly, DCAF1's contribution to the growth of some cancers may be CRL4-DCAF1 independent. DCAF1 protein expression is upregulated in high-grade serous ovarian tumours, which correlates with an increase in FOXM1 activation (Wang *et al.*, 2017). In addition, in bladder, breast and prostate cancer tissues there was a correlation between DCAF1 expression and H2AT120p, a substrate downstream of DCAF1 kinase activity (Kim *et al.*, 2013). H2A phosphorylation inhibits gene transcription of tumour suppressor genes and DCAF1 depletion by Short hairpin RNA (shRNA) led to a decrease in H2AT120p as well as a decrease in proliferation and viability (Kim *et al.*, 2013). Importantly, overexpression of kinase-dead DCAF1 (K194R) did not restore proliferation of colony formation suggesting DCAF1 kinase activity has a pertinent oncogenic role in some tumour types (Kim *et al.*, 2013).

1.6.3 Targeting CRL4-DCAF1 and DCAF1 kinase activity

There are no specific CRL4-DCAF1 inhibitors. However, MLN4921 (and its successor MLN3651) are NAE inhibitors that bind to the NAE active site and prevent the neddylation and activation of Cullins (Brownell *et al.*, 2010). Interestingly, neddylation also has roles in the activation and/or the inactivation of proteins such as p53 and Mouse double minute 2 homolog (MDM2), independent of Cullins (Dohmesen, Koeppel & Dobbelstein, 2008; Xirodimas *et al.*, 2004). E3 ubiquitin ligase dependent ubiquitination of substrates is reduced following MLN4924 treatment (Zhou *et al.*, 2018). Accordingly, MLN4924 leads to the accumulation of Cullin substrates such as Chromatin Licensing And DNA Replication Factor 1 (CDT1), Hypoxia-inducible factor 1-alpha (HIF1α) and CYCLIN E (Soucy *et al.*, 2009). The accumulation of Cullin–RING ligase

(CRL) substrates following MLN4924 treatment in cancer cells leads to DNA re-replication (Soucy *et al.*, 2009), apoptosis (Lin *et al.*, 2010; Swords *et al.*, 2010), senescence (Jia, Li & Sun, 2011) and protective autophagy (Luo *et al.*, 2012). MLN4924 was also able to inhibit the growth of tumour xenografts derived from HCT-116 or H522 cells (Soucy *et al.*, 2009).

MLN4924 inhibited LATS1/2 ubiquitination suggesting that the drug effectively prevents CRL4-DCAF1 neddylation (Cooper *et al.*, 2017). Furthermore, MLN4924 treatment in the mouse schwannoma cell line, FC-1801 led to increased YAP phosphorylation at S127 (downstream of LATS1/2) and decreased neddylated Cullins (Cooper *et al.*, 2017). Importantly, MLN4924 suppressed growth of Merlin-deficient FC-1801 cells but not the Merlin expressing FH-912 Schwann cells at 0.28 μM showing that Merlin-deficient cells are particularly sensitive to neddylation inhibition which could be CRL4-DCAF1 dependent (Cooper *et al.*, 2017). Whilst YAP phosphorylation was increased, downstream YAP target genes were unchanged in both cell lines (FC-1801 and FH-912) therefore suggesting that MLN4924's growth suppressive effects are not dependent on Hippo pathway activation (Cooper *et al.*, 2017).

Cooper *et al.* noticed that MLN4924 did not inhibit the MTOR pathway or S6 phosphorylation and therefore suggested that combination of MLN4924 and GDC-0980, a dual mTOR/PI3K inhibitor, may be beneficial in inhibiting Merlin-deficient cell growth (Cooper *et al.*, 2017). Indeed, combination of MLN4924 and GDC-0980 completely suppressed tumour growth of the malignant mesothelioma cell line, VAMT-1 when injected into the flanks of mice (Cooper *et al.*, 2017). Treatment of primary schwannoma cells with both MLN4924 and GDC-0980 led to a significant decrease in proliferation compared with MLN4924 treatment alone (Cooper *et al.*, 2017). This

demonstrates that neddylation inhibition can be combined with inhibitors of other pertinent pathways in Merlin-deficient cells to enhance treatment efficacy.

Using *in vitro* kinase assays, DCAF1 and H2A were incubated with various compounds to identify a DCAF1 kinase inhibitor (Kim *et al.*, 2013). B32B3 was identified and shown to reduce H2AT120p after 24 hours with an IC50 of 0.5 μM in DU145 cells (Kim *et al.*, 2013). This reduction correlated with a reduction in the number of colonies after cells were plated on soft agar (Kim *et al.*, 2013). Mice were then inoculated with DU145 cells and treated with B32B3 for three weeks leading to reduced tumour growth and reduced H2AT120p in tumour xenografts demonstrating the potential of B32B3 as a therapeutic agent (Kim *et al.*, 2013).

1.7 KSR1

The KSR proteins are encoded by *Ksr1* and Kinase suppressor of RAS 2 (*Ksr2*) genes with significant homology and 43% sequence identity (Channavajhala *et al.*, 2003; Therrien *et al.*, 1995). KSR1 is highly expressed in the brain with expression also detected in bladder, ovary, testis and lung mouse tissue whereas KSR2 protein is only detected in the brain (Costanzo-Garvey *et al.*, 2009; Giblett *et al.*, 2002). A novel splice variant of KSR1, named Brain isoform-Kinase suppressor of RAS-1 (B-KSR1) has also been identified in mouse brain tissues (Müller *et al.*, 2000). Both KSR1 and KSR2 contain five conserved domains (CA1-CA5) and interact with the RAF/MEK/ERK pathway (Channavajhala *et al.*, 2003; Therrien *et al.*, 1995). KSR1 and KSR2 also have distinct roles. For example, KSR2 regulates proliferation through Adenosine monophosphate-activated protein kinase (AMPK) in a RAF/MEK/ERK-independent fashion (Fernandez, Henry & Lewis, 2012; Liu *et al.*, 2009). We chose to investigate KSR1 as its roles in cancer are better defined than KSR2. In addition, KSR1 deficiency

prevented v-Ha-RAS-mediated skin tumour formation in mice whereas the role of KSR2 in resistance to tumour formation has not yet been explored (Lozano *et al.*, 2003).

1.7.1 KSR1 roles and regulation

KSR1 is a cytoplasmic scaffold protein of the RAF/MEK/ERK pathway, which brings the three components together to allow sequential activation of the pathway following growth factor stimulation at the cell membrane (Matallanas *et al.*, 2011). Activated RAF induces a change in KSR1 that stimulates phosphorylation of the constitutively bound MEK1/2 to allow ERK1/2 activation (Brennan *et al.*, 2011). MEK1/2 and RAF bind to the CA5 putative kinase domain within the C terminus of the protein whilst ERK1/2 binds to the S/T-rich CA4 domain (Morrison, 2001). KSR1 is classified as a pseudokinase which lacks the lysine residue responsible for ATP orientation and hydrolysis within its CA5 kinase domain and is therefore thought not to have enzymatic activity (Clapéron & Therrien, 2007; Roy *et al.*, 2002). However, recent evidence suggests that some pseudokinases can adopt a conformation which is permissive of autophosphorylation and phosphorylation of specific substrates meaning that the possibility of KSR1 kinase activity cannot be excluded (Zhang *et al.*, 2012).

Increasing levels of KSR1 promote RAF/MEK/ERK signalling and proliferation (Kortum & Lewis, 2004; Zhou *et al.*, 2016a). However, at high concentrations KSR1 can inhibit signalling, a phenomenon common to many scaffold proteins (Kortum & Lewis, 2004). Therefore, KSR1 concentrations are tightly regulated within the cell by nuclear shuttling, phosphorylation and sub-cytoplasmic partitioning, which is regulated predominantly by the cysteine-rich CA3 domain, summarized in figure 1.3 (Brennan *et al.*, 2002; Müller *et al.*, 2001; Razidlo *et al.*, 2004). For example, KSR1 shuttles out of the nucleus in a manner dependent on both T274 and S392 phosphorylation (around

the CA3 domain) and association with MEK1/2 (CA5 domain) (Brennan *et al.*, 2002; Razidlo *et al.*, 2004). In addition, phosphorylation of S392 by CDC25C-associated kinase 1 (C-TAK1) regulates 14-3-3 protein binding to KSR1 leading to increased cytoplasmic accumulation (Müller *et al.*, 2001). Conversely, Protein phosphatase 2A (PP2A) dephosphorylates KSR1 at S392 leading to KSR1 and 14-3-3 dissociation and subsequent KSR1 plasma membrane recruitment to activate signalling (Ory *et al.*, 2003). KSR1's scaffolding function are also regulated by Casein kinase 2 (CK2) which modulates RAF/MEK/ERK activation. CK2 binds within the CA3 domain of KSR1 and facilitates Raf kinase activity (Ritt *et al.*, 2007). Accordingly, loss of CK2 inhibits RAF/MEK/ERK activation without affecting KSR1 localization or RAF/MEK/ERK binding to KSR1 (Ritt *et al.*, 2007).

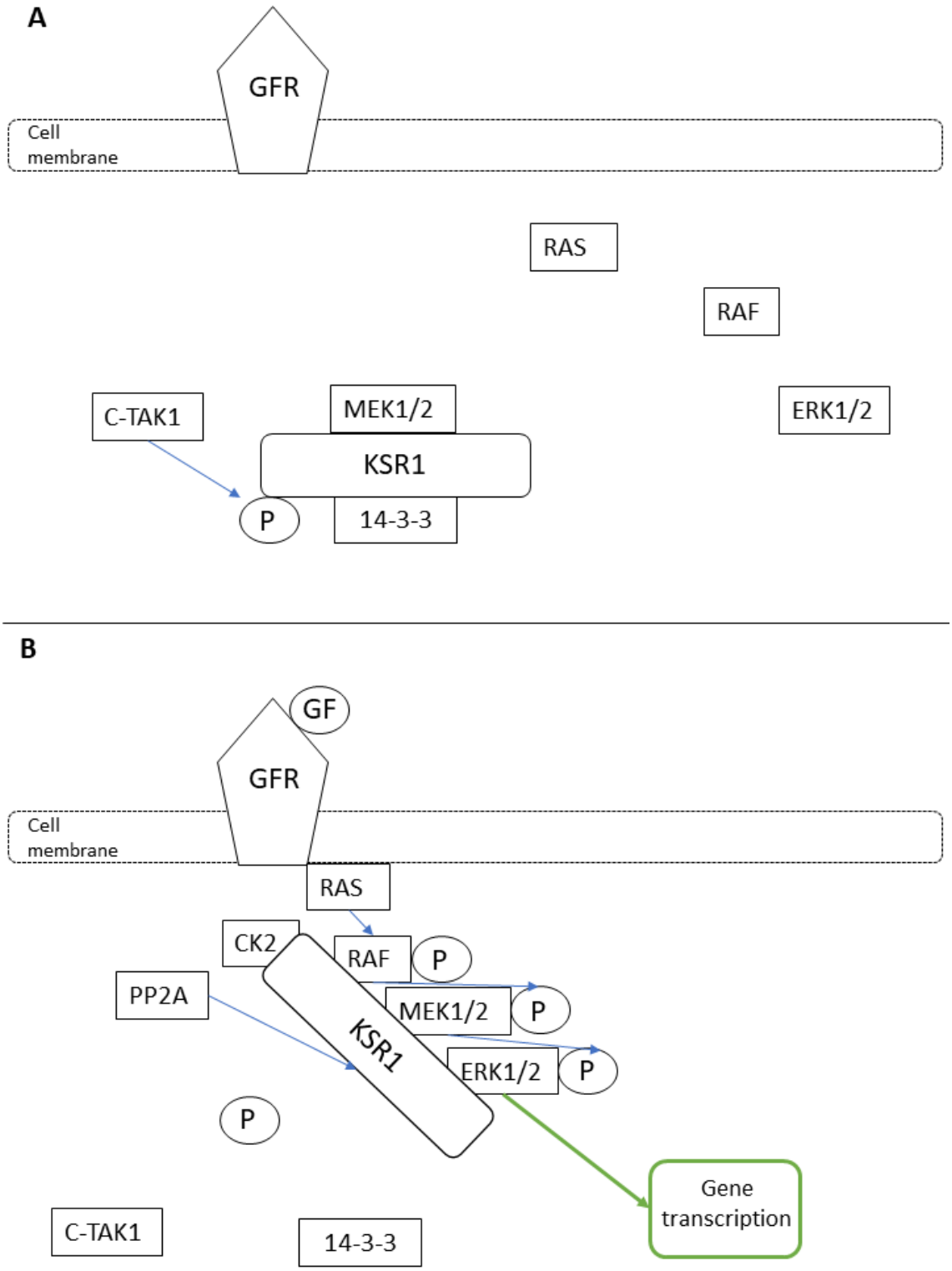

Figure 1.3 - KSR1 regulation. A. Inactive KSR1 signalling. In the absence of growth factors (GF) and growth factor receptor (GFR) activation, KSR1 is maintained in an inactive state by 14-3-3 which retains KSR1 in the cytoplasm and prevents RAF/MEK/ERK activation (Jagemann *et al.*, 2008). 14-3-3 binding to KSR1 is mediated by C-TAK1-dependent KSR1 phosphorylation (P) at S392 (Müller *et al.*, 2001). **B.** Active KSR1 signalling. When a growth factor binds and activates a growth factor receptor, RAS is phosphorylated which mediates RAF/MEK/ERK pathway activation. KSR1 is dephosphorylated by PP2A which leads to the release of 14-3-3 and allows translocation to the cell membrane (Ory *et al.*, 2003). RAF kinase activity is also regulated by CK2 binding to KSR1 (Ritt *et al.*, 2007). KSR1 is a scaffold protein that enhances RAF/MEK/ERK activation leading to ERK1/2 nuclear translocation to alter gene transcription.

The known roles of KSR1 are predominantly related to regulation of RAF/MEK/ERK activity. However, there is some evidence that suggests there may be RAF/MEK/ERK independent roles of KSR1. Zhang *et al.* identified that KSR1 suppresses Deleted in bladder cancer protein 1 (DBC1) phosphorylation whilst Stebbing *et al.* showed that KSR1 increased Breast cancer 1 (BRCA1)-associated RING domain protein 1 (BARD1) protein levels in breast cancer cells line which may be independent of MEK1/2 (Stebbing *et al.*, 2015; Zhang *et al.*, 2013). Furthermore, Zhou *et al.* described a MEK1/2 independent role of KSR1 in schwannoma adhesion (Zhou *et al.*, 2016a).

1.7.2 Roles in cancer

Despite multifaceted regulation, KSR1 is frequently overexpressed in several cancers including colorectal cancer (Fisher *et al.*, 2015), endometrial carcinoma (Llobet *et al.*, 2011), breast cancer (Stebbing *et al.*, 2015) and schwannoma (Zhou *et al.*, 2016a). Increased KSR1 expression in colorectal cancer is inversely correlated with expression of microRNA-497 (Wang *et al.*, 2016). Wang *et al.* discovered that overexpression of microRNA-497 led to a significant reduction of KSR1 expression and mutation of KSR1 at the proposed microRNA-497 binding site abrogated this change, suggesting that microRNA-497 directly regulates KSR1 expression (Wang *et al.*, 2016). In addition, overexpression of KSR1 led to increases in cell proliferation, migration and invasion in the colorectal cell line model (Wang *et al.*, 2016). Llobet *et al.* demonstrated that KSR1 was overexpressed in endometrial carcinoma compared with normal endometrium. Furthermore, KSR1 knockdown in two endometrial cancer cell lines reduced proliferation which correlated with decreased pERK1/2 and CYCLIN D1 (Llobet *et al.*, 2011). Interestingly, KSR1 was not required for tumourigenesis in a K-RAS driven pancreatic cancer mouse model with heterozygous loss of p53 (Germino *et al.*, 2018).

Finally, Yu *et al.* showed that mRNA and protein expression of Tissue factor protein is partly dependent on KSR1 (Yu *et al.*, 2010). Tissue factor is a key component of the coagulation process and is also upregulated and involved in cancer metastasis suggesting a role for KSR1 in invasion (Ruf *et al.*, 2011). KSR1 is also significantly upregulated in primary schwannoma cells at both the mRNA and protein level (Zhou *et al.*, 2016a). Two KSR1 short hairpin RNA (shRNA) constructs significantly reduced proliferation, increased apoptosis, reduced focal adhesions, and altered cells from a multipolar to a bipolar shape demonstrating that KSR1 contributes to schwannoma pathology (Zhou *et al.*, 2016a).

Conversely, KSR1 was shown to act as a tumour suppressor in breast cancer (Stebbing *et al.*, 2015). Stebbing *et al.* discovered a significant association between KSR1 expression and disease-free survival (Stebbing *et al.*, 2015). In addition, overexpression of KSR1 in breast cancer cell lines led to inhibition of tumour growth demonstrating that KSR1 protein function is dependent on cell type (Stebbing *et al.*, 2015).

The RAF/MEK/ERK pathway, which is often dependent on active KSR1 signalling, is commonly upregulated in cancer cells due to hyper-activation of receptor tyrosine kinases as well as mutated forms of RAS or RAF in some tumours leading to increased proliferation and decreased apoptosis (Niault & Baccarini, 2010; Tsuda, Kanje & Dahlin, 2011). RAF/MEK/ERK signalling is also upregulated in Merlin-deficient tumours and drives cell proliferation as a result of PDGFR-β overexpression (Ammoun *et al.*, 2008). This upregulation is also illustrated clearly by immunohistochemical staining of traumatic neuroma and human schwannoma tissue showing a large increase in both phosphorylated MEK1/2 and phosphorylated ERK1/2 expression, particularly within the nucleus (Hilton, Ristic & Hanemann, 2009).

1.7.3 Targeting KSR1

Terbinafine is a potent inhibitor of squalene epoxidase, a component of the cholesterol biosynthetic pathway essential for the growth of pathogenic fungi (Nowosielski *et al.*, 2011). At higher concentrations Terbinafine also inhibits mammalian squalene epoxidase (Ryder & Dupont, 1985), as reviewed by Jain and Sehgal (Jain & Sehgal, 2000). Terbinafine also has anti-proliferative effects in many cancers (Brown *et al.*, 2016; Lee *et al.*, 2003; Li *et al.*, 2013; Yang *et al.*, 2006). It has been suggested by Li *et al.* that Terbinafine anti-tumour effects are dependent on KSR1 inhibition (Li *et al.*, 2013). Indeed, Terbinafine treatment in the oral squamous cell carcinoma cell line, KB, led to reduced KSR1 protein expression as well as significant decreases in pRaf, pMEK1/2 and pERK1/2 (Li *et al.*, 2013). Unfortunately, a concentration of 291 µM (85 µg/µl) was required to reduce the proliferative rate of KB cells by half demonstrating that terbinafine is not particularly potent (Li *et al.*, 2013). In contrast, Terbinafine anti-cancer activity in breast cancer cell lines was attributed to its mammalian squalene epoxidase activity known to be amplified in breast cancer (Brown *et al.*, 2016). Terbinafine has modest anti-cancer activity and the mechanism of action is yet to be conclusively determined. Therefore, terbinafine was not used in this study.

A phosphorothioate antisense oligonucleotide was designed to target KSR1 nucleotides 214–231, which resulted in a 90% reduction of KSR1 expression in epidermoid carcinoma (A431) and pancreatic carcinoma (PANC-1) cell lines (Xing *et al.*, 2003). Continuous infusion of KSR1-specific antisense oligonucleotide 2 days before A431 or PANC1 implantation reduced tumour growth in a tumour model compared with no infusion (Xing *et al.*, 2003). However, phosphorothioate oligonucleotides may interact with growth factor receptors such as EGFR and a non-specific

phosphorothioate oligonucleotide suppressed glioblastoma growth in a mouse model demonstrating potential non-target anti-tumourigenic effects (Rockwell *et al.*, 1997).

The KSR inhibitor, APS_2_79, was shown to block the dimerization of RAF with MEK1/2 by maintaining KSR2 in an inactive state, whereby preventing MEK1/2 phosphorylation (Dhawan, Scopton & Dar, 2016). Importantly, KSR1-dependent phosphorylation of MEK1/2 and ERK1/2 was reduced with the addition of APS_2_79 for two hours in HEK293H cells overexpressing both KSR1 and MEK1/2 (Dhawan, Scopton & Dar, 2016). This suggests that APS_2_79 inhibits both KSR1 and KSR2 signalling. APS_2_79 activity was dependent on disruption of ATP binding as treatment of 293H HEK cells overexpressing the active site mutant, KSR1(A690F) had less of an effect on MEK1/2 and ERK1/2 phosphorylation than wild-type KSR1 (Dhawan, Scopton & Dar, 2016). Unfortunately, this drug has limited efficacy alone in RAS-mutant cell lines (HCT-116 and A549) and B-RAF-mutant cell lines (SK-MEL-239 and A375) (Dhawan, Scopton & Dar, 2016). However, APS_2_79 has synergistic activity with the MEK1/2 inhibitor, trametinib, specifically in K-RAS-mutant cell lines (Dhawan, Scopton & Dar, 2016). Dhawan *et al.* proposed that APS_2_79 potentiates the negative feedback loop induced by MEK1/2 inhibition in RAS mutant cancers (Dhawan, Scopton & Dar, 2016). The efficacy of APS_2_79 alone or in combination with a MEK1/2 inhibitor in other indications is not yet known (Dhawan, Scopton & Dar, 2016).

1.8 Aims

There is evidence that KSR1 is upregulated in schwannoma but DCAF1 expression has not been explored. In addition, DCAF1 and KSR1 expression in Merlin-deficient meningioma have not been reported. The first aim of this project was to analyse DCAF1 and KSR1 expression in schwannoma and meningioma. We also aimed to

determine the role of DCAF1 in Merlin-deficient cells. We hypothesised that DCAF1 regulates KSR1 expression, localization or activity and thus contributes to Merlin-deficient tumourigenesis.

CRL4-DCAF1 and KSR1 interact and therefore our second aim was to characterise the DCAF1 and KSR1 interaction. Whilst DCAF1 and overexpressed KSR1 have been shown to interact in schwannoma, we wanted to show that the endogenous proteins interact. In addition, we used overexpressed proteins to determine the domains involved in the DCAF1/KSR1 interaction and the cellular location of the interaction, which may inform the relevance of the interaction. Finally, we assessed if DCAF1 knockdown changed the binding of KSR1 and RAF/MEK/ERK proteins to regulate the pathway.

Our third and final aim was to assess the therapeutic potential of DCAF1 and KSR1 inhibitors, particularly in combination. Combined shRNA knockdown of both KSR1 and DCAF1 had an additive effect on reducing proliferation of schwannoma cells implying that combination of DCAF1 and KSR1 inhibitors may be beneficial (Zhou *et al.*, 2016a). We tested the potential of the neddylation inhibitor, MLN3651, the DCAF1 kinase inhibitor, B32B3, the KSR1 inhibitor, APS_2_79, as well as the RAF/MEK/ERK inhibitor, AZD6244, using *in vitro* models of schwannoma and meningioma.

Chapter 2 - Materials and Methods

2.1 Buffers and reagents

Transport medium (TM) - Dulbecco's modified eagle medium (DMEM) (Gibco), 10% (v/v) foetal bovine serum (FBS) (Sigma), 500 U/ml penicillin/streptomycin (Gibco), 2.5 µg/ml amphotericin B (Sigma)

Schwannoma digestion medium - DMEM, 10% FBS, 500 U/ml penicillin/streptomycin, 1.25 U/ml dispase grade I (Sigma), 160 U/ml collagenase type 1A (Sigma)

Meningioma digestion medium - DMEM, 10% FBS, 100 U/ml penicillin/streptomycin, 20 U/ml collagenase type III (Sigma)

Nerve digestion medium - DMEM, 10% FBS, 500 U/ml penicillin/streptomycin, 0.8 U/ml dispase grade I, collagenase type 1A 160 U/ml

Freezing medium - 45% FBS, 45% cell culture medium and 10% Dimethyl sulphoxide (DMSO) (Sigma)

Low salt lysis buffer - 30 mM Trizma-base (Sigma) pH 8, 75 mM sodium chloride (Sigma), 10% v/v glycerol (for molecular biology) (Sigma), 1% v/v Triton X-100 (Sigma)

4X sample reducing buffer - 1M Trizma-base pH 6.8, 200 mM Dithiothreitol (DTT) (Sigma), 8% Sodium dodecyl sulphate (SDS) (Fisher), 40% glycerol, 0.04% bromophenol blue

Immunohistochemistry citrate buffer - 10 mM citric acid (Sigma), pH 6

Immunohistochemistry Tris-Ethylenediaminetetraacetic acid (EDTA) buffer - 20 mM Trizma-base, 1 mM EDTA, pH 9

Immunohistochemistry Tris-buffered saline-Tween 20 (TBST) buffer - 50 mM Trizma-base, 140 mM sodium chloride, pH 7.6 with 0.045% v/v Tween 20 (Sigma

Copper sulphate 3’3 diaminobenzidine (DAB) enhancer - 50 mM copper sulphate (Sigma), 250 mM sodium chloride

Lentiviral reagent mix - 3 µg of packaging plasmid (pCMV-dR8.91), 0.3 µg of envelope plasmid (VSV-G) and 3 µg of the hairpin-pLKO.1 vector dilute in Opti-mem® previously incubated with 18 µl of FuGENE® 6 transfection reagent (in Opti-mem® medium)

Restriction enzyme plasmid digestion reaction - 0.5 µg Plasmid DNA, 0.2 µl acetylated Bovine serum albumin (BSA), 2 µl buffer, 0.5 µl restriction enzyme (NEB) and water to a total of 20 µl

Radioimmunoprecipitation assay (RIPA) buffer - 50 mM Trizma-base pH 8, 150 mM sodium chloride, 1 mM EDTA pH 7.4, 1% nonidet p40 (NP-40), 0.5% sodium deoxycholate (Sigma), 0.1% SDS

Western blot running buffer - 25 mM Trizma-base, 20 mM glycine, 3.5 mM SDS

Western blot transfer buffer - 25 mM Trizma-base, 20 mM glycine and 15% v/v methanol

Western blot TBST - 20 mM Trizma-base, 150 mM sodium chloride, 0.1% v/v Tween 20

Western blot blocking buffer- 5% w/v milk (Sigma), 2% w/v BSA in TBST

Western blot wash buffer - 100 mM glycine pH 2.4, 2 mM ethylene glycol-bis(β-aminoethyl ether)-N,N,N',N'-tetraacetic acid (EGTA) (Sigma) in deionised water

Western blot stripping buffer - 1M Trizma-base pH 6.8, 10% w/v SDS, 0.7% v/v β-metacarpoethanol (Sigma) in deionised water

2.2 Cell culture

2.2.1 Sample collection

All primary schwannoma, meningioma and normal tissues used throughout this project were obtained from consented individuals following the ethical guideline included in the 'Investigation into the expression of signalling molecules in human brain tumour samples (Research Ethics Committee (REC) number 6/Q2103/123)' and the 'Identifying and validating molecular targets in low grade brain tumours (REC number 14/SW/0119) study'.

Peripheral nerves for Schwann cell culture were retrieved from donors post mortem after consent. The NHS Blood and Transplant (NHSBT) research study is entitled 'Collection of peripheral nerves for control cells for brain tumour treatment research', NHSBT study reference: 61. Full research project title was 'Identifying and validating molecular targets in low grade brain tumours; REC number: 14/SW/0119'.

2.2.2 Tumour digestion

Tumour specimens were collected and transported in Falcon tubes containing a transport medium (TM), in order to maintain live cells. In our laboratory, TM was removed and the tumour specimen washed with Dulbecco's phosphate buffered saline (DPBS) (Gibco) and then transferred into a 10 cm petri dish with 20 ml of fresh TM. When possible tumours were processed obtaining primary cells, DNA, RNA, protein lysates and optimal cutting temperature (OCT) inclusions for immunofluorescence.

Primary cells were obtained by incubating the tumour specimen in a digestion medium following two different protocols: one for schwannoma and another for meningioma. Schwannoma digestion medium or meningioma digestion medium were freshly made

and filtered with a 0.22 µM millex GP filter unit Millipore express Polyethersulfone (PES) membrane (Millipore) before applying the digestion procedure.

In addition, tumour specimens were minced in smaller pieces using a sterile scalpel and tissues mechanically disrupted after 24 hours of incubation by pipetting using glass pipettes of decreasing diameter size. The digested sample was collected and centrifuged for seven minutes at 400 x g, the supernatant was removed and the pellet containing the cells was re-suspended in schwannoma or meningioma culture medium, according to the tissue type. After digestion, cells obtained from schwannoma tissues were plated on coated plates and incubated at 37 ˚C/10% CO_2 whilst cells obtained from meningioma cells were plated on uncoated plates and incubated at 37 ˚C/5% CO_2. All schwannoma plates were coated with 0.1 mg/ml poly-L-lysine (PLL) (Sigma) for 30 minutes at room temperature and 4 µg/ml laminin (Fisher) overnight at 4 ˚C. Tumour digestion was performed by the author and members of the research group but primarily by Dr Emanuela Ercolano.

Phosphorylated Merlin and Merlin expression were checked by Western blot and only samples with no expression were used in subsequent experiments (figure 2.1).

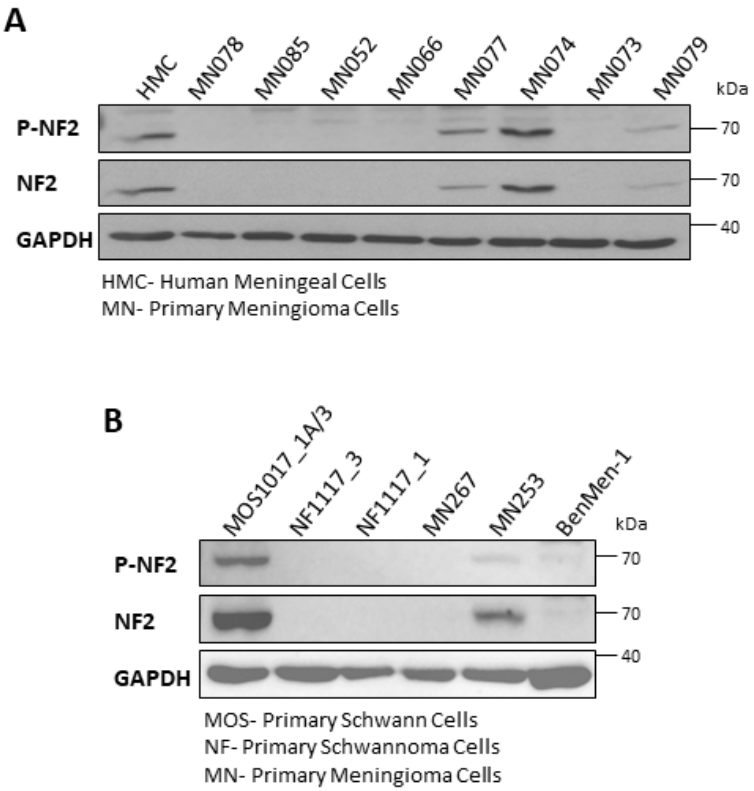

Figure 2.1 - Determining schwannoma and meningioma Merlin status. A: Representative Western blot showing pNF2 and Merlin (NF2) expression in human meningeal cells (HMC) and primary meningioma cells (MN), GAPDH- loading control. HMC were used as a positive control for the expression of pNF2 and NF2. Meningioma samples with no Merlin expression were used for experiments and assumed to have a *Nf2* mutation in at least one allele. **B:** Representative Western blot showing pNF2 and Merlin (NF2) in primary Schwann cells (MOS), primary schwannoma cells (NF), meningioma cells (MN) and Benign Meningioma 1 (BenMen-1) cells. MOS were used as a positive control for pNF2 and NF2 whilst BenMen-1 was used as a negative control. Schwannoma samples with no Merlin expression were used for experiments.

2.2.3 Normal nerve digestion

Normal nerves were dissected at Derriford hospital and transported using TM as described above. TM was removed and the nerve was washed with DPBS before adding incubation media and transferring the sample to a 10 cm plate. Fascicles were pulled out of the nerve using sterile forceps under a microscope in a horizontal flow hood. The fascicles were incubated at 37 ˚C/10% CO_2 for 7-14 days. Nerve digestion was performed by adding nerve digestion medium and incubating overnight. The nerve was then cut into small pieces and mechanically digested using glass pipettes of decreasing diameter size. The digested sample was centrifuged at 400 x g for seven minutes and the pellet containing cells was resuspended before plating on a coated six well plate. Digestion of normal nerve was performed by Dr Emanuela Ercolano.

2.2.4 Cell splitting and storage

Cell medium was replaced every 3 days and cells were split when they reached confluency. Passaging the cells was performed by washing with DPBS and adding 0.05% trypsin-ethylenediaminetetraacetic acid (EDTA) (Gibco). The cells were incubated for up to five minutes at 37 ˚C before neutralizing trypsin with cell culture medium. Cells were then collected, centrifuged and re-suspended accordingly into fresh vessels.

Primary cell and cell line storage was performed by re-suspending cell pellets in a freezing medium using cryogenic tubes. Freezing procedure was performed by maintaining cells in a freezing container overnight at -80 ˚C and transferring to liquid nitrogen the following day for long-term use.

2.2.5 Cells and medium

Cells	Type	Obtained from	Medium	Supplements
Primary human Schwann cells (mos)	Adherent primary human Schwann cells	Post mortem nerve tissue	DMEM (low glucose) (gibco)	10% FBS (Sigma), 100 U/ml penicillin/streptomycin (Gibco), 0.5 µM forskolin (Tocris), 2.5 µg/ml amphotericin, 2.5 µg/ml insulin (Thermo Fisher Scientific), 10 nM β1-heregulin (Bio-teche), 0.5 mM 3-isobutyl-1-methylxanthine (IBMX) (Sigma)
Primary human schwannoma (NF)	Adherent primary human cell	Tumour tissue	DMEM (gibco)	10% FBS, 100 U/ml penicillin/streptomycin, 0.5 µM forskolin, 2.5 µg/ml amphotericin, 2.5 µg/ml insulin, 10 nM β1-heregulin, 0.5 mM IBMX
Primary WHO I meningioma (MN)	Adherent primary human cell	Tumour tissue	DMEM (gibco)	10% FBS, 100 U/ml penicillin/streptomycin, 2 mM L-glutamine (Gibco) and 1% v/v D(+) glucose solution (Sigma).
Primary WHO II meningioma (MN)	Adherent primary human cell	Tumour tissue	DMEM/F-12 (1:1) + glutamax (gibco)	20% FBS, 1% v/v D(+) glucose solution and 100U/ml penicillin/streptomycin
BenMen-1	Benign WHO I immortalised meningioma cell line	Puttman *et al.,* 2005	DMEM (gibco)	10% FBS, 100 U/ml penicillin/streptomycin, 2 mM L-glutamine and 1% v/v D(+) glucose solution.
KT21-MG1-Luc5D	WHO III immortalised cell line	Chow *et al.,* 2015	DMEM (gibco)	10% FBS, 100 U/ml penicillin/streptomycin, 2 mM L-glutamine and 1% v/v D(+) glucose solution.
HMC	Human meningeal cells	Sciencell	Meningeal cell medium (Sciencell)	2% FBS, 1% meningeal cell growth supplement , 1% penicillin/streptomycin solution (all Sciencell).
HEK293T and HEK293FT	Human embryonic kidney cells	ATCC	DMEM (gibco)	10% FBS and 1% penicillin/streptomycin.

Table 2.1 Cells and medium used.

2.3 Co-immunoprecipitation

2.3.1 Endogenous DCAF1 IP

Confluent 10 cm plates of Benign meningioma cell line 1 (BenMen-1) cells were lysed and scraped in 250 µl low salt lysis buffer with Halt protease and phosphatase inhibitors (Thermo Fisher Scientific) (1:1000). Alternatively, schwannoma or meningioma tissue was homogenised in 1 ml low salt lysis buffer. BenMen-1 lysates were concentrated using Amicon Ultra-15 Centrifugal Filter Unit with Ultracel-10 membrane (Millipore) to maximise amount of protein used for immunoprecipitation. At least 3 mg of protein were used for BenMen-1 experiments.

50µl of protein G sepharose 4 fast flow (GE healthcare) was added to fresh Eppendorf tubes using a 200µl pipette tip with the end cut off to prevent damage to the beads. The beads were washed three times with low salt lysis buffer followed by a 1 minute centrifuge at 7000 x g at 4 ˚C. Ready-to-use beads were added to 3 mg of protein and rotated for 1 hour at room temperature to remove any proteins that bind to the beads (pre-clearing). The pre-cleared protein lysate was then collected after centrifuging the beads and DCAF1 antibody (Santa Cruz Biotechnology) or normal mouse IgG (Santa Cruz Biotechnology) was added at a concentration of 4 µg for each milligram of protein. The pre-cleared protein and antibody complex were further rotated overnight at 4 ˚C.

The beads used to pre-clear the protein were washed a further three times with low salt lysis buffer and 40 µl 2X sample reducing buffer was added. 2X sample reducing buffer was made by diluting 4X sample reducing buffer with low salt lysis buffer. The beads were heated at 95 ˚C and stored at -80 ˚C.

Fresh beads were washed three times with low salt lysis buffer and added to the pre-cleared protein and antibody complex for one hour rotated at room temperature. Following the incubation, the beads were washed three times using a low salt lysis buffer and 40 µl 2X sample reducing buffer. The beads were heated at 95 ˚C for five minutes and stored at -80 ˚C.

2.3.2 FLAG IP

A 10 cm plate of HEK293T cells transfected with FLAG-tagged proteins were lysed in 1 ml of low salt lysis buffer. 40 µl of anti-FLAG M2 affinity gel (Sigma) for each experimental condition was washed with low salt lysis buffer followed by centrifugation at 7000 x g for 1 minute at 4 ˚C. Low salt lysis buffer was removed and 0.1 M glycine (Santa Cruz Biotechnology) pH 3.5 was added to remove any unbound anti-FLAG antibody from the resin suspension. This was followed by three further washes with low salt lysis buffer and the addition of at least 1 mg of protein lysate (except the cytoplasmic and nuclear fractionation FLAG immunoprecipitation in which at least 100 µg of protein was added).

The volume of each experimental condition was equalised using low salt lysis buffer and resin was rotated overnight at 4 ˚C. The protein-resin complex was then washed three times with low salt lysis buffer and 40 µl 2X sample reducing buffer was added. The resin was heated at 95 ˚C for five minutes and stored at -80 ˚C.

2.3.3 Myc IP

A 10 cm plate of HEK293T cells transfected with myc-tagged proteins was lysed in 1ml low salt lysis buffer. Two protocols were used for myc IP.

Protocol one (#) - 50 µl protein G sepharose 4 fast flow was washed three times with low salt lysis buffer at 4 ˚C and then 1 mg of protein was added and rotated for one hour at room temperature. The pre-cleared protein was removed from the beads and placed in a fresh Eppendorf. 1 µl of Myc-tag antibody (Cell Signalling Technology) was then added to the pre-cleared protein and rotated overnight at 4 ˚C. The next day 50 µl protein G sepharose 4 fast flow were washed three time with low salt lysis buffer and added to the protein-antibody complex for 1 hour rotating at room temperature. The complex was then washed three times with low salt lysis buffer and 40 µl 2X sample reducing buffer was added. The beads were heated for five minutes at 95 ˚C and stored at -80 ˚C until needed.

Protocol two (*) – 50 µl protein G sepharose 4 fast flow was washed three times with low salt lysis buffer at 4 ˚C and then 1 mg of protein and 1 µl of Myc-tag antibody (Cell Signalling Technology) was added. The beads were rotated overnight at 4 ˚C and then the protein-bead complex was washed three times with low salt lysis buffer. 40 µl 2X sample reducing buffer was added and the beads were heated for five minutes at 95 ˚C and stored at -80 ˚C until needed.

Antibody	Type	Clone	Company	Catalog	Dilution
DCAF1	Mouse monoclonal	C-8	Santa Cruz Biotechnology	Sc-376850	4 µg/mg
Normal mouse IgG			Santa Cruz Biotechnology	Sc-2025	4 µg/mg
Myc tag	Mouse monoclonal	9B11	CST	2276	1 µl/ml

Table 2.2 - Antibodies used for co-immunoprecipitation experiments.

2.4 Cytoplasmic and nuclear fractionation

Cells were fractionated using the nuclear and cytoplasmic extraction reagents (NE-PER) kit (Thermo Fisher Scientific) using the recommended protocol. Briefly, cells were collected using trypsin and re-suspended in ice-cold DPBS. Cells were then centrifuged at 500 x g for 2 minutes at 4 ˚C to remove DPBS and re-suspended in the recommended amount of ice-cold Cytoplasmic Extraction Reagent I (CER I) (with protease and phosphatase inhibitors). The cell pellet was vortexed for 15 seconds and incubated on ice for 10 minutes followed by the addition of Cytoplasmic Extraction Reagent I (CER II) to rupture the cell membrane. The supernatant containing cytoplasmic extract was collected and ice-cold Nuclear extraction reagent (NER) (with protease and phosphatase inhibitors) was added to the nuclear pellet. The nuclear pellet was vortexed repeatedly and centrifuged to release the nuclear extract which was collected and stored at -80 ˚C. Protein estimation was calculated for both the cytoplasmic and nuclear fraction and all experiments using these lysates were based on equal protein.

2.5 Drug treatments

2.5.1 Drugs used

MLN3651, a neddylation inhibitor, was provided by Takeda pharmaceuticals at a concentration of 10 mM. MLN3651 was diluted in DMSO to make stocks of 0.1 mM, 0.3 mM, 0.6 mM, 1 mM, 3 mM, 6 mM and 10 mM. These drug stocks were further diluted in phenol-free cell culture medium (DMEM; Gibco, 11880-028) at 1:1000 for drug treatments.

B32B3, a DCAF1 kinase inhibitor, was purchased from Sigma and re-suspended in DMSO to make stocks of 20 mM and 60 mM. Final dilutions were made in phenol-free cell culture medium at a concentration of 1:1000 from the DMSO stocks.

Selumetinib (AZD6244), a MEK1/2 inhibitor, was purchased from Selleckchem and re-suspended in DMSO to make stock of 50 mM and 100 mM. Final dilutions were made in phenol-free cell culture medium to achieve a final concentration of 0.1% DMSO.

2.5.2 ATP viability assay

Cells were plated in clear bottom, opaque walled 96 well plates (4000 cells per well for primary cells and 3000 cells per well for cell lines). After 24 hours, the medium was removed and replaced with varying concentrations of B32B3 or MLN3651 diluted in phenol-free cell culture medium. After the drug treatment (see figures for drug treatment times), the plate was placed at room temperature for 30 minutes following the Celltiter-Glo® luminescent cell viability assay (Promega) instructions. The reagents were equilibrated to room temperature and 100 µl of reconstituted reagent was added to each well using fresh filter tips to avoid ATP contamination. The plate was placed on an orbital shake for two minutes and incubated at room temperature for 10 minutes before reading the luminescent signal with the BMG Labtech Fluostar Omega plate reader. A Repeated Measures Analysis of Variance (ANOVA) with Tukey's Multiple Comparison Post Test was used to test statistical significance between drug-treated cells and DMSO control ($p < 0.05$). IC50 was determined using Graphpad Prism 5 with automatic outlier elimination. Cell viability experiments for MLN3651-treated cells were performed by Dr Emaneula Ercolano and the author as part of a Takeda-funded study.

2.5.3 Caspase 3/7 assay

As above, except 100 µl of reconstituted Caspase-Glo 3/7 assay (Promega) reagents are added to the cells. The plate was then placed on an orbital shaker for 30 seconds and incubated at room temperature for 1 hour before reading the luminescent signal with the BMG Labtech Fluostar Omega plate reader. A Repeated Measures ANOVA with Tukey's Multiple Comparison Post Test was used to test statistical significance between drug-treated cells and DMSO control ($p < 0.05$). Caspase 3/7 experiments for MLN3651-treated cells were performed by Dr Emaneula Ercolano and the author as part of a Takeda-funded study.

2.6 Immunocytochemistry

2.6.1 Ki-67

Immunocytochemistry on cells were performed using 8-well chamber slides (Nunc™ Lab-Tek™ Chamber Slide System, Thermo Fisher Scientific) Briefly, 10000 cells were plated in each well of the labtek and left to grow overnight before adding drug treatments. After the drug treatment, the medium was removed, cells washed with phosphate buffered saline (PBS) (Thermo Fisher Scientific) and fixed with 4% paraformaldehyde (PFA) diluted from 16% PFA weight/volume (w/v) (Thermo Fisher Scientific)/PBS. Cells were permeabilised and fixed with ice-cold methanol at -20˚C for 10 minutes; blocking was performed with 10% v/v goat serum (Abcam) in 1% w/v bovine serum albumin (BSA) (Thermo Fisher Scientific)/PBS for 1 hour. Cells were incubated overnight with Ki-67 (1:200) (DAKO) in 1% BSA/PBS and Goat anti-Mouse IgG (H+L) Cross-Adsorbed Secondary Antibody, Alexa Fluor 594 (Thermo Fisher Scientific) (1:500) in 1% BSA/PBS for 1 hour at room temperature. Finally, 4',6-diamidino-2-phenylindole (DAPI) nuclear stain was added 1:500 in DPBS for 15 minutes

and the chamber of the labtek was removed. A cover slip was added with vectashield mounting medium for fluorescence (Vector Laboratories) and sealed with nail polish before imaging with an inverted Leica DMi8 microscope.

Ki-67 staining was quantified by taking in account at least three 20x images of each condition and manually counting the number of Ki-67 positive cells versus the total number of cells (positive for DAPI staining) using ImageJ software. Statistical analysis was performed, on raw data, using a Repeated Measures ANOVA (with Tukey's Multiple Comparison Test) or Student's Paired T-test, $p< 0.05$.

2.6.2 FLAG

Immunocytochemistry on cells was performed using 8-well chamber slides (Nunc™ Lab-Tek™ Chamber Slide System, Thermo Fisher Scientific). 10000 cells were plated in each well of the labtek and left to grow overnight before adding KSR1 constructs. 48 hours after transfection, the medium was removed, cells washed with phosphate buffered saline (PBS) (Thermo Fisher Scientific) and fixed with 4% PFA diluted from 16% PFA weight/volume (w/v) (Thermo Fisher Scientific)/PBS. Cells were permeabilised with 0.2 Triton X-100 for 5 minutes; blocking was performed with 10% v/v goat serum (Abcam) in 1% w/v bovine serum albumin (BSA) (Thermo Fisher Scientific)/PBS for 1 hour. Cells were incubated overnight with FLAG (1:500) (Sigma) in 1% BSA/PBS and Goat anti-Mouse IgG (H+L) Cross-Adsorbed Secondary Antibody, Alexa Fluor 488 (Thermo Fisher Scientific) (1:500) in 1% BSA/PBS for 1 hour at room temperature. Finally, DAPI nuclear stain was added 1:500 in DPBS for 15 minutes and the chamber of the labtek was removed. A cover slip was added with vectashield mounting medium for fluorescence (Vector Laboratories) and sealed with nail polish before imaging with an inverted Leica DMi8 microscope.

2.6.3 S100

Schwann cell culture quality was assessed by S100 immunocytochemistry, as described above but with S100 (Dako, Z0311, rabbit polyclonal) antibody diluted (1:100) in 1% BSA in DPBS. Only Schwann cell cultures with more than 90% S100 positive cells were used in experiments (figure 2.2).

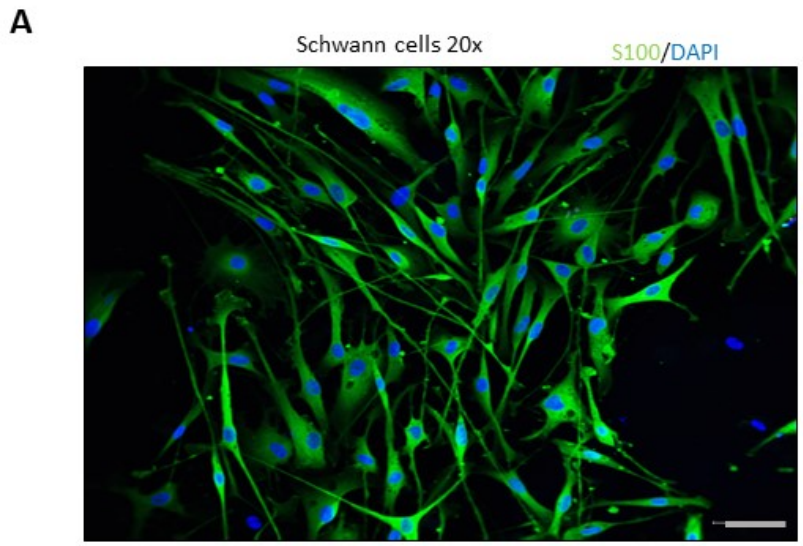

Figure 2.2 - Proportion of S100-positive cells in Schwann cell cultures. A: Representative Schwann cell culture stained with a S100 antibody and counter-stained with the nuclear marker, DAPI. The image shows cells at 20x magnification and demonstrates that the majority of the culture is S100-positive and therefore Schwann cells. Schwann cell cultures with more than 90% S100-positive cells were used in experiments.

2.7 Immunohistochemistry

Formalin fixed paraffin embedded sections (4 µM) were provided by Derriford hospital, Plymouth, UK (Dr D. Hilton, Cellular and Anatomical Pathology). Briefly, slides were baked at 60˚C for one hour and rehydrated using xylene followed by two ethanol washes. The slides were washed in running tap water for five minutes and then blocked in 3% H_2O_2/methanol for 30 minutes at room temperature. Slides were equilibrated with citrate (10 mM citric acid (Sigma), pH 6) or Tris-EDTA (20 mM Trizma-base, 1 mM EDTA, pH 9) buffer dependent on the antibody being used. Slides for KSR1 (H70) (Santa Cruz Biotechnology) were equilibrated in citrate buffer whilst slides for CUL4A (Proteintech) and VPRBP (DCAF1) (Proteintech) staining were equilibrated in Tris-EDTA buffer. Slides were then heated for 30 minutes in the microwave (700 W).

The slides were washed in immunohistochemistry TBST buffer (50 mM Trizma-base, 140 mM sodium chloride, pH 7.6 with 0.045% v/v Tween 20 (Sigma)) and blocking solution from the Vectastain universal elite ABC kit (Vector Laboratories) was made and added for 30 minutes. Primary antibody (CUL4A 1:100, VPRBP (DCAF1) 1:1000, KSR1 (H-70) 1:500) was diluted in TBST and added to the slides overnight at 4 ˚C.

A universal biotinylated secondary antibody (which contains a mixture of rabbit and mouse antibodies) and a streptavidin/biotin complex (provided with the Vectastain universal elite ABC kit) was then applied to the slides for 30 minutes each, at room temperature. Sigmafast 3’3 diaminobenzidine (DAB) tablets (Sigma) were used to make a DAB solution which is added to the slides for five minutes followed by copper sulphate DAB enhancer (50 mM copper sulphate (Sigma), 250 mM sodium chloride) for 2–5 minutes. The slides are then washed with tap water and counterstained with Mayers haemotoxylin (Sigma) for two minutes. Finally, slides were dehydrated in

ethanol and then xylene and mounted onto cover slips using Distyrene, plasticizer, and xylene (DPX) mountant for histology (Fluka).

Slides were kindly imaged and quantified by Dr David Hilton. DCAF1 antibody staining for schwannoma was conducted at the Cellular and Anatomical Pathology (Dr D. Hilton, Derriford hospital, Plymouth, UK) whereas all other staining was performed by the author. A score of 1-4 was given to each sample corresponding to 0–25%, 25–50%, 50–75%, 75-100%, respectively. Percentage refers to the proportion of cells that are positive for the protein of interest. A Mann-Whitney test, Wilcoxon signed rank test or Kruskal-Wallis test with Dunn Multiple Comparison's Post Tests was used to assess statistical significance, $p< 0.05$.

Antibody	Type	Clone	Company	Catalog	Dilution
CUL4A	Rabbit polyclonal		Abcam	Ab72548	1:1000
CUL4A	Rabbit polyclonal		Proteintech	10693-1-AP	1:100
KSR1 H-70	Rabbit polyclonal	H-70	Santa Cruz Biotechnology	Sc-25416	1:500
VPRBP (DCAF1)	Rabbit polyclonal		Proteintech	11612-1-AP	1:1000

Table 2.3 - Antibodies used for immunohistochemistry experiments.

2.8 Lentivirus production and infection

2.8.1 Lentivirus production

HEK293FT cells (passage < 15) were plated in DMEM, 10% FBS into 10 cm culture plates and left growing overnight. A lentiviral reagent mix was added when cells reached 70% of confluence and maintained for 24 hours to facilitate cell infection. The lentiviral reagent mix consists of 3 µg of a packaging plasmid (pCMV-dR8.91), 0.3 µg of an envelope plasmid (VSV-G) and 3 µg of the hairpin-pLKO.1 vector in Opti-mem® previously incubated with 18 µl of FuGENE® 6 transfection reagent (in Opti-mem® medium) for 30 minutes at room temperature.

After 24 hours, the medium containing the lentiviral reagent mix was removed and replaced with fresh medium (DMEM, 20% FBS, 100 U/ml penicillin/streptomycin). Supernatant, containing lentiviruses, was collected after 24 hours: medium was centrifuged at 400 x g for five minutes to remove cell debris. Lentiviral medium was aliquoted and stored at -80˚C.

2.8.2 Lentivirus infection

HEK293T, schwannoma or meningioma cells were grown to at least 70% confluency before infection. Medium was replaced with medium supplemented with 16 µg/ml hexadimethrine bromide (Sigma) (cell lines) or protamine sulphate (Sigma) (primary cells). Homemade virus (DCAF1 shRNA, KSR1 overexpression) was then added at 1:1 ratio with medium for 24 hours. Commercially available viruses (TRCN0000006230, KSR1 shRNA) were added at an Multiplicity of infection (MOI) of 20 to medium supplemented with 8 µg/ml polybrene or protamine sulphate. After 24 hours, fresh medium was added. After a further 24 hours, medium supplemented with 4 µg/ml

puromycin (Sigma) was added and replaced every 3–4 days for a total of seven days. Protein upregulation and downregulation was assessed by Western blot.

2.8.3 Lentiviral information

MISSION® pLKO.1-puro Non-Mammalian shRNA Control Plasmid DNA was used as a Scramble control for all DCAF1 and KSR1 knockdown experiments and was purchased from Sigma. Scramble control lentiviral particles were produced in-house using methods mentioned above.

The shDCAF1 lentivirus clone, TRCN0000129909, was purchased from Open Biosystem with a sequence of CCGGGCTGAGAATACTCTTCAAGAACTCGAGTT CTTGAAGAGTATTCTCAGCTTTTTTGGCTGAGAATACTCTTCAAGAA. Lentiviral particles were produced in-house using methods mentioned above.

The shKSR1 lentivirus clones, TRCN0000006230, was purchased from Sigma with a sequence of CCGGGTGCCAGAAGAGCATGATATTCTCG AGAATATCATGCTCTTCTGGCACTTTTT. Lentiviral particles were purchased and manufactured by Sigma.

A custom overexpression vector was used to produce a lentiviral plasmid that overexpressed human KSR1 (VectorBuilder; Cyagen). The human KSR1 sequence, NM _014238.1, with a C-terminal FLAG tag was cloned into the vector under the CMV promoter. A cleavage linker followed by Enhanced green fluorescent protein (EGFP) was used to allow co-expression of both human KSR1 and EGFP without compromising KSR1 structure and/or function. The plasmid contained ampicillin resistance for bacterial amplification and puromycin resistance for mammalian cell selection. A control plasmid was used that contained EGFP and puromycin resistance in a similar

vector. The control and KSR1 overexpression lentiviral particles were produced in-house using methods mentioned above.

Control plasmid, pLV[Exp]-EGFP:T2A:Puro-EF1A>mCherry, and human KSR1 overexpression plasmid, pLV[Exp]-Puro-CMV>hKSR1[NM_014238.1](ns)/3xFLAG:T2A:EGFP maps are shown (figure 2.3).

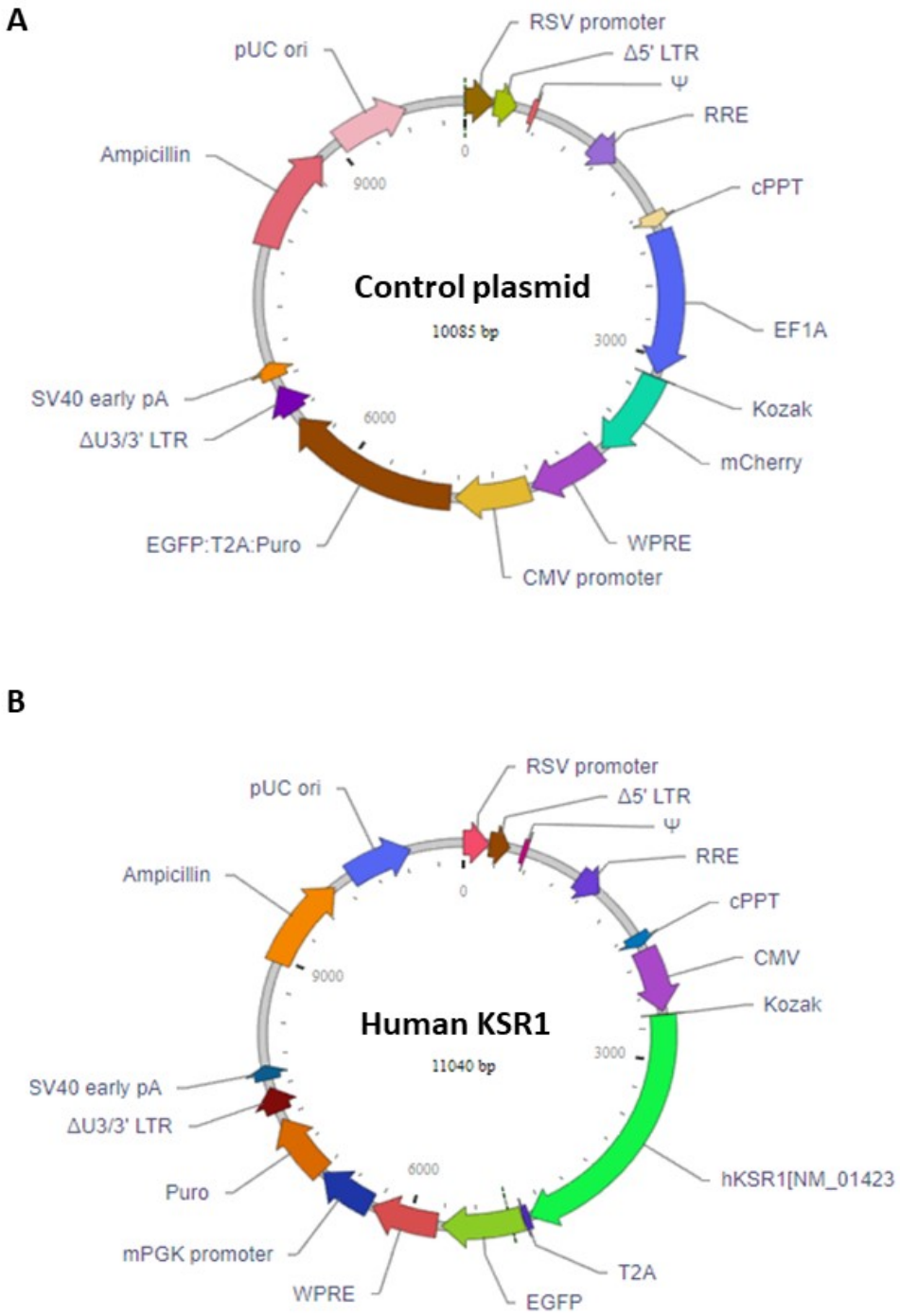

Figure 2.3- Control and human KSR1 overexpression plasmid maps used for lentiviral production.
(Designed using VectorBuilder software)

2.9 Plasmids

2.9.1 Plasmid information

pCMV5 WT KSR1 (K1) was a gift from Rob Lewis (Addgene plasmid # 25970) and contained the KSR1 sequence (NM_013571) with a C-terminal FLAG tag between the 5' cloning site EcoR1 and the 3' cloning site Kpn1 of pCMV5 (Yu *et al.*, 1998).

pCMV5 N539 (KN) was a gift from Rob Lewis (Addgene plasmid # 25972) and contained the KSR1 sequence (NM_013571) with deleted amino acids 540–873. A FLAG tag was added to the C-terminal and the sequence was between the 5' cloning site EcoR1 and the 3' cloning site Xba1 of pCMV5 (Yu *et al.*, 1998).

pCMV5 C540 (KC) was a gift from Rob Lewis (Addgene plasmid # 25971) and contained the KSR1 sequence (NM_013571) with deleted amino acids 1–539. A FLAG tag was added to the C-terminal and the sequence was between the 5' cloning site EcoR1 and the 3' cloning site Kpn1 of pCMV5 (Yu *et al.*, 1998).

pRK5-Myc-DCAF1 (D1), pRK5-Myc-DCAF1 (1–744)(D2) and pRK5-Myc-DCAF1 (D3) (745–1507) plasmids were produced and kindly provided by Li *et al.* (Li *et al.*, 2010).

2.9.2 Plasmid amplification

Plasmids were transformed into DH5α competent cells (Thermo Fisher Scientific) by adding 5 µl plasmid DNA into 50 µl competent cells in an Eppendorf tube. The plasmid/competent cell mix was incubated on ice for 30 minutes, heat shocked for 45 seconds at 42 ˚C and incubated on ice for 2 minutes. 250 µl sterile Luria Bertani (LB) broth (Sigma) was added and the plasmid/competent cell mix was then incubated in an orbital incubator shaker for 1 hour at 150 rpm, 37 ˚C. Transformed competent cells

were plated onto sterile LB agar (Sigma) plates with ampicillin (100µg/ml) (Sigma) and incubated overnight at 37 ˚C for selection.

Plasmid amplification was performed from a single colony grown initially into 5 ml LB broth supplemented with (100 µg/ml) ampicillin overnight at 37 ˚C in an orbital incubator shaker (150 rpm); 200 µl of this bacteria suspension was transferred into 100 ml LB broth supplemented with (100 µg/ml) ampicillin and incubated overnight in an orbital incubator shaker at 150 rpm/37 ˚C.

Plasmid DNA was obtained from the bacteria culture using the Qiagen plasmid mini kit (Qiagen) following manufacturer's protocol. We conducted a digestion of the plasmid DNA of interest using specific restriction enzymes to check whether the digested bands obtained are as expected for the individual plasmid.

2.9.3 Restriction enzyme plasmid digestion

A solution of 0.5 µg Plasmid DNA, 0.2 µl acetylated BSA, 2 µl buffer, 0.5 µl restriction enzyme (NEB) (specific enzymes listed in figures) and water to a total of 20 µl was incubated at 37 ˚C for one hour. 6X DNA loading buffer was added and the samples were loaded onto a 1% agarose/Tris/Borate/EDTA (TBE) gel with gel red. The DNA was separated at 120 volts for 40 minutes and imaged. Restriction digests for DCAF1 and KSR1 plasmids are shown in figure 2.4 and figure 2.5 respectively.

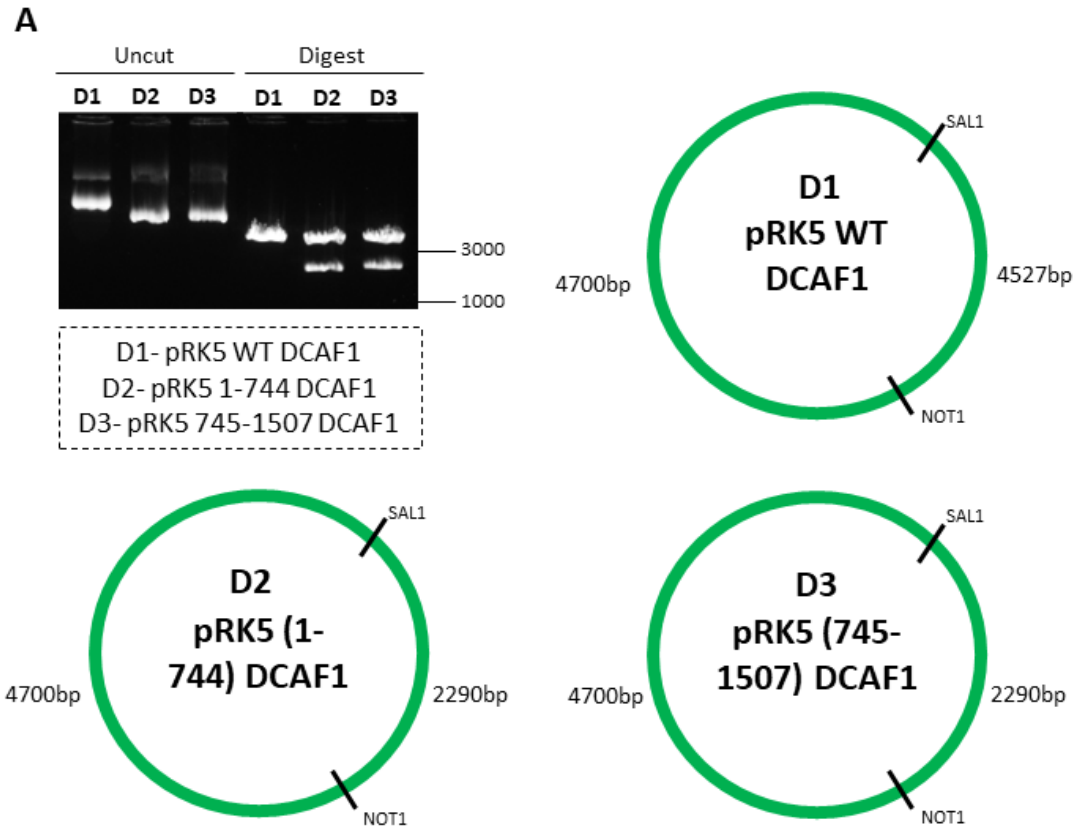

Figure 2.4 - DCAF1 plasmid digests. A: pRK5 wild type (WT) DCAF1 (D1), pRK5 (1–744 amino acids) DCAF1 (D2) and pRK5 (745–1507 amino acids) DCAF1 (D3) were digested with restriction enzymes as indicated on the plasmid maps. The agarose gel shows uncut plasmids and digested plasmid fragments confirming plasmid identity.

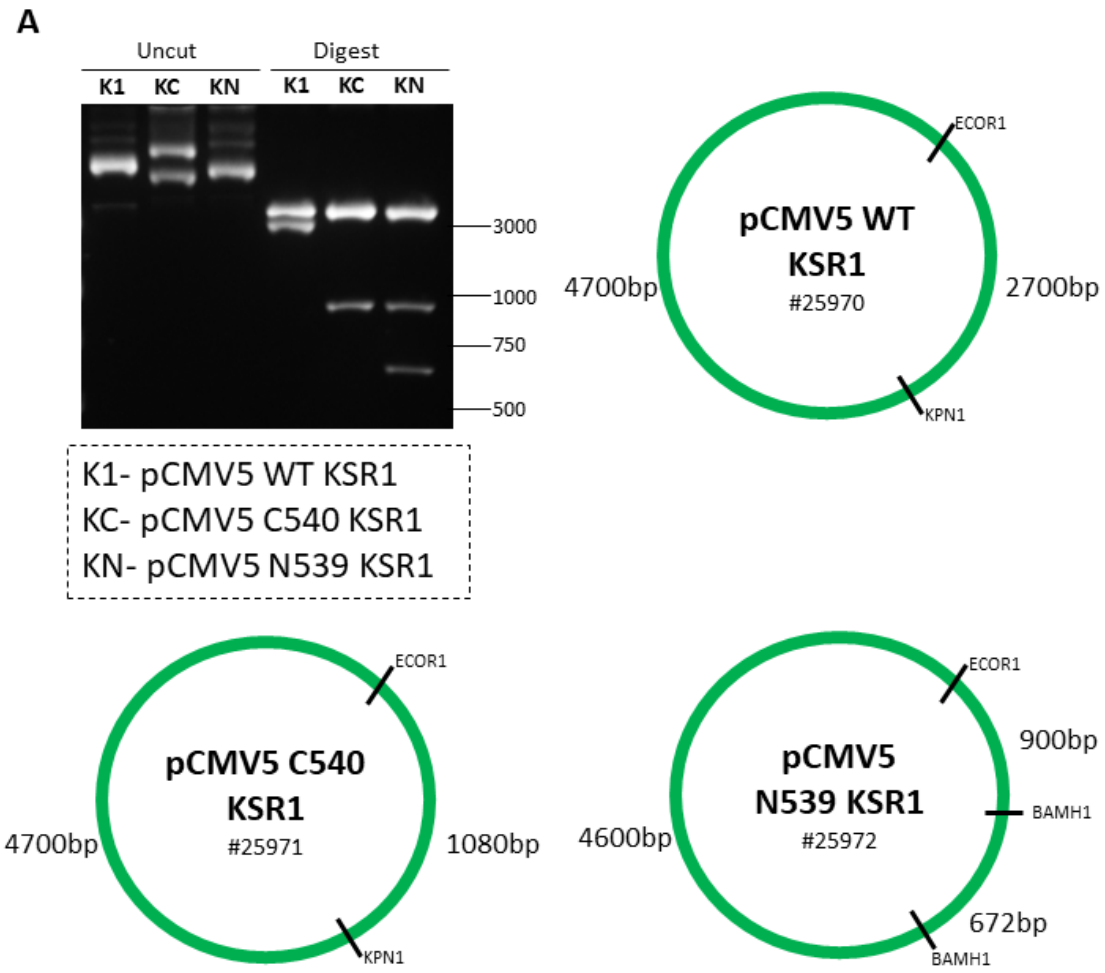

Figure 2.5 - KSR1 plasmid digests. A: pCMV5 wild type (WT) KSR1 (K1), pCMV5 (C540) KSR1 (KC) and pCMV5 (N539) KSR1 (KN) were digested with restriction enzymes as indicated on the plasmid maps. The agarose gel shows uncut plasmids and digested plasmid fragments confirming plasmid identity.

2.9.4 Plasmid transfection

HEK293T cells were transfected at 60% confluency with FuGENE® 6 transfection reagent (Promega) at a ratio of 3:1 to the amount of plasmid added. For a 10 cm plate, 6 µg K1, 4 µg KC, 2 µg KN, 4.5 µg D1, 3 µg D2 or 2.5 µg D3 was added to Opti-mem® (Gibco). The FuGENE® 6 transfection reagent/plasmid mix was then added to cells after 45 minutes incubation at room temperature. Fresh medium was added to cells 24 hours after transfection and cells were lysed 48 hours post-transfection.

2.10 Western blotting

2.10.1 Cell lysis/tissue homogenisation

Cells were lysed by removing medium, washing with DPBS and adding RIPA buffer with Halt protease and phosphatase inhibitors (1:1000). Cells were removed using a plate scraper and stored at -80˚C overnight before centrifuging at 13000 x g for 15 minutes at 4˚C. The supernatant containing protein was then stored at -80˚C before protein estimation and Western blot analysis.

Tissue was washed in DPBS before adding low salt lysis buffer and digested using a glass homogeniser. The tissue was stored overnight at -80˚C before centrifuging at 13000 x g for 15 minutes.

2.10.2 Protein estimation

BSA protein standards were prepared in RIPA or low salt lysis buffer at varying concentrations between 0–2 mg/ml. Protein standards and samples were added to a 96-well plate and 100 µl of Pierce™ bicinchoninic acid (BCA) protein assay kit (Thermo Fisher Scientific) reagents (A:B at a ratio of 50:1) was added to each well. The 96 well

plate was incubated for 30 minutes at 37 ˚C and protein concentration was established using a BMG Labtech Fluostar Omega plate reader.

Protein concentrations were determined using a standard curve formed from the BSA protein standards.

2.10.3 Gels

The resolving gel was made using the following recipe and added to glass plates:-

1 gel	**6%**	**8%**	**10%**	**12%**	**15%**
30% acrylamide (Biorad)	2ml	2.67ml	3.33ml	4ml	5ml
1.5 M Tris-Hydrochloric acid (HCL) pH 8.8	2.5ml	2.5ml	2.5ml	2.5ml	2.5ml
10% SDS	100µl	100µl	100µl	100µl	100µl
Water	5.29ml	4.62ml	3.96ml	3.29ml	2.29ml
10% Ammonium persulphate (APS) (Sigma)	100µl	100µl	100µl	100µl	100µl
Tetramethylethylenediamine (TEMED)(Thermo Fisher Scientific)	10µl	10µl	10µl	10µl	10µl

Table 2.4- Western blot resolving gel recipe.

Stacking gel was made and added using the following recipe:-

4% Stacking gel	**5ml (one gel)**	**10ml (two gel)**
30% acrylamide	650µl	1.3ml
1 M Tris-HCL pH 6.8	625µl	1.25ml
10% SDS	50µl	100µl
Water	3.68ml	7.34ml
10% APS	50µl	100µl
TEMED	10µl	20µl

Table 2.5 - Western blot stacking gel recipe.

2.10.4 Protein separation and transfer

The gels were set up in the running apparatus in running buffer (25 mM Trizma-base, 20 mM glycine, 3.5 mM SDS). Most commonly, 20 µg of protein with 4X sample reducing buffer was loaded into the gels and separated at a constant voltage of 120V for 70 minutes. Transfer onto polyvinylidene fluoride (PVDF) membrane (Biorad) (after pre-wetting with methanol) was set up in transfer buffer (25 mM Trizma-base, 20 mM glycine and 15% v/v methanol) and transferred at a constant current of 400mA for 80 minutes. The ice pack was exchanged half way through the transfer and a magnetic stirrer maintained an even temperature throughout the tank.

2.10.5 Membrane probing

Following the transfer the membrane was washed in TBST (20 mM Trizma-base, 150 mM sodium chloride, 0.1% v/v Tween 20) blocked using blocking buffer (5% w/v milk (Sigma), 2% w/v BSA in TBST) for one hour at room temperature on a rocker. The membrane was then washed three times with TBST and primary antibody was added overnight at 4 °C. Primary antibody was diluted in 5% BSA/TBST (see antibody table for dilutions). After three TBST washes, secondary HRP-conjugated antibody (Biorad) was added for one hour at room temperature diluted at 1:5000 in 2.5% milk, 1% BSA in TBST. The membrane was washed with TBST and then twice with TBS before developing.

Pierce Enhanced chemiluminescent substrate (ECL) Western blotting substrate or Pierce ECL plus Western blotting substrate (Thermo Fisher Scientific) was added to the membranes and incubated for two minutes. Then the membranes were either manually developed using Amersham hyperfilm ECL (GE healthcare) and a Xograph film

processor or using the PXi gel imaging system (Syngene) with automatically adjusted exposure times.

Antibody	Type	Clone	Company	Catalog	Dilution
C-RAF	Rabbit polyclonal		CST	9422	1:1000
CYCLIN D1	Rabbit polyclonal		CST	2922	1:1000
DDB1	Rabbit polyclonal		Bethyl	A300-462A	1:1000
ERK1/2	Rabbit monoclonal		CST	9102	1:1000
FLAG	Mouse monoclonal	M2	Sigma	F1804	1:5000
GAPDH	Mouse monoclonal	6C5	Millipore	MAB374	1:20000
HDAC1	Mouse monoclonal	10E2	CST	5356	1:1000
KSR1	Rabbit polyclonal		CST	4640S	1:500
KSR1 H-70	Rabbit polyclonal	H-70	Santa Cruz Biotechnology	Sc-25416	1:500
LATS1	Rabbit polyclonal		CST	9153	1:1000
LATS2	Rabbit monoclonal	D83D6	CST	5888	1:1000
MEK1/2	Rabbit polyclonal		CST	9122	1:1000
Merlin	Rabbit polyclonal	D1D8	CST	6995	1:1000
Myc tag	Mouse monoclonal	9B11	CST	2276	1:1000
NEDD8	Rabbit polyclonal		CST	2745	1:1000
p-ERK (T202/Y204)	Rabbit polyclonal		CST	9101	1:2000
p-MEK1/2 (S217/S221)	Rabbit monoclonal	41G9	CST	9154	1:1000
p-Merlin (S518)	Rabbit polyclonal		CST	9163	1:500
p-YAP (S127)	Rabbit polyclonal		CST	4911	1:1000
Ubiquitin	Rabbit polyclonal		CST	3933	1:1000
VPRBP (DCAF1)	Rabbit polyclonal		Proteintech	11612-1-AP	1:1000

Table 2.6 - Antibodies used for Western blotting.

2.10.6 Stripping and storing membranes

Stripping membranes was avoided when possible as protein may also be removed. Stripping was conducted by adding a wash buffer (100 mM glycine pH 2.4, 2 mM ethylene glycol-bis(β-aminoethyl ether)-N,N,N',N'-tetraacetic acid (EGTA) (Sigma) in deionised water) followed by incubation with stripping buffer (1M tris-HCL pH 6.8, 10% w/v SDS, 0.7% v/v β-metacarpoethanol (Sigma) in deionised water) pre-heated to 56˚C for 10 minutes. The membrane was then re-blocked with blocking milk and re-probed. Membranes were stored at -20˚C when no longer needed.

2.10.7 Western blot analysis

Manually developed films were scanned in at 600dpi in greyscale. Image J was used for quantification of all Western blot bands, using Glyceraldehyde 3-phosphate dehydrogenase (GAPDH) as a loading control. Statistical analysis was performed on the raw densitometry values using Graphpad Prism 5, $p< 0.05$. Student's Paired T test or Student's Unpaired T test was used to assess statistical significance when there was two samples whereas a one-way ANOVA/Repeated Measures ANOVA was used if there were more than two samples with Tukey's Multiple Comparison Test ($p< 0.05$).

Chapter 3 - DCAF1 and KSR1 expression and regulation of KSR1 by DCAF1 in Merlin-deficient tumours

3.1 Introduction

The aim of this chapter was to examine DCAF1 expression in schwannoma, determine if DCAF1 and KSR1 expression was increased in Merlin-deficient models, focussing on meningioma in particular, and to determine if DCAF1 regulated KSR1 in these cells. In addition, we wanted to determine if targeting both DCAF1 and KSR1 expression in meningioma and BenMen-1 would have an additive effect on reducing RAF/MEK/ERK activity and proliferation compared with DCAF1 or KSR1 knockdown alone.

3.2 DCAF1 is overexpressed in schwannoma

DCAF1 and KSR1 are frequently overexpressed or dysregulated in cancer (Cooper *et al.*, 2017; Fisher *et al.*, 2015; Kim *et al.*, 2013; Llobet *et al.*, 2011; Stebbing *et al.*, 2015; Wang *et al.*, 2017; Zhou *et al.*, 2016a). Merlin is a suppressor of DCAF1 activity and therefore, DCAF1 is activated in Merlin-deficient tumours (Li *et al.*, 2014; Li *et al.*, 2010). We have previously shown that KSR1 protein expression is increased in schwannoma tissue compared with normal nerve and traumatic neuroma, by immunohistochemistry (Zhou *et al.*, 2016a). We wanted to determine if DCAF1 protein expression was also increased in Merlin-deficient schwannoma. We stained normal nerve, traumatic neuroma and schwannoma with DCAF1 antibody counterstained with haematoxylin to stain the nucleus and compared DCAF1 protein expression. Figure 3.1A shows representative images at 400x magnification of five replicates showing that there is little DCAF1 staining in normal nerve and traumatic neuroma compared with schwannoma tissue, in which DCAF1 is highly expressed, particularly in the nucleus. The five replicates of each tissue type were given a score of 1, 2, 3 or 4 according to the percentage of cells expressing DCAF1. A score of 1 is given when less than 25% of cells expressed protein, a score of 2 for between 25% and 50% of cells expressing

protein, a score of 3 for between 51% and 75% of cells and a score of 4 for more than 75% of cells expressing the protein. Figure 3.1B shows that four out of five schwannoma tissue samples were scored as 4 and one was scored as 3 whereas scoring for normal nerve and traumatic neuroma was much lower. A Kruskal-Wallis test was used to test statistical significance of differences in the medians of each group and Dunn's multiple comparison post test showed that median DCAF1 protein expression was significantly higher in schwannoma tissue compared with normal nerve ($p< 0.01$). There was no significant difference in protein expression between normal nerve and traumatic neuroma or between traumatic neuroma and schwannoma ($p> 0.05$).

To confirm the results from immunohistochemistry, we used an alternative method to determine DCAF1 and KSR1 protein expression in normal nerve and schwannoma tissue (figure 3.1C). The Western blot shows there was increased DCAF1 protein expression in three schwannomas compared with one normal nerve. KSR1 expression was relatively absent in normal nerve and 1 schwannoma whereas there was clear KSR1 expression in two schwannoma (figure 3.1C). We did not quantify this Western blot as there was only one normal nerve tissue sample.

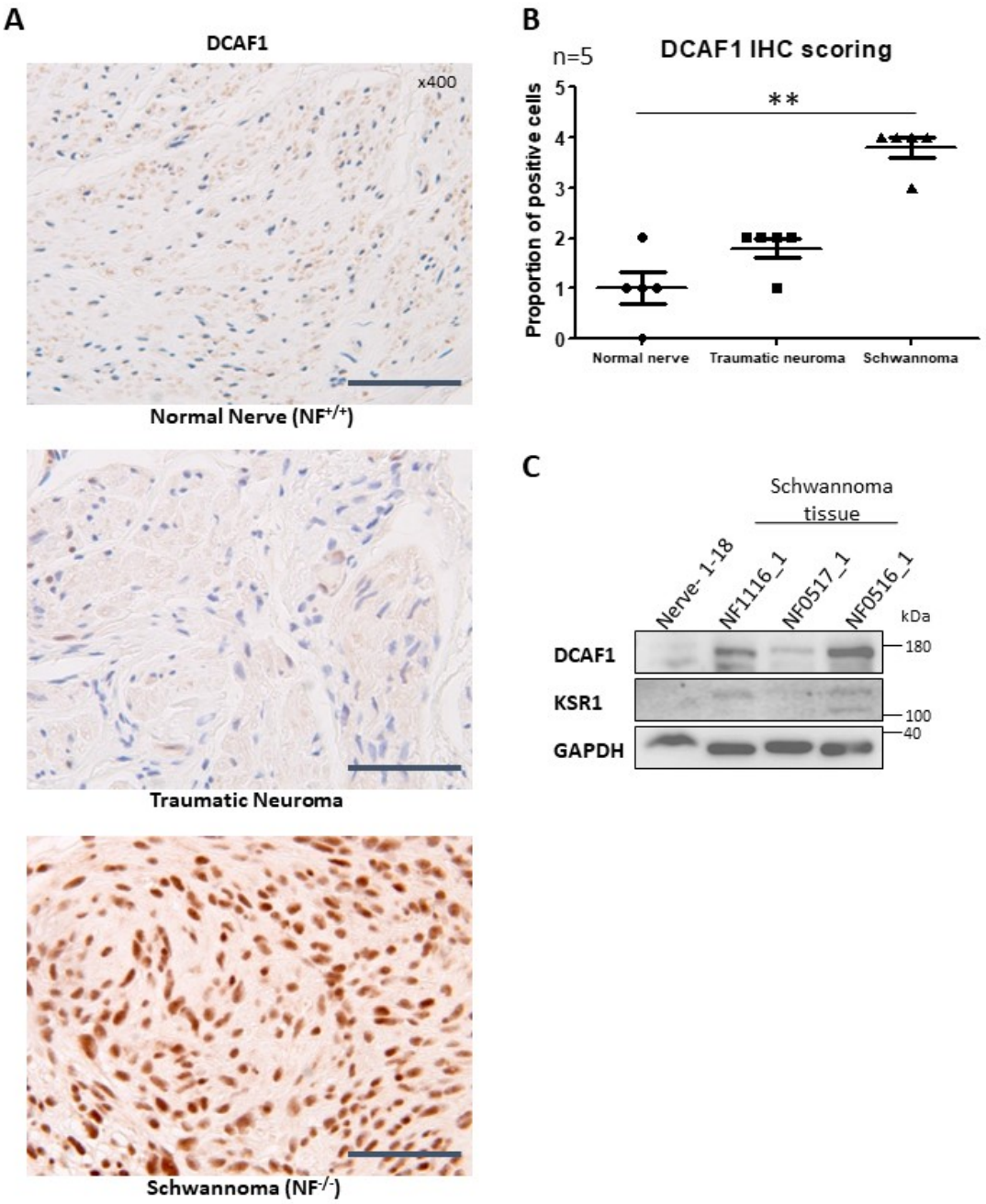

Figure 3.1 - DCAF1 is overexpressed in schwannoma tissue. **A:** Representative immunohistochemical images of normal nerve ($NF^{+/+}$), traumatic neuroma and merlin-deficient schwannoma ($NF^{-/-}$) tissue stained with DCAF1 antibody and counterstained with haematoxylin are shown at 400x magnification. DCAF1 expression was increased in schwannoma compared to normal nerve and traumatic neuroma, particularly in the nucleus, scale bar- 50 µM. Immunohistochemical staining, imaging and scoring was carried out by Dr David Hilton. **B:** The graph shows the proportion of DCAF1 positive cells in five normal nerves, five traumatic neuromas and five schwannoma tissues where a score of 1 was less than 25% of cells expressing DCAF1, a score of 2 was between 25% and 50%, a score of 3 was between 51% and 75% and a score of 4 was more than 75%. Schwannoma tissue had significantly more cells expressing DCAF1 than normal nerve, **- $p< 0.01$. **C:** Western blot showing DCAF1 and KSR1 expression in one normal nerve (Nerve-1–18 and three schwannoma tissue (NF) samples. DCAF1 was increased in schwannoma compared with normal nerve. KSR1 were increased in two schwannoma samples (NF1116_1 and NF0516_1) compared with normal nerve whereas NF0517_1 had similar KSR1 expression as the normal nerve.

Previously, we demonstrated that KSR1 protein was upregulated in schwannoma cells compared with Schwann cells, derived from schwannoma tissue and normal nerve respectively, via Western blot (Zhou *et al.*, 2016a). We analysed DCAF1 protein expression in Schwann cells and Merlin-deficient schwannoma cells, shown in figure 3.2A and B. We confirmed loss of Merlin protein expression by Western blot (figure 2.1). DCAF1 expression was highly variable in Schwann cell and schwannoma samples. Figure 3.2C shows densitometry quantification of DCAF1 (normalized to Glyceraldehyde 3-phosphate dehydrogenase (GAPDH)) and whilst the mean expression in schwannoma samples was higher than the mean expression in Schwann cell samples, this was not statistically significant (Unpaired Student's T test, $p > 0.05$). Overall, the results suggest that both DCAF1 and KSR1 proteins are overexpressed in schwannoma compared with normal controls.

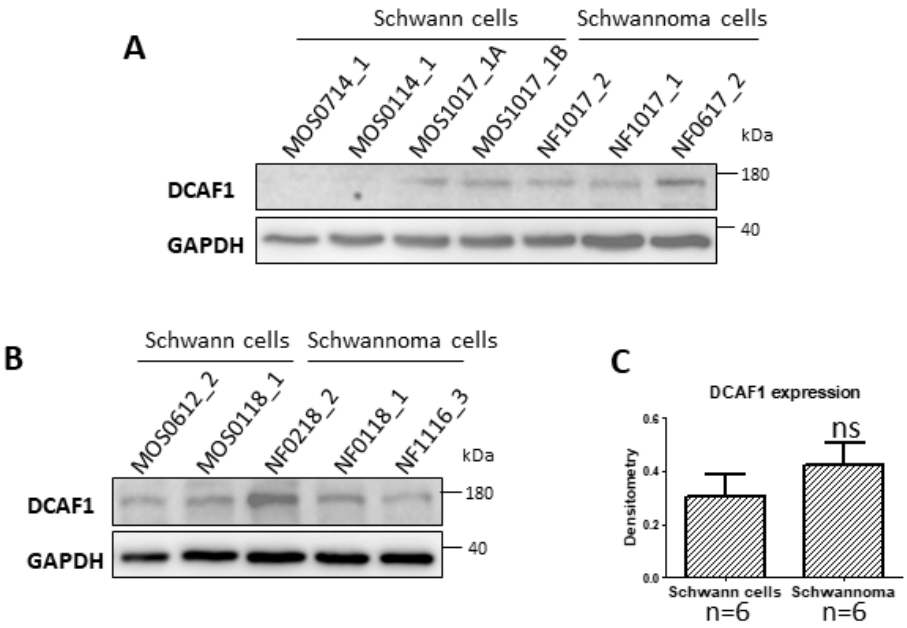

Figure 3.2 - DCAF1 expression is highly variable in schwannoma cells. A, B: Western blots showing DCAF1 expression in Schwann (MOS) and schwannoma (NF) cells. DCAF1 expression is highly variable in Schwann and schwannoma cells. **C:** Mean DCAF1 expression and standard error of the mean (SEM) in Schwann cells and schwannoma from blots shown in A and B normalized to the loading control, GAPDH. DCAF1 expression was unchanged, ns- not significant ($p > 0.05$)**.**

3.3 DCAF1 and KSR1 are overexpressed in meningioma

DCAF1 and KSR1 expression in Merlin-deficient meningioma has never been explored and is important for this project where the aim was to test inhibitors of DCAF1 and KSR1 activity. Therefore, we analysed DCAF1 and KSR1 expression in human meninges and Merlin-deficient meningioma. Figure 3.3A shows representative images of normal brain with intact meninges (as shown by the insert) and Merlin-deficient meningioma tissue stained with DCAF1 and counterstained with the nuclear stain, haematoxylin. DCAF1 protein was mostly nuclear with some diffuse cytoplasmic expression. DCAF1 was scored, by Dr David Hilton, according to the criteria described in figure 3.1B and shown in figure 3.3C. The proportion of cells expressing DCAF1 was significantly higher in meningioma (n=7) than in meninges (n=9) ($p< 0.01$, Mann-Whitney test). Figure 3.3B shows representative images of normal brain with intact meninges and Merlin-deficient meningioma tissue stained with KSR1 and counterstained with the nuclear stain, haematoxylin. KSR1 was diffuse and granular in the cytoplasm with strong paranuclear nuclear expression in four out of seven meningioma samples. KSR1 was scored, by Dr David Hilton, according to the criteria described in figure 3.1B and the results are displayed in figure 3.3D. Interestingly, all seven meningioma samples had more than 75% of cells expressing KSR1 and thus were scored as 4. The proportion of cells expressing KSR1 was significantly higher in meningioma (n=7) compared with meninges (n=9) and this difference was statistically significant ($p< 0.05$, Wilcoxon signed rank test).

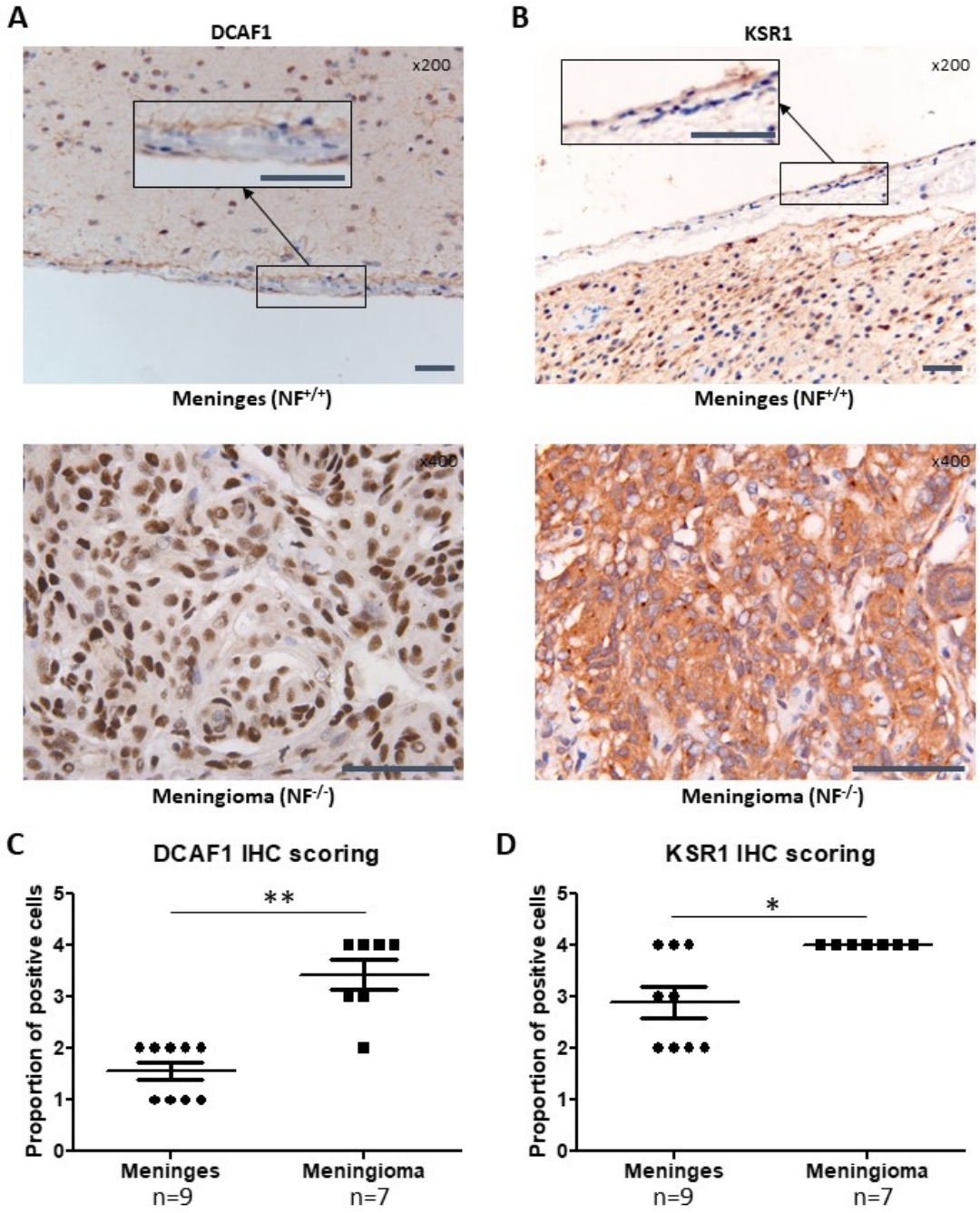

Figure 3.3 - DCAF1 and KSR1 are overexpressed in meningioma tissue. A: Representative immunohistochemical images of normal meninges (200x with 400x insert) and meningioma (400x) tissue stained with DCAF1 antibody and counterstained with haematoxylin. DCAF1 expression was mostly nuclear with some diffuse cytoplasmic expression in meningioma. Immunohistochemical staining was carried out by the author whereas the images were taken and scored by Dr David Hilton. **B:** Representative Immunohistochemical images of normal meninges (200x with 400x insert) and meningioma (400x) tissue stained with KSR1 antibody and counterstained with haematoxylin. KSR1 expression was diffuse and granular in the cytoplasm with some strong paranuclear nuclear expression in meningioma. Scale bar- 50 µM. **C:** Proportion of DCAF1 positive cells in nine normal meninges and seven meningioma tissues are plotted where a score of 1 was less than 25% of cells expressing DCAF1, a score of 2 was between 25% and 50%, a score of 3 was between 51% and 75% and a score of 4 was more than 75%. Meningioma tissue had significantly more cells expressing DCAF1 than normal meninges, **- $p < 0.01$. **D:** Proportion of KSR1 positive cells in nine normal meninges and seven meningioma tissues are plotted. Meningioma tissue had significantly more cells expressing KSR1 than normal meninges, *- $p < 0.05$.

To confirm overexpression of both DCAF1 and KSR1 in meningioma tissue compared with normal meningeal tissue, we analysed protein expression in three normal meninges samples and three Merlin-deficient meningioma samples via Western blot (figure 3.4A). Figure 3.4B shows the raw densitometry values obtained when quantifying figure 3.4A using Image J software confirming the overexpression of both DCAF1 and KSR1 in Merlin-deficient meningioma (Student's Unpaired T-test, $p< 0.05$).

Human meningeal cells (HMC) were purchased from Sciencell and meningioma cells were derived from Merlin-deficient meningioma tissue. We confirmed loss of Merlin protein expression by Western blot (figure 2.1). HMC and meningioma protein lysate were probed with DCAF1 and KSR1 antibodies via Western blot and are shown in figure 3.4C. DCAF1 and KSR1 expression were highly variable across the meningioma samples, hence a large sample size was analysed. In figure 3.4D, densitometry analysis of DCAF1 and the two KSR1 bands in HMC and meningioma cells is reported. DCAF1 and KSR1 expression were significantly increased in meningioma compared with HMC (Student's unpaired T test; $p< 0.05$ and $p< 0.01$ respectively). Therefore, DCAF1 and KSR1 expression are consistently overexpressed in both meningioma cells and tissue compared to normal controls.

We used the WHO I Benign meningioma cell line, BenMen-1 and WHO III meningioma cell line, KT21-MG1-Luc5D as models of Merlin-deficient meningioma for drug treatment experiments, *in vitro*. Therefore, we wanted to determine if DCAF1 and KSR1 protein were overexpressed in these models when compared with HMC cells. We analysed DCAF1 and KSR1 protein expression by Western blot (figure 3.4E). The bar chart in figure 3.4F shows the mean DCAF1 and KSR1 expression in each cell line and the SEM normalized to the loading control, GAPDH. A one-way ANOVA with Tukey's

Multiple Comparison Test was performed using GraphPad Prism software and DCAF1 expression was significantly higher in KT21-MG1-Luc5D than in HMC ($p < 0.05$). On the contrary, the mean DCAF1 expression in BenMen-1 was increased but not statistically significant when compared with HMC. There was no statistical significance for KSR1 expression between HMC, BenMen-1 or KT21-MG1-Luc5D.

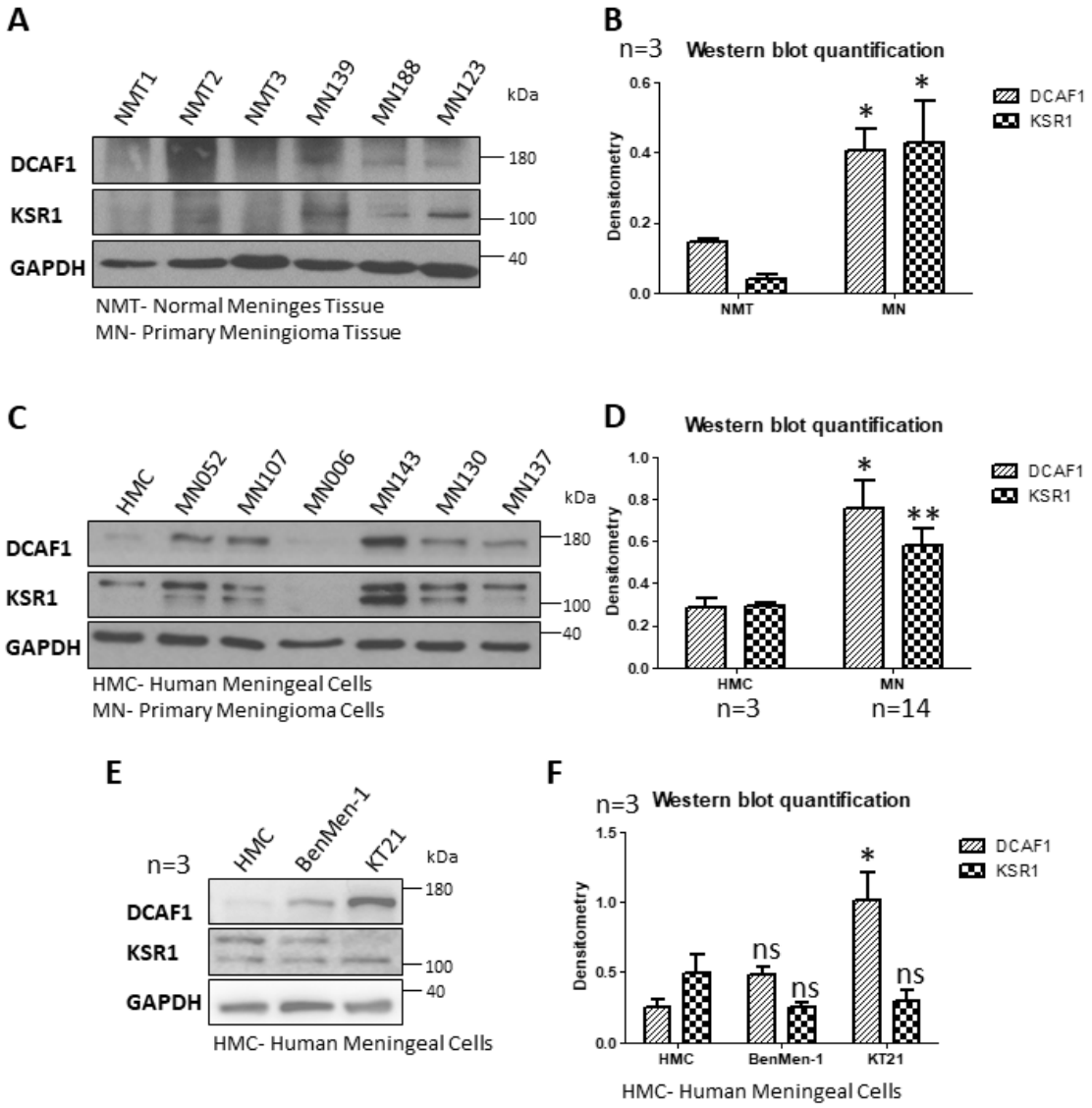

Figure 3.4 - DCAF1 and KSR1 are overexpressed in meningioma cells. A: Western blot showing DCAF1 and KSR1 expression in normal meninges tissue (NMT) and primary meningioma tissue (MN), GAPDH-loading control. **B:** Mean DCAF1 and KSR1 expression and SEM in NMT and MN normalized to the loading control. DCAF1 and KSR1 expression were significantly increased in MN compared with NMT, *- $p< 0.05$. **C:** Western blot showing DCAF1 and KSR1 expression in human meningeal cells (HMC) and meningioma cells (MN). DCAF1 and KSR1 expression are highly variable in primary meningioma cells. **D:** Mean DCAF1 and KSR1 expression and SEM in three HMC and 14 MN normalized to the loading control, GAPDH. DCAF1 and KSR1 expression were significantly increased in MN compared with HMC, *- $p< 0.05$, **- $p< 0.01$. **E:** Representative Western blot, of three replicates (n=3), to show DCAF1 and KSR1 expression in HMC, Benign meningioma 1 (BenMen-1) and WHO III meningioma cell line (KT21-MG1-Luc5D) (KT21). **F:** Mean DCAF1 and KSR1 expression and SEM in three HMC, BenMen-1 and KT21 normalized to the loading control, GAPDH. DCAF1 was significantly increased in KT21 compared with HMC, *- $p< 0.05$. DCAF1 and KSR1 were unchanged in BenMen-1 compared to HMC and KSR1 was unchanged in KT21 compared to HMC, $p>0.05$ (not significant (ns)).

We also analysed DCAF1 and KSR1 expression in alternative models of Merlin-deficiency including the mouse model, described in Mindos *et al.* (data not shown) (Mindos *et al.*, 2017). In uninjured (Control) sciatic nerve, DCAF1 and KSR1 expression could not be detected or was very low in both wild type and Merlin conditional null nerve tissue and therefore could not be quantified accurately.

Altogether, these data suggest that DCAF1 and KSR1 proteins are overexpressed in primary Merlin-deficient meningioma whereas expression was more variable in meningioma cell lines, BenMen-1 and KT21-MG1-Luc5D.

3.4 The higher molecular weight KSR1 band

Interestingly, there were two bands detected in figure 3.4C and 3.1C using the Cell Signalling Technology KSR1 antibody that binds to the region surrounding G910 of human KSR1. One of these bands at 100 kDa is the expected size and the additional band is around 10 kDa larger at 110 kDa. We showed that two bands were also present using an alternative KSR1 antibody (Abcam) that binds to human KSR1 around the region of S392 and were present in Schwann cell, schwannoma and BenMen-1 cell protein (data not shown).

We suspected that the additional band was a post-translationally modified form of KSR1 yet there was no shift in molecular weight using lambda phosphatase or Peptide: N-glycosidase F (PNGase F) (data not shown). Therefore, the additional band is not due to phosphorylation or N-glycosylation. Furthermore, DCAF1 knockdown did not lead to a shift in the molecular weight of KSR1 further excluding DCAF1-dependent ubiquitination as the identity of the band (Zhou *et al.*, 2016a and figure 3.5A). Ubiquitin is a small protein around 8.5 kDa in size and therefore the additional band could represent DCAF1-independent mono-ubiquitination of KSR1 (Terrell *et al.*, 1998).

As we have shown that the additional KSR1 band is detected by two antibodies that target different KSR1-specific sequences, is not phosphorylated or glycosylated and is diminished with the use of a KSR1 targeting shRNA construct (Zhou *et al.*, 2016a), we decided to quantify both Western blot bands in all subsequent experiments.

3.5 DCAF1 does not regulate KSR1 expression or localization

As CRL4-DCAF1's primary role is to ubiquitinate substrates and the most common result of this ubiquitination is protein degradation, we determined whether DCAF1 regulates KSR1 degradation (Ahn *et al.*, 2011). We previously demonstrated that DCAF1 did not regulate KSR1 expression in schwannoma cells (Zhou *et al.*, 2016a). We wanted to confirm this result in primary meningioma cells and BenMen-1 cells as protein function can be context dependent. We used a shRNA construct targeting DCAF1 to knock down DCAF1 expression in primary meningioma cells and observed changes in KSR1 expression. Scramble or DCAF1 lentivirus was added for 24 hours followed by a 24 hour recovery period. Puromycin was then added for seven days to select cell with puromycin resistance which have therefore been successfully transduced with the lentivirus. DCAF1 expression was significantly decreased, by an average of 53%, in DCAF1 knockdown cells compared with the scramble (Sc) control (Student's Paired T-test, $p< 0.01$; figure 3.5A and B). Figure 3.5A show that KSR1 expression is unchanged between scramble and DCAF1 knockdown in primary meningioma cells (quantified in figure 3.5B, $p> 0.05$). We then confirmed this result in BenMen-1 cells (figure 3.5C and D). Therefore, DCAF1 does not regulate KSR1 protein expression in Merlin-deficient schwannoma or meningioma cells.

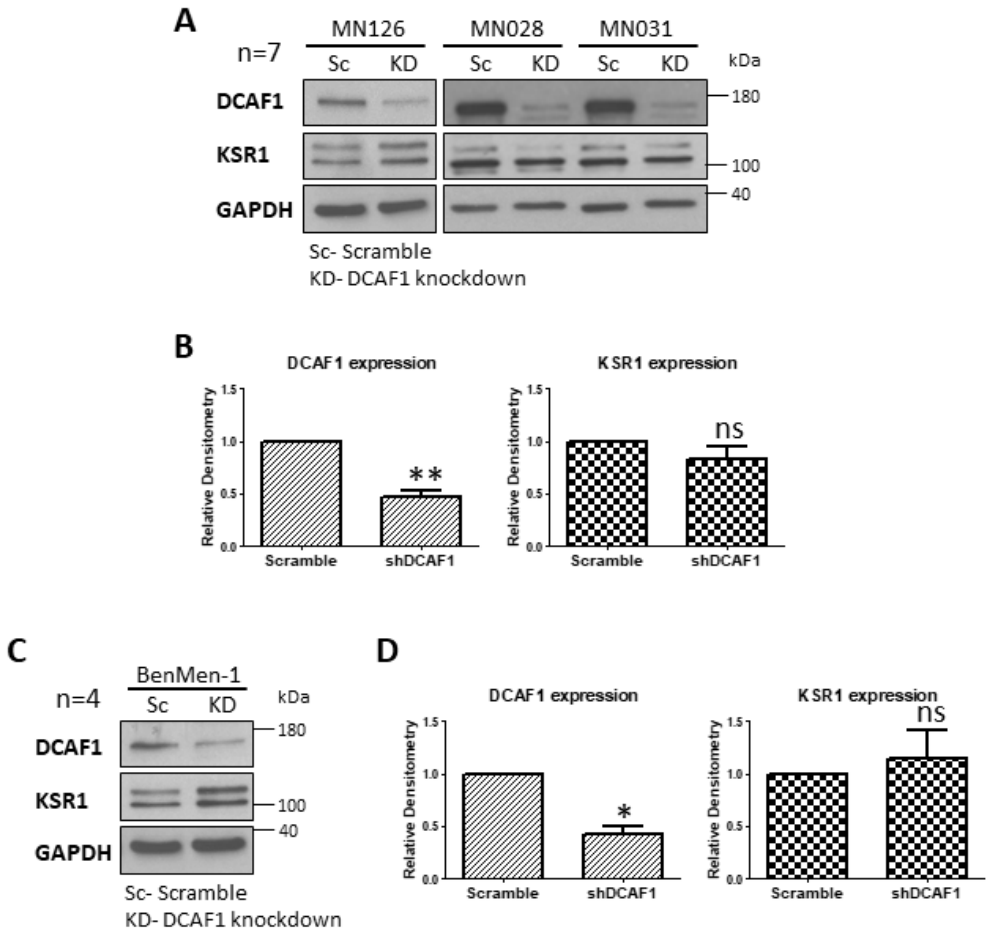

Figure 3.5 - DCAF1 does not regulate KSR1 degradation in meningioma. A: Western blots of DCAF1 and KSR1 expression after DCAF1 knockdown in three meningiomas (MN) representative of seven replicates. Scramble (Sc) or DCAF1 (KD) lentivirus was added to cells for 24 hours followed by a 24 hour recovery period and then seven days of puromycin selection before cell lysis. **B:** The graph shows the mean DCAF1 and KSR1 expression with SEM in shDCAF1 treated MN cells normalized to the loading control, GAPDH and relative to scramble. DCAF1 expression was reduced whilst KSR1 was unchanged in shDCAF1 treated cells compared with scramble. **- p< 0.01, ns- not significant. **C:** Western blots of DCAF1 and KSR1 expression after DCAF1 knockdown in the WHO I benign meningioma 1 cell line, BenMen-1. Scramble (Sc) or DCAF1 (KD) lentivirus was added to cells for 24 hours followed by a 24 hour recovery period and then seven days of puromycin selection before cell lysis. **D:** The graph shows the mean DCAF1 and KSR1 expression with SEM in shDCAF1 treated BenMen-1 cells normalized to the loading control, GAPDH and relative to scramble. DCAF1 expression was reduced whilst KSR1 was unchanged in shDCAF1 treated cells compared with scramble. *- p< 0.05, ns- not significant.

We used a cytoplasmic and nuclear extraction kit to establish DCAF1 and KSR1 localization in Schwann and schwannoma cells. In order to assess protein cross-contamination between the two cellular compartments, we used GAPDH as a cytoplasmic control and Histone deacetylase 1 (HDAC1) as a nuclear control. Figure 3.6A shows that DCAF1 and KSR1 are predominantly nuclear in Schwann cells with some cytoplasmic DCAF1 expression in two out of four Schwann cells analysed. Figure 3.6B shows the localization of DCAF1 and KSR1 in schwannoma. DCAF1 was predominantly nuclear in schwannoma with a faint band observed in the cytoplasm of three out of three schwannomas analysed. KSR1 is localised in the cytoplasm and the nucleus in two out of three schwannoma and exclusively in the nucleus of one schwannoma. In one schwannoma, the upper KSR1 band was predominantly cytoplasmic whereas the lower KSR1 band was nuclear.

Mono-ubiquitination has been reported to alter cellular localization of substrates (Wu *et al.*, 2011). As KSR1 expression in the cytoplasm was increased in schwannoma compared with Schwann cells we determined if DCAF1 regulated KSR1 localization, possibly in a mono-ubiquitin dependent manner. We knocked down DCAF1 expression using an shRNA construct and performed cytoplasmic and nuclear extraction. The Western blots in figure 3.7A-C demonstrate that KSR1 localization was unchanged after DCAF1 knockdown in schwannoma. Therefore, DCAF1 does not regulate KSR1 localization in schwannoma.

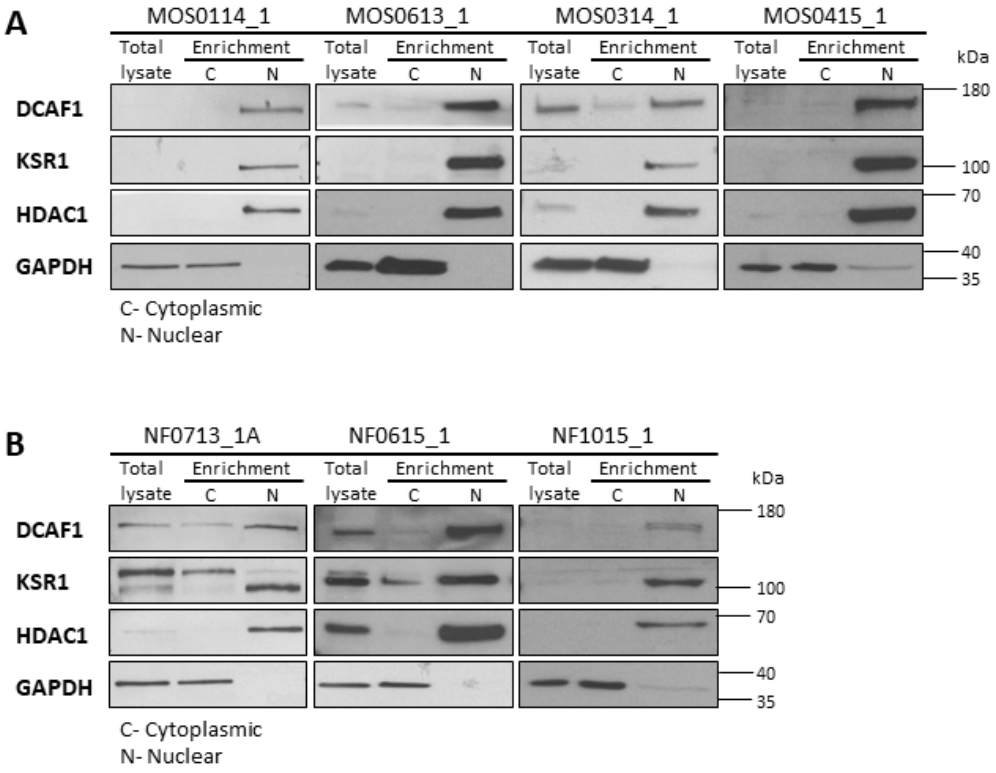

Figure 3.6 - Cytoplasmic KSR1 is increased in schwannoma compared with Schwann cells. A: Western blots of Schwann cell (MOS) total, cytoplasmic (C) and nuclear (N) lysates after cytoplasmic and nuclear enrichment. DCAF1 and KSR1 were predominantly nuclear in MOS. **B:** Western blots of schwannoma (NF) total, cytoplasmic and nuclear lysates after cytoplasmic and nuclear enrichment. DCAF1 and KSR1 were mostly nuclear but also expressed in the cytoplasm of NF. GAPDH-cytoplasmic control and HDAC1-nuclear control.

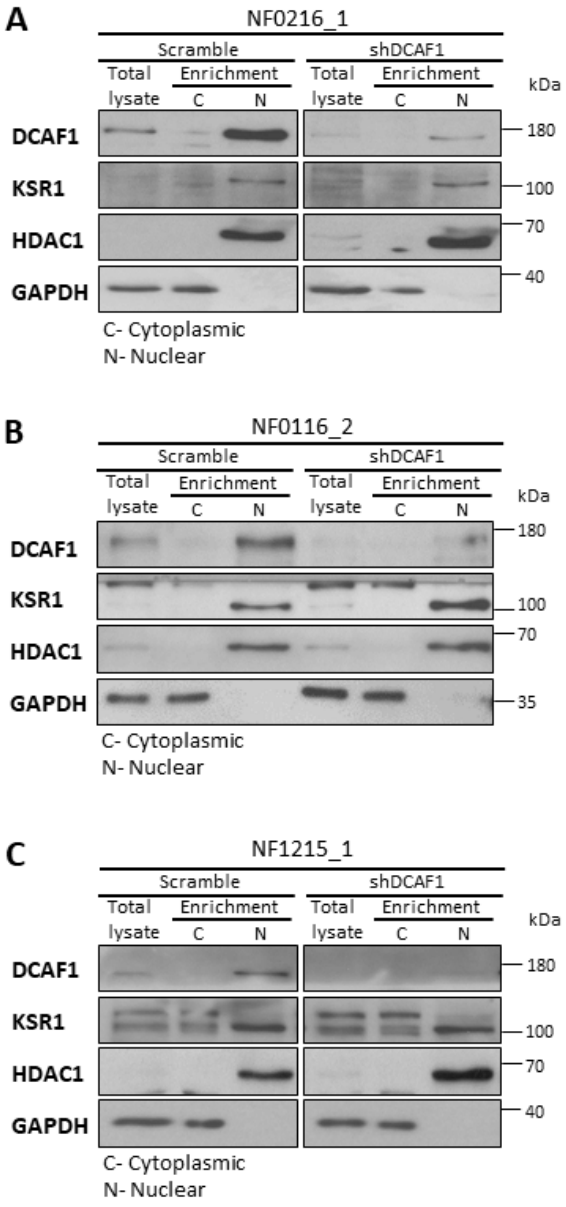

Figure 3.7 - DCAF1 does not regulate KSR1 localization in schwannoma. A, B, C: Western blots to show KSR1 localization after DCAF1 knockdown in schwannoma (NF). Scramble or DCAF1 lentivirus was added for 24 hours followed by a 24 hour recovery period and then seven days of puromycin selection before cytoplasmic (C) and nuclear (N) enrichment. KSR1 localization did not change after DCAF1 knockdown. GAPDH-cytoplasmic control and HDAC1 - nuclear control.

In contrast to Schwann cells and schwannoma, Figure 3.8 and supplementary figure 1 illustrate that DCAF1 and KSR1 localization were unchanged in the benign meningioma cell line, BenMen-1 compared with HMC. We then performed DCAF1 knockdown in primary meningioma cells and performed cytoplasmic and nuclear extraction. Figure 3.9A-B shows that KSR1 localization was unchanged after DCAF1 knockdown in meningioma. Similarly, we knocked down DCAF1 in BenMen-1 and KSR1 localization did not change consistent with results in schwannoma demonstrating that DCAF1 does not regulate KSR1 localization in meningioma (figure 3.9D and supplementary figure 2A-B).

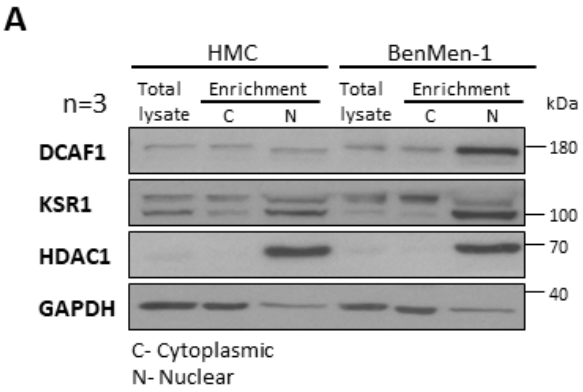

Figure 3.8 - Cytoplasmic KSR1 is not upregulated in BenMen-1 compared with HMC. A: Western blot of DCAF1 and KSR1 in total, cytoplasmic (C) and nuclear (N) lysate of human meningeal cells (HMC) and the Benign meningioma cell line BenMen-1, representative of three replicates. Nuclear DCAF1 was increased in BenMen-1 compared with HMC whilst KSR1 localization was unchanged. GAPDH-cytoplasmic control and HDAC1-is the nuclear control.

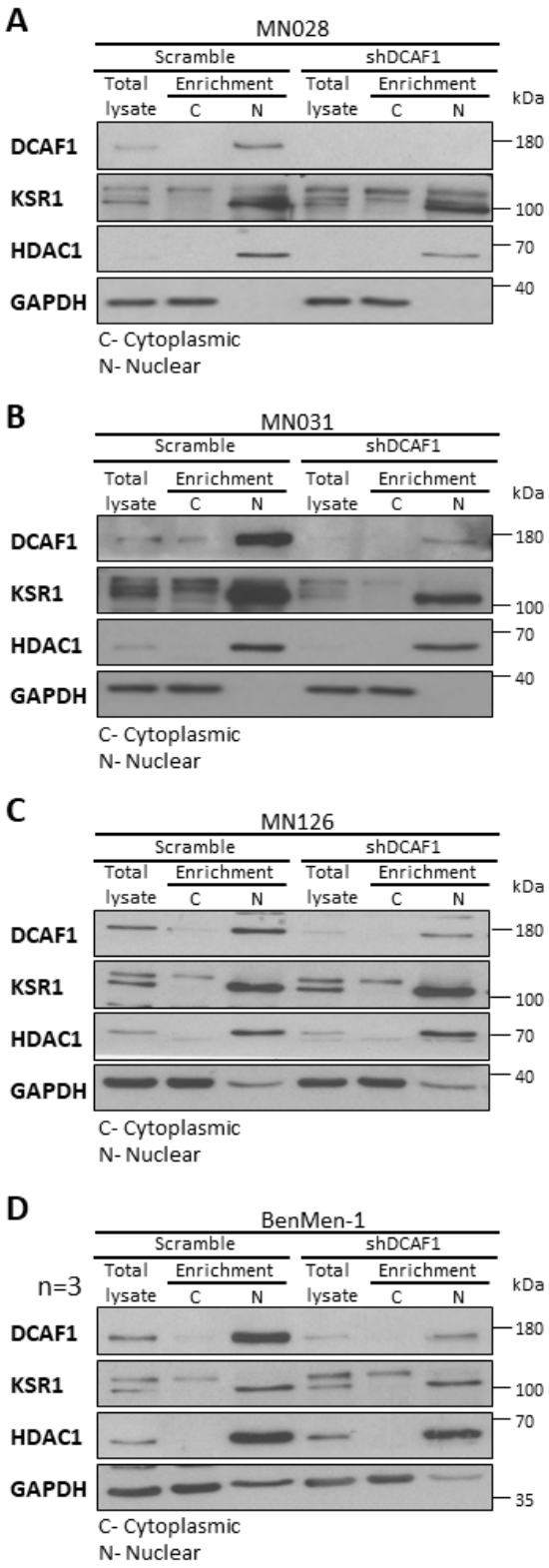

Figure 3.9 - DCAF1 does not regulate KSR1 localization in meningioma or BenMen-1. A, B, C: Western blots to show KSR1 localization after DCAF1 knockdown in meningioma (MN). Scramble or DCAF1 lentivirus was added for 24 hours followed by a 24 hour recovery period and then seven days of puromycin selection before cytoplasmic and nuclear enrichment. KSR1 localization did not change after DCAF1 knockdown. **D:** Western blot to show KSR1 localization in the Benign meningioma cell line, BenMen-1 after DCAF1 knockdown followed by cytoplasmic (C) and nuclear (N) enrichment representative of three replicates. KSR1 localization did not change after DCAF1 knockdown. GAPDH-cytoplasmic control and HDAC1-nuclear control.

3.6 DCAF1 regulates RAF/MEK/ERK activity in schwannoma and reduces proliferation of schwannoma and meningioma

Mono-ubiquitination can also modulate protein activity and we hypothesised that DCAF1 regulates KSR1 activity in the form of RAF/MEK/ERK activation (Chen, 2005). We knocked down DCAF1 expression in schwannoma and analysed the expression of phosphorylated ERK1/2 relative to total ERK1/2 to capture changes in activity. ShRNA-mediated DCAF1 knockdown efficiency was evaluated by Western blot in schwannoma cells (figure 3.10A). Quantification of six independent experiments demonstrated a significant 71% reduction of DCAF1 expression between scramble and DCAF1 knockdown (Student's paired T test, $p< 0.01$; figure 3.10B), which led to a significant reduction in pERK1/2 expression (35% reduction; $p< 0.05$) when quantified taking into account both ERK1/2 and GAPDH expression (figure 3.10B). Therefore, DCAF1 regulates RAF/MEK/ERK signalling in schwannoma. CYCLIN D1 is a downstream target of pERK1/2 so we monitored its protein levels following DCAF1 knockdown. Interestingly, our results demonstrated that CYCLIN D1 expression was unchanged suggesting that RAF/MEK/ERK inhibition by DCAF1 knockdown was not sufficient to influence the expression of downstream proteins such as CYCLIN D1 (figure 3.10B).

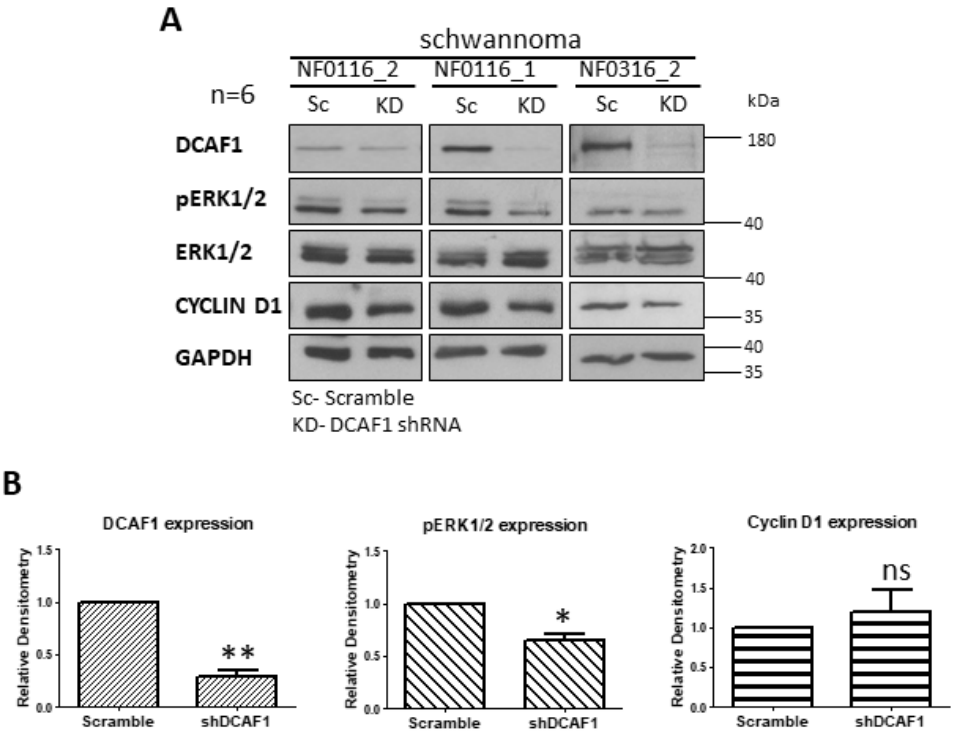

Figure 3.10 - DCAF1 knockdown reduces pERK1/2, but not CYCLIN D1 in schwannoma. A: Western blots of DCAF1, pERK1/2, ERK1/2 and CYCLIN D1 expression after DCAF1 knockdown in three schwannoma (NF) representative of six replicates. Scramble (Sc) or DCAF1 (KD) lentivirus was added to cells for 24 hours followed by a 24 hour recovery period and then seven days of puromycin selection before cell lysis. **B:** Mean DCAF1, pERK1/2 and CYCLIN D1 expression and SEM in shDCAF1 treated NF cells normalized to the loading control and relative to scramble. DCAF1 and pERK1/2 expression were reduced whilst CYCLIN D1 was unchanged in shDCAF1 treated cells compared with scramble. *- $p < 0.05$, **- $p < 0.01$, ns- not significant. GAPDH- loading control, pERK1/2 normalized to ERK1/2 and GAPDH.

To determine if DCAF1 regulates RAF/MEK/ERK signalling in meningioma, we performed the same experiment in primary meningioma and BenMen-1 cells. Whilst in some meningioma samples pERK1/2 expression was reduced, in others DCAF1 knockdown led to an increase in pERK1/2 (figure 3.11A). In addition, in BenMen-1, DCAF1 knockdown did not alter pERK1/2 or CYCLIN D1 expression (figure 3.12A-B). Therefore, DCAF1 does not regulate RAF/MEK/ERK signalling in meningioma.

Interestingly, DCAF1 knockdown resulted in a significant reduction in proliferation (as measured by proportion of Ki-67 cells) in both primary meningioma cells and BenMen-1 cells, consistent with schwannoma ($p< 0.05$) (Zhou *et al.*, 2016). Figure 3.11C and 3.12C show representative Ki-67 images at 20x magnification of meningioma and BenMen-1, respectively. DCAF1 knockdown reduced proliferation to an average of 35% of the scramble control in meningioma and to an average of 61% in BenMen-1 (figure 3.11C and 3.12D) (Student's Paired T test; $p< 0.05$). Altogether, these data suggest that RAF/MEK/ERK activity is regulated by DCAF1 in schwannoma but not in meningioma and that DCAF1 regulates proliferation in meningioma independently of RAF/MEK/ERK activity.

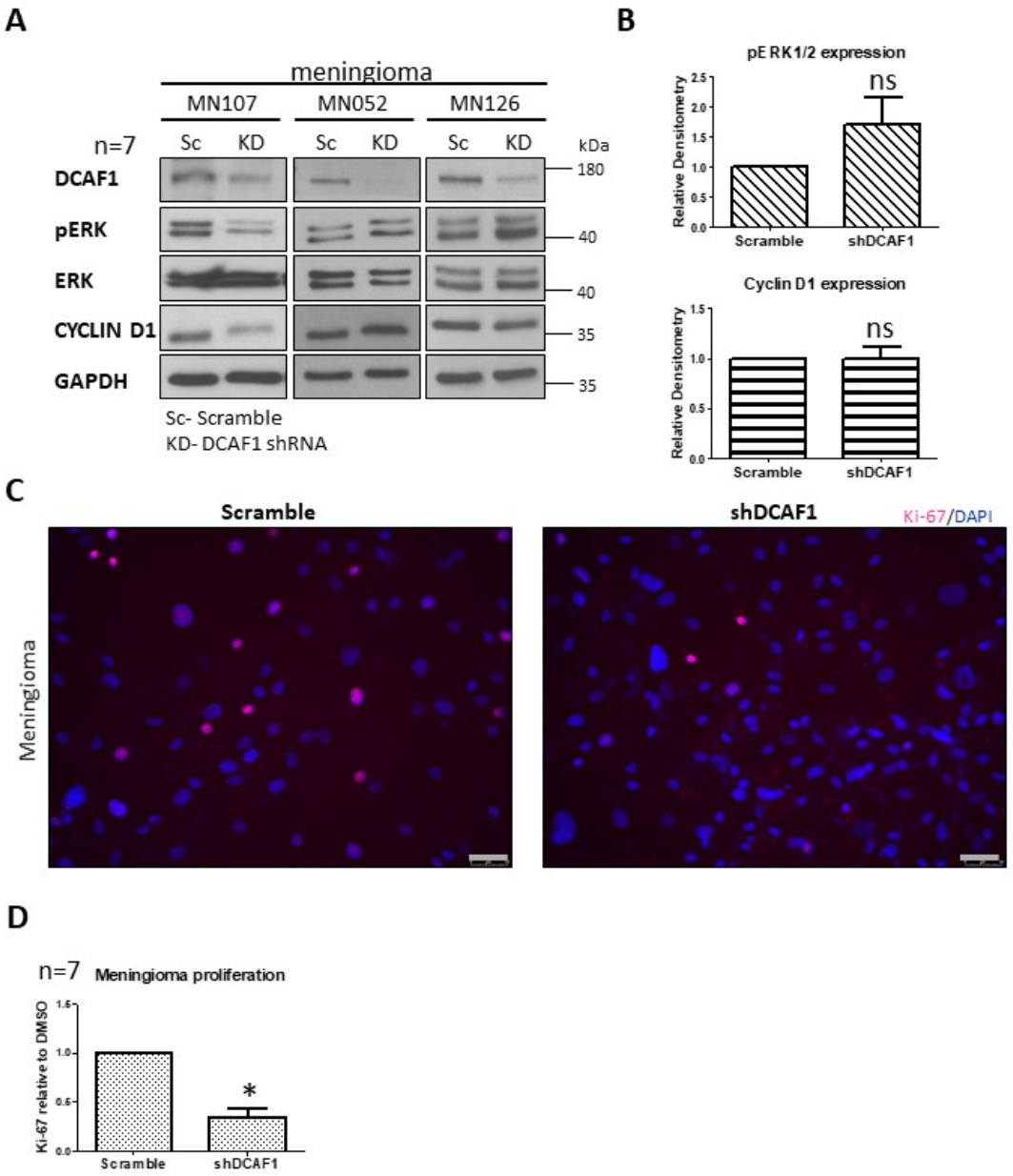

Figure 3.11 - DCAF1 knockdown does not alter pERK1/2 but significantly reduces proliferation in meningioma. A: Western blots of DCAF1, pERK1/2, ERK1/2 and CYCLIN D1 expression after Scramble (Sc) or DCAF1 knockdown (KD) in three meningioma (MN) representative of seven replicates. Scramble or DCAF1 lentivirus was added to cells for 24 hours followed by a 24 hour recovery period and then seven days of puromycin selection before cell lysis. **B:** Mean pERK1/2 and CYCLIN D1 expression and SEM in shDCAF1 treated NF cells normalized to the loading control, GAPDH and relative to scramble. pERK1/2 and CYCLIN D1 were unchanged in shDCAF1 treated cells compared with scramble (ns- not significant, $p>0.05$). pERK1/2 was normalized to both ERK1/2 and GAPDH **C:** Representative immunocytochemistry images, at 20x magnification, of scramble and shDCAF1 meningioma cells stained with Ki-67 antibody and 4',6-diamidino-2-phenylindole (DAPI), Scale bar- 50 µM. **D:** Mean proportion of Ki-67 positive cells in DCAF1 knockdown meningioma cells relative to scramble control and SEM. At least three images each of seven biological replicates were quantified. DCAF1 knockdown significantly decreased proliferation in primary meningioma,*- $p< 0.05$.

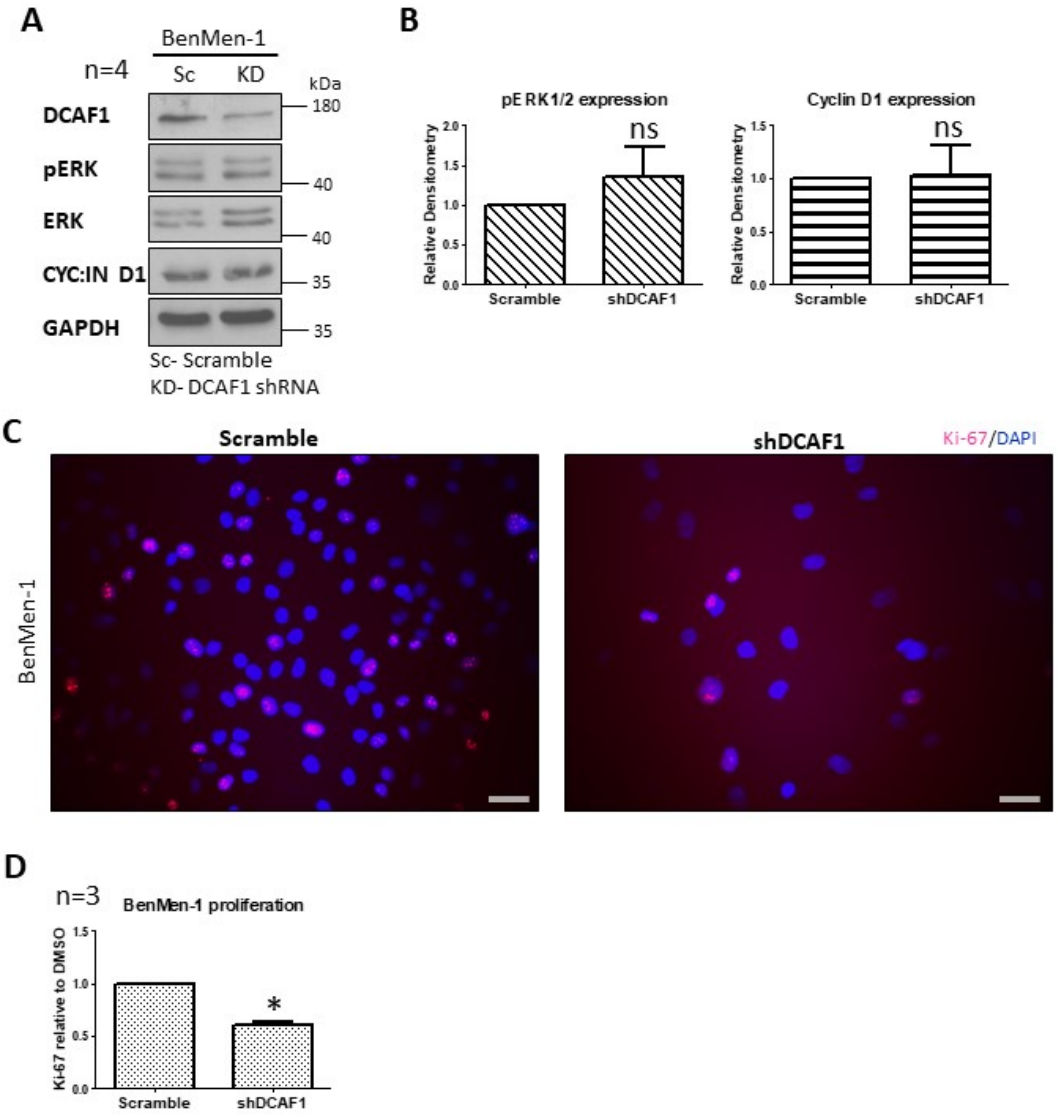

Figure 3.12 - DCAF1 knockdown does not alter pERK1/2 but significantly reduces proliferation in BenMen-1. A: Western blots of DCAF1, pERK1/2, ERK1/2 and CYCLIN D1 after DCAF1 knockdown (KD) in the Benign meningioma cell line BenMen-1, representative of four replicates. Scramble (Sc) or DCAF1 lentivirus was added to cells for 24 hours followed by a 24 hour recovery period and then seven days of puromycin selection before cell lysis. **B:** Mean pERK1/2 and CYCLIN D1 expression with SEM in shDCAF1 treated BenMen-1 cells normalized to the loading control, GAPDH and relative to scramble (ns- not significant, $p > 0.05$). pERK1/2 and CYCLIN D1 were unchanged in shDCAF1 treated cells compared with scramble. pERK1/2 was normalized to both ERK1.2 and GAPDH. **C:** Representative immunocytochemistry images, at 20x magnification, of scramble and shDCAF1 BenMen-1 cells stained with Ki-67 antibody and DAPI, Scale bar- 50 µM. **D:** Mean proportion of Ki-67 positive cells in DCAF1 knockdown BenMen-1 cells relative to scramble control with SEM. At least three images each of three replicates were quantified. DCAF1 knockdown significantly decreased proliferation in BenMen-1,*- $p < 0.05$.

3.7 Targeting DCAF1 and KSR1 together reduces proliferation in BenMen-1 similar to schwannoma

Several reports suggest that DCAF1 and KSR1 have important roles in Merlin-deficient tumourigenesis; in fact, DCAF1 and KSR1 knockdown led to a significant reduction of schwannoma cell proliferation, determined by Ki-67 index, compared with DCAF1 of KSR1 knockdown alone (Li *et al.*, 2010; Zhou *et al.*, 2016a). Therefore, we explored the hypothesis that targeting both DCAF1 and KSR1 in Merlin-deficient schwannoma, meningioma and BenMen-1 would have an additive benefit when compared with DCAF1 or KSR1 knockdown alone. We also wanted to determine if this additive effect was due to RAF/MEK/ERK pathway inhibition and therefore we examined pMEK1/2, MEK1/2, pERK1/2, ERK1/2 and CYCLIN D1 expression by Western blot in schwannoma (figure 3.13A). DCAF1 and KSR1 expression were quantified and normalized to GAPDH for three independent experiments in schwannoma (figure 3.13B). DCAF1 and KSR1 knockdown reduced DCAF1 and KSR1 protein expression levels in individual experiments, as reported in figure 3.13A but this was not significant (One-way ANOVA with Tukey Multiple Comparison Post Test, $p > 0.05$). We quantified pMEK1/2 (relative to MEK1/2 and GAPDH), pERK1/2 (relative to ERK1/2 and GAPDH) and CYCLIN D1 (relative to GAPDH) and found that adding the DCAF1 or KSR1 shRNA construct individually did not significantly reduce protein expression. pERK1/2 expression was not significantly reduced in this experimental setup, in contradiction to earlier results in this chapter as well as Zhou *et al.,* 2016a. This could be due to the different sample sizes used and different shRNA KSR1 construct used, respectively. However, we found a significant decrease in pMEK1/2 expression when DCAF1 and KSR1 shRNA constructs were added together compared with the scramble control suggesting a possible

additive effect of DCAF1 and KSR1 knockdown on RAF/MEK/ERK activity (figure 3.13B; $p < 0.05$).

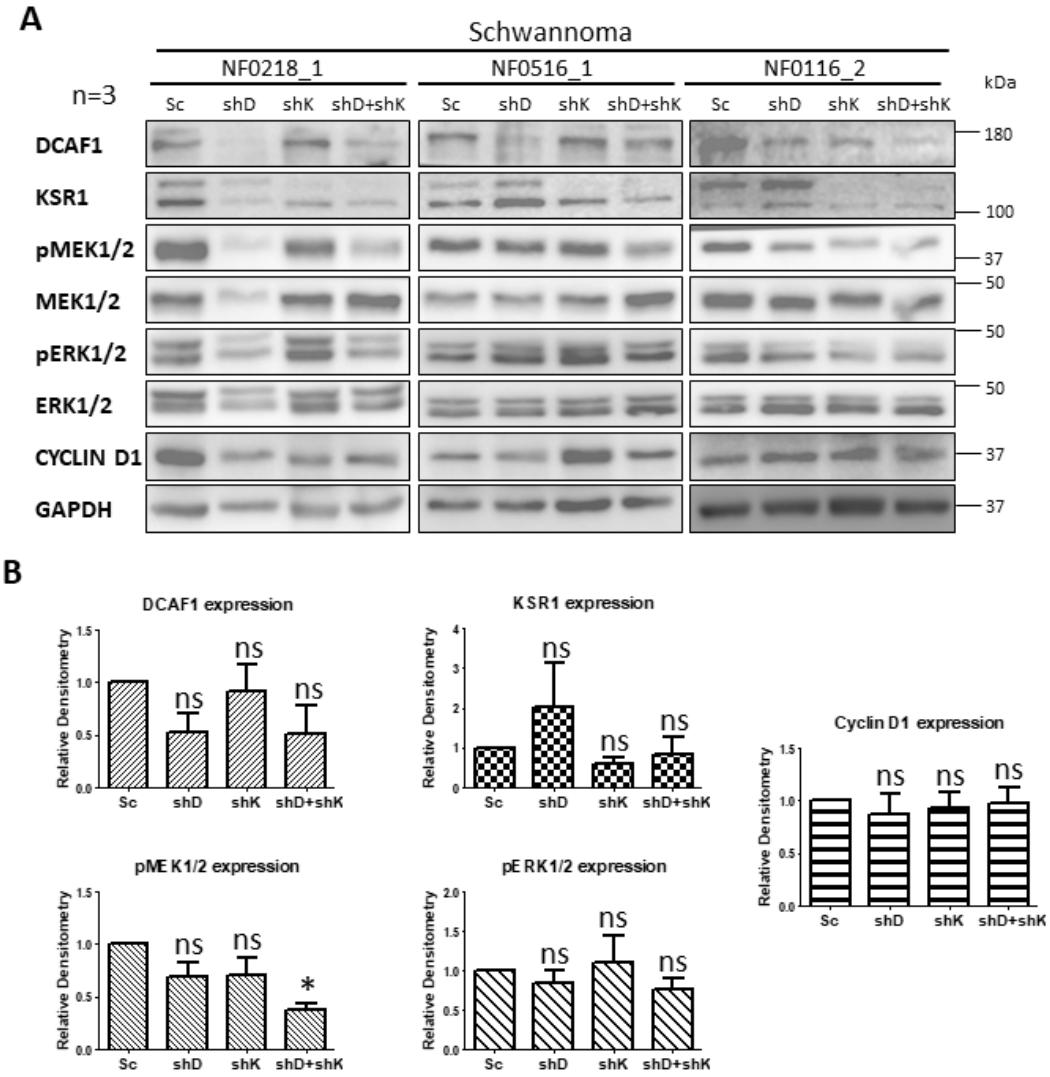

Figure 3.13 - DCAF1 and KSR1 knockdown reduces pMEK1/2 but not pERK1/2 or CYCLIN D1 in schwannoma. A: Western blots of DCAF1, KSR1, pMEK1/2, MEK1/2, pERK1/2, ERK1/2 and CYCLIN D1 expression after DCAF1, KSR1 or DCAF1 and KSR1 knockdown in schwannoma (NF) cells. Scramble, DCAF1 and/or KSR1 lentivirus was added to cells for 24 hours followed by a 24 hour recovery period and then seven days of puromycin selection before cell lysis. **B:** Mean DCAF1, KSR1, pMEK1/2, pERK1/2 and CYCLIN D1 expression and SEM in shDCAF1 (shD), shKSR1 (shK) or shDCAF1 and shKSR1 treated schwannoma cells normalized to the loading control, GAPDH and relative to scramble (Sc). pMEK1/2 was reduced in shDCAF1 and shKSR1 treated cells compared with scramble,*- $p < 0.05$. pMEK1/2 and pERK1/2 were unchanged in shDCAF1 or shKSR1 treated cells (ns- not significant, $p > 0.05$). pMEK1/2 was normalized to MEK1/2 and GAPDH, pERK1/2 was normalized to ERK1/2 and GAPDH.

We repeated the experiment in primary meningioma cells and the cell line, BenMen-1. Unfortunately, DCAF1 and KSR1 knockdown was not successful in primary meningioma cells and therefore, only data from BenMen-1 is shown. DCAF1 knockdown was significantly reduced in BenMen-1 following the addition of a DCAF1 shRNA construct ($p< 0.05$). However, whilst KSR1 was reduced after adding a KSR1 shRNA construct in individual experiments, this was not significant ($p> 0.05$, figure 3.14A-B). Unfortunately, the KSR1 shRNA construct used did not significantly reduce pERK1/2 or CYCLIN D1 expression. This is in contrast to KSR1 knockdown in schwannoma which significantly reduced both pERK1/2 and CYCLIN D1 (Zhou *et al.*, 2016a). In addition, DCAF1 and KSR1 shRNA constructs added together did not significantly affect RAF/MEK/ERK activity or CYCLIN D1 expression. Therefore, there was no additive effect of DCAF1 and KSR1 knockdown on RAF/MEK/ERK activity in meningioma.

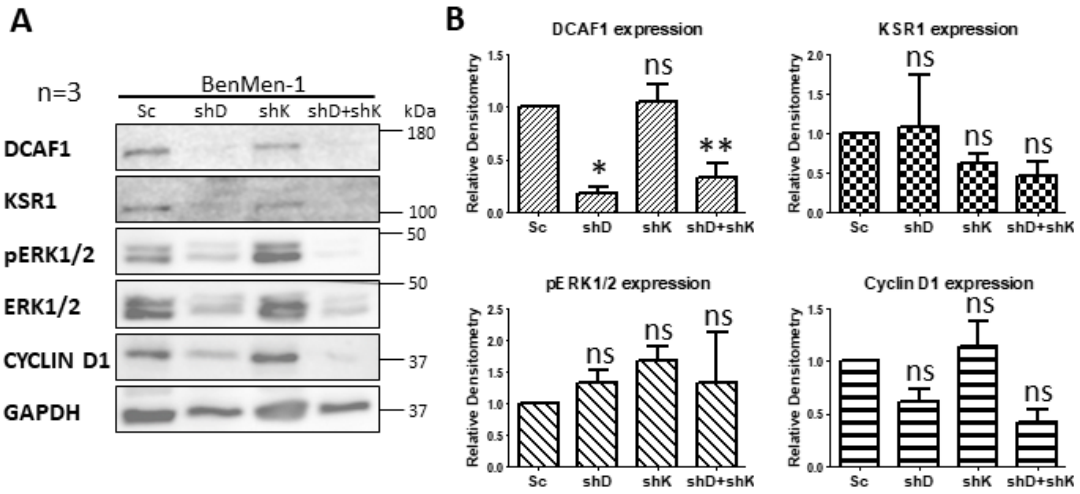

Figure 3.14 - DCAF1 and KSR1 knockdown does not reduce pERK1/2 in BenMen-1. A: Western blots of DCAF1, KSR1, pERK1/2, ERK1/2 and CYCLIN D1 expression after DCAF1, KSR1 or DCAF1 and KSR1 knockdown in the Benign meningioma cell line, BenMen-1. Scramble, DCAF1 or KSR1 lentivirus was added to cells for 24 hours followed by a 24 hour recovery period and then seven days of puromycin selection before cell lysis. **B:** Mean DCAF1, KSR1, pERK1/2 and CYCLIN D1 expression and SEM in shDCAF1 (shD), shKSR1 (shK) or shDCAF1 and shKSR1 treated BenMen-1 cells normalized to the loading control, GAPDH and relative to scramble (Sc). pERK1/2 and CYCLIN D1 were unchanged in shDCAF1 and shKSR1 treated cells compared with scramble,*- $p< 0.05$, **- $p< 0.01$, ns- not significant. pERK1/2 was normalized to ERK1/2 and GAPDH.

Interestingly, DCAF1 and KSR1 knockdown in BenMen-1 cells significantly reduced proliferation compared with scramble control and compared with either DCAF1 or KSR1 knockdown alone (figure 3.15A and B). Figure 3.15A illustrates the reduction in the proportion of Ki-67 positive cells following DCAF1 knockdown and is representative of images taken across three biological replicates. The proportion of Ki-67 cells was calculated and plotted relative to scramble control in figure 3.15B. Both DCAF1 and KSR1 knockdown alone significantly reduced proliferation whilst DCAF1 and KSR1 added together had an additive effect on proliferation (Repeated Measures ANOVA with Tukey Multiple Comparison Post Test; $p< 0.01$). This suggests that DCAF1 or KSR1 are potential targets for meningioma and that targeting both proteins can have a therapeutic benefit by contrasting tumour cell growth.

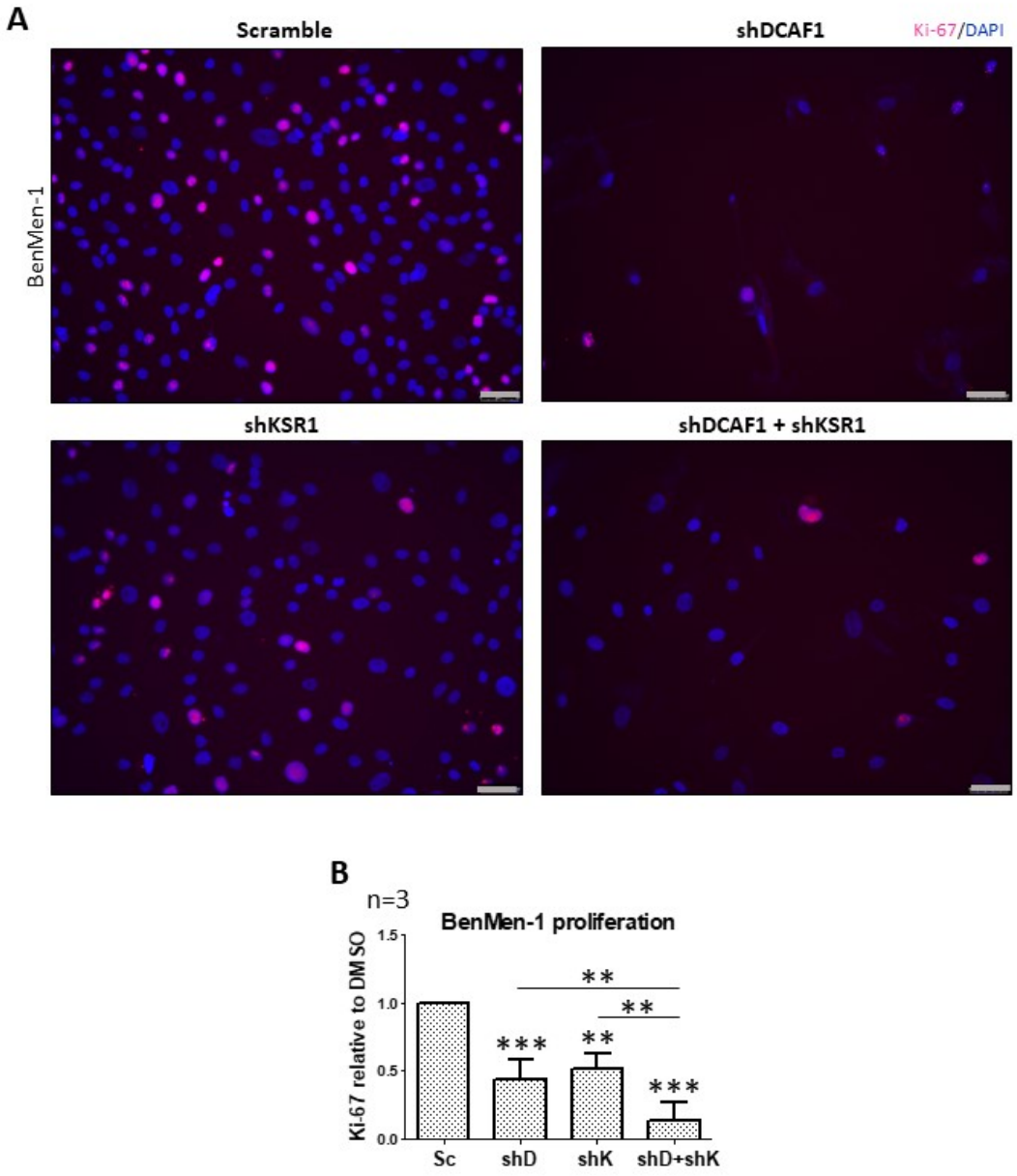

Figure 3.15 - DCAF1 and KSR1 knockdown reduces proliferation of BenMen-1 cells. A: Representative immunocytochemistry images, at 20x magnification, of scramble, shDCAF1, shKSR1 and shDCAF1 and shKSR1 in BenMen-1 cells stained with Ki-67 antibody and DAPI, Scale bar- 50 µM. **B:** Mean proportion of Ki-67 positive cells in knockdown BenMen-1 cells relative to scramble control and SEM. At least three images each of three replicates were quantified. DCAF1 and KSR1 knockdown significantly decreased proliferation compared with either DCAF1 or KSR1 knockdown alone, **- $p < 0.01$, ***- $p < 0.001$.

3.8 Discussion

Whilst DCAF1 protein was clearly over-expressed in tissue samples, the expression was much more variable in schwannoma cells derived from schwannoma tumour tissue (figure 3.1 and 3.2). There was also a large variation in DCAF1 expression in Schwann cells, most probably due to variation in proliferative rates *in vitro* (figure 3.2). Growth factors are added to cell culture medium to stimulate Schwann cell growth and can have varying effects at different passages. We excluded the possibility of cell contamination by confirming more than 90% S100 protein expression (figure 2.2), characteristic of Schwann cells. Analysis of tissue samples is more reflective of *in vivo* protein expression than analysis of cells derived from tissue. However, cells have the added benefit of allowing *in vitro* drug testing and analysis of cell signalling mechanisms; therefore, they represent a highly relevant model.

Both, DCAF1 and KSR1 were highly expressed in meningioma tissue and were significantly higher than the expression levels in meninges (figure 3.3). However, there was also a large proportion of cells in the meninges that expressed KSR1. Often with immunohistochemistry, there is more non-specific staining around the edges of the tissue, coincidently, the location of the meninges (True, 2008). Therefore, some DCAF1 and KSR1 staining may be artefact and may not reflect real meningeal expression. We also analysed DCAF1 and KSR1 expression in tissue by Western blot to confirm overexpression (figure 3.4). There were a lot of non-specific staining of DCAF1 and KSR1 in the meninges but DCAF1 and KSR1 expression in meningioma was significantly higher and the Western blot band corresponding to the correct protein size was much clearer in meningioma tissue than in meninges demonstrating that DCAF1 and KSR1 are overexpressed in meningioma tissue.

We derived meningioma cells from meningioma tissue and compared DCAF1 and KSR1 expression with that of human meningeal cells (HMC), which were derived from embryonic/fetal meningeal cells and grown in medium enriched with growth factors. This can make comparison between HMC and adult meningioma tissue difficult. Despite this, DCAF1 and KSR1 protein expression was significantly increased in meningioma cells compared with HMC (figure 3.4). As expected, we detected some variability in expression between tumours, similar to schwannoma. In addition, one particular meningioma sample had very low DCAF1 and KSR1 expression (MN006). We analysed the clinical data and discovered that the tumour was removed after radiation treatment. Therefore, we did not include this tumour in the subsequent Western blot analysis.

There were a number of samples with loss of Merlin expression and a confirmed heterozygous *Traf7* mutation including MN078, MN036 and MN056. *Nf2* and *Traf7* mutations are mutually exclusive in meningioma and therefore it is unlikely that the *Traf7* mutant meningioma samples also have an *Nf2* mutation (Clark *et al.*, 2013; Zotti *et al.*, 2017). Therefore, we removed these samples from Western blot analysis and subsequent experiments. The absence of Merlin protein in *Traf7* mutant samples suggests that TRAF7 could regulate Merlin expression. The expression of Merlin protein in non-Merlin mutant meningioma tumours has not yet been reported in the literature. Sequencing of the *Nf2* gene to identify and confirm the Merlin mutation in each tumour would be beneficial, although this would be expensive considering the number of samples used.

We discovered that DCAF1 and KSR1 were not significantly upregulated in BenMen-1 compared with HMC (figure 3.4). DCAF1 was significantly overexpressed in KT21-MG1-

Luc5D compared with HMC whereas KSR1 was unchanged. These results were disappointing as we had hoped for a Merlin-deficient meningioma model with high levels of DCAF1 and KSR1 expression so we could more easily investigate the DCAF1 and KSR1 interaction.

DCAF1 knockdown did not lead to an increase in KSR1 protein, confirming that KSR1 degradation is not regulated by DCAF1 in meningioma (figure 3.5). Whilst it may seem logical to overexpress DCAF1 to show that KSR1 protein is not downregulated, DCAF1 exists in an E3 ubiquitin complex containing several proteins (Cullin 4A/B and DDB1), which modulate its ubiquitination function, therefore, overexpressing DCAF1 alone would be unlikely to alter ubiquitin functions.

KSR1 overexpression had been previously reported in schwannoma; therefore, we wanted to determine the localization of KSR1 (Zhou *et al.*, 2016a). In Schwann cells, KSR1 was predominantly nuclear, which is in contrast to published data suggesting KSR1 is cytoplasmic and is redistributed to the cell membrane when signalling is activated (Müller *et al.*, 2001). KSR1 cycles through the nucleus similar to MEK1/2 and ERK1/2 (Kortum *et al.*, 2005; Razidlo *et al.*, 2004). However, there is no known role of nuclear KSR1. In schwannoma, KSR1 was localized to the cytoplasm and nucleus suggesting increased cytoplasmic signalling which may be Merlin-dependent. However, there was no increase in cytoplasmic KSR1 in BenMen-1 compared with HMC demonstrating that the increase in cytoplasmic KSR1 observed in schwannoma may not be Merlin-dependent.

If KSR1 localization was regulated by DCAF1, we would see a decrease in cytoplasmic KSR1 upon DCAF1 knockdown. However, we did not see any significant changes in KSR1 localization in schwannoma (figure 3.7). We replicated these experiments in

meningioma to confirm DCAF1's role (figure 3.9 and supplementary figure 2). As expected, DCAF1 knockdown did not consistently alter KSR1 localization in primary meningioma or BenMen-1. Therefore, DCAF1 does not regulate KSR1 expression or localization in Merlin-deficient cells.

Phosphorylated ERK1/2 was significantly reduced upon DCAF1 knockdown in schwannoma; however, there was only a 35% reduction suggesting that KSR1 activity is only partly dependent on DCAF1 (figure 3.10). Conversely, it could also suggest that RAF/MEK/ERK activity is only partially dependent on active KSR1 in schwannoma. CYCLIN D1 expression, a downstream target of pERK1/2, did not change demonstrating that the inhibition of ERK1/2 phosphorylation was not sufficiently high enough to affect CYCLIN D1. Unfortunately, DCAF1-dependent inhibition of pERK1/2 was not translatable to meningioma. In some experiments, pERK1/2 was reduced upon DCAF1 knockdown, whereas in others it was increased (figure 3.11 and figure 3.12). This suggests that there is much more variability in the primary meningioma cohort than in primary schwannoma. In addition, there was a much smaller reduction in DCAF1 expression upon DCAF1 knockdown in meningioma compared with schwannoma that may not have been sufficient to inhibit RAF/MEK/ERK activity.

DCAF1 knockdown significantly reduced the proliferation of both primary meningioma cells and BenMen-1 (figure 3.11 and 3.12). As there were no significant changes in pERK1/2 expression upon DCAF1 knockdown, this suggests that DCAF1 knockdown reduces proliferation independent of KSR1 and RAF/MEK/ERK activity in meningioma. However, there may be a proportion of cells that have a greater DCAF1 knockdown and therefore some cells stop proliferating in a RAF/MEK/ERK dependent manner whereas others retain more DCAF1 protein and continue to proliferate. This is more

the case in BenMen-1 as a greater proportion of cells are still proliferating upon DCAF1 knockdown (figure 3.12). Whilst the best method of protein knockdown is to isolate individual clones, this was not possible with primary schwannoma or meningioma cells (including BenMen-1) as they need close contact with other tumour cells in order to proliferate.

We previously demonstrated that targeting both DCAF1 and KSR1 in schwannoma had an additive effect on reducing proliferation in schwannoma (Zhou *et al.*, 2016a). We wanted to determine if DCAF1 and KSR1 together had an additive effect on RAF/MEK/ERK inhibition to demonstrate potential for a combination therapy targeting these two proteins. Unfortunately, there was no significant DCAF1 or KSR1 knockdown in schwannoma (figure 3.13). This is possibly because the sample size used (n=3) did not have enough power to detect the change in DCAF1 and KSR1 expression. In individual experiments, a decrease in DCAF1 and KSR1 can be clearly seen. We used a different shRNA construct targeting KSR1 than has previously been published in schwannoma because we had difficulty transfecting primary meningioma and BenMen-1. This KSR1 construct did not reduce pERK1/2 or CYCLIN D1 in schwannoma, in contrast to published data (Zhou *et al.*, 2016a). This is probably because the knockdown was less successful and therefore KSR1 was still active in KSR1 knockdown lysates. However, DCAF1 and KSR1 knockdown significantly reduced pMEK1/2 in schwannoma suggesting more robust and consistent inhibition of MEK1/2 activity in comparison to DCAF1 or KSR1 knockdown alone.

We added DCAF1 and KSR1 shRNA constructs to BenMen-1 cells and probed for the RAF/MEK/ERK pathway (figure 3.14). DCAF1 was successfully knocked down whereas the reduction in KSR1 expression was not significant. DCAF1 and KSR1 knockdown did

not reduce pERK1/2 or CYCLIN D1 expression. KSR1-dependent RAF/MEK/ERK activation has not been fully explored in meningioma and therefore future experiments should use a more effective shRNA construct to knockdown KSR1. Interestingly, KSR1 knockdown significantly reduced BenMen-1 proliferation, suggesting that the Western blot experiment did not have enough statistical power to detect the knockdown (figure 3.15). In addition, DCAF1 and KSR1 knockdown significantly reduced proliferation compared with either construct alone. This demonstrates the additive value of targeting both DCAF1 and KSR1 in schwannoma and meningioma.

DCAF1 also leads to Hippo pathway inactivation and therefore activation of gene transcription (Li *et al.*, 2014). The inhibitory effect of DCAF1 knockdown on Merlin-deficient schwannoma and meningioma proliferation could be Hippo pathway-dependent rather than RAF/MEK/ERK-dependent and this possibility must be further investigated. Indeed, it has been shown that the Hippo pathway is inhibited in Merlin-deficient cells, contributing to tumourigenesis (Li *et al.*, 2014; Serrano *et al.*, 2013; Striedinger *et al.*, 2008).

3.9 Conclusion

DCAF1 and KSR1 are upregulated in Merlin-deficient cells, including schwannoma and meningioma. The expression of these proteins is variable between individual tumours and the meningioma cell line, BenMen-1. DCAF1 regulates RAF/MEK/ERK activity in schwannoma which may be KSR-1-dependent. DCAF1 does not significantly affect RAF/MEK/ERK activity in primary meningioma or BenMen-1; however, DCAF1 knockdown significantly reduces proliferation of schwannoma, meningioma and BenMen-1, suggesting that DCAF1 is a potential therapeutic target for Merlin-deficient

tumours. In addition, DCAF1 and KSR1 knockdown further reduced proliferation of BenMen-1 cells compared with either knockdown alone, therefore, targeting both DCAF1 and KSR1 may be beneficial.

Chapter 4 - Characterising the DCAF1/KSR1 interaction

4.1 Introduction

Merlin has been shown to inhibit DCAF1 ubiquitin ligase activity in the nucleus (Li *et al.*, 2014; Li *et al.*, 2010). In Merlin-deficient tumours, DCAF1 is therefore activated and contributes to tumourigenesis. The mechanisms of DCAF1-mediated tumourigenesis is not fully understood. We previously showed that KSR1 was upregulated and important in Merlin-deficient tumourigenesis (Zhou *et al.*, 2016a).

We co-immunoprecipitated overexpressed Merlin and overexpressed KSR1 in a HEK293T model (Zhou *et al.*, 2016a). Mass spectrometry revealed CRL4-DCAF1 components as common interactors between Merlin and KSR1 (Zhou *et al.*, 2016a). The DCAF1/KSR1 interaction was confirmed by immunoprecipitating overexpressed KSR1 in HEK293T cells and probing for DCAF1 via Western blot (Zhou *et al.*, 2016a). Therefore elucidating KSR1's involvement in DCAF1-mediated tumourigenesis is pertinent. The aim of this chapter is to show that endogenous DCAF1 and KSR1 interact in a Merlin-deficient model, to identify if DCAF1 and KSR1 interact in the nucleus and to further characterize the DCAF1/KSR1 interaction using overexpressed protein in HEK293T cells.

4.2 Endogenous DCAF1 and KSR1 interact in Merlin-deficient meningioma

To show that there is an endogenous DCAF1/KSR1 interaction in Merlin-deficient cells we used the benign Merlin-deficient meningioma cell line, BenMen-1. BenMen-1 protein lysate was concentrated and DCAF1 was immunoprecipitated from 3 mg of protein using a DCAF1 antibody. We used IgG as a negative immunoprecipitation control to determine any proteins interacting with IgG of the same species of the DCAF1 antibody. The immunoprecipitated samples were separated by Western blot along with an input sample of BenMen-1 lysate (to show endogenous protein

expression) and probed for DCAF1, KSR1 and DDB1 (figure 4.1A and supplementary figure 3B-C). DCAF1 and DDB1 (positive control) were detected in the DCAF1 lane and was absent in the IgG lane demonstrating successful DCAF1 immunoprecipitation. A band corresponding to KSR1 was detected when DCAF1 was immunoprecipitated suggesting that endogenous DCAF1 and KSR1 interact in Merlin-deficient cells (figure 4.1A and supplementary figure 3B-C).

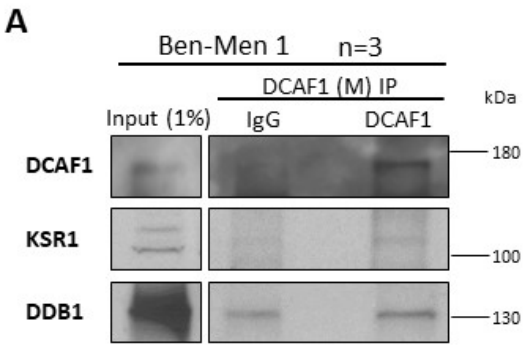

Figure 4.1 - Endogenous DCAF1 and KSR1 interact in BenMen-1. A: Western blot of DCAF1, KSR1 and DDB1 in the benign meningioma cell line, BenMen-1 (input), immunoprecipitated IgG and immunoprecipitated DCAF1 from 3mg BenMen-1 protein lysate, representative of three replicates. DCAF1 was immunoprecipitated from BenMen-1 lysates using a mouse (M) DCAF1 antibody (Proteintech). KSR1 and DDB1 were present in the DCAF1 complex.

Interestingly, an additional band, 130–180 kDa in size, was visible when probing with a KSR1 antibody that was specific to immunoprecipitated DCAF1 and was absent in the IgG lane (supplementary figure 3A-C). This additional band was also present when immunoprecipitating DCAF1 using 3 mg of protein from KT21-MG1-Luc5D cells (supplementary figure 3D) (n=1). We were unable to detect KSR1 in the DCAF1 complex when DCAF1 was immunoprecipitated from an alternative Merlin-deficient model (schwannoma lysate and tissue) although much less protein was available (< 1 mg) (data not shown). To confirm the DCAF1/KSR1 interaction, we immunoprecipitated the KSR1 complex in BenMen-1 using 3 mg protein and unfortunately we were unable to detect DCAF1 probably due to the low endogenous expression of KSR1 in BenMen-1 (data not shown).

4.3 The C-terminus of DCAF1 interacts with the N-terminus of KSR1 in the cytoplasm and nucleus

We wanted to identify the DCAF1 domains responsible for KSR1 binding to determine a possible function of the DCAF1/KSR1 interaction. DCAF1 plasmids corresponding to the wild type DCAF1 sequence (D1), the N terminus (1–744 amino acids (aa)) (D2) and the C terminus (745–1507 aa) (D3), all with a myc-tag were used and figure 4.2A illustrates the domains in each plasmid sequence. D2 contained the armadillo-like and cromo-like domains whereas D3 contained the LisH, WD40 and acidic domains of DCAF1. The restriction enzymes, SalI and NotI were used to digest the plasmids and we confirmed the expected DNA bands for D1, D2 and D3 digestion by agarose gel electrophoresis (figure 2.4). We transfected HEK293T cells with the D1, D2 and D3 plasmids and confirmed DCAF1 overexpression using a myc-tag antibody. We then used a myc-tag antibody to immunoprecipitate the DCAF1-containing complexes, from 1 mg of

HEK293T protein, and separated these proteins by Western blot. We probed the membrane for myc-tag and confirmed that overexpressed DCAF1 protein was successfully immunoprecipitated (figure 4.2B and supplementary figure 4A-B). We also immunoprecipitated myc-tag containing complexes in non-transfected HEK293T cells which identified non-specific protein binding to the myc-tag antibody. The D1 immunoprecipitated complex did not contain KSR1, as there was no specific band visible (that was also absent in the non-transfected control) around 100 kDa when probing with KSR1 antibody. The D2 (N-terminal DCAF1) immunoprecipitated complex also did not contain KSR1 whereas the D3 (C-terminal DCAF1) immunoprecipitated complex did contain KSR1. The D3 complex had a clear band, around 100 kDa, when probing with KSR1 antibody in all three repeats (indicated by an arrow) (figure 4.2B and supplementary figure 4A-B). DDB1 was present in the D1 and D3 complexes, as expected, suggesting that the DCAF1 immunoprecipitation successfully pulled down DCAF1-interacting proteins. Unexpectedly, there was an additional KSR1 reactive band, around 180 kDa, detected in the D1 complexes which was absent in the non-transfected control and D2. A faint 180 kDa band can also be seen in two out of three repeats in the D3 complex (figure 4.2B and supplementary figure 4B). We repeated the experiment using an alternative myc-tag antibody to determine if the results seen in figure 4.2 could be replicated (supplementary figure 4C). We immunoprecipitated the DCAF1 containing complexes and identified KSR1 in the D3 complex and a 180 kDa KSR1-reactive band in the D1 complex (n=1).

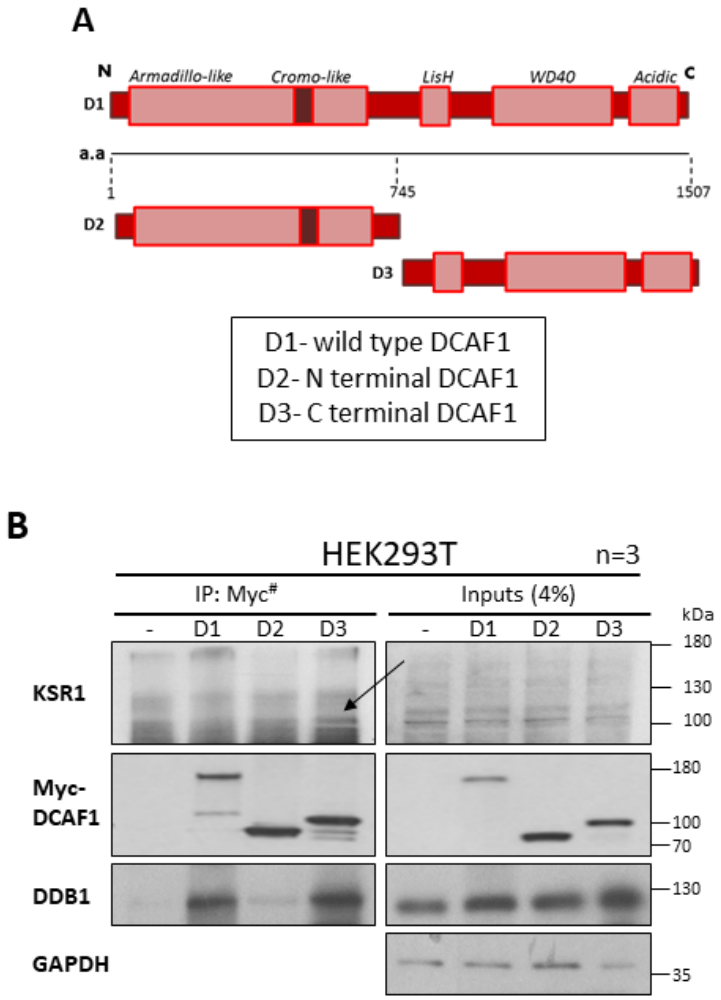

Figure 4.2 - DCAF1 interacts with KSR1 via the C terminal of DCAF1. A: DCAF1 domains within sequences used. wild type DCAF1 (D1) contained an armadillo-like and cromo-like domain at the N terminal followed by a LisH domain, a WD40 domain and an acidic C-terminal domain. The N-terminal DCAF1 (D2) sequence (1–744 amino acids (a.a)) contained the armadillo-like and cromo-like domain. The C-terminal DCAF1 (D3) sequence (745–1507 a.a) contained the LisH, WD40 and acidic domains. **B:** The DCAF1 sequences D1, D2 and D3, with a Myc-tag, were overexpressed in HEK293T and immunoprecipitated from 1 mg HEK293T using a Myc-tag antibody. The Western blot shown is representative of three repeats and was probed for KSR1, Myc, DDB1 and GAPDH. KSR1 was present in the C-terminal DCAF1 complex (D3) (indicated by the arrow) and a high molecular weight KSR1-reactive band was present in the wild-type DCAF1 (D1) complex. Myc-tag antibody reactive proteins were immunoprecipitated from non-transfected HEK293T (-) as a negative control.

To explore the DCAF1/KSR1 interaction further we used KSR1 plasmids corresponding to wild-type KSR1 (K1), N-terminal KSR1 (1–539 aa) (KN) and C-terminal KSR1 (540–873 aa) (KC), all with a FLAG tag, to determine the domains responsible for DCAF1 binding (figure 4.3A). We confirmed plasmid identity using restriction enzymes to digest the plasmid at specific known sites producing bands of expected sizes (figure 2.5). For example, the pCMV5 vector containing the wild-type KSR1 sequence (K1) was digested using the EcorI and KpnI restriction enzymes producing DNA bands at 4700 bp and 2700 bp as expected according to the plasmid map (figure 2.5). We transfected HEK293T with the K1, KC and KN plasmids to overexpress the KSR1 proteins and immunoprecipitated these complexes using a FLAG tag antibody. We separated the protein complexes by Western blot and probed for DCAF1, DDB1, FLAG and MEK1/2 (figure 4.3B and supplementary figure 5A-B). We confirmed successful FLAG-KSR1 immunoprecipitation and identified MEK1/2 in the K1 and KC complexes as expected. DCAF1 and DDB1 were identified in the K1 and KN complex demonstrating that the CRL4-DCAF1 complex interacts with the N-terminal of KSR1 (1–539 aa). In two out of three replicates, DCAF1 and DDB1 were also present in the KC immunoprecipitated complex, however, the band was much weaker suggesting decreased DCAF1 binding in the absence of the CA1-CA4 domains.

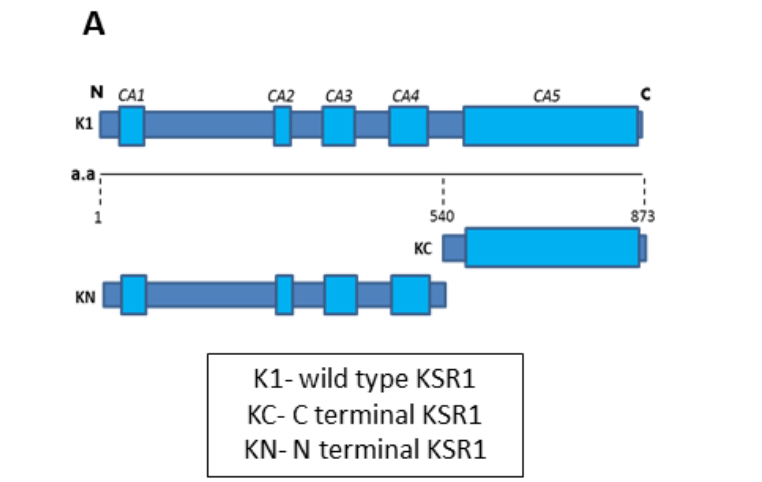

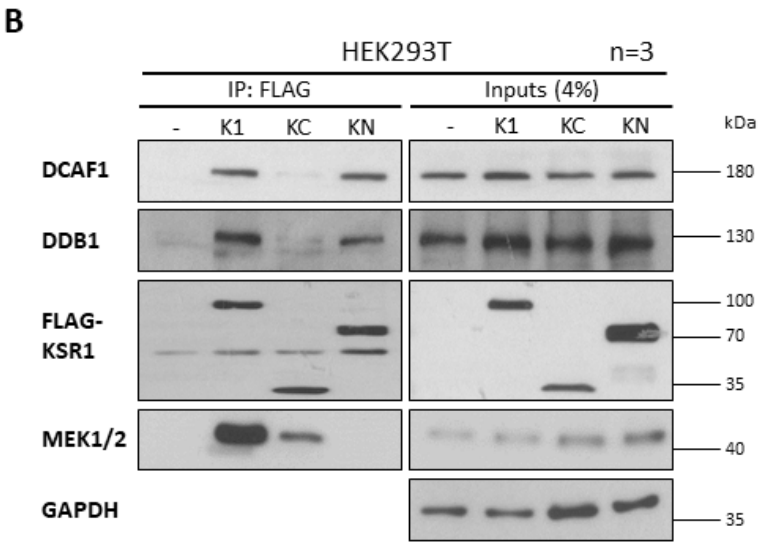

Figure 4.3 - KSR1 interacts with the CRL4-DCAF1 complex via the N-terminal of KSR1. A: KSR1 domains within the sequences used**.** Wild type KSR1 (K1) contained CA1–5 domains. The N-terminal KSR1 (KN) sequence (1–539 amino acids (a.a)) contained CA1–4 domains. The C-terminal KSR1 (KC) sequence (540–873a.a) contained the CA5 domain. **B:** The KSR1 sequences K1, KC and KN, with a FLAG-tag, were overexpressed in HEK293T and immunoprecipitated from 1 mg HEK293T using a FLAG-tag antibody. The Western blot shown is representative of three repeats and was probed for DCAF1, DDB1, FLAG, MEK1/2 and GAPDH. DCAF1 and DDB1 were present in the wild-type and N-terminal KSR1 complexes. FLAG-tag interacting proteins were immunoprecipitated from non-transfected HEK293T (-) as a negative control.

As the Merlin/DCAF1 interaction occurs in the nucleus, we wanted to determine if the DCAF1/KSR1 interaction is also nuclear and thus highlight the possible nature of the interaction. First, we wanted to establish where the KSR1 constructs localized in the cell (figure 4.4A). We transfected K1, KC and KN in HEK293T cells and stained the cells with a FLAG-tag antibody counterstained with DAPI. K1 predominantly localized to the cytoplasm with some nuclear expression observed (figure 4.4A). Similarly, KC was predominantly cytoplasmic with stronger peri-nuclear staining and some nuclear expression. Conversely, KN was mostly nuclear with weaker cytoplasmic expression. As all three complexes were present in both the cytoplasm and the nucleus of HEK293T cells, the DCAF1 interaction may occur in either of these locations.

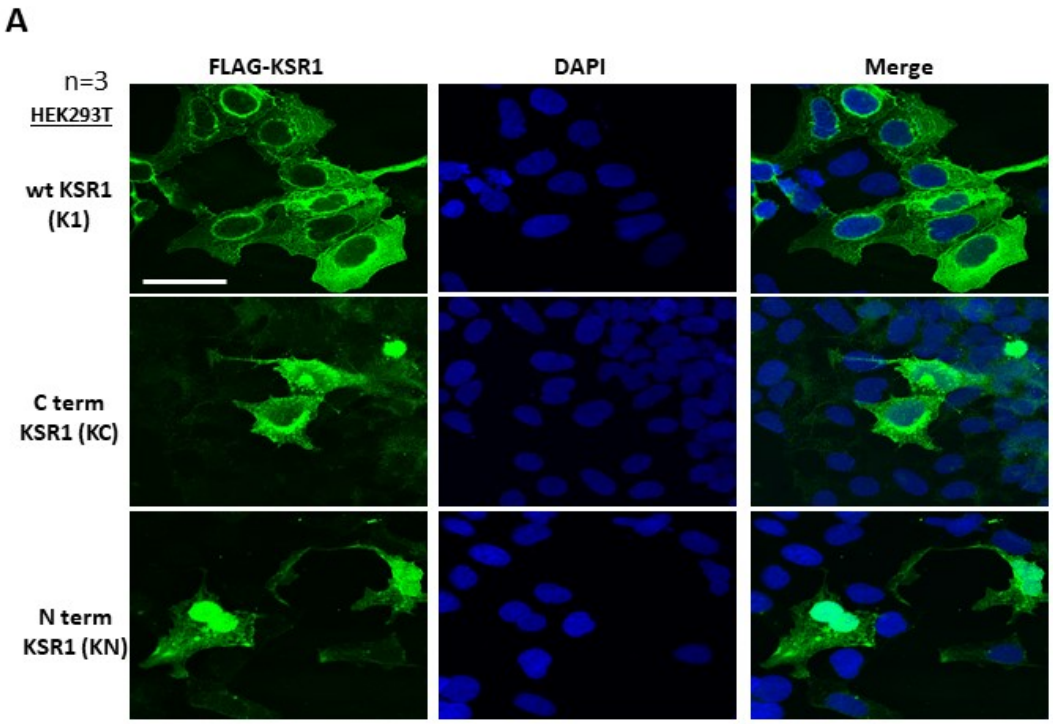

Figure 4.4 - KSR1 construct localization in HEK293T cells. A: HEK293T cells were transfected with wild type KSR1 (K1), C-terminal KSR1 (KC) sequence (540–873 amino acids (a.a)) or N-terminal KSR1 (KN) sequence (1–539 a.a) and stained with FLAG-tag antibody (Sigma) (green) and DAPI nuclear stain. Images were taken at 60x magnification, scale bar- 50 µM. The images show that K1 is predominantly localized to the cytoplasm. KC is also predominantly expressed in the cytoplasm. KN is predominantly expressed in the nucleus but is also present in the cytoplasm.

We overexpressed K1 in HEK293T cells and then performed cytoplasmic and nuclear extraction. Figure 4.5A shows successful fractionation as HDAC1 was mostly nuclear and GAPDH was mostly cytoplasmic as expected. K1 was also confirmed to be present in the cytoplasm and the nucleus of transfected cells although there was much more cytoplasmic expression. Endogenous DCAF1 and DDB1 were confirmed in the cytoplasm and nucleus of HEK293T cells. Interestingly, DCAF1 was mostly cytoplasmic in contrast to Schwann and schwannoma cells in which DCAF1 is mostly nuclear.

We immunoprecipitated the K1 complex using a FLAG-tag antibody in at least 100 µg of K1 transfected total, cytoplasmic and nuclear HEK293T lysates (figure 4.5B). We also immunoprecipitated FLAG-tag binding proteins from non-transfected total, cytoplasmic and nuclear HEK293T lysates as a control to determine non-specific binding to the FLAG-tag antibody. Figure 4.5B shows that DCAF1 and DDB1 interact in the cytoplasm and the nucleus of HEK293T cells in a complex with MEK1/2. There was more DCAF1 in the cytoplasmic KSR1 complex than the nuclear complex, however, the predominant cytoplasmic DCAF1 distribution in the immunoprecipitation input samples should be considered.

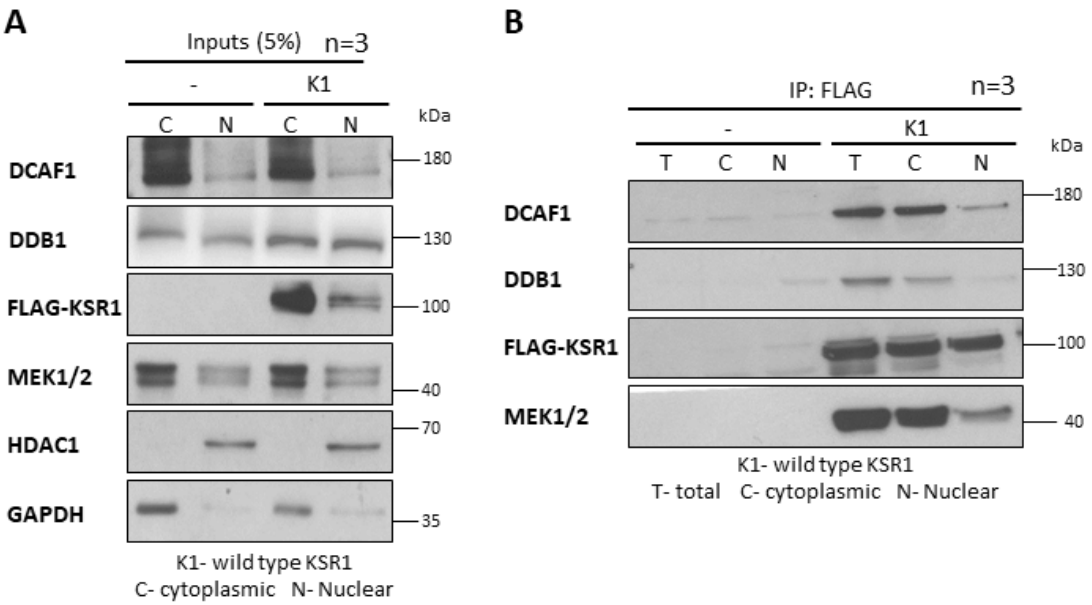

Figure 4.5 - The DCAF1/KSR1 interaction occurs both in the cytoplasm and nucleus of HEK293T cells. A: Wild-type KSR1 (K1) with a FLAG-tag was overexpressed in HEK293T cells and the cytoplasm and nucleus was extracted from HEK293T lysate. The Western blot shows that DCAF1, DDB1, FLAG and MEK1/2 are present in the cytoplasmic (C) and nuclear (N) fractions. HDAC1 and GAPDH are nuclear and cytoplasmic respectively and determine cross-contamination between fractions. **B:** K1 was immunoprecipitated from the total (T), cytoplasmic and nuclear fractions using a FLAG-tag antibody. The Western blot shows DCAF1, DDB1, FLAG and MEK1/2 in non-transfected (-) and K1-transfected immunoprecipitates, representative of three repeats. DCAF1 and DDB1 were in the cytoplasmic KSR1 complex. DCAF1 was also present in the nuclear KSR1 complex.

4.4 C-terminal KSR1 ubiquitination is not dependent on DCAF1

We suspected that KSR1 was a CRL4-DCAF1 substrate for ubiquitination and therefore we immunoprecipitated overexpressed truncated KSR1 constructs to determine if KSR1 was ubiquitinated. We overexpressed K1, KC and KN in HEK293T followed by FLAG-KSR1 immunoprecipitation and Western blotting in the same experimental set up as figure 4.3. We probed the entire membrane with an ubiquitin antibody and found that K1 and KC are poly-ubiquitinated (figure 4.6A).

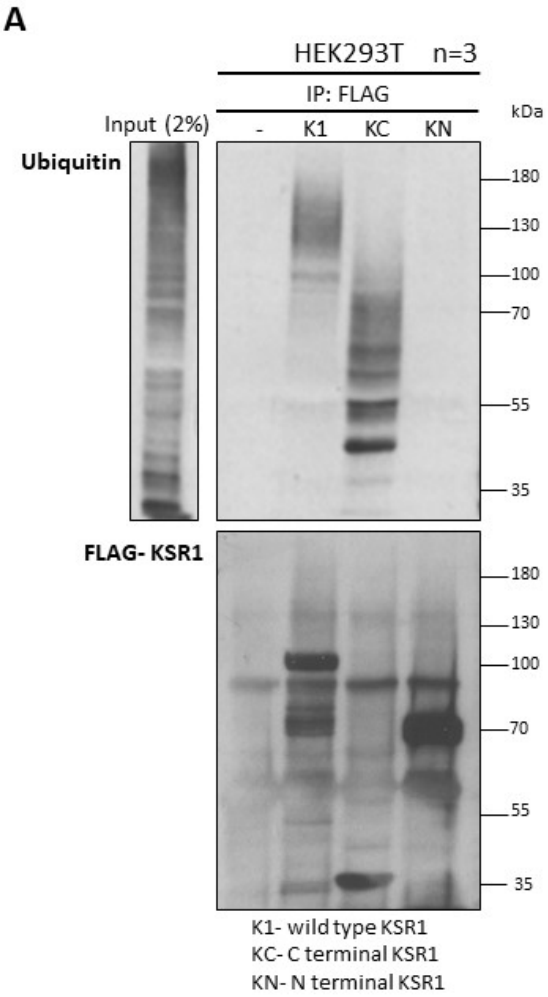

Figure 4.6 - Wild type KSR1 and C-terminal KSR1 are ubiquitinated in HEK293T cells. A: The KSR1 sequences K1, KC and KN, with a FLAG-tag, were overexpressed in HEK293T and immunoprecipitated from 1 mg HEK293T protein lysate using a FLAG-tag antibody. The Western blot shown is representative of three repeats and was probed for Ubiquitin and FLAG-tag. Ubiquitin was present in the K1 and KC complexes and not the KN complex. FLAG-tag interacting proteins were immunoprecipitated from non-transfected HEK293T (-) as a negative control. HEK293T protein lysate (input) was probed with ubiquitin to show endogenous expression prior to the immunoprecipitation.

We then wanted to determine if KSR1 poly-ubiquitination was dependent on DCAF1 expression. In the HEK293T model we used a shRNA construct targeting DCAF1 expression and then overexpressed human wild type KSR1 (hK1) tagged with FLAG using an overexpression lentiviral vector. We confirmed successful DCAF1 knockdown and hK1 overexpression by Western blot using DCAF1, FLAG and KSR1 (H70) antibodies (figure 4.7A). We used these lysates as well as appropriate scramble control lysates and immunoprecipitated hK1 with a FLAG tag antibody. The immunoprecipitated proteins were separated by Western blot and probed with an ubiquitin antibody (figure 4.7B). There were no clear or consistent differences in the amount of ubiquitin present in the hK1 complexes between scramble and DCAF1 knockdown lysates. Successful and comparable FLAG-hK1 immunoprecipitation was confirmed in figure 4.8A and supplementary figure 6A-B.

4.5 DCAF1 facilitates the association of KSR1 with MEK1/2 and ERK1/2

To understand the purpose of the DCAF1/KSR1 interaction, we immunoprecipitated hK1 complexes and experimental input samples from the previous experiment and probed for components of the RAF/MEK/ERK pathway by Western blot (figure 4.7). KSR1 is a scaffold protein that facilitates RAF/MEK/ERK pathway activation and therefore we also probed for phosphorylated MEK1/2 and ERK1/2. Figure 4.8A and supplementary figure 6A-B shows that DCAF1 knockdown reduced the amount of total MEK1/2 and ERK1/2 in the KSR1 complex. Total C-RAF (figure 4.8) was decreased in one replicate and increased in one replicate (supplementary figure 6A) when DCAF1 expression is reduced, whilst it was absent in supplementary figure 6B. Phosphorylated MEK1/2 and ERK1/2 were reduced in the KSR1 complex upon DCAF1 knockdown.

Altogether, this evidence suggests that DCAF1 enhances the binding of MEK1/2 and ERK1/2 to KSR1 and promotes KSR1-dependent MEK1/2 and ERK1/2 phosphorylation.

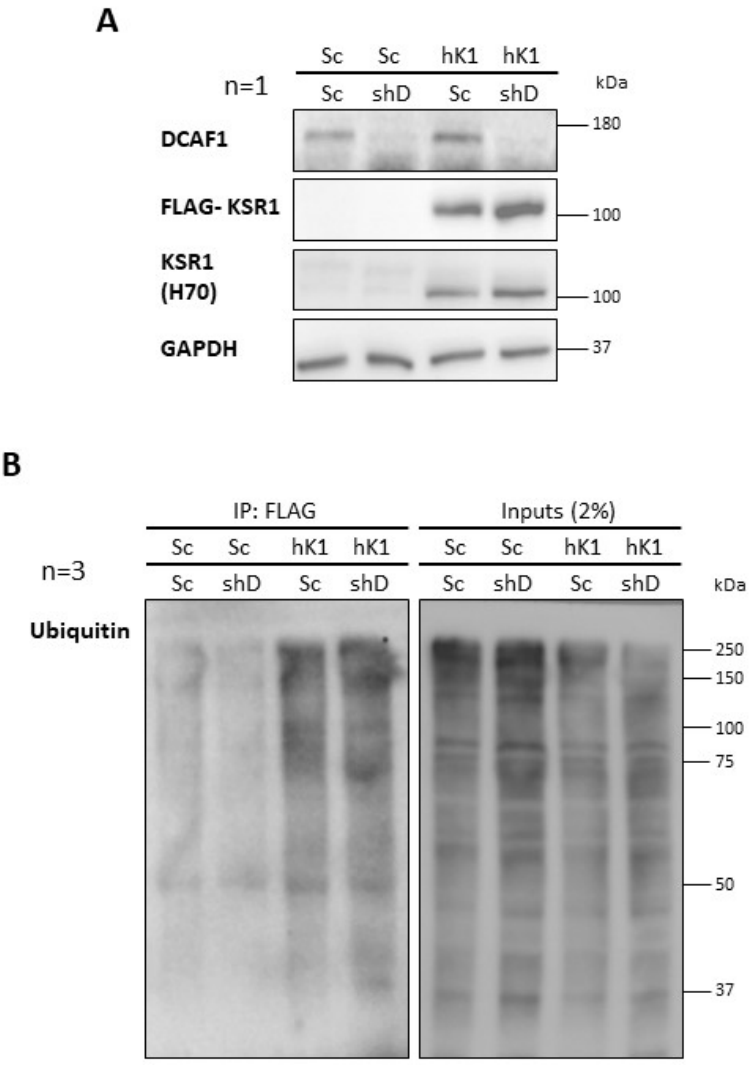

Figure 4.7 - KSR1 poly-ubiquitination is not dependent on DCAF1 in HEK293T cells. A: DCAF1 expression was knocked down in HEK293T cells and then human KSR1 (hK1) with a FLAG-tag was overexpressed. Scramble (Sc) or DCAF1 shRNA (shD) lentivirus was added for 24 hours and then fresh medium for 24 hours followed by four days of puromycin selection. Cells were split and Sc or hK1 lentivirus was added after 24 hours, for 48 hours before cell lysis. The Western blot confirmed DCAF1 knockdown and hK1 overexpression. **B:** hK1 complexes were immunoprecipitated using a FLAG antibody from 1 mg of HEK293T lysate. Western blot shows immunoprecipitated FLAG complexes (IP) and input lysates probed with ubiquitin, representative of three repeats. The amount of Ubiquitin in the hK1 complexes was not affected by DCAF1 knockdown. FLAG-tag interacting proteins were immunoprecipitated from Sc/sc and Sc/shD as negative controls. The input lanes shows endogenous ubiquitin expression and represents 2% of the total protein used for the immunoprecipitation.

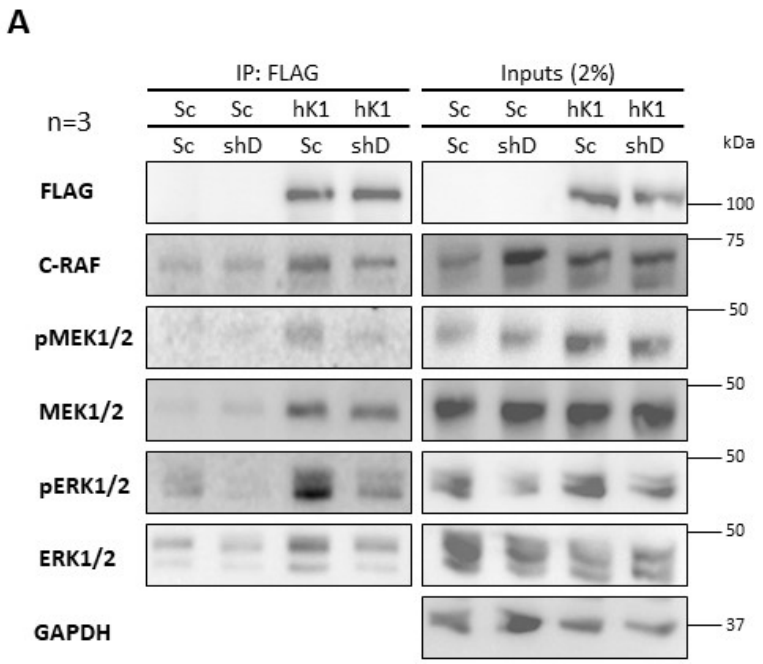

Figure 4.8 - KSR1 and RAF/MEK/ERK binding is partly dependent on DCAF1 in HEK293T cells. A: DCAF1 expression was targeted with a shRNA lentiviral plasmid in HEK293T cells and then human KSR1 (hK1) with a FLAG-tag was overexpressed. DCAF1 lentivirus was added for 24 hours and then fresh medium was added for 24 hours followed by four days of puromycin selection. Cells were then split and 24 hours later hK1 lentivirus was added for 48 hours followed by cell lysis. hK1 complexes were immunoprecipitated using a FLAG antibody from 1 mg of HEK293T lysate. Western blot shows immunoprecipitated FLAG complexes and input lysates probed with FLAG, C-RAF, pMEK1/2, MEK1/2, pERK1/2. ERK1/2 and GAPDH, representative of three repeats. The amount of pMEK1/2, MEK1/2, pERK1/2 and ERK1/2 in the hK1 complex was reduced when DCAF1 expression was knocked down. FLAG-tag interacting proteins were immunoprecipitated from Scramble (Sc)/Sc and Sc/DCAF1 knockdown (shD) lysates as a negative control. Input lysates show endogenous expression in lysates prior to the immunoprecipitation. 2% of the total protein amount used for the immunoprecipitation was used for the input lanes.

4.6 Discussion

We have shown for the first time that endogenous DCAF1 and KSR1 interact in a Merlin-deficient model (figure 4.1A). However, the KSR1 band at 100 kDa was faint in all experiments which is probably reflective of low endogenous expression. Interestingly, there was also a higher molecular weight KSR1 band specific to immunoprecipitated DCAF1. This band was between 130 kDa and 180 kDa (much higher than the additional KSR1 band present in BenMen-1 input lysate). The higher molecular weight band was not specific to BenMen-1 lysate as we also identified the same band in immunoprecipitated DCAF1 from KT21-MG1-Luc5D lysate (supplementary figure 3D). In addition, a band of the same size was detected when immunoprecipitating overexpressed DCAF1 using a myc-tag antibody demonstrating that the band was not a non-specific signal caused by the DCAF1 antibody used for immunoprecipitation (figure 4.2). Indeed, a multiprotein KSR1 complex has previously been reported by Stewart *et al.* (Stewart *et al.*, 1999). This complex remained even under high-salt conditions (up to 1 M sodium chloride) or in the presence of 0.1% SDS and contained Heat shock protein 70 (HSP70), Heat shock protein 90 (HSP90), MEK1/2 and 14-3-3 proteins (Stewart *et al.*, 1999). However, this complex was reported to be around 1000 kDa in size, dissimilar to the size of the band we detected. Nonetheless, it is interesting that the higher molecular weight band was present exclusively when full length DCAF1 is expressed and not when the C-terminal of DCAF1 was expressed. Thus, suggesting that wild-type DCAF1 is required for high molecular weight KSR1 complexes to be formed.

We found that KSR1 binds specifically to the C-terminal of DCAF1 between 745–1507 amino acids (figure 4.2). This portion of the protein contains a LisH domain regulating

DCAF1 dimerization, a WD40 domain responsible for DCAF1 interaction with DDB1 and an acidic C-terminus which is required for Merlin binding (Nakagawa, Mondal & Swanson, 2013). Further analysis is required to determine the role of KSR1 binding and elucidate if KSR1 is a substrate for ubiquitination via the CRL4-DCAF1 complex. We then overexpressed truncated KSR1 constructs and identified that DCAF1 binding was specific to the N-terminal of KSR1 (figure 4.3). Interestingly, there was also a weak band in the C-terminal KSR1 lane suggesting that DCAF1 may bind to multiple locations on KSR1. The C-terminal contained the kinase domain responsible for MEK1/2 and C-RAF binding and facilitating RAF/MEK/ERK activation whereas the N-terminal (1–539 amino acids) contained domains CA1-CA4 that also bind C-RAF (CA1) as well as ERK1/2 (CA4) and are responsible for KSR1 regulation by 14-3-3 proteins (Morrison, 2001).

We performed cytoplasmic and nuclear fractionation of HEK293T overexpressing FLAG-KSR1 (K1) and immunoprecipitated the KSR1 complex discovering that the DCAF1/KSR1 interaction surprisingly occurred in the cytoplasm of HEK293T cells (although some nuclear protein was detected in some replicates) (figure 4.5B). However, endogenous DCAF1 protein in HEK293T was mostly cytoplasmic, in contrast to Merlin-deficient cells in which it was mostly nuclear (figure 4.5A). Therefore, it is important to repeat this experiment in a relevant Merlin-deficient model to confirm the location of the interaction in Merlin-deficient cells. Unfortunately, attempts to overexpress KSR1 in the Merlin-deficient cell line BenMen-1 failed using both lipofectamine and lentiviral methods (data not shown).

We showed that KSR1 was poly-ubiquitinated at the C-terminal containing CA5 domains and was not dependent on DCAF1 expression (figure 4.6 and 4.7). This is in keeping with the previous data in chapter 3 that excludes the possibility that DCAF1

regulates KSR1 degradation, often mediated by poly-ubiquitination. In addition, it has recently been shown that KSR1 poly-ubiquitination is dependent on PRAJA2 (Rinaldi *et al.*, 2016). Unfortunately, we could not determine if KSR1 was mono-ubiquitinated as there are no specific mono-ubiquitin antibodies. We also did not overexpress ubiquitin, therefore, the assay used may not have been sensitive enough to detect N-terminal KSR1 mono-ubiquitination. However, we cannot exclude the possibility that DCAF1 mono-ubiquitinates KSR1 and in this manner regulates RAF/MEK/ERK activity.

We used the previous experimental setup to determine if DCAF1 regulates KSR1 binding to RAF/MEK/ERK. We identified a reduction in pMEK, MEK1/2, pERK1/2 and ERK1/2 bound to KSR1 when DCAF1 expression was knocked down (figure 4.8 and supplementary figure 6). Therefore, demonstrating that DCAF1 enhances RAF/MEK/ERK activity in a KSR1-dependent manner. Interestingly, C-RAF bound to KSR1 is unchanged upon DCAF1 knockdown suggesting that DCAF1 specifically enhances MEK1/2 binding to KSR1 and subsequent phosphorylation. MEK1/2 binds to the CA5 domain of KSR1 whereas DCAF1 binds to a domain between CA1 and CA4 (Morrison, 2001). How DCAF1 enhances KSR1 binding to MEK1/2 is a mystery but it may involve DCAF1-dependent changes in KSR1 spatial conformation or changes in membrane localization that must be further investigated.

4.7 Conclusion

We have shown, for the first time that endogenous DCAF1 and KSR1 interact in a Merlin deficient model (BenMen-1 cells). In addition, there was a high molecular weight KSR1 complex in DCAF1 immunoprecipitated from BenMen-1 lysates. This complex was also present when overexpressed DCAF1 is isolated from HE293T lysates but not when C-terminal DCAF1 was overexpressed and immunoprecipitated.

Therefore, suggesting that DCAF1 facilitates the formation of a high molecular weight KSR1 complex which is dependent on full length DCAF1.

We have also shown evidence that KSR1 interacts with a DCAF1 domain between 745–1507 amino acids and that DCAF1 interacts with KSR1 domains between 1–539 amino acids. There may also be a DCAF1 and KSR1 interaction between 540–873 amino acids but this is at least partly dependent on the presence of amino acids 1–539 of KSR1.The DCAF1/KSR1 interaction occurred in the cytoplasm of HEK293T cells but they may also interact in the nucleus, particularly when nuclear DCAF1 expression is increased. We have shown evidence that the DCAF1/KSR1 interaction enhances KSR1 binding to MEK1/2 and ERK1/2 and increases MEK1/2 and ERK1/2 phosphorylation. Therefore, DCAF1 regulates RAF/MEK/ERK activity in a KSR1-dependent manner and may be a good therapeutic target for tumours driven by RAF/MEK/ERK activity, in particular, Merlin-deficient tumours.

Chapter 5 - Targeting DCAF1 in Merlin-deficient tumours

5.1 Introduction

There are currently no specific inhibitors of CRL4-DCAF1 activity. As CRL4-DCAF1 is activated by neddylation, we identified the neddylation inhibitor, MLN3651, a successor of MLN4924. MLN3651 (Takeda, UK) was developed to overcome the problems with MLN4924 such as its bioavailability. MLN3651 is an orally available inhibitor with pre-clinical activity. We aimed to determine if MLN3651 had significant anti-tumour activity in Merlin-deficient schwannoma and meningioma.

We identified that DCAF1 protein expression was increased in schwannoma and meningioma in previous chapters. Thus, we hypothesised that DCAF1 kinase activity was also upregulated in Merlin-deficient tumours. Therefore, we also aimed to investigate the potency of the DCAF1 kinase inhibitor, B32B3 in Merlin-deficient cells.

5.2 MLN3651 treatment reduces NEDD8-conjugates and activates the Hippo pathway in Merlin-deficient cells

We confirmed MLN3651 drug activity by observing NEDD8-conjugates, by Western blot. In preliminary experiments we found that a 24 hour MLN3651 treatment in schwannoma cells was not sufficient to reduce cell viability (data not shown). Therefore, we treated primary schwannoma cells for 72 hours whereas primary meningioma and BenMen-1 cells were treated for 24 hours with MLN3651 and then NEDD8-conjugates were analysed using a neddylation antibody (figure 5.1A-C). BenMen-1 cells were treated with a lower concentration of MLN3651 as we determined BenMen-1 cells were much more sensitive to MLN3651 (data not shown). In all treated cells, NEDD8-conjugates were dramatically reduced demonstrating that MLN3651 treatment of cells in culture successfully inhibits neddylation.

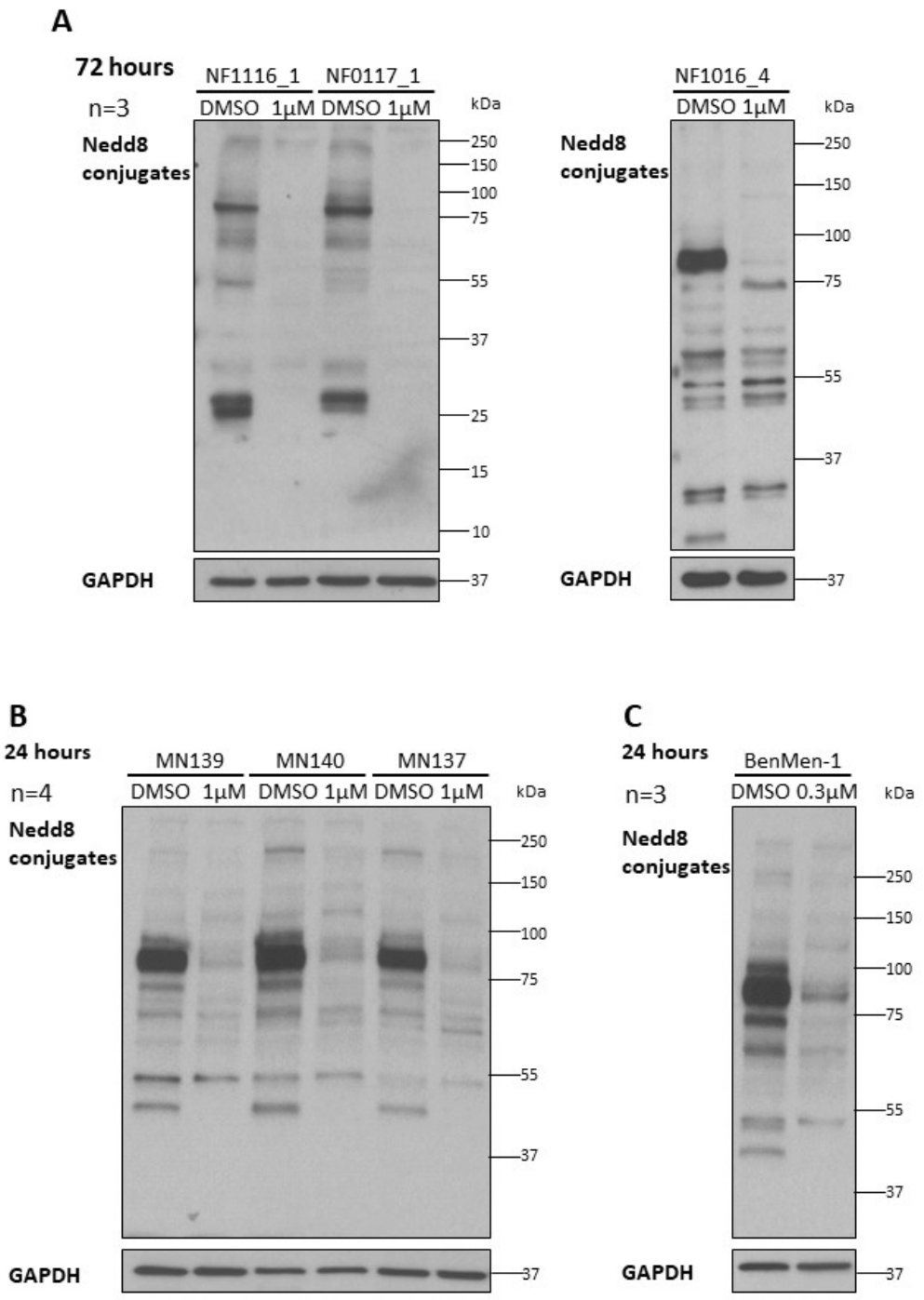

Figure 5.1 - MLN3651 reduces NEDD8-conjugates in Merlin-deficient tumours. A: Western blot of three primary schwannomas treated with DMSO or 1 μM MLN3651 for 72 hours and probed for NEDD8-conjugates and GAPDH, the loading control. MLN3651 led to a clear reduction in NEDD8-conjugates in schwannoma. **B:** Western blot of three primary meningiomas (MN) treated with DMSO or 1 μM MLN3651 for 24 hours and probed for NEDD8-conjugates and GAPDH, representative of nine replicates. MLN3651 led to a clear reduction in NEDD8-conjugates in meningioma. **C:** Western blot of the benign meningioma cell line, BenMen-1 treated with DMSO or 0.3 μM MLN3651 for 24 hours and probed for NEDD8-conjugates and GAPDH, representative of three replicates. MLN3651 led to a clear reduction in NEDD8-conjugates in BenMen-1.

CRL4-DCAF1 is more active in Merlin-deficient cells and leads to Hippo pathway inhibition by ubiquitinating LATS1/2 (Li *et al.*, 2014). LATS1/2 ubiquitination causes changes in LATS1/2 degradation and activity preventing phosphorylation of YAP (Li *et al.*, 2014). Therefore, Merlin-deficient cells have an increase in nuclear YAP which activates transcription of genes involved in tumourigenesis (Li *et al.*, 2014; Zhang *et al.*, 2010). Merlin-deficient cells have more active CRL4-DCAF1 and this may make them more sensitive to neddylation inhibition. We analysed the expression of LATS2 and pYAP after MLN3651 treatment of schwannoma cells to determine if MLN3651 inhibits CRL4-DCAF1 activity and to investigate the effects on downstream Hippo pathway signalling.

We treated schwannoma cells for 72 hours with MLN3651 as they were less sensitive to the drug than other tumours in preliminary experiments. Figure 5.2A shows Western blots from schwannoma lysates treated with MLN3651 for 72 hours and probed with LATS2 and pYAP. LATS2 and pYAP expression were significantly increased with MLN3651 treatments as low as 0.3 μM indicating activation of the Hippo pathway and suggesting that MLN3651 inhibits CRL4-DCAF1 activity (Repeated Measures ANOVA with Tukey's Multiple Comparison Post Test; $p< 0.05$) (figure 5.2B).

In primary meningioma, a four hour treatment with MLN3651 was sufficient to lead to a significant increase in LATS1 expression (Student's Paired T test; $p< 0.05$) (figure 5.3A-B). However, there was only an average increase in LATS1 expression of 23% whereas there was an average increase of 88% LATS2 expression that was not statistically significant ($p= 0.06$). After four hours treatment in meningioma, pYAP expression was not increased but there was a clear increase in two out of the three meningioma samples treated figure 5.3A-B). Therefore, we analysed LATS2 and pYAP

expression after 24 hours MLN3651 treatment to determine whether Hippo pathway activation would occur at a later time point (figure 5.3C-D). Indeed, 24 hours treatment with 1 μM MLN3651 led to a significant increase in LATS2 expression. In addition, pYAP expression was increased in four out of the six replicates but this was not significant. Altogether suggesting that MLN3651 inhibits CRL4-DCAF1 activity in primary meningioma and leads to Hippo pathway activation.

MLN3651 treatment of BenMen-1 cells did not lead to any significant changes in Hippo pathway activation at four hours or 24 hours (figure 5.4A-D). However, increases in LATS1 and LATS2 were observed in some Western blot replicates (data not shown). Therefore, there is no strong evidence that MLN3651 inhibits CRL4-DCAF1 activity in BenMen-1 cells.

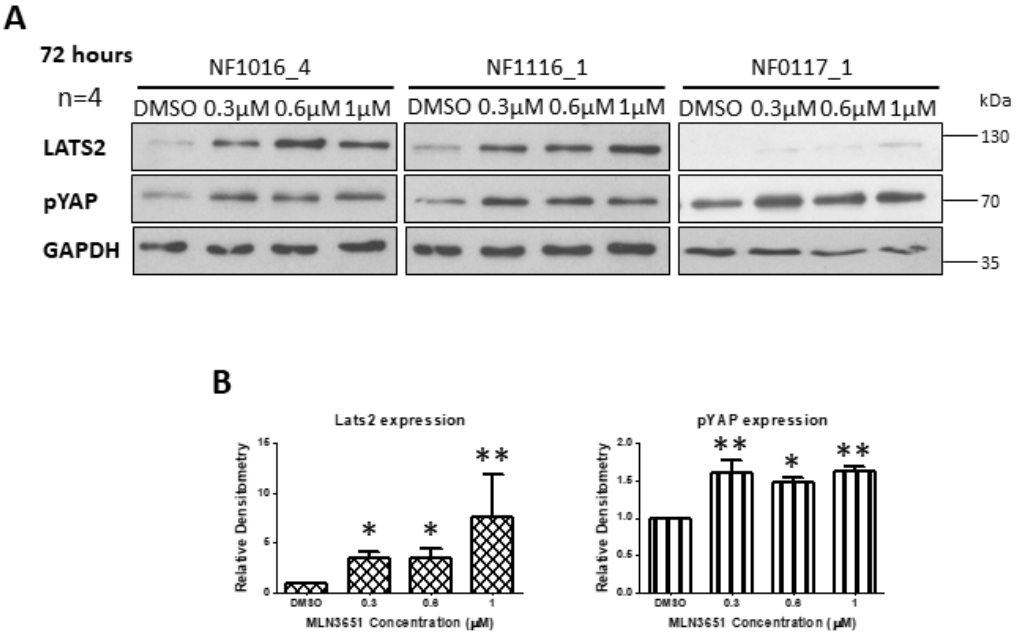

Figure 5.2 - MLN3651 activates the Hippo pathway in schwannoma. A: Western blot of three primary schwannomas treated with DMSO, 0.3 µM, 0.6 µM or 1 µM MLN3651 for 72 hours and probed for LATS2 and pYAP of the Hippo pathway and GAPDH (loading control). MLN3651 led to an increase in the expression of LATS2 and pYAP in schwannoma showing Hippo pathway activation after treatment. **B:** Mean LATS2 and pYAP expression and SEM in MLN3651 treated schwannoma cells normalized to the loading control and relative to DMSO. LATS2 and pYAP were significantly increased with MLN3651 treatment compared with the DMSO control, *- $p < 0.05$, **- $p < 0.01$.

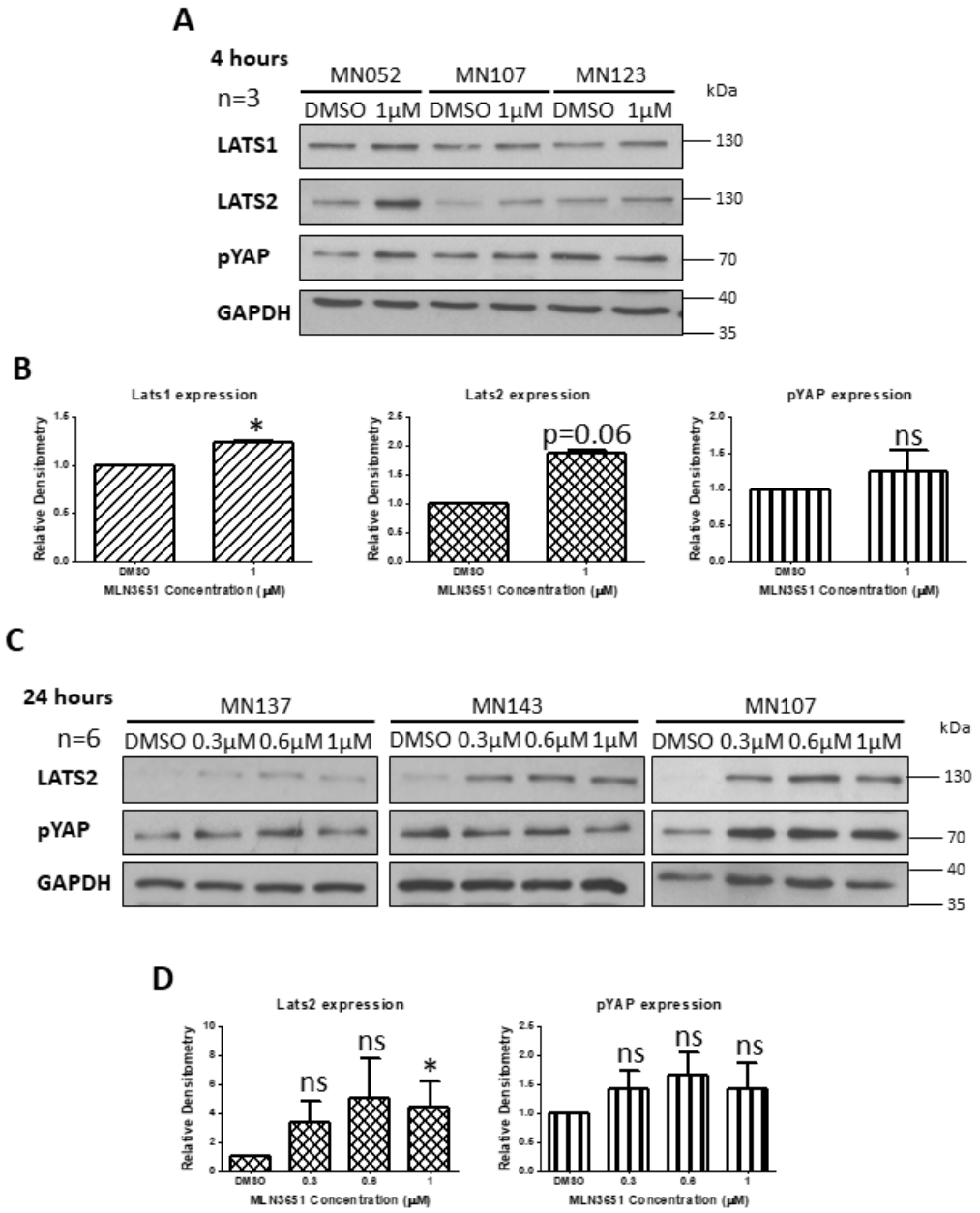

Figure 5.3 - MLN3651 activates the Hippo pathway in meningioma. A: Western blot of three primary meningiomas treated with DMSO or 1 μM MLN3651 for four hours and probed for LATS1, LATS2, pYAP (Hippo pathway) and GAPDH (loading control). **B:** Mean LATS1, LATS2 and pYAP expression and SEM in MLN3651 treated meningioma cells normalized to the loading control and relative to DMSO. LATS1 was significantly increased with MLN3651 treatment compared with the DMSO control, *- p< 0.05. The mean expression of LATS2 and pYAP was increased in MLN3651 treated meningioma cells but this was not significant, ns- not significant showing some evidence for Hippo pathway activation. **C:** Western blot of three meningiomas treated with DMSO, 0.3 μM, 0.6 μM or 1 μM MLN3651 for 24 hours and probed for LATS2, pYAP and GAPDH, representative of six replicates. LATS2 expression increased with MLN3651 treatment. **D:** Mean LATS2 and pYAP expression and SEM in MLN3651 treated meningioma cells normalized to the loading control and relative to DMSO. LATS2 was significantly increased with 1 μM MLN3651 treatment compared with the DMSO control, *- p< 0.05. The mean expression of pYAP was increased in MLN3651 treated meningioma cells but it was not significant showing some evidence of Hippo pathway activation.

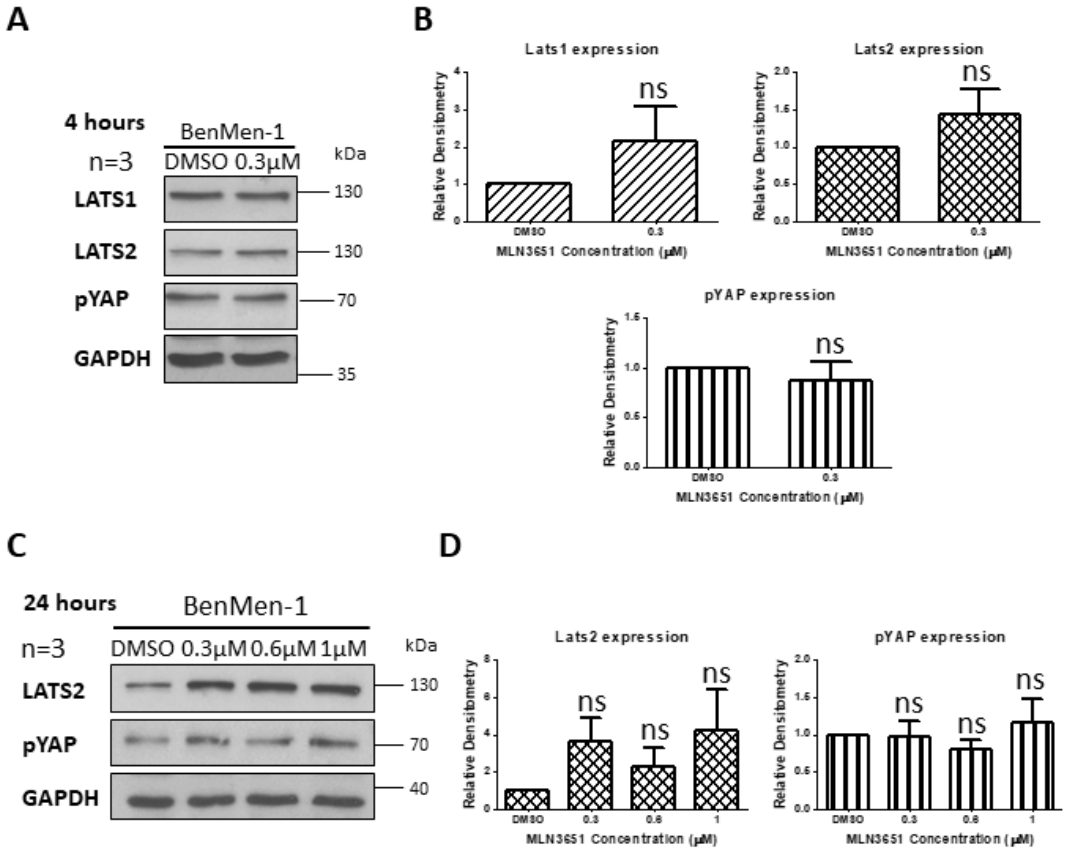

Figure 5.4 - MLN3651 does not activate the Hippo pathway in BenMen-1. A: Western blot of the benign meningioma cell line (BenMen-1) treated with DMSO or 0.3 µM MLN3651 for four hours and probed for LATS1, LATS2, pYAP and GAPDH (loading control), representative of three replicates. **B:** Mean LATS1, LATS2 and pYAP expression and SEM in MLN3651 treated meningioma cells normalized to the loading control and relative to DMSO. The mean expression of LATS1 and LATS2 were increased in MLN3651 treated BenMen-1 cells but this was not significant, ns- not significant, therefore there is no evidence for Hippo pathway activation in this cell model. **C:** Western blot of BenMen-1 cells treated with DMSO, 0.3 µM, 0.6 µM or 1 µM MLN3651 for 24 hours and probed for LATS2, pYAP and GAPDH, representative of three replicates. LATS2 expression increased with MLN3651 treatment. **D:** Mean LATS2 and pYAP expression and SEM in MLN3651 treated BenMen-1 cells normalized to the loading control and relative to DMSO. The mean expression of LATS2 was increased in MLN3651 treated BenMen-1 cells but this was not significant, pYAP expression was not increased by MLN3651, ns- not significant. There is no evidence for Hippo pathway activation in the BenMen-1 model after 24 hours MLN3651 treatment.

5.3 MLN3651 treatment leads to enhanced RAF/MEK/ERK activity in Merlin-deficient cells

We hypothesised that CRL4-DCAF1 regulates KSR1 activity and therefore RAF/MEK/ERK activity. As MLN3651 targets CRL4-DCAF1 neddylation, we suspected that MLN3651 treatment would inhibit the RAF/MEK/ERK pathway. Therefore, we analysed pERK1/2 and ERK1/2 expression following MLN3651 treatment of Merlin-deficient cells. Figure 5.5A-B shows that pERK1/2 was significantly increased in schwannoma cells after 72 hours MLN3651 treatment (0.6 μM) (Repeated Measures ANOVA with Tukey's Multiple Comparison Post Test; $p< 0.05$). Similarly, 24 hours MLN3651 treatment of primary meningioma cells significantly increased phosphorylation of ERK1/2 ($p< 0.05$) (figure 5.6A-B). In contrast, 24 hours MLN3651 treatment of BenMen-1 cells did not significantly increase pERK1/2 expression.

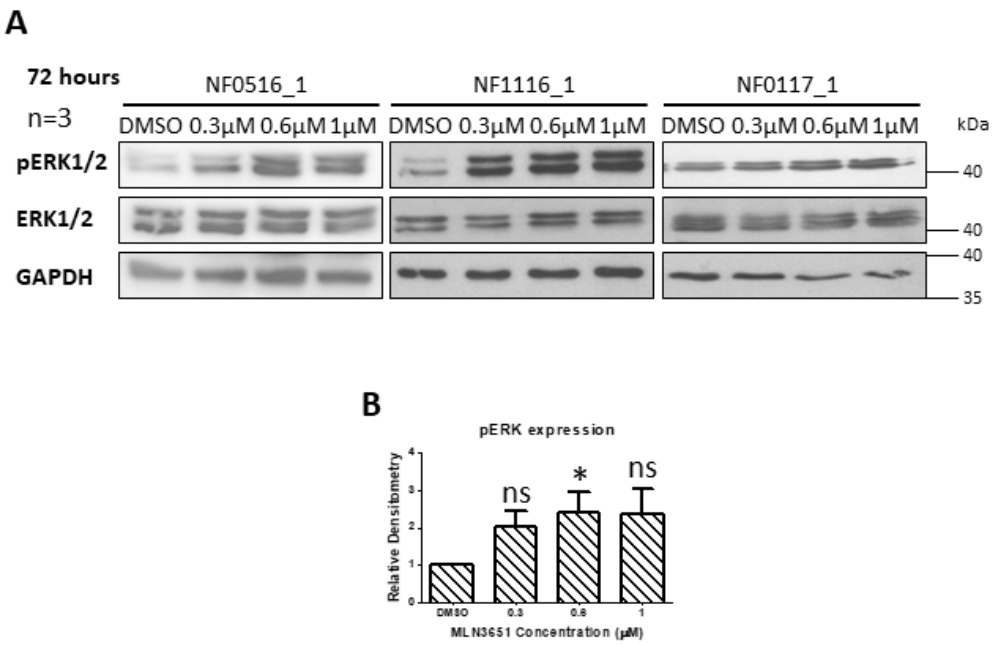

Figure 5.5 - MLN3651 increases pERK1/2 in schwannoma. A: Western blot of three primary schwannomas (NF) treated with DMSO, 0.3 µM, 0.6 µM or 1 µM MLN3651 for 72 hours and probed for pERK1/2 (showing activation), ERK1/2 and GAPDH (loading control). MLN3651 led to an increase in the expression of pERK1/2 in schwannoma. **B:** Mean pERK1/2 expression and SEM in MLN3651 treated schwannoma cells normalized to total ERK1/2 and the loading control (GAPDH), relative to DMSO. pERK1/2 expression was significantly increased with 0.6 µM MLN3651 treatment compared with the DMSO control, *- p< 0.05. ns- not significant showing that MLN3651 activates the RAF/MEK/ERK pathway in schwannoma.

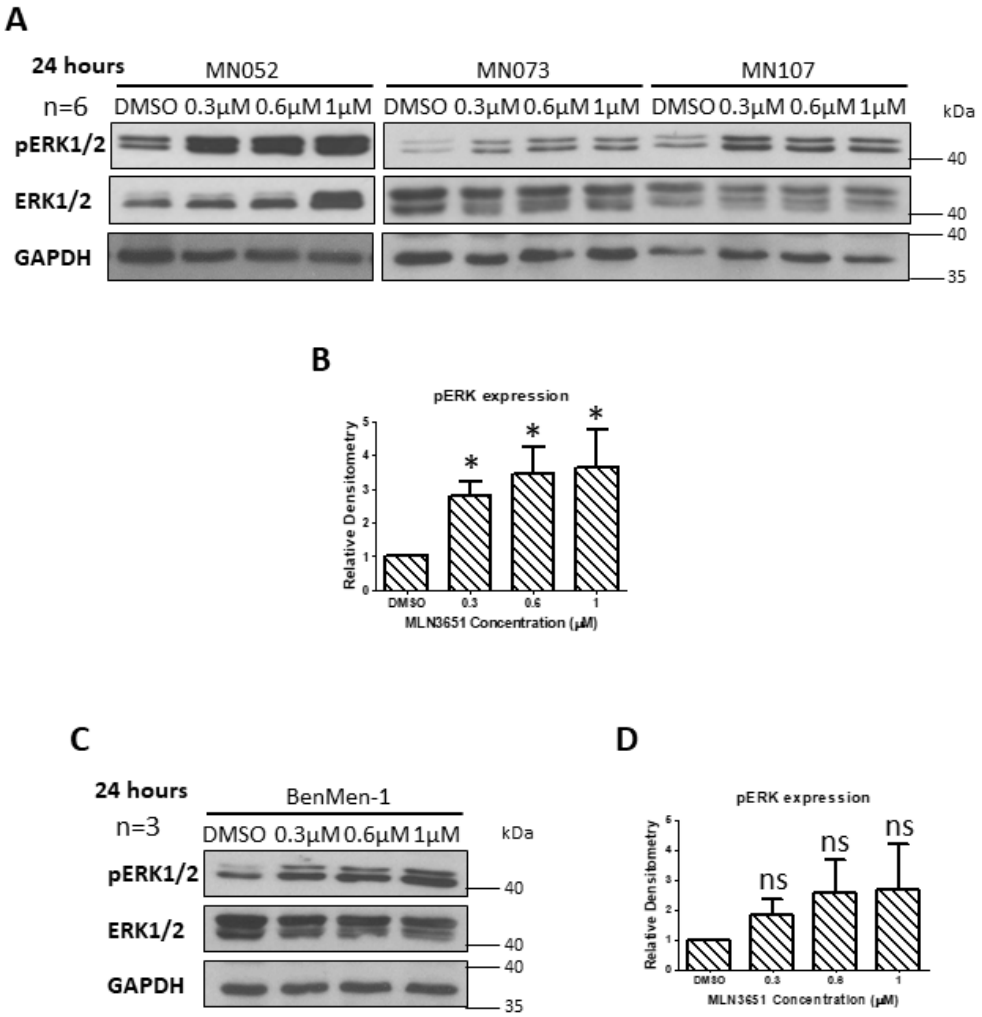

Figure 5.6 - MLN3651 increases pERK1/2 in meningioma but not BenMen-1. A: Western blot of three primary meningiomas (MN) treated with DMSO, 0.3 μM, 0.6 μM or 1 μM MLN3651 for 24 hours and probed for pERK1/2 (showing activation), ERK1/2 and GAPDH (loading control). MLN3651 led to an increase in the expression of pERK1/2 in meningioma demonstrating increased RAF/MEK/ERK activation in response to MLN3651. **B:** Mean pERK1/2 expression and SEM in MLN3651 treated meningioma cells normalized to total ERK1/2 and the loading control (GAPDH), relative to DMSO. pERK1/2 expression was significantly increased with MLN3651 treatment compared with the DMSO control, *- $p < 0.05$. **C:** Western blot of the benign meningioma cell line (BenMen-1) treated with DMSO, 0.3 μM, 0.6 μM or 1 μM MLN3651 for 24 hours and probed for pERK1/2, ERK1/2 and GAPDH, representative of three replicates. MLN3651 led to an increase in the expression of pERK1/2 in BenMen-1. **D:** Mean pERK1/2 expression and SEM in MLN3651 treated meningioma cells normalized to total ERK1/2 and the loading control (GAPDH), relative to DMSO. The mean expression of pERK1/2 was increased in MLN3651 treated BenMen-1 cells but this was not significant, ns- not significant. Therefore, there is no evidence that MLN3651 activates the RAF/MEK/ERK pathway in BenMen-1.

5.4 MLN3651 reduces cell viability and proliferation of Merlin-deficient schwannoma

To assess the efficacy of MLN3651, we analysed the viability of Merlin-deficient cells after treatment with concentrations of 0.1-10 μM MLN3651. We treated primary schwannoma cells, in triplicate, for 72 hours with different concentrations of MLN3651 (stable for up to 72 hours). Figure 5.7A shows the average luminescent signal, correlating with ATP concentration, relative to DMSO control for each drug concentration with the SEM where each line represents a different tumour (biological replicate) (n=3). The average IC50, the concentration at which cell viability was halved, was 23.76 μM. However, viability was significantly reduced from 1 μM demonstrating that MLN3651 has an effect on a proportion of cells (Repeated Measures ANOVA with Tukey's Multiple Comparison Post Test; $p< 0.01$). A 72 hour treatment was not long enough to induce reductions in viability below 50% and therefore we extended the treatment time.

We hypothesised that a longer treatment would have more of an effect on viability and therefore, we treated cells for 72 + 72 hours. MLN3651 is stable for 72 hours but longer time points have not been investigated and therefore we added fresh drug after 72 hours (personal communication with Takeda). Two 72 hours treatments (144 hours) of primary Merlin-deficient schwannoma significantly reduced viability at concentrations of 0.3 μM ($p< 0.001$) (figure 5.7B). The average IC50 was 3.14 μM with a 2.34 μM standard error of the mean. As the standard error was relatively large, we removed the 'non-responder' and the average IC50 was reduced to 1.01 μM with a standard error of 0.18 μM.

We treated primary schwannoma cells, in triplicate, with 0.3–1 μM of MLN3651 for 72 hours and analysed cleaved Caspase 3/7 expression using a luminescent assay. Figure

5.7C shows the average changes in Caspase 3/7 activity in three biological replicates after MLN3651 treatment. MLN3651 significantly increased cleaved Caspase 3/7 at all concentrations tested (Repeated Measures Analysis of Variance (ANOVA) with Tukey's Multiple Comparison Post Test; $p< 0.05$). Therefore, reduced viability after MLN3651 treatment was caused by changes in apoptosis in schwannoma.

Changes in proliferation and cell death can affect cell viability and therefore we determined the effect of MLN3651 treatment on primary schwannoma cell proliferation. Figure 5.8A shows representative images of schwannoma cells stained with Ki-67 antibody and counterstained with 4', 6-diamidino-2-phenylindole (DAPI) after 72 hours of MLN3651 treatment at 0.3 µM, 0.6 µM and 1 µM. There is a clear decrease in the proportion of Ki-67 cells, representing active proliferation, as well as a decrease in the total number of cells. We quantified the proportion of Ki-67 positive cells in at least three images from each of four biological replicates (figure 5.8B). Figure 5.8B shows that 0.6 µM MLN3651 significantly reduced proliferation, of schwannoma cells, by an average of 68% (Repeated Measures ANOVA with Tukey's Multiple Comparison Post Test; $p< 0.01$).

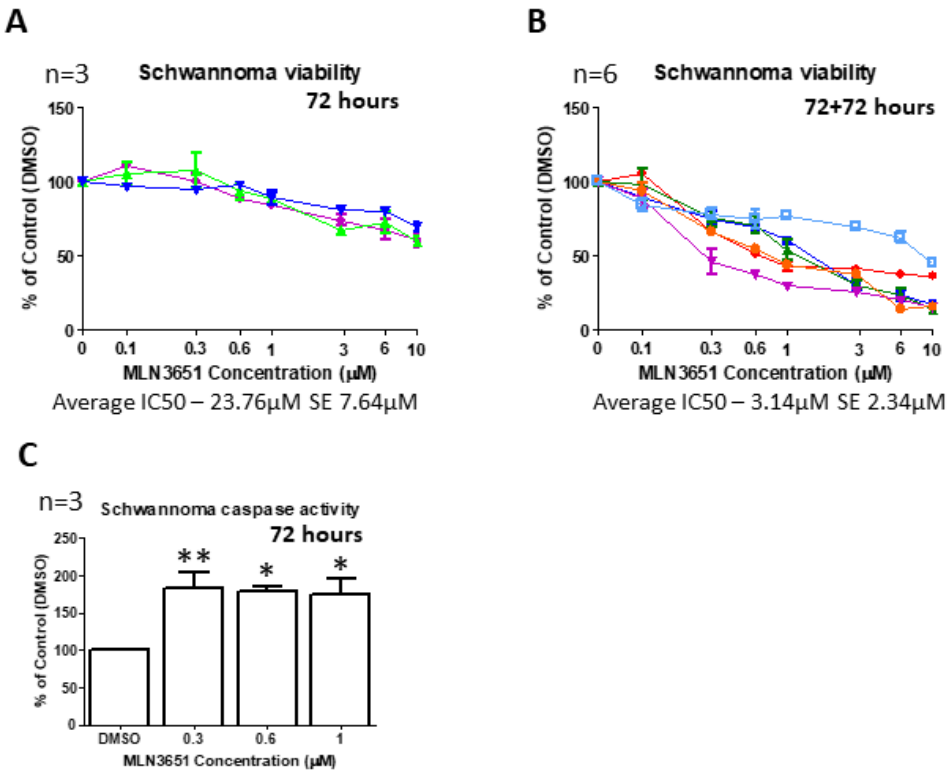

Figure 5.7 - MLN3651 reduces cell viability and increases apoptosis in schwannoma. A: Merlin-deficient schwannoma cells were treated with MLN3651, in triplicate, and subjected to CellTiter-Glo® luminescent cell viability assay after 72 hours (n=3). Viability of MLN3651-treated cells was normalized to respective DMSO-treated controls. The concentration of MLN3651 required to reduce cell viability by 50% (IC50) is indicated with the standard error of the mean (SEM). Each colour in the graph represents a different primary schwannoma sample. Error bars show the SEM of technical replicates. MLN3651 was ineffective at the 72 hour timepoint. **B:** Merlin-deficient schwannoma cells were treated with increasing doses of MLN3651 every 72 hours, in triplicate, and subjected to CellTiter-Glo® luminescent cell viability assay after 144 hours (n=6). The IC50 is indicated with the SEM. Each colour in the graph represents a different primary schwannoma sample and the error bars show the SEM of the technical replicates. MLN3651 reduced schwannoma viability after 144 hours treatment. **C:** Merlin-deficient schwannoma cells were treated with MLN3651, in triplicate, and subjected to Caspase-Glo® 3/7 assay after 72 hours (n=3). Caspase 3/7 activity in MLN3651-treated cells was normalized to respective DMSO-treated controls. Caspase 3/7 activity was significantly higher in MLN3651-treated cells compared with DMSO-treated cells showing that MLN3651 activates apoptosis, *-p< 0.05, **- p< 0.01, ns- not significant, error bars are ±SEM.

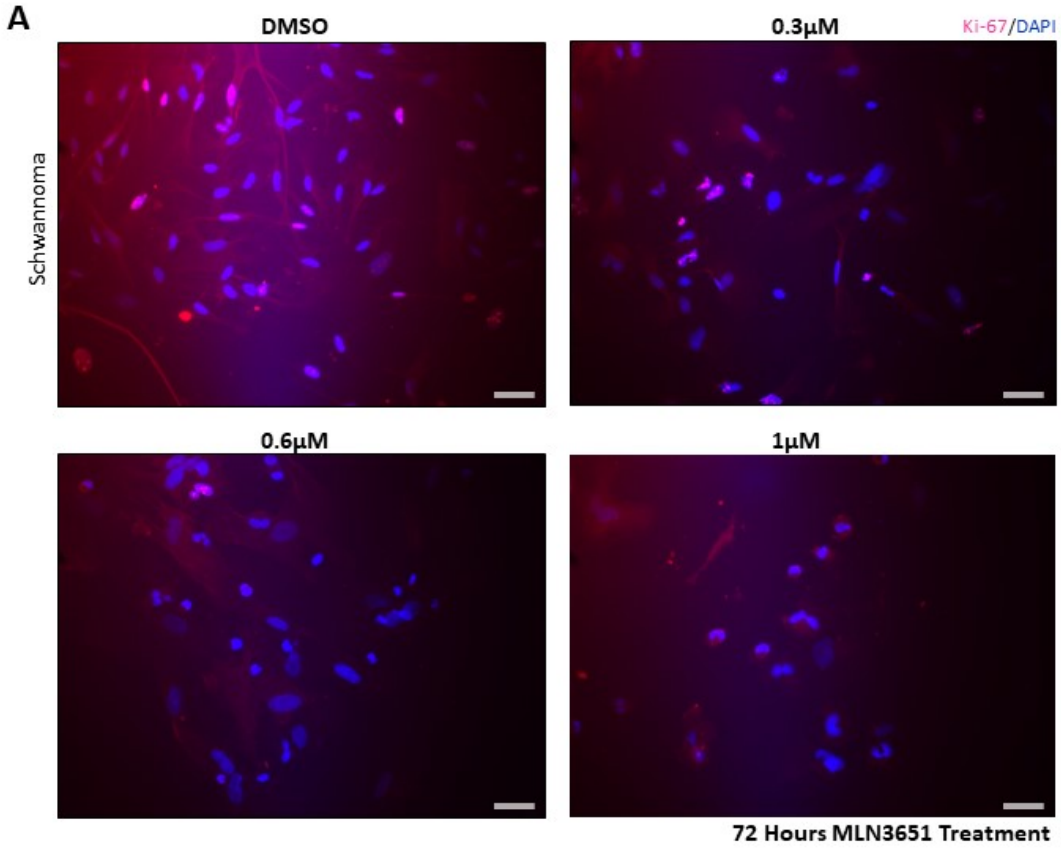

Figure 5.8 - MLN3651 reduces proliferation of schwannoma. A: Representative immunocytochemistry images, at 20x magnification, of Merlin-deficient schwannoma cells treated with DMSO, 0.3 µM, 0.6 µM or 1 µM MLN3651 for 72 hours and stained with Ki-67 antibody and DAPI, Scale bar- 50 µM. **B:** At least three images from each treatment group in A was quantified to calculate the proportion of Ki-67 positive cells in each group. Four different schwannoma tumours were treated with MLN3651 and quantified in this way. The mean proportion of Ki-67 positive cells in MLN3651-treated schwannoma cells relative to DMSO control is plotted and SEM in B. 0.6 µM and 1 µM MLN3651 significantly reduced proliferation of schwannoma compared with DMSO.

5.5 MLN3651 reduces cell viability and proliferation of Merlin-deficient meningioma

As MLN3651 reduced the viability of primary Merlin-deficient schwannoma cells we tested the efficacy of MLN3651 in primary Merlin-deficient meningioma cells. Meningioma cells were treated with 0.1-10 μM MLN3651, in triplicate, for 72 hours. An ATP luminescent assay was used to determine the viability of meningioma after treatment. There were two distinct groups of meningioma after MLN3651 treatment; those that had an IC50 of less than 3 μM and those that had an IC50 of more than 7 μM. These groups were defined as 'responders' and 'non-responders' and plotted separately in figure 5.9A-B. The graphs show the average luminescent signal for each tumour (each in a different colour) relative to the luminescent signal in the DMSO control. Viability was significantly reduced in cells treated with 0.3 μM (Repeated Measures ANOVA with Tukey's Multiple Comparison Post Test; $p< 0.01$) in the 'responder' group and 3 μM ($p< 0.001$) in the 'non-responder' group. Interestingly, viability was significantly increased after 0.1 μM MLN3651 treatment in the 'non-responder' group ($p< 0.05$). The average IC50, that reduced cell viability by half, was 1.31 μM in the 'responder' group and 12.81 μM in the 'non-responder' group. As there was a large amount of variability in viability response to MLN3651 treatment after 72 hours, we increased the treatment time to 144 hours (two 72 hour treatments).

After a 144 hour MLN3651 treatment of primary meningioma cells from both the 'responder' and 'non-responder' groups, viability was significantly reduced at 0.1 μM ($p< 0.05$) demonstrating increased sensitivity to MLN3651 compared with a 72 hour treatment. There was no significant difference between the IC50 of 'responder' and 'non-responder' tumours after 144 hours MLN3651 treatment and the average IC50 was 0.38 μM with a standard error of 0.18 μM, shown in figure 5.9C. The colours of the

lines representing individual tumours were consistent between figure 5.9A-B and C for comparison. Therefore, prolonged treatment can effectively reduce cell viability of the 'non-responder' group. Furthermore, 0.3 μM MLN3651 treatment for 24 hours significantly increased Caspase 3/7 activity in meningioma (figure 5.9D) (n=10) (Repeated Measures ANOVA with Tukey's Multiple Comparison Post Test; $p< 0.001$).

Figure 5.10A shows representative images of primary meningioma cells stained with Ki-67 and DAPI after a 72 hour treatment of MLN3651 at concentrations of 0.3 μM, 0.6 μM and 1 μM. At least three images from each of nine biological replicates were analysed and the proportion of Ki-67 positive cells relative to DMSO control was plotted in figure 5.10B. Treatment of meningioma cells with 0.3 μM significantly reduced proliferation, by an average of 51%, relative to DMSO control (Repeated Measures ANOVA with Tukey's Multiple Comparison Post Test; $p< 0.001$). Similar to schwannoma, MLN3651 reduced viability of meningioma cells by inducing apoptosis and reducing proliferation.

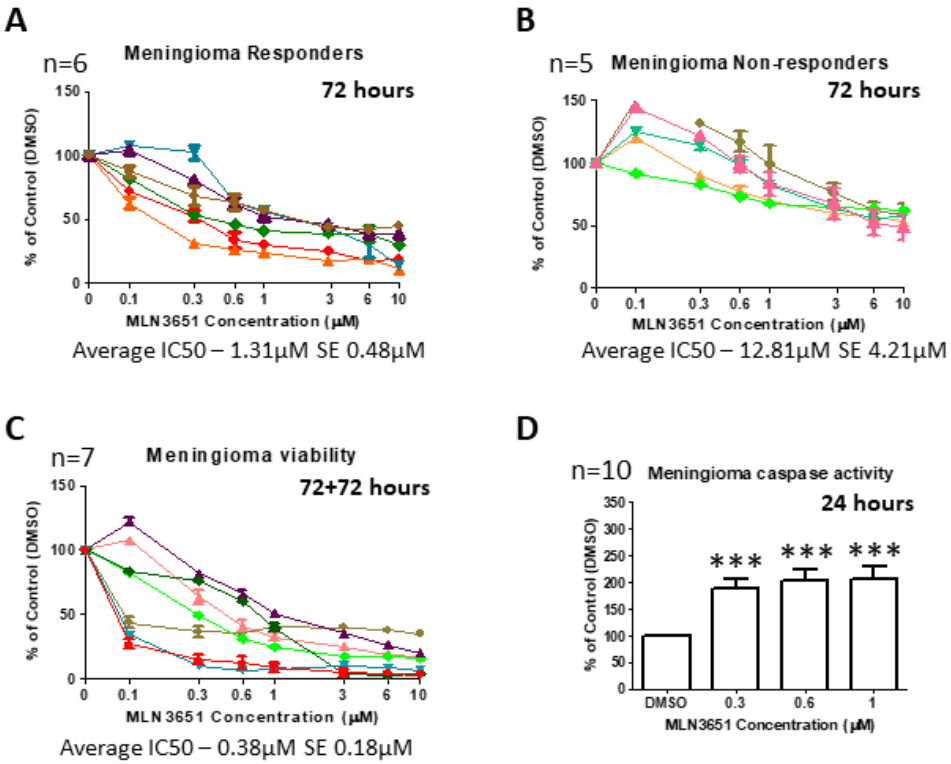

Figure 5.9 - MLN3651 reduces cell viability and increases apoptosis in meningioma. A,B: Merlin-deficient meningioma cells were treated with increasing doses of MLN3651, in triplicate, and subjected to CellTiter-Glo® luminescent cell viability assay after 72 hours (n=11). Viability of MLN3651-treated cells was normalized to respective DMSO-treated controls. The concentration of MLN3651 required to reduce cell viability by 50% (IC50) is indicated with the standard error of the mean (SEM). meningioma cells with an average IC50 < 3 μM were plotted in A (n=6) and considered to be sensitive to MLN3651 whereas meningioma cells with an average IC50 > 7 μM were plotted in B (n=5). Each colour represents a different primary meningioma tumour and the error bars show the SEM of technical replicates for each tumour. **C:** Merlin-deficient meningioma cells were treated with increasing doses of MLN3651 every 72 hours, in triplicate, and subjected to CellTiter-Glo® luminescent cell viability assay after 144 hours (n=7). The IC50 is indicated with the SEM. Colours in the graph are consistent with those in A, B and represent different primary meningioma tumours. MLN3651 reduced the viability of all meningioma tumours after 144 hours treatment. **D:** Merlin-deficient meningioma cells were treated with increasing doses of MLN3651, in triplicate, and subjected to Caspase-Glo® 3/7 assay after 72 hours (n=10). Caspase 3/7 activity in MLN3651-treated cells was normalized to respective DMSO-treated controls. Caspase 3/7 activity was significantly higher in MLN3651-treated cells compared with DMSO-treated cells MLN3651 activated apoptosis in meningioma tumours., ***-p< 0.001, error bars are ±SEM.

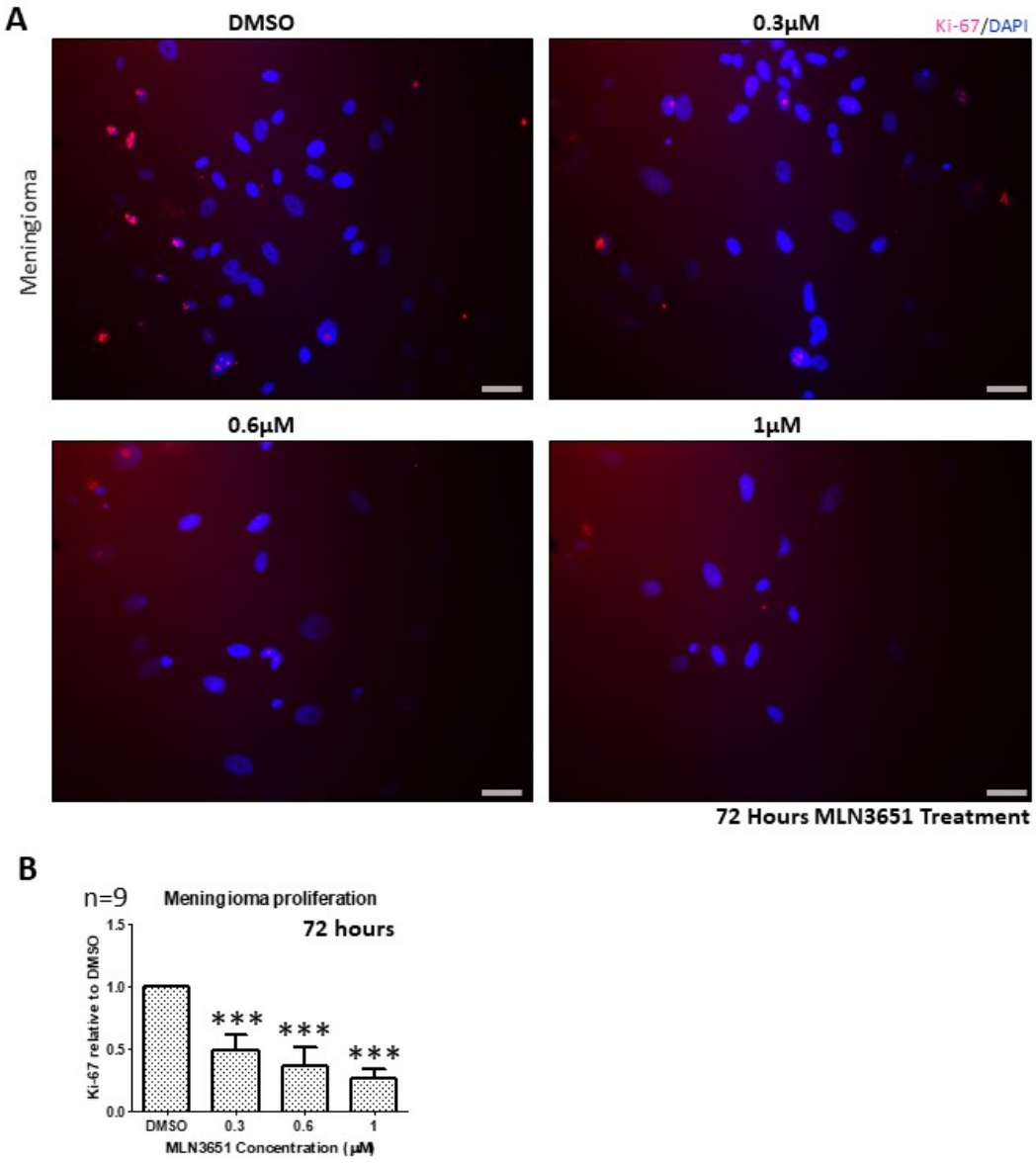

Figure 5.10 – MLN3651 reduces proliferation of meningioma cells. A: Representative immunocytochemistry images, at 20x magnification, of Merlin-deficient meningioma cells treated with DMSO, 0.3 µM, 0.6 µM or 1 µM MLN3651 for 72 hours and stained with Ki-67 antibody and DAPI, Scale bar- 50 µM. **B:** Mean proportion of Ki-67 positive cells in MLN3651-treated meningioma cells relative to DMSO control and SEM. At least three images each of nine replicates were quantified. MLN3651 significantly reduced proliferation of meningioma compared with DMSO. ***- $p<0.001$.

We treated BenMen-1 cells with MLN3651 at concentrations between 0.1–10 μM and analysed the amount of ATP, consistent with number of cells, after 72 hours. The graph in figure 5.11A shows the ATP concentrations at each concentration, relative to DMSO, for seven replicates. Cell viability was significantly reduced when cells were treated with as little as 0.1 μM MLN3651 and the average IC50 was 0.28 μM (Repeated Measures ANOVA with Tukey's Multiple Comparison Post Test; $p < 0.05$). An extended treatment was not required in this case as BenMen-1 cells are much more sensitive to MLN3651 than primary cells. We showed that Caspase 3/7 activity was significantly increased after 0.1 μM MLN3651 treatment for 24 hours ($p < 0.01$) (figure 5.11B). Proliferation was significantly reduced after 72 hours at 0.3 μM to less than 50% of the DMSO control ($p < 0.05$) (figure 5.12A-B).

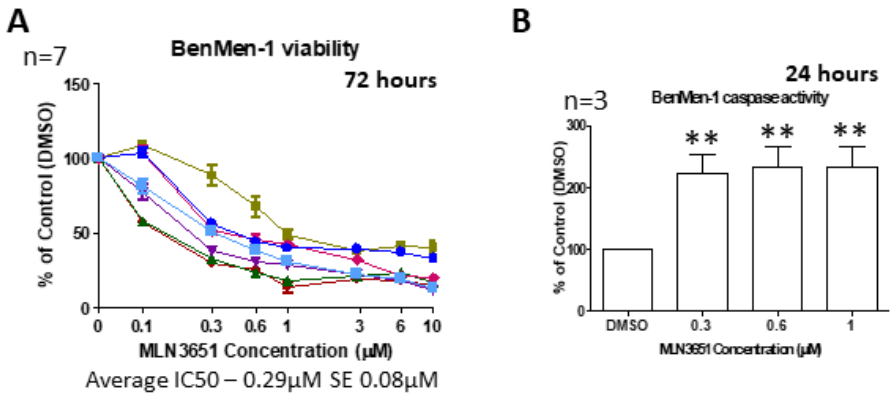

Figure 5.11 - MLN3651 reduces cell viability and increases apoptosis in BenMen-1. A: The benign meningioma cell line (BenMen-1) was treated with increasing doses of MLN3651, in triplicate, and subjected to CellTiter-Glo® luminescent cell viability assay after 72 hours (n=7). Viability of MLN3651-treated cells was normalized to respective DMSO-treated controls. The concentration of MLN3651 required to reduce cell viability by 50% (IC50) is indicated with the standard error of the mean (SEM). Each colour represents a technical replicate of the experiment. The error bars show the SEM in each individual experiment. MLN3651 reduced the viability of BenMen-1 cells. **B:** BenMen-1 cells were treated with increasing doses of MLN3651, in triplicate, and subjected to Caspase-Glo® 3/7 assay after 24 hours (n=3). Caspase 3/7 activity in MLN3651-treated cells was normalized to respective DMSO-treated controls. Caspase 3/7 activity was significantly higher in MLN3651-treated cells compared with DMSO-treated cells, *-p< 0.05, **-p< 0.01, error bars are ±SEM. MLN3651 activated apoptosis in BenMen-1 cells.

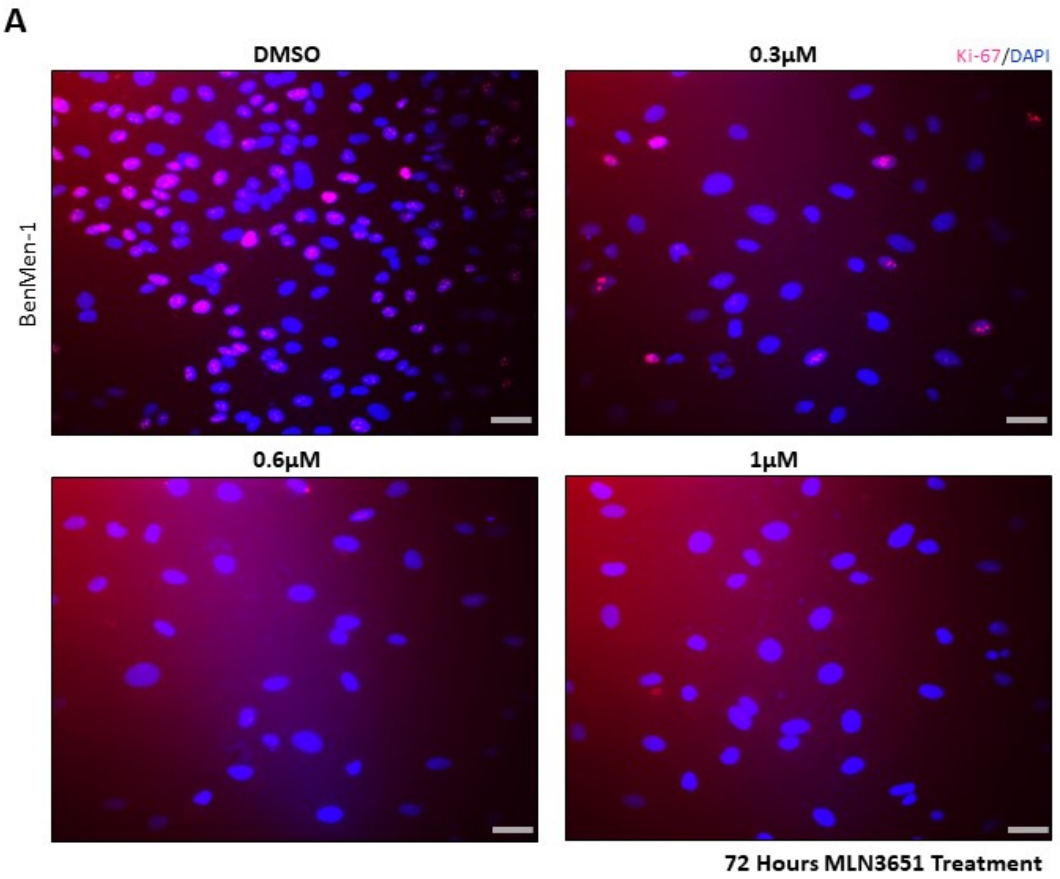

Figure 5.12 – MLN3651 reduces proliferation of BenMen-1 cells. A: Representative immunocytochemistry images, at 20x magnification, of BenMen-1 cells treated with DMSO, 0.3 µM, 0.6 µM or 1 µM MLN3651 for 72 hours and stained with Ki-67 antibody and DAPI, Scale bar- 50 µM. **B:** Mean proportion of Ki-67 positive cells in MLN3651-treated BenMen-1 cells relative to DMSO control and SEM. At least three images each of three replicates were quantified. MLN3651 significantly reduces proliferation of meningioma compared with DMSO.

We also tested MLN3651's effect on viability of WHO II Merlin-deficient meningioma (figure 5.13A-B). The availability of WHO II meningioma was limited and therefore we were only able to test two samples after 72 hours MLN3651 treatment and one sample after 144 hours treatment. A 72 hours treatment reduced viability of both tumours with an average IC50 of 3.10 µM (figure 5.13A). Furthermore, the IC50 of the WHO II sample tested after 144 hours MLN3651 treatment was 0.75 µM, comparable to the IC50's identified in WHO I meningiomas demonstrating equivalent MLN3651 sensitivity in higher grade meningiomas (figure 5.13B).

There were no WHO III primary Merlin-deficient tumours that we could successfully culture. Therefore, we utilised the Merlin-deficient WHO III meningioma cell line, KT21-MG1-Luc5D and identified an average IC50 of 0.18 µM with a small SEM of 0.02 µM between technical repeats when cells were treated with MLN3651 for 72 hours (figure 5.13C). Thus, demonstrating that KT21-MG1-Luc5D WHO III cells were more sensitive to MLN3651 than WHO I BenMen-1 cells and MLN3651 may be a potential therapeutic in WHO III meningioma tumours.

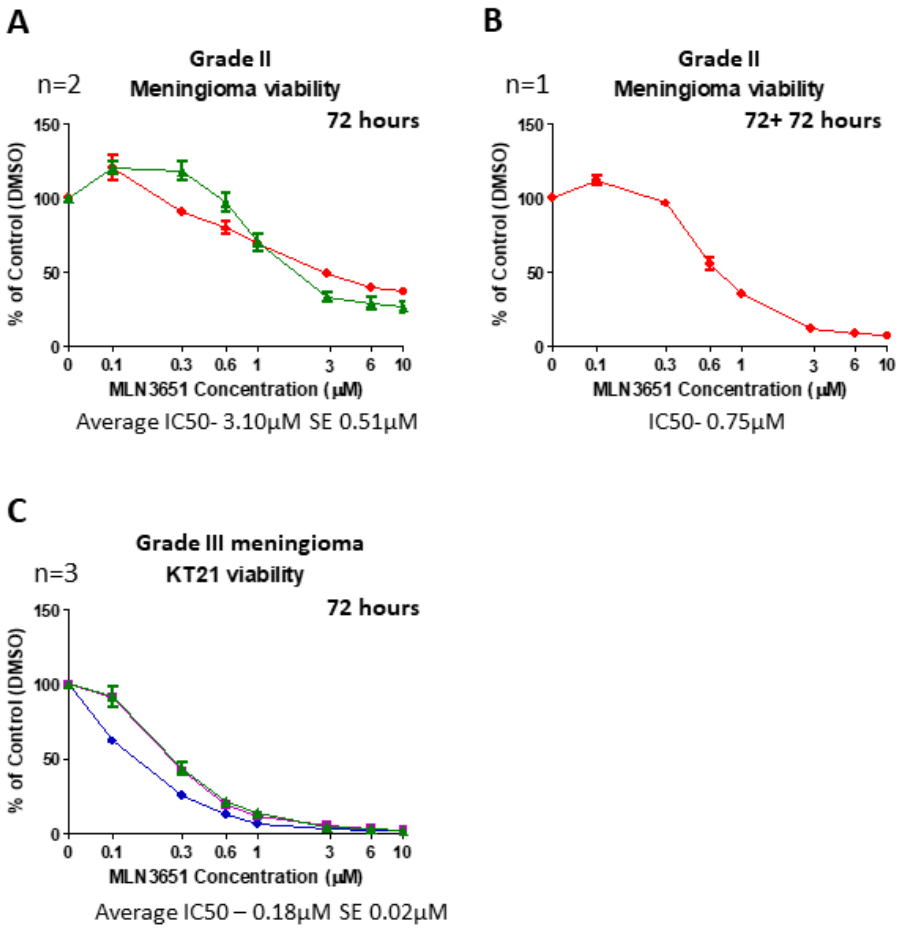

Figure 5.13 - Viability of WHO II and III meningiomas after MLN3651 treatment. A: Merlin-deficient WHO II meningioma cells were treated with increasing doses of MLN3651, in triplicate, and subjected to CellTiter-Glo® luminescent cell viability assay after 72 hours (n=2). Viability of MLN3651-treated cells was normalized to respective DMSO-treated controls. The concentration of MLN3651 required to reduce cell viability by 50% (IC50) is indicated with the standard error of the mean (SEM). Each colour represents a different meningioma tumour. **B:** Merlin-deficient WHO II meningioma cells were treated with increasing doses of MLN3651 every 72 hours, in triplicate, and subjected to CellTiter-Glo® luminescent cell viability assay after 144 hours (n=1). The IC50 of the one sample tested is indicated. **C:** The Merlin-deficient WHO III cell line KT21-MG1-Luc5D (KT21), was treated with MLN3651, in triplicate, and subjected to CellTiter-Glo® luminescent cell viability assay after 144 hours (n=3). The average IC50 is indicated. KT21 is sensitive to low doses of MLN3651. The experiments in this figure were carried out by Dr Emanuela Ercolano and the author analysed the data.

5.6 Merlin-positive schwannoma and meningioma cells are less sensitive to MLN3651 than Merlin-negative cells

Figure 5.14 illustrates the effect of MLN3651 on the viability of Merlin-positive schwannoma and meningioma cells. The viability curve for the only schwannoma tested after 72 hours treatment and three schwannomas after 144 hours treatment did not converge demonstrating that an IC50 was not detected (figure 5.14A-B). In addition, one schwannoma sample after 24 hours had an IC50 of 6.7 μM, less sensitive than Merlin-deficient schwannoma at the same time point. We treated three Merlin-positive meningioma with MLN3651 for 72 hours and assessed viability (figure 5.14C). The average IC50 was 10.04 μM with an SEM of 2.52 μM, again, less sensitive than Merlin-deficient meningiomas at the same time point. We analysed the viability of one Merlin-positive meningioma after 144 hours MLN3651 treatment (two 72 hour treatments) and the concentration that reduced the viability by half was 2.75 μM (figure 5.14D). Finally, we treated one Merlin-positive grade II meningioma sample for 72 hours and 144 hours, at 72 hours the viability curve did not converge whereas after 144 hours the IC50 was 2.93 μM (figure 5.14E-F).

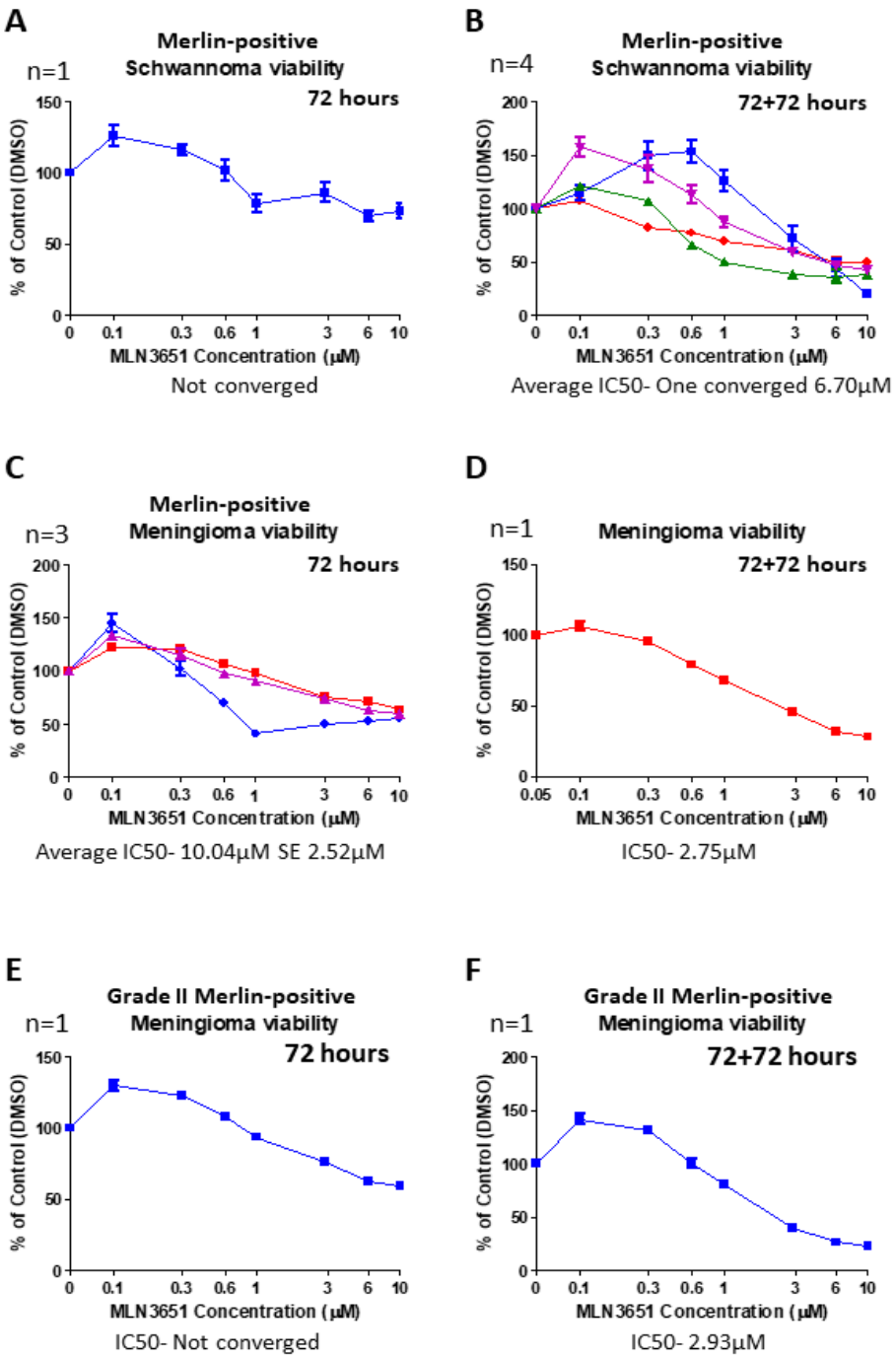

Figure 5.14 - Viability of Merlin-positive schwannoma and meningioma after MLN3651 treatment. A: Merlin-positive schwannoma cells were treated with MLN3651, in triplicate, and subjected to CellTiter-Glo® luminescent cell viability assay after 72 hours (n=1). Viability of MLN3651-treated cells was normalized to respective DMSO-treated controls. The curve did not converge and therefore the concentration of MLN3651 required to reduce cell viability by 50% (IC50) could not be calculated. Each colour represents a different tumour. **B:** Merlin-positive schwannoma cells were treated with MLN3651 every 72 hours, in triplicate, and subjected to CellTiter-Glo® luminescent cell viability assay after 144 hours (n=4). One sample converged and had an IC50 of 6.70 μM. **C:** Merlin-positive meningioma cells were treated with MLN3651, in triplicate, and subjected to CellTiter-Glo® luminescent cell viability assay after 72 hours (n=3). **D:** Merlin-positive meningioma cells were treated with MLN3651 every 72 hours, in triplicate, and subjected to CellTiter-Glo® luminescent cell viability assay after 144 hours (n=1). The IC50 of the one sample tested is indicated. **E:** Merlin-positive WHO II meningioma cells were treated with MLN3651, in triplicate, and subjected to CellTiter-Glo® luminescent cell viability assay after 72 hours (n=1). The sample did not converge and therefore an IC50 cannot be calculated. **F:** Merlin-positive WHO II meningioma cells were treated with MLN3651 every 72 hours, in triplicate, and subjected to CellTiter-Glo® luminescent cell viability assay after 144 hours (n=1).

5.7 Control cells are less sensitive to MLN3651 than Merlin-deficient tumour cells

Primary Schwann cells were plated in 96 well plates, in triplicate, and treated with MLN3651 for 72 hours (figure 5.15A) and 144 hours (two 72 hour treatments) (figure 5.15B) to assess the effects of MLN3651 on normal cells. Four different primary Schwann cells were assessed for viability after a 72 hour MLN3651 treatment and the average IC50 for three samples was 8.44 μM whereas one sample did not converge. There was also a large standard of error of 8.11 μM representing the variability observed in the graph (figure 5.15A). After two 72 hour MLN3651 treatments (144 hours), three different Schwann cells had an average IC50 of 7.78 μM, with a large standard error of 4.46 μM. Overall, primary Schwann cells were less sensitive to MLN3651 than Merlin-deficient schwannoma but viability was significantly reduced with treatment and some individual Schwann cell samples were particularly sensitive (Repeated Measures ANOVA with Tukey's Multiple Comparison Post Test; $p< 0.05$).

We treated HMC with MLN3651 for 72 hours or 144 hours (two 72 hour treatments) (figure 5.15C-D). Two out of the three replicates did not converge and therefore an IC50 could not be calculated. One replicate had an IC50 of 8.55 μM after a 72 hour treatment (figure 5.15C). We also analysed cell viability after 144 hours of MLN3651 treatment and none of the three replicates converged (figure 5.15D). Interestingly, 0.1 μM of MLN3651 significantly increased the viability of HMC after 72 hours and concentrations up to 1 μM significantly increased HMC viability after a 144 hour treatment (Repeated Measures ANOVA with Tukey's Multiple Comparison Post Test; $p< 0.001$). We also analysed apoptosis of HMC after 72 hours of MLN3651 treatment (figure 5.15E). Caspase 3/7 activity was significantly increased in HMC cells after treatment with 0.6 μM MLN3651 ($p< 0.05$). As HMC experiments were cultured and

experiments carried out in a medium enriched with growth factors (as provided by the manufacturer), we decided to repeat the viability assay with HMC cultured in meningioma medium to ensure consistency with primary meningioma experiments and allow the experiments to be directly comparable (figure 5.15F). The meningioma medium made HMC much more sensitive to MLN3651 after 72 hours with an average IC50 of 0.72 µM, lower than the average IC50 of Merlin-deficient meningioma cells after 72 hours MLN3651 treatment.

There is a stark difference in the sensitivity between HMC cultured in HMC medium and meningioma medium and therefore, HMC medium may lead to MLN3651 resistance. We tested the difference in sensitivity between Merlin-deficient meningioma cells cultured in meningioma medium and the same samples cultured in HMC medium (figure 5.16A-B). HMC medium dramatically reduced the sensitivity of all three meningioma samples assessed after a 72 hour MLN3651 treatment, and of two samples after 144 hours. Therefore, suggesting that a component of HMC medium protects both HMC and meningioma cells from MLN3651 induced changes in viability (figure 5.16A-B).

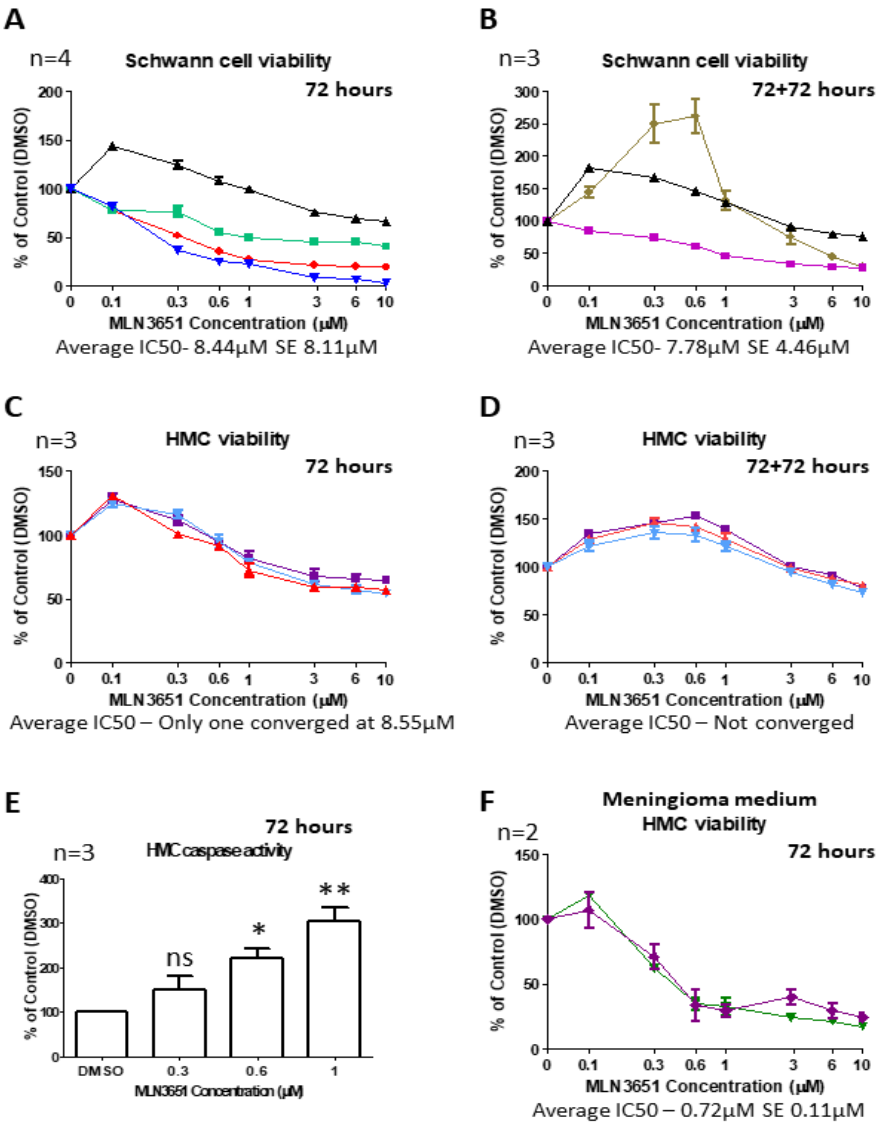

Figure 5.15 - Human Schwann cells and HMC are less sensitive to MLN3651 than tumour cells. A: Primary Schwann cells were treated with MLN3651 (at concentrations indicated), in triplicate, and subjected to CellTiter-Glo® luminescent cell viability assay after 72 hours (n=4). Viability of MLN3651-treated cells was normalized to respective DMSO-treated controls. The concentration of MLN3651 required to reduce cell viability by 50% (IC50) is indicated with the standard error of the mean (SEM). Each colour represent a different primary Schwann cell sample. MLN3651 reduced the viability of some Schwann cell samples. The error bars show the SEM of technical replicates for each experiment. **B:** Primary Schwann cells were treated with MLN3651 every 72 hours, in triplicate, and subjected to CellTiter-Glo® luminescent cell viability assay after 144 hours (n=3). Each colour represents a different primary Schwann cell sample. MLN3651 reduced the viability of some Schwann cell samples. **C:** Human meningeal cells (HMC) were treated with MLN3651, in triplicate, and subjected to CellTiter-Glo® luminescent cell viability assay after 72 hours (n=3). Each colour represents a technical replicate of the experiment. **D:** Human meningeal cells (HMC), a normal meningeal control cell line were treated with MLN3651 every 72 hours, in triplicate, and subjected to CellTiter-Glo® luminescent cell viability assay after 144 hours (n=3). Each colour represents a technical replicate of the experiment. HMC cells were not as sensitive to MLN3651 as meningioma cells. MLN3651 did not reduce the viability of HMC cells. **E:** HMC were treated with MLN3651, in triplicate, and subjected to Caspase-Glo® 3/7 assay after 72 hours (n=3). Caspase 3/7 activity in MLN3651-treated cells was normalized to respective DMSO-treated controls. Caspase 3/7 activity was significantly higher in 0.6 μM and 1 μM MLN3651-treated cells compared with DMSO-treated cells, *-p< 0.05, **-p< 0.01, ns- not significant. **F:** HMC were grown in meningioma medium for at least a week and then treated with MLN3651, in triplicate, and subjected to CellTiter-Glo® luminescent cell viability assay after 72 hours (n=2). HMC cells were very sensitive to MLN3651 when grown in meningioma medium.

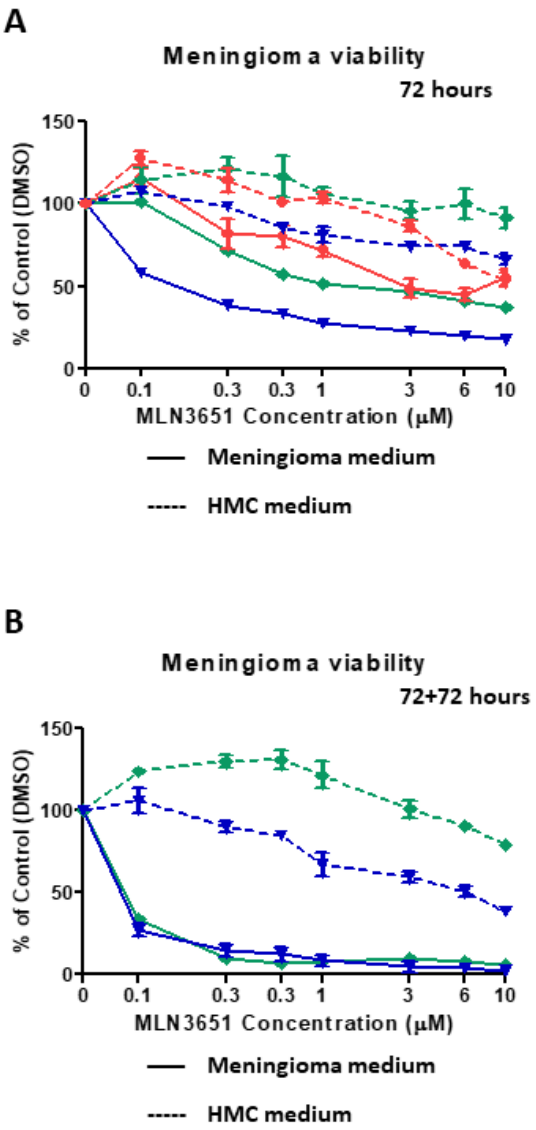

Figure 5.16 - Viability of meningioma in HMC or meningioma medium after MLN3651 treatment. A: Merlin-deficient meningioma cells were grown in meningioma medium or HMC medium for at least a week and then treated with increasing doses of MLN3651, in triplicate, and subjected to CellTiter-Glo® luminescent cell viability assay after 72 hours (n=3). Viability of MLN3651-treated cells was normalized to respective DMSO-treated controls. Coloured lines represent samples cultured in meningioma medium whereas dotted lines represent samples culture in HMC medium. Viability of meningioma cells grown in HMC medium was much higher than meningioma grown in meningioma medium after MLN3651 treatment demonstrating that HMC medium decreases the sensitivity of meningioma cells to MLN3651. **B:** Merlin-deficient meningioma cells were grown in meningioma medium or HMC medium for at least a week and then treated with increasing doses of MLN3651 every 72 hours, in triplicate, and subjected to CellTiter-Glo® luminescent cell viability assay after 144 hours (n=2). Coloured lines represent samples cultured in meningioma medium whereas dotted lines represent samples culture in HMC medium. Viability of meningioma cells grown in HMC medium was much higher than meningioma grown in meningioma medium after MLN3651 treatment demonstrating that HMC medium decreases the sensitivity of meningioma cells to MLN3651. The experiments in this figure were carried out by Dr Emanuela Ercolano and analysis was performed by the author.

5.8 B32B3 reduces viability and proliferation of Merlin-deficient cells

We tested the effect of B32B3 treatment on the viability of primary Merlin-deficient schwannoma cells by quantifying the proportion of ATP present in each treated well compared with DMSO control (figure 5.17A). We treated cells with 0.1–20 μM B32B3 for 72 hours and assessed viability. A B32B3 treatment of 10 μM significantly reduced cell viability (Repeated Measures ANOVA with Tukey's Multiple Comparison Post Test; $p<0.001$) and the average IC50 was 11.07 μM (figure 5.17A) whereas one sample did not converge. We also analysed the proliferation of schwannoma cells after 72 hours B32B3 treatment. We identified a significant decrease in the proportion of Ki-67 positive cells at 5 μM and 10 μM compared with DMSO (Repeated Measures ANOVA with Tukey's Multiple Comparison Post Test; $p< 0.05$) (figure 5.17B). Figure 5.17C shows representative images of a schwannoma treated with B32B3 and stained with a Ki-67 antibody and DAPI which was then quantified in figure 5.17B.

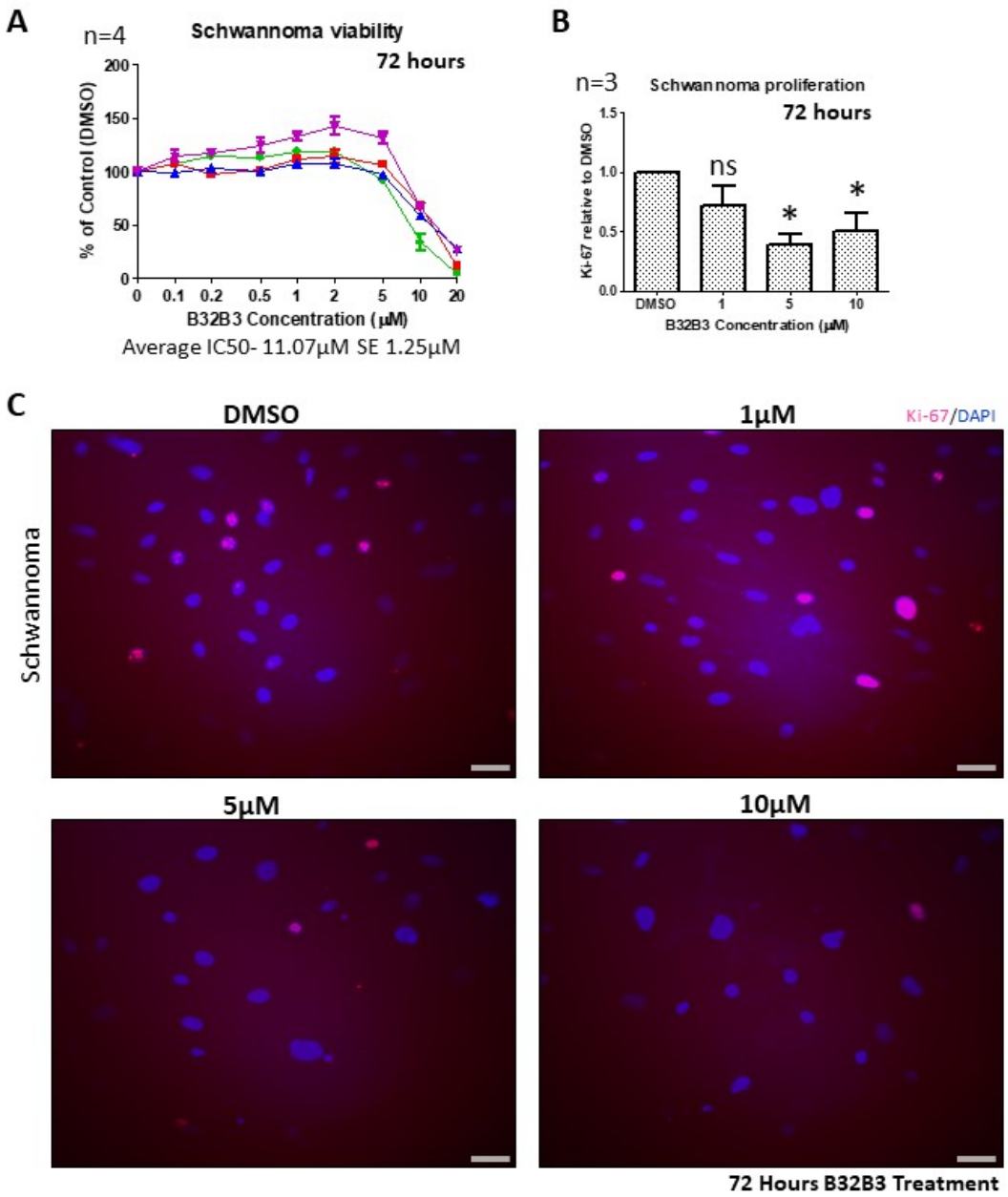

Figure 5.17 - B32B3 effect on viability and proliferation of schwannoma. A: Merlin-deficient schwannoma cells were treated with increasing doses of B32B3, in triplicate, and subjected to CellTiter-Glo® luminescent cell viability assay after 72 hours (n=4). Viability of B32B3-treated cells was normalized to respective DMSO-treated controls. The concentration of B32B3 required to reduce cell viability by 50% (IC50) is indicated with the standard error of the mean (SEM). Each colour represents a different primary schwannoma tumour. The error bars show the SEM of the technical replicates for each schwannoma tumour. B32B3 reduces schwannoma viability at high concentrations. **B:** Mean proportion of Ki-67 positive cells in B32B3-treated schwannoma cells relative to DMSO control and SEM. At least three images each of three replicates from C were quantified. 5 μM and 10 μM B32B3 significantly reduced proliferation of schwannoma compared with DMSO, *-p< 0.05, ns- not significant, error bars are ±SEM. **C:** Representative immunocytochemistry images, at 20x magnification, of Merlin-deficient schwannoma cells treated with DMSO, 1 μM, 5 μM or 10 μM B32B3 for 72 hours and stained with Ki-67 antibody and DAPI, Scale bar- 50 μM.

Primary Merlin-deficient meningioma cells were treated with B32B3 for 72 hours and assessed for changes in cell viability (figure 5.18A). Meningioma cells had a similar sensitivity to B32B3 as schwannoma cells with an average IC50 of 13.92 μM and a standard error of 1.84 μM. Viability was significantly reduced at 10 μM (Repeated Measures ANOVA with Tukey's Multiple Comparison Post Test; $p< 0.001$). We also treated meningioma cells with B32B3 for 72 hours and assessed proliferation via Ki-67 staining (representative images shown in figure 5.18C). Quantification of proportion of Ki-67 positive cells from at least three images of six different meningiomas is shown in figure 5.18B. B32B3 significantly reduces meningioma proliferation, by an average of 50%, at 1 μM (Repeated Measures ANOVA with Tukey's Multiple Comparison Post Test; $p< 0.05$). BenMen-1 cells treated with B32B3 for 72 hours had a significantly increased cell viability up to 2 μM ($p< 0.05$) and a significantly reduced proliferation at 1 μM ($p< 0.05$) (figure 5.19A). The average IC50 across the three repeats was 9.22 μM and proliferation was also significantly reduced at 5 μM, as measured by Ki-67 index (Repeated Measures ANOVA with Tukey's Multiple Comparison Post Test; $p< 0.01$) (figure 5.19B-C).

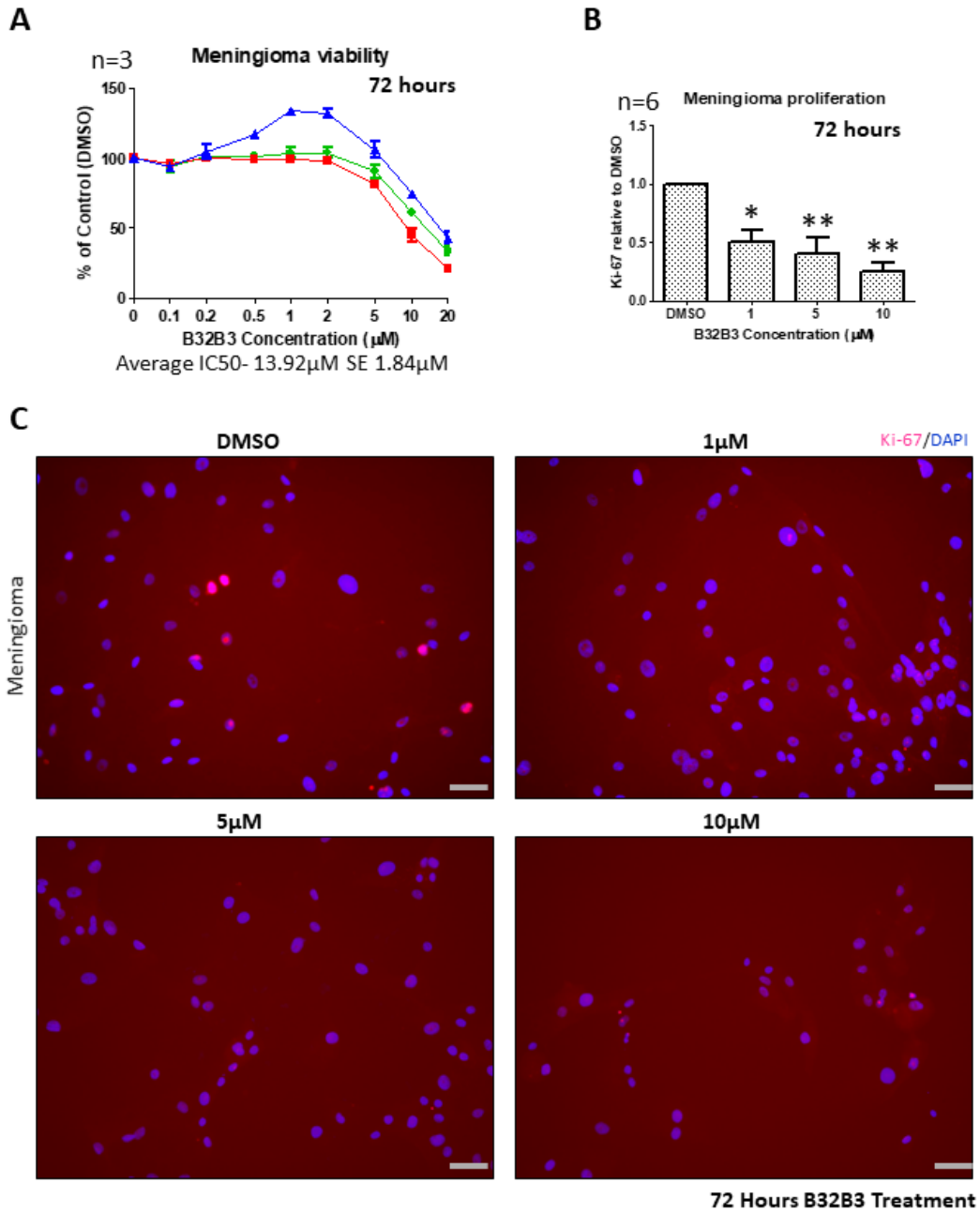

Figure 5.18 - B32B3 effect on viability and proliferation of meningioma. A: Merlin-deficient meningioma cells were treated with increasing doses of B32B3, in triplicate, and subjected to CellTiter-Glo® luminescent cell viability assay after 72 hours (n=3). Viability of B32B3-treated cells was normalized to respective DMSO-treated controls. The concentration of B32B3 required to reduce cell viability by 50% (IC50) is indicated with the standard error of the mean (SEM). Each colour on the graph represents a different primary meningioma tumour. The error bars show the SEM of technical replicates for each meningioma tumour. B32B3 reduced meningioma viability at higher concentrations. **B:** Mean proportion of Ki-67 positive cells in B32B3-treated meningioma cells relative to DMSO control and SEM. At least three images each of six replicates from C were quantified. 1 μM, 5 μM and 10 μM B32B3 significantly reduced proliferation of meningioma compared with DMSO, *-p< 0.05, **-p< 0.01, ns- not significant, error bars are ±SEM. **C:** Representative immunocytochemistry images, at 20x magnification, of Merlin-deficient meningioma cells treated with DMSO, 1 μM, 5 μM or 10 μM B32B3 for 72 hours and stained with Ki-67 antibody and DAPI, Scale bar- 50 μM.

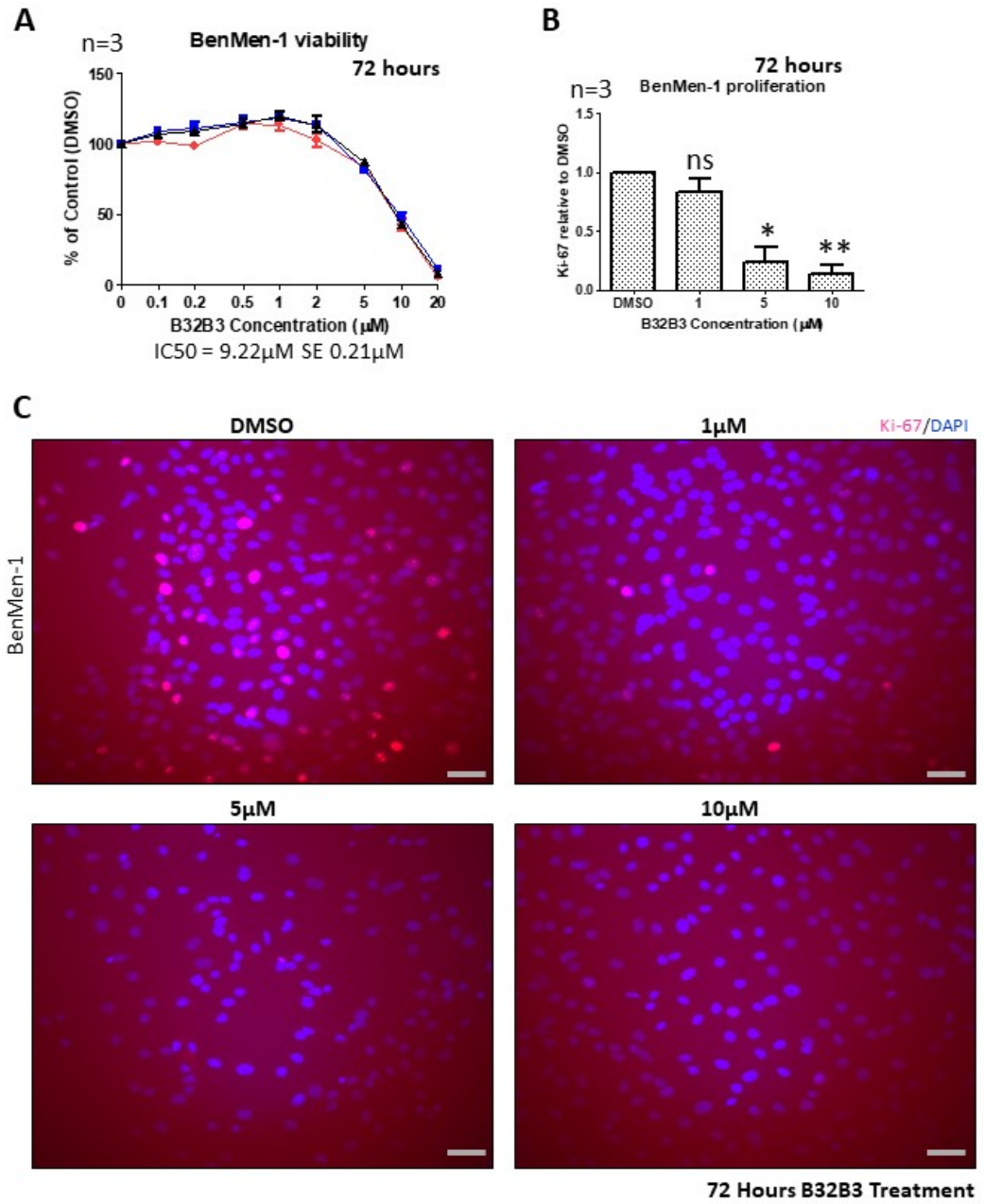

Figure 5.19 - B32B3 effect on viability and proliferation of BenMen-1. A: The Benign meningioma cell line (BenMen-1) was treated with increasing doses of B32B3, in triplicate, and subjected to CellTiter-Glo® luminescent cell viability assay after 72 hours (n=3). Viability of B32B3-treated cells was normalized to respective DMSO-treated controls. The concentration of B32B3 required to reduce cell viability by 50% (IC50) is indicated with the standard error of the mean (SEM). Each colour on the graph represents a technical replicate of the experiment. Error bars show the SEM of the technical replicates for each experiment. B32B3 reduced BenMen-1 viability at higher concentrations. **B:** Mean proportion of Ki-67 positive cells in B32B3-treated BenMen-1 cells relative to DMSO control and SEM. At least three images each of three replicates were quantified from C. 5 µM and 10 µM B32B3 significantly reduced proliferation of BenMen-1 compared with DMSO, *-p< 0.05, **-p< 0.01, ns- not significant, error bars are ±SEM. **C:** Representative immunocytochemistry images, at 20x magnification, of BenMen-1 cells treated with DMSO, 1 µM, 5 µM or 10 µM B32B3 for 72 hours and stained with Ki-67 antibody and DAPI, Scale bar- 50 µM.

5.9 Discussion

MLN4924 is a first in class NAE inhibitor that inhibits neddylation and has activity in a number of tumours to induce cell cycle arrest and apoptosis (Lin *et al.*, 2010; Luo *et al.*, 2012; Milhollen *et al.*, 2010; Swords *et al.*, 2015; Wei *et al.*, 2012; Yang *et al.*, 2012; Zhang *et al.*, 2016; Zhao *et al.*, 2012). Previous research in schwannoma and Merlin-deficient mesothelioma has demonstrated increased sensitivity to MLN4924 compared with Merlin-positive samples (Cooper *et al.*, 2017). MLN3651 has significant pre-clinical activity equal to or exceeding MLN4924 (personal communication with Takeda) and therefore we tested the potential of MLN3651 in Merlin-deficient tumours. As the drug mechanisms are very similar, we hypothesised that Merlin-deficient cells would be more sensitive to MLN3651 compared with Merlin-positive cells.

We confirmed drug activity by observing NEDD8-conjugates after MLN3651 treatment. In all treated cells (schwannoma, meningioma and BenMen-1) neddylation was significantly reduced with minimal signal in treated samples (figure 5.1). Many proteins are neddylated, most important are Cullins (between 75–100 kDa), which inhibit ubiquitin ligase complex formation and activation (Deshaies, Emberley & Saha, 2010). We confirmed that neddylation of Cullins was inhibited as the protein bands around 75–100 kDa were reduced.

CRL4-DCAF1 ubiquitinates both LATS1 and LATS2 leading to LATS1 degradation and inhibition of LATS2 kinase activity (Li *et al.*, 2014). Therefore, inhibiting CRL4-DCAF1 inhibition should lead to an increase in LATS1 and not LATS2. However, Cooper *et al.* reported no significant changes in LATS1 following MLN4924 treatment (Cooper *et al.*, 2017). We identified a significant increase in LATS1 protein following four hours MLN3651 treatment in primary meningioma but these differences were small (figure

5.3A). There was a much larger change in the average LATS2 expression after MLN3651 treatment (although not significant) and therefore we decided to analyse LATS2 in all other MLN3651 experiments (figure 5.3B). After 24 hours MLN3651 treatment, in meningioma, we detected a significant increase in LATS2 protein expression confirming Hippo pathway activation (figure 5.3C). However, there were no significant changes in pYAP. As phosphorylation of YAP leads to nuclear exclusion and subsequent degradation, changes in pYAP may be undetectable at this time point (Sayedyahossein *et al.*, 2016; Zhao *et al.*, 2010; Zhao *et al.*, 2007). A longer treatment of 72 hours may show significant changes in pYAP similar to schwannoma.

MLN3651 treatment in BenMen-1 for four hours or 24 hours did not induce any significant changes in LATS2 or pYAP expression suggesting that MLN3651 does not activate the Hippo pathway in this cell line (figure 5.4). Therefore, MLN3651's effects on proliferation and apoptosis in BenMen-1 is independent of CRL4-DCAF1 activity. MLN4924 induced accumulation of CDT1, p21 and p27 to induce cell cycle arrest in gastric cancer and this may be the MLN3651 mechanism of action in BenMen-1 cells rather than Hippo pathway activation (Lan *et al.*, 2016).

Surprisingly, MLN3651 treatment increased pERK1/2 and therefore ERK1/2 activity (Figure 5.5 and 5.6). This is possibly in a CRL4-DCAF1 independent manner as in previous chapters DCAF1 depletion led to a decrease in RAF/MEK/ERK activity (figure 3.10). Although we expected a decrease in RAF/MEK/ERK activity, the increase seen provides an additional rationale for combination therapy of MLN3651 with a RAF/MEK/ERK activity or KSR1 inhibitor.

Both cell proliferation and cell death contributed to the changes in cell viability observed after MLN3651 treatment (figure 5.7-5.12). A 72 hour MLN3651 treatment

significantly reduced proliferation and significantly increased apoptosis suggesting that MLN3651 inhibits cell cycle progression and activates apoptosis in schwannoma consistent with MLN4924 treatment in other cancers (Lin *et al.*, 2010; Lin *et al.*, 2018; Luo *et al.*, 2012), including schwannoma (Cooper *et al.*, 2017).

Elucidating the reason for differences in drug sensitivity of Merlin-deficient meningioma is particularly important to determine which patients may benefit from MLN3651. One potential reason for the 'responder' and 'non-responder' sub-groups could be the *Nf2* mutation type (figure 5.9). Yang *et al.* reported that missense *Nf2* mutations are transcribed at the same rate as wild-type *Nf2* genes in meningioma and that the decreased Merlin protein levels observed in *Nf2* mutant meningiomas are due to increased protein degradation (Yang *et al.*, 2011). Indeed, treatment of missense *Nf2* meningioma cells with Celastrol, a proteasome inhibitor, led to increased Merlin protein expression and decreased proliferation (Yang *et al.*, 2011). Therefore meningiomas with missense *Nf2* mutations may be more sensitive to MLN3651 compared with other *Nf2* mutation types. We could not confirm this as we did not determine the type of *Nf2* mutation in 'responder' or 'non-responder' meningiomas sub-groups.

Interestingly, low concentrations significantly increased the cell viability of tumours in the non-responder group suggesting that drug concentrations at the site of the tumour should be closely monitored in future patients dosed with MLN3651 (figure 5.9B) ($p < 0.05$). Consistent with this, Zhou *et al.* identified that low doses of MLN4924 (nanomolar) significantly increased the proliferation of lung cancer (H1299), breast cancer (MCF7 and SUM159) and colorectal cancer (HCT116) cell lines when cultured in serum-free medium (Zhou *et al.*, 2016b).

We confirmed that increased MLN3651 sensitivity was Merlin-dependent by treating Merlin-positive schwannoma and meningioma for 72 hours and 144 hours (figure 5.14). The average IC50 of all Merlin-deficient schwannoma (including the outlier) was 3.14 µM whereas only one of four Merlin-positive schwannoma converged at 6.70 µM demonstrating reduced drug sensitivity (figure 5.7B and figure 5.14). Cooper *et al.* predicted a 10 fold increased sensitivity of Merlin-deficient schwannoma cell to MLN4924 compared with Merlin-positive Schwann cells (Cooper *et al.*, 2017). However, this was using a mouse model and normal Merlin-positive cells whereas we compared the response between primary human Merlin-deficient and Merlin-positive meningioma to MLN3651. Unfortunately, as most of the Merlin-positive samples did not converge, we cannot calculate a fold change of sensitivity (figure 5.14). Future experiments should determine if Merlin-deficient cells are more sensitive because of increased CRL4-DCAF1 activity or hyper-activation of other pathways.

In the meningioma model, we tested three Merlin-positive meningioma at 72 hours and found an average IC50 of 10.04 µM (figure 5.14). As the average IC50 of Merlin-deficient meningiomas in the 'responder' sub-group at the same time point was 1.31 µM, we estimate a 7.5 fold increased sensitivity of Merlin-deficient meningioma cells compared with Merlin-positive cells (figure 5.9A). However, this does not take into account the 'non-responder' sub-group and this group had an IC50 of 12.81 µM which is higher than the average IC50 of Merlin-positive meningioma tumours (figure 5.9B). Although we only tested one Merlin-positive meningioma after 144 hours MLN3651 treatment, the IC50 was 2.75 µM and again, Merlin negative meningiomas had an approximate 7.5 fold increased sensitivity at the same time point (figure 5.9C and

figure 5.14D). This is particularly interesting because the 144 hour Merlin-deficient meningioma tumours included both 'responders' and 'non-responders'. This suggests that prolonged treatment sensitizes 'non-responders' meningioma cells but prolonged treatment in Merlin-positive meningioma cells does not have the same effect.

Human Merlin-positive Schwann cells were treated with MLN3651 for 72 hours or 144 hours (figure 5.15A-B). Two Schwann cell samples were particularly sensitive to a 72 hour treatment of MLN3651 whereas two were not. The average IC50 was 8.44 µM but, as expected, had a large standard error. Indeed, there was a similar pattern observed after a 144 hour MLN3651 treatment. Two out of the three Schwann cells tested were resistant whereas one sample showed sensitivity. Only one sample was tested at both a 72 hour and a 144 hour timepoint, and interestingly, this sample was less sensitive after 144 hours than after 72 hours (black line) (figure 5.15A-B). This could be due to the proliferative rate or passage at the time of the experiment as the time points were performed independently and at different times due to primary Schwann cell availability. Therefore, it is difficult to ascertain if Schwann cells are sensitive to MLN3651 or not. It could be that the sensitive Schwann cells were proliferating at a much faster rate than the other two samples. Importantly, differentiated Schwann cells do not divide *in vivo* in the absence of nerve injury; therefore non-proliferating Schwann cells may respond differently to MLN3651 (Kim *et al.*, 2000; Webster, Martin & O'Connell, 1973). The suitability of using *in vitro* primary human Schwann cells as a drug control is in question. Further information is needed from planned *in vivo* testing of MLN3651 to determine potential toxicity to Schwann cells.

HMC are much less sensitive to MLN3651 compared with the 'responder' meningiomas after 72 hours (figure 5.15C). However, HMC were more sensitive to MLN3651 than the 'non-responder' group and lower doses of MLN3651 significantly increased viability in both HMC and 'non-responders' (figure 5.9B). We also confirmed that MLN3651 activated apoptosis in HMC similar to meningioma tumours (figure 5.15E). Therefore, suggesting that MLN3651 may be toxic to normal cells. However, after two 72 hours MLN3651 treatments (144 hours), HMC viability did not converge suggesting that HMC cells can recover with prolonged treatment and are resistant to MLN3651 (figure 5.15D). Conversely, 'non-responder' meningiomas did not recover after prolonged MLN3651 treatment and all meningiomas have a lower IC50 than HMC after 144 hours MLN3651 (figure 5.9B).

Unfortunately, HMC cultured in meningioma medium were very sensitive to MLN3651 which induced a significant reduction in viability at low concentrations (figure 5.15F). Furthermore, the average IC50 was 0.72 µM after a 72 hour MLN3651 treatment, much lower than 'responder' and 'non-responder' meningiomas (figure 5.9B). Whether MLN3651 is truly toxic to HMC, or if meningioma medium prevents the optimal culture of HMC (therefore rendering them sensitive to many chemicals) remains to be determined. In addition, HMC in culture proliferate and are derived from fetal/embryonic meningeal cells whereas adult meningeal cells do not proliferate. Furthermore, only a small proportion of meningeal cells, named meningeal stem cells, retain the ability to self-renew and proliferate following injury (Decimo *et al.*, 2012). Therefore, the use of *in vitro* HMC cells as a toxicity control for drugs is dubious and *in vivo* toxicity studies are essential.

Interestingly, cells cultured in HMC medium were more resistant to MLN3651 than cells, derived from the same tumours, cultured in meningioma medium (figure 5.16). This difference in sensitivity was more obvious after two 72 hour treatments, providing further evidence that a component of HMC medium promotes resistance to MLN3651 (figure 5.16B). This is an interesting and important future area of investigation. Growth factors and nutrients are often added to enhance conditions for *in vitro* cell culture. Overproduction of growth factors could also be the potential mechanism of MLN3651 resistance observed in the 'non-responder' meningioma sub-group after 72 hours MLN3651 treatment (figure 5.9B). Alternatively, MLN3651 could be inhibited or degraded by a component of the HMC medium. As HMC medium causes MLN3651 resistance and HMC cells in meningioma medium are sensitive to MLN3651, further experiments are needed to assess MLN3651's effect on normal cells; *in vivo* experiments are planned which will provide reliable data on toxicity.

DCAF1 has ubiquitin ligase activity and kinase activity independent or the CRL4-DCAF1 complex. As we found that DCAF1 expression was commonly upregulated, we hypothesised that targeting DCAF1 kinase activity may have a therapeutic effect. The DCAF1 kinase inhibitior B32B3, significantly reduced the viability of schwannoma cells with an average IC50 of 11.07 µM (figure 5.17A). In addition, 5 µM B32B3 treatment significantly decreased proliferation (figure 5.17B). In DU145 cells, 0.5 µM B32B3 treatment for 24 hours was sufficient to inhibit H2A phosphorylation downstream of kinase activity (Kim *et al.*, 2013). Therefore, the effect of B32B3 on schwannoma viability is unlikely to be dependent on DCAF1 kinase activity and may be due to inhibition of off-target proteins.

The effect of B32B3 on meningioma viability is similar to that in schwannoma, again suggesting that DCAF1 activity is not significant in Merlin-deficient tumours (figure 5.18). However, B32B3 reduced meningioma cell proliferation at 1 μM, demonstrating some anti-tumourigenic activity that should be further explored (figure 5.18B). We did not analyse H2A phosphorylation in Merlin-deficient tumours and without significant evidence of B32B3 activity, we cannot determine if DCAF1 kinase activity is increased or significant in these tumours.

5.10 Conclusion

We have shown that MLN3651 inhibits neddylation in Merlin-deficient tumours and that this inhibition is sufficient to activate the Hippo pathway in schwannoma and meningioma but not in BenMen-1. The Hippo pathway is downstream of CRL4-DCAF1 in Merlin-deficient cells and therefore MLN3651 possibly inhibits CRL4-DCAF1 activity in schwannoma and meningioma. In addition, MLN3651 also activates RAF/MEK/ERK signalling in Merlin-deficient tumours. RAF/MEK/ERK drives growth in Merlin-deficient tumours and therefore may limit the efficacy of MLN3651 as a monotherapy.

MLN3651 treatment significantly reduces cell viability, proliferation and increases apoptosis in Merlin-deficient cells, at therapeutically relevant concentrations. MLN3651 sensitivity is dependent on Merlin loss as Merlin-positive tumours were much more resistant to treatment. However, we could not accurately assess MLN3651 toxicity due to variability of response observed in Merlin-positive Schwann cells and cell culture medium-dependent MLN3652 resistance in HMC. MLN3651 toxicity must therefore be assessed *in vivo* before translation to the clinic. In addition, the evidence suggests that MLN3651 sensitivity is not completely dependent on CRL4-DCAF1

inhibition as BenMen-1 cells (in which the Hippo pathway was not activated by MLN3651) were equally or more sensitive to MLN3651 than primary cells.

Finally, we tested the efficacy of the DCAF1 kinase inhibitor, B32B3. Whilst B32B3 was effective at reducing cell viability of schwannoma and meningioma, the concentrations required were much higher than those that inhibit DCAF1 kinase activity. Therefore, DCAF1 kinase activity is unlikely to be significant in Merlin-deficient tumourigenesis, despite increased DCAF1 protein expression in many primary tumours. However, we did not directly assess DCAF1 kinase activity in Merlin-deficient cells.

Chapter 6 - Targeting DCAF1 and KSR1 in Merlin-deficient tumours

6.1 Introduction

This chapter investigates the potential of targeting both DCAF1 and KSR1 activity together. We previously showed that targeting DCAF1 and KSR1 expression together had an additive effect on proliferation and therefore we expected that utilizing drugs targeting both these pathways would be beneficial (Zhou *et al.*, 2016a and chapter 3). APS_2_79 was identified as an inhibitor of KSR1 activity by inhibiting the activation of KSR-bound MEK1/2 and therefore preventing MEK1/2 and ERK1/2 phosphorylation (Dhawan, Scopton & Dar, 2016). As KSR1 was overexpressed in Merlin-deficient schwannomas and meningiomas, we tested APS_2_79 as a potential therapeutic.

In addition, we tested the neddylation inhibitor, MLN3651 in combination with the MEK1/2 inhibitor, AZD6244. AZD6244 has potential as a therapeutic to treat schwannoma and successfully reduced PDGF-induced proliferation (Ammoun *et al.*, 2010b). We tested if the combination of MLN3651 with a MEK1/2 inhibitor would inhibit the increase in RAF/MEK/ERK activity observed with MLN3651 alone and therefore target multiple pathways simultaneously.

6.2 APS_2_79 has no effect on RAF/MEK/ERK activity or proliferation of Merlin-deficient schwannoma and meningioma

To test the effect of inhibiting KSR1-dependent RAF/MEK/ERK activity in Merlin-deficient tumours we treated primary schwannoma cells with 5 µM APS_2_79 for 24 hours. There was no clear change in pMEK1/2 or pERK1/2 protein expression (data not shown). There was also no significant changes in pERK1/2 protein expression when Merlin-deficient primary meningioma cells were treated with 10µM APS_2_79 for 24 hours (data not shown).

In addition, a 72 hour treatment of schwannoma cells with 1, 5 or 10 μM APS_2_79 did not affect cell proliferation (data not shown). A treatment of 10 μM APS_2_79 for 72 hours significantly reduced meningioma cell proliferation (data not shown). However, BenMen-1 proliferation was not reduced by any concentration of APS_2_79 treatment for 72 hours (data not shown). Therefore, APS_2_79 is not effective as a monotherapy in Merlin-deficient tumours.

6.3 MLN3651 and AZD6244 treatment inhibits RAF/MEK/ERK activity and activates the Hippo pathway

As APS_2_79 was ineffective at reducing RAF/MEK/ERK activity in Merlin-deficient tumours, we did not investigate the combinational potential of APS_2_79 with MLN3651. Instead, we used the MEK1/2 inhibitor AZD6244 in combination with MLN3651. We treated Merlin-deficient cells with MLN3651 and AZD6244 to determine if the drug combination would inhibit the RAF/MEK/ERK activation observed when Merlin-deficient cells were treated with MLN3651 alone.

Primary schwannoma cells were treated with 0.1 μM AZD6244, 1 μM AZD6244, 1 μM MLN3651, or a combination of the two drugs for 72 hours and probed for LATS2 (to indicate Hippo pathway activation), pERK1/2, ERK1/2 and CYCLIN D1 (for RAF/MEK/ERK activity) and GAPDH (the loading control) (figure 6.1A). Figure 6.1B shows that LATS2 expression was significantly increased when MLN3651 is added alone, and in combination with 0.1 μM and 1 μM AZD6244 indicating that combination of MLN3651 and AZD6244 maintained MLN3651-mediated Hippo pathway activation (Repeated Measures ANOVA with Tukey's Multiple Comparison Post Test; $p < 0.01$). Ammoun *et al.* demonstrated that 1 μM AZD6244 was sufficient to reduce schwannoma ERK1/2 activity (Ammoun *et al.*, 2010b). Figure 6.1B demonstrates that

both 0.1 µM and 1 µM AZD6244 significantly reduced pERK1/2 expression in schwannoma, as expected ($p< 0.05$). Combining MLN3651 and AZD6244 reduced the average pERK1/2 expression to baseline levels although this reduction was not significant compared with MLN3651 treatment alone. Therefore, AZD6244 treatment cannot inhibit RAF/MEK/ERK activation observed after MLN3651 treatment alone in schwannoma.

To further investigate the combinatorial benefits of MLN3651 and AZD6244, We analysed the effect of the combination on schwannoma cell proliferation (figure 6.2A and B). We chose the MLN3651 concentration that was closest to the IC50 for schwannoma viability (excluding the outlier). We found that AZD6244 or MLN3651 treatment alone did not significantly reduce proliferation in contrast to Ammoun *et al.*,2010b and chapter 5 (figure 6.2). This results shows that AZD6244 alone has no potential as a therapeutic in schwannoma. The combination of 1 µM MLN3651 and 1 µM AZD6244 significantly reduced proliferation compared with 1 µM AZD6244 alone but not compared with 1 µM MLN3651 alone (Repeated Measures ANOVA with Tukey's Multiple Comparison Post Test; $p< 0.05$).

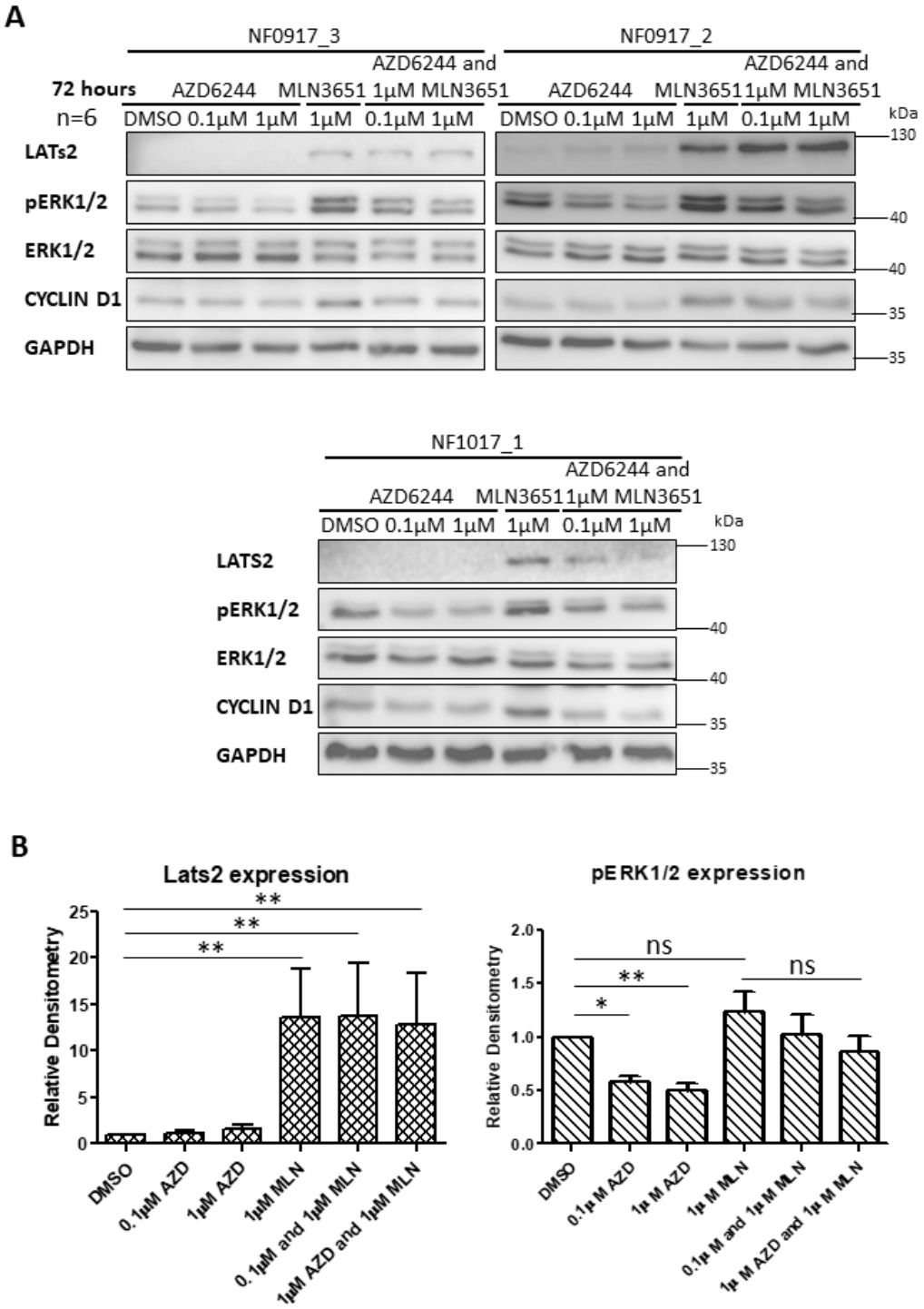

Figure 6.1 - MLN3651 and AZD6244 treatment activates the Hippo pathway in schwannoma. A: Western blot of three primary schwannomas treated with MLN3651 and/or AZD6244 (MEK1/2 inhibitor) for 72 hours and probed for LATS2 (Hippo pathway), pERK1/2 (activated ERK), ERK1/2, CYCLIN D1 and GAPDH (loading control), representative of six replicates. **B:** Mean LATS2 and pERK1/2 expression ±SEM in drug treated schwannoma cells normalized to the loading control (ERK1/2 and/or GAPDH), relative to DMSO. LATS2 expression was significantly increased by MLN3651 and, MLN3651 and AZD6244 compared with DMSO control showing that MLN3651 activates the Hippo pathway even when treated in combination with AZD6244. pERK1/2 expression was significantly decreased with AZD6244 alone showing that AZD6244 inhibits RAF/MEK/ERK activity. However, combination of MLN3651 and AZD6244 did not inhibit RAF/MEK/ERK activity compared to MLN3651 treatment alone., *- p< 0.05, **- p< 0.01, ns- not significant.

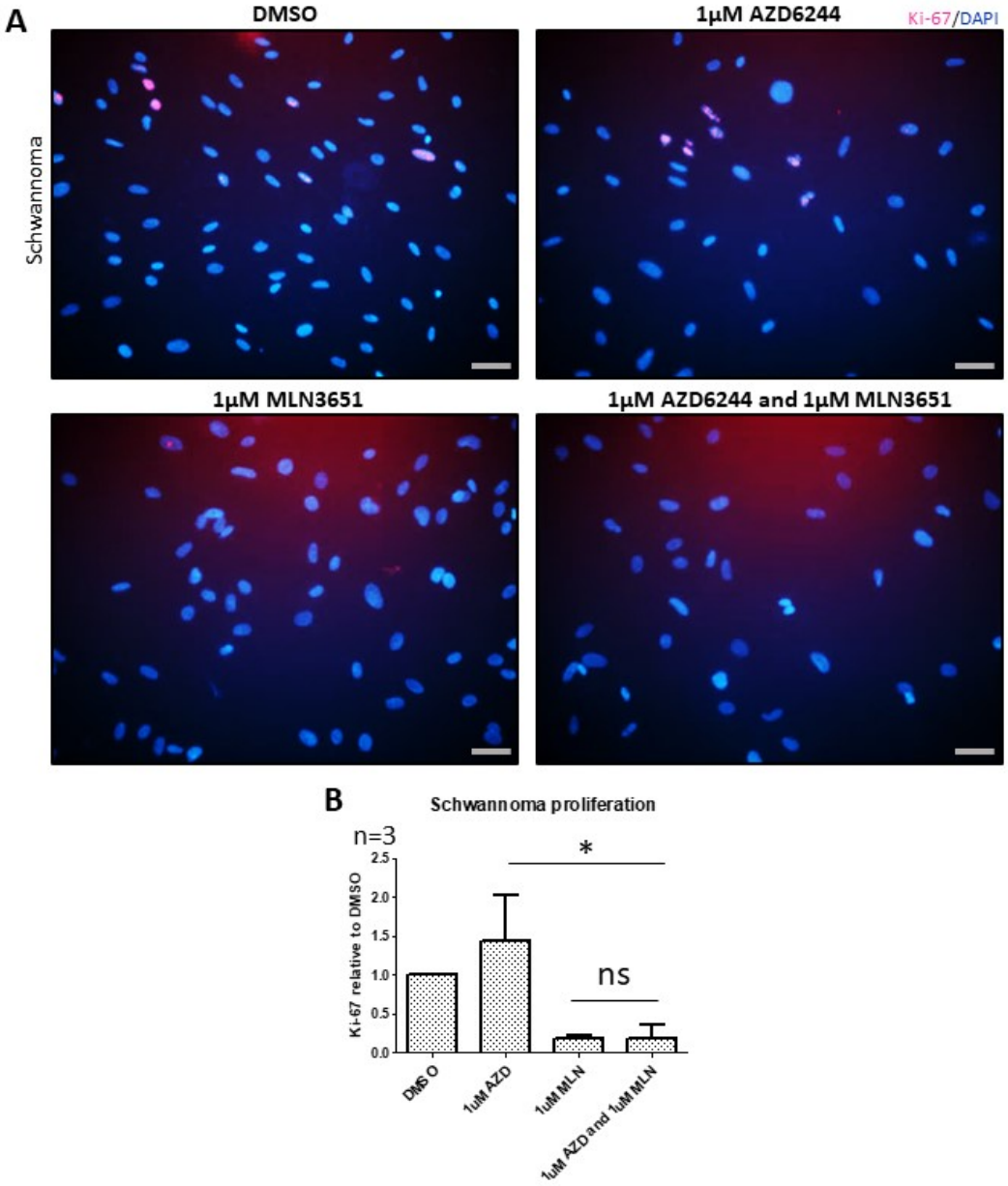

Figure 6.2 - MLN3651 and AZD6244 effect on proliferation in schwannoma. A: Representative immunocytochemistry images, at 20x magnification, of schwannoma cells treated with DMSO, 1 µM AZD6244 (MEK1/2 inhibitor), 1 µM MLN3651 or 1 µM AZD6244 and 1 µM MLN3651 for 72 hours and stained with Ki-67 antibody and DAPI, Scale bar- 50 µM. **B:** Mean proportion of Ki-67 positive cells in drug treated schwannoma cells relative to DMSO control ±SEM. At least three images each of three replicates were quantified. AZD6244 did not inhibit schwannoma proliferation. Combination of AZD6244 and MLN3651 significantly reduced proliferation compared with AZD6244 alone but not compared with MLN3651 alone, *-p< 0.05, ns- not significant.

We replicated the MLN3651 and AZD6244 combination experiment in meningioma cells and probed Western blots for LATS2, pERK1/2, ERK1/2, CYCLIN D1 and GAPDH (figure 6.3A). MLN3651 treatment (1 μM) alone did not significantly increase Hippo pathway activation, via LATS2 expression (figure 6.3B). However, combination of 1 μM MLN3651 with 1 μM AZD6244 significantly increased LATS2 expression compared with DMSO control demonstrating robust Hippo pathway activation ($p< 0.05$). We also analysed ERK1/2 activation and identified a significant increase in pERK1/2 expression after a 72 hour treatment of cells with 1 μM MLN3651 ($p< 0.01$). We also discovered that combining 0.1 μM AZD6244 or 1 μM AZD6244 with 1 μM MLN3651 significantly decreased pERK1/2 expression compared with MLN3651 alone ($p< 0.01$) (figure 6.3B). Unfortunately, none of the treatments, shown in figure 5.4A and B, significantly reduced proliferation of meningioma cells. However, the average rate of proliferation was much lower in cells treated with 1 μM MLN3651 and 1 μM AZD6244 compared with either treatment alone.

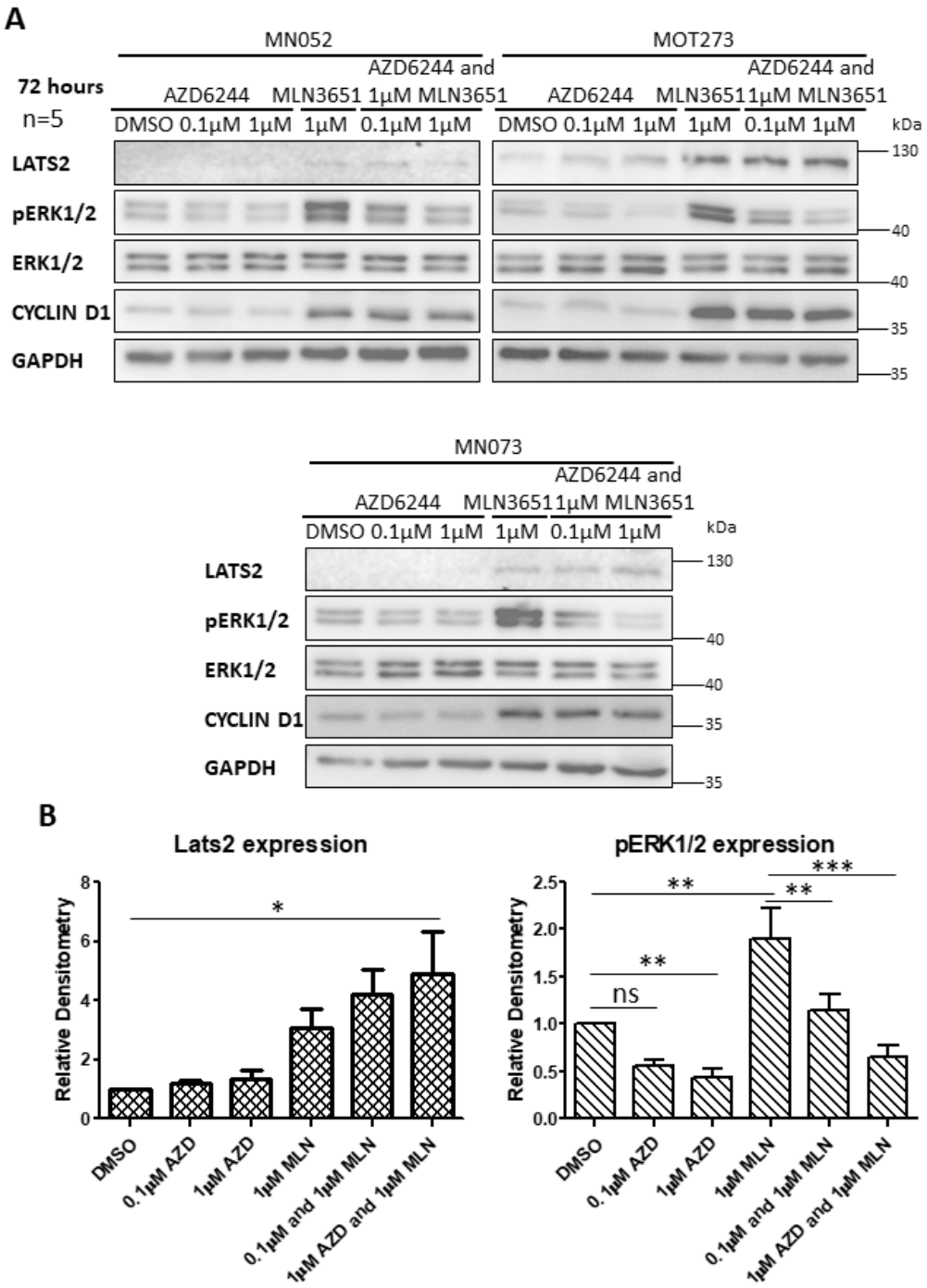

Figure 6.3 - MLN3651 and AZD6244 treatment activates the Hippo pathway and prevents ERK1/2 activation in meningioma. A: Western blot of three primary meningiomas treated with MLN3651 and/or AZD6244 (MEK1/2 inhibitor) for 72 hours and probed for LATS2 (Hippo pathway), pERK1/2 (activated ERK), ERK1/2, CYCLIN D1 and GAPDH (loading control), representative of five replicates. **B:** Mean LATS2 and pERK1/2 expression ±SEM in drug treated schwannoma cells normalized to the loading control (ERK1/2 and/or GAPDH), relative to DMSO. LATS2 expression was significantly increased by the combination of AZD6244 and MLN3651 compared with DMSO control showing sustained Hippo pathway activation when the drugs are combined. pERK1/2 expression was significantly decreased when AZD6244 and MLN3651 are combined compared with MLN3651 alone showing that RAF/MEK/ERK activity is inhibited, *- p< 0.05, **- p< 0.01, ***- p< 0.001, ns- not significant.

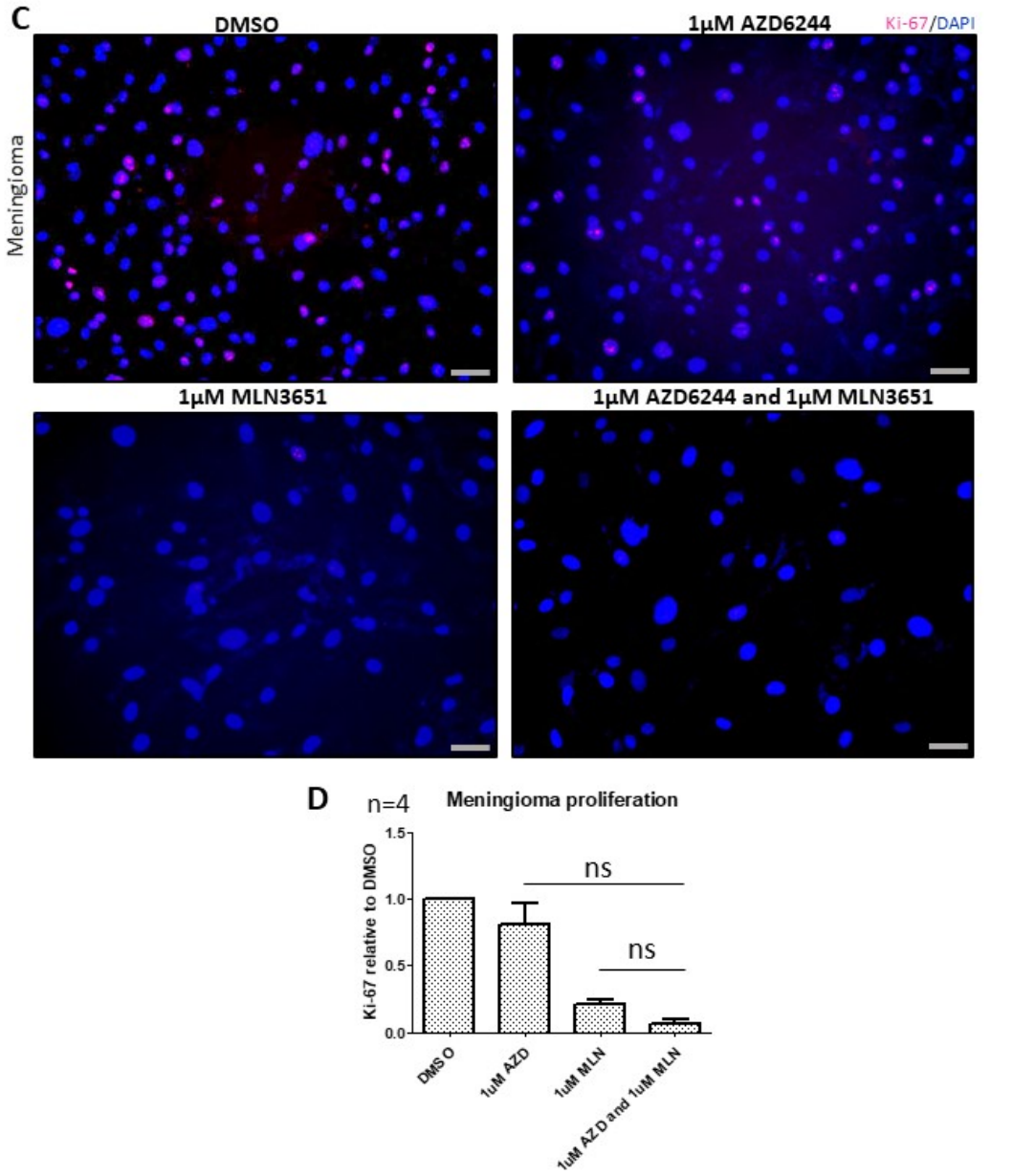

Figure 6.4 - MLN3651 and AZD6244 effect on proliferation in meningioma. A: Representative immunocytochemistry images, at 20x magnification, of meningioma cells treated with DMSO, 1 µM AZD6244 (MEK1/2 inhibitor), 1 µM MLN3651 or 1 µM AZD6244 and 1 µM MLN3651 for 72 hours and stained with Ki-67 antibody and DAPI, Scale bar- 50 µM. **B:** Mean proportion of Ki-67 positive cells in drug treated meningioma cells relative to DMSO control ±SEM. At least three images each of four replicates were quantified. Combination of AZD6244 and MLN3651 significantly reduced the mean proliferation rate compared with either treatment alone but this was not significant (ns).

We also assessed the effect of combining MLN3651 and AZD6244 treatment in BenMen-1 cells. We postulated that BenMen-1 results would be more consistent than primary cells and therefore, the Ki-67 proliferation assay would be more sensitive. In addition, we used a lower MLN3651 concentration of 0.3 μM compared with 1 μM used in primary cells. This was because the average IC50 for BenMen-1 viability after MLN3651 treatment was 0.3 μM after 72 hours, much lower than primary tumours. Treatment with 0.3 μM MLN3651 and 1 μM AZD6244, for 72 hours, significantly increased LATS2 expression compared with DMSO whereas MLN3651 alone did not ($p< 0.05$) (figure 6.5A-B). This indicates that combination of MLN3651 and AZD6244 produces a more robust and prolonged activation of the Hippo pathway compared with MLN3651 alone. Similar to meningioma, MLN3651 treatment significantly increased pERK1/2 expression after 72 hours ($p< 0.01$) (figure 6.5B). Addition of 1 μM AZD6244 significantly decreased ERK1/2 activation of BenMen-1 cells compared with MLN3651 whilst 0.1 μM was not able to reduce pERK1/2 expression ($p< 0.05$) (figure 6.5B). We treated cells for 72 hours with 1 μM AZD6244, 0.3 μM MLN3651 or both drugs and analysed proliferation by Ki-67 index (figure 6.6A and B). AZD6244 and MLN3651 significantly reduced proliferation compared with DMSO and either drug alone suggesting the drugs have an additive effect on proliferation ($p< 0.05$).

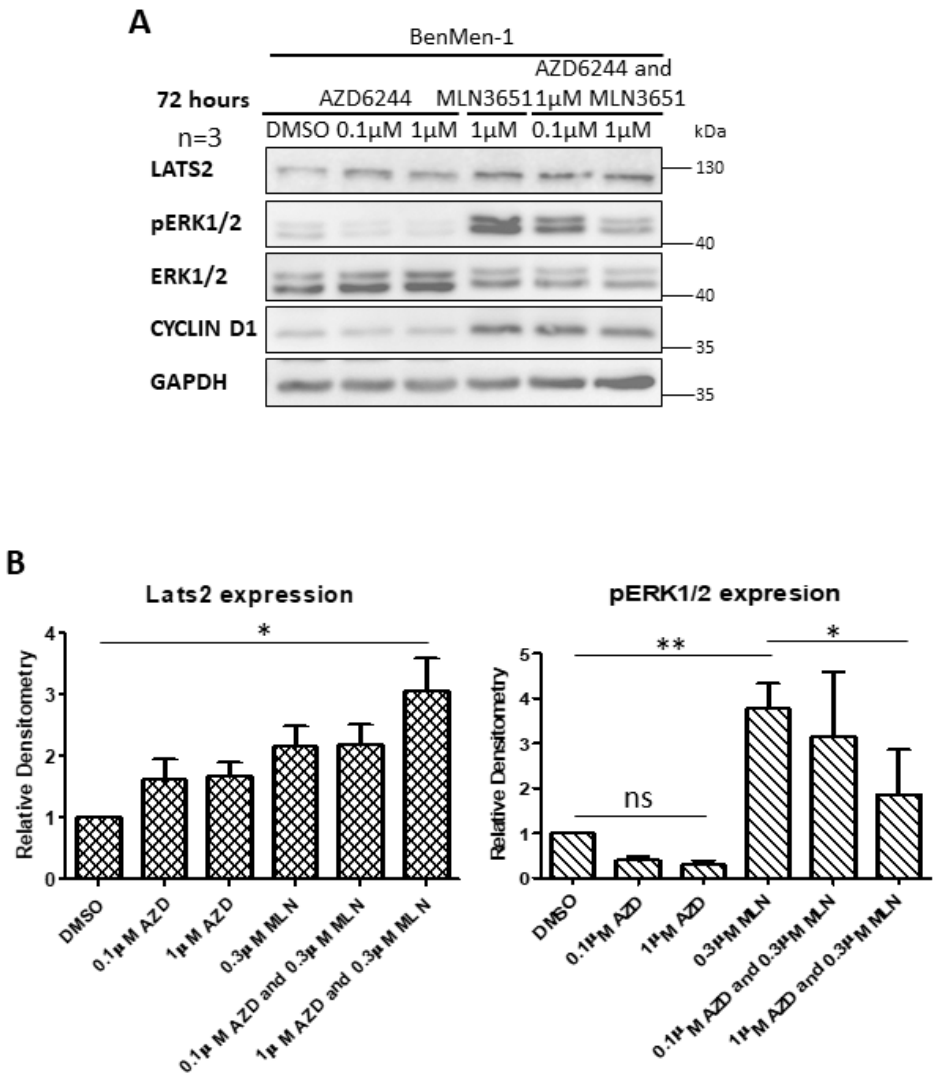

Figure 6.5 - MLN3651 and AZD6244 activates the Hippo pathway and prevents ERK1/2 activation in BenMen-1. A: Western blot of the benign meningioma cell line, BenMen-1, treated with MLN3651 and/or AZD6244 (MEK1/2 inhibitor) for 72 hours and probed for LATS2 (Hippo pathway), pERK1/2 (activated ERK), ERK1/2, CYCLIN D1 and GAPDH (loading control), representative of three replicates. **B:** Mean LATS2 and pERK1/2 expression ±SEM in drug treated schwannoma cells normalized to the loading control (ERK1/2 and/or GAPDH), relative to DMSO. LATS2 expression was significantly increased by the combination of AZD6244 and MLN3651 compared with DMSO control showing sustained Hippo pathway activation when combining both drugs. pERK1/2 expression was significantly decreased when AZD6244 and MLN3651 are combined compared with MLN3651 alone demonstrating RAF/MEK/ERK inhibition, *- $p< 0.05$, **- $p< 0.01$, ***- $p< 0.001$, ns- not significant.

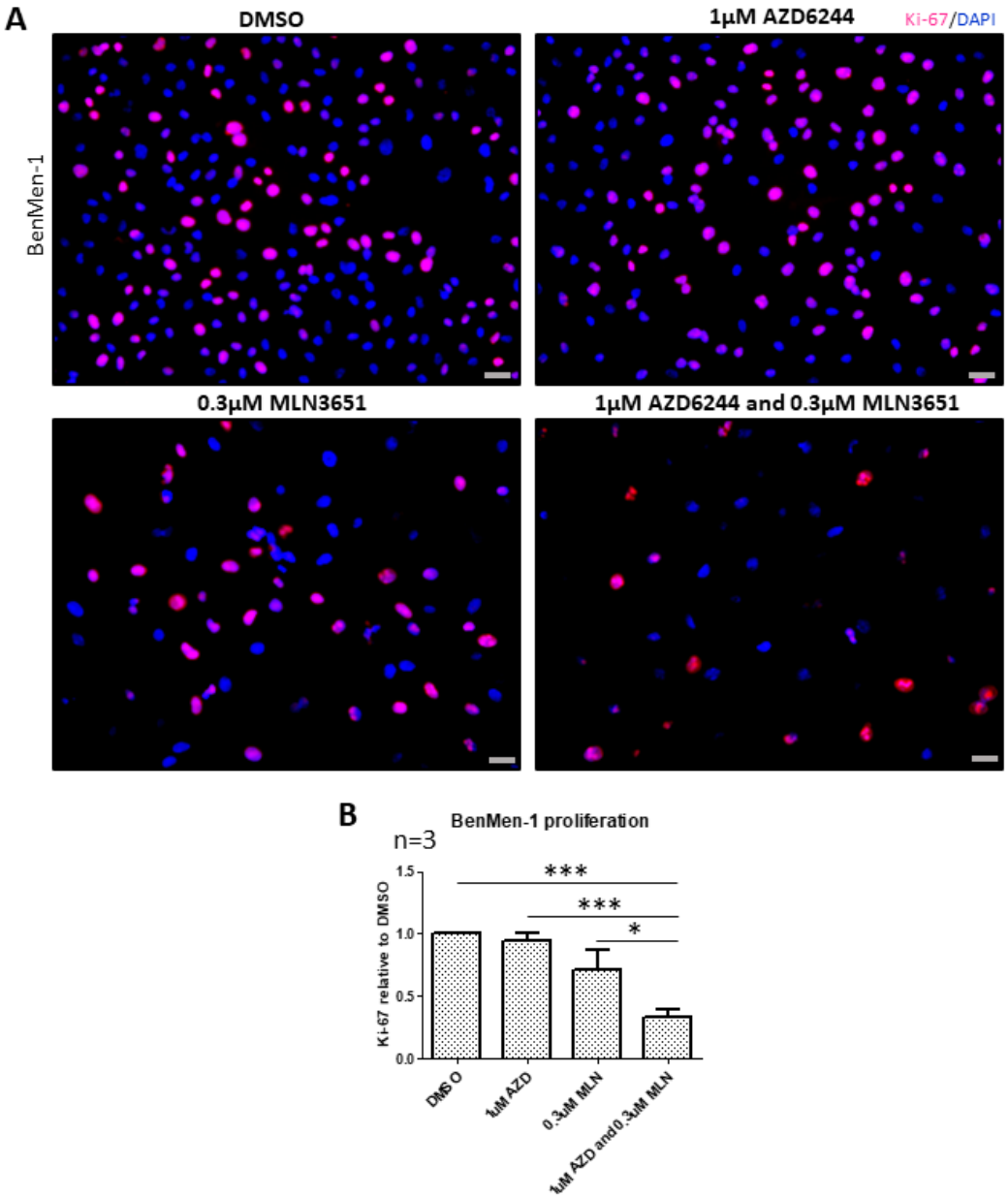

Figure 6.6 - MLN3651 and AZD6244 reduces proliferation in BenMen-1. A: Representative immunocytochemistry images, at 20x magnification, of a benign meningioma cell line (BenMen-1) treated with DMSO, 1 µM AZD6244 (MEK1/2 inhibitor), 0.3 µM MLN3651 or 1 µM AZD6244 and 0.3 µM MLN3651 for 72 hours and stained with Ki-67 antibody and DAPI, Scale bar- 50 µM. **B:** Mean proportion of Ki-67 positive cells in drug treated BenMen-1 cells relative to DMSO control ±SEM. At least three images each of three replicates were quantified. Combination of AZD6244 and MLN3651 significantly reduced the proliferation rate compared with either treatment alone demonstrating the additive benefit of combining the two drugs in meningioma, *- p< 0.05, ***- p< 0.001.

We could not confirm an additive effect of MLN3651 and AZD6244 on proliferation in primary schwannoma or meningioma so we wanted to determine if there was a synergistic effect of the drugs on cell viability. We tested the effect of AZD6244 on cell viability of schwannoma and meningioma (data not shown). There was no significant changes to viability at any concentration (0.1–20 μM) and therefore we concluded it was inappropriate to combine MLN3651 and AZD6244 in this assay.

6.4 Discussion

Dhawan, Scopton & Dar, 2016 found that the KSR1 inhibitor APS_2_79, was ineffective as a monotherapy. However, we postulated that as KSR1 and RAF/MEK/ERK are hyper-active in Merlin-deficient tumours, APS_2_79 alone would be sufficient to inhibit KSR1-dependent RAF/MEK/ERK activation and proliferation. Unfortunately, we found that neither RAF/MEK/ERK activity or proliferation were reduced by APS_2_79 in Merlin-deficient tumours (data not shown). It can be hypothesised that APS_2_79 did not reach a high enough intracellular concentration to inhibit all KSR1-MEK1/2 binding at the concentrations tested. Alternatively, the compound purchased may have differed to the one used in Dhawan *et al.* such as purity, manufacturing method or concentration. Future experiments should determine if the APS_2_79 we purchased matches the efficacy of the compound used in Dhawan *et al.* (Dhawan, Scopton & Dar, 2016).

We found that a 72 hour treatment of 1 μM AZD6244 in primary schwannoma did not significantly reduce proliferation in contrast to Ammoun *et al* (Ammoun *et al.*, 2010b)(figure 6.2). However, Ammoun *et al.* stimulated cells with PDGF before AZD6244 treatment whereas we did not which could explain the discrepancy (Ammoun *et al.*, 2010b). In addition, 1 μM MLN3651 did not significantly reduce

proliferation compared with DMSO, in contrast to the previous chapter. This discrepancy is probably due to the small number of samples used in this experiment therefore limiting the statistical power. Further experiments should assess the efficacy of combining a wider range of MLN3651 and AZD6244 concentrations in schwannoma.

In meningioma, a 72 hour treatment of 1 μM MLN3651 did not significantly increase LATS2 expression (figure 6.3). In the previous chapter, a 24 hour 1 μM MLN3651 treatment was sufficient to increase LATS2 expression and therefore Hippo pathway activation. At 72 hours, there may be a signalling feedback mechanism that prevents LATS2 activation. Interestingly, combination of 1 μM MLN3651 with 1 μM AZD6244 significantly increased LATS2 expression compared with DMSO, suggesting that the RAF/MEK/ERK pathway is upstream of the Hippo pathway in Merlin-deficient cells (figure 6.3). We also analysed the RAF/MEK/ERK pathway after treatment. A 72 hour treatment of 1 μM AZD6244 significantly reduced pERK1/2 expression whilst a 1 μM MLN3651 treatment significantly increased pERK1/2 in meningioma (figure 6.4). Combination of 0.1 μM or 1 μM AZD6244 significantly decreased pERK1/2 expression compared with 1 μM MLN3651 treatment suggesting there is a therapeutic benefit of combining both drugs. Whilst there was a trend in reduced proliferation of combination-treated meningioma cells compared to either drug treatment alone; this was not statistically significantly (figure 6.4). However, the sample size was much lower than that reported in previous chapters limiting the statistical power of this experiment. The sample size must be increased in order to assess the efficacy of combining MLN3651 and AZD6244 in meningioma. In addition, variability in baseline proliferation rates of meningioma is a confounding factor. Indeed, we removed samples that were proliferating at a rate lower than 8% in the DMSO control as it was

difficult to assess drug efficacy with such low baseline proliferation. We concluded that measuring proportions of Ki-67 cells was not the most sensitive method to assess drug combinations.

Consistent with chapter 5, LATS2 expression was not significantly increased in BenMen-1 after MLN3651 treatment alone, even after 72 hours (figure 6.5). However, combination of MLN3651 with 1 µM AZD6244 significantly increased LATS2 expression compared with DMSO control. Therefore suggesting that AZD6244 enhances Hippo pathway activation in MLN3651 treated cells. Additionally, the combination of MLN3651 with 1 µM AZD6244 significantly decreased pERK1/2 expression compared with MLN3651 treatment alone, in agreement with primary meningioma data (figure 6.3 and 6.5).

Interestingly, proliferation was significantly decreased with the combination of 0.3 µM MLN3651 and 1 µM AZD6244 compared with DMSO and either drug alone (figure 6.6). The lower MLN3651 concentration used may enhance the sensitivity of the Ki-67 proliferation assay. In addition, BenMen-1 baseline proliferation was much higher than primary meningioma cells which may make them more sensitive to drug treatment.

6.5 Conclusion

The KSR1 inhibitor, APS_2_79 has little therapeutic potential in Merlin-deficient cells as it was unable to reduce RAF/MEK/ERK activity or proliferation at relevant concentrations. Previous research shows that APS_2_79 must be combined with a MEK1/2 inhibitor in order to be efficacious. We did not test this combination in Merlin-deficient cells but it may be necessary in order to successfully reduce RAF/MEK/ERK activity and proliferation.

As direct and specific CRL4-DCAF1 and KSR1 inhibition was not possible, we combined MLN3651 and AZD6244 to demonstrate therapeutic potential of combination therapy targeting the two main downstream pathways (Hippo and RAF/MEK/ERK activity). We have shown that combination of MLN3651 and AZD6244 has three additional benefits compared with either treatment alone. Firstly, LATS2 expression and therefore the Hippo pathway is consistently elevated in combination treated cells (schwannoma, meningioma and BenMen-1). Secondly, the increase in RAF/MEK/ERK activity observed after MLN3651 treatment is inhibited with the addition of AZD6244 (meningioma and BenMen-1). Finally, combination of 0.3 μM MLN3651 and 1 μM AZD6244 reduced BenMen-1 cell proliferation compared with either treatment alone. Therefore, combination of MLN3651 and AZD6244 is a potential therapeutic option for schwannoma and meningioma that should be further explored.

Chapter 7 – Discussion

7.1 Introduction

The aims of this project were to assess the potential of targeting CRL4-DCAF1 and KSR1 in Merlin-deficient schwannoma and meningioma. As CRL4-DCAF1 is a master regulator and KSR1 has many roles in Merlin-deficient tumours, we hypothesised that CRL4-DCAF1 and KSR1 could be targeted together to improve efficacy compared with targeting only one protein or pathway (Li *et al.*, 2010). In order to assess this we first needed to determine DCAF1 and KSR1 expression and the meaning of the CRL4-DCAF1 and KSR1 interaction in Merlin-deficient tumours. We hypothesised that targeting CRL4-DCAF1 and KSR1 activity individually, with MLN3651 and APS_2_79 respectively, would be efficacious in schwannoma and meningioma. Finally, we hypothesised that targeting both CRL4-DCAF1 and KSR1 activity together would have additional benefits.

KSR1 has been shown to be upregulated in Merlin-deficient schwannoma and contributes to tumourigenesis (Zhou *et al.*, 2016a). In addition, targeting DCAF1 and KSR1 expression in schwannoma led to an enhanced effect on proliferation compared with targeting DCAF1 or KSR1 alone (Zhou *et al.*, 2016a). KSR1 expression has not been previously explored in Merlin-deficient meningioma, and DCAF1 expression has not been explored in Merlin-deficient schwannoma or meningioma. We found that DCAF1 and KSR1 were upregulated in Merlin-deficient schwannoma and meningioma. In addition, targeting DCAF1 and KSR1 together enhanced the effect on proliferation in meningioma.

CRL4-DCAF1 is inhibited by Merlin in the nucleus; therefore, loss of Merlin leads to CRL4-DCAF1 hyper-activity (Li *et al.*, 2010). CRL4-DCAF1 has been described as a master regulator in Merlin-deficient tumours and targets the Hippo pathway, among others (Li *et al.*, 2014; Zhou & Hanemann, 2012). We showed that CRL4-DCAF1 and

KSR1 interact in Merlin-deficient tumours (Zhou *et al.*, 2016a). As KSR1 has an important role in Merlin-deficient schwannoma, it is important to understand how CRL4-DCAF1 may regulate KSR1 to enhance KSR1 signalling. We showed that CRL4-DCAF1 enhances KSR1 association with MEK1/2 and ERK1/2 and their subsequent phosphorylation. Accordingly, we showed that DCAF1 knockdown in schwannoma reduced RAF/MEK/ERK activity, presumably in a KSR1-dependent manner. This observation provided the mechanistic basis for combination therapy of a DCAF1 and KSR1 inhibitor.

The treatment options for schwannoma, meningioma and ependymoma are limited to surgery and radiotherapy and therefore, a therapeutic strategy is urgently required, particularly for NF2 patients who have numerous tumours (Evans, 2009). CRL4-DCAF1 is a potential therapeutic target for Merlin-deficient tumours and can be targeted by the neddylation inhibitor, MLN4924 (Cooper *et al.*, 2017). MLN3651 is a second-generation NAE inhibitor which can be taken orally and has not yet been tested in any indication. We showed that MLN3651 has potential as a treatment for Merlin-deficient tumours. KSR1 is also a therapeutic target as it regulates; proliferation, apoptosis, adhesion and cell morphology in schwannoma (Zhou *et al.*, 2016a). APS_2_79 is an inhibitor of KSR1-dependent RAF/MEK/ERK activity, which has activity when combined with a MEK1/2 inhibitor in K-RAS driven tumours (Dhawan, Scopton & Dar, 2016). APS_2_79 has not yet been tested in Merlin-deficient tumours. We showed that APS_2_79 alone has no or little potential as a treatment for Merlin-deficient tumours. Finally, we showed that combination treatment of MLN3651 and AZD6244 had additive effects on proliferation in meningioma. We also showed that RAF/MEK/ERK activation by MLN3651 could be prevented with the addition of AZD6244.

Combination of MLN3651 and AZD6244 had the unexpected effect of activating the Hippo pathway more robustly than MLN3651 treatment alone.

7.2 DCAF1 and KSR1 expression is increased in schwannoma and meningioma

We have shown for the first time that DCAF1 expression is increased in Merlin-deficient schwannoma and meningioma compared with normal cells (figure 3.1–4). Merlin inhibits CRL4-DCAF1 activity and therefore Merlin-deficient cells have increased CRL4-DCAF1 activity (Li *et al.*, 2010). We identified increased DCAF1 expression as another mechanism that contributes to increased CRL4-DCAF1 activity and possibly increased DCAF1 kinase activity in Merlin-deficient cells.

We found that KSR1 protein expression was significantly increased in primary meningiomas compared with normal meningeal cells supporting the notion that KSR1 expression is regulated by Merlin (figure 3.3 and 3.4). However, KSR1 expression was not increased in the benign meningioma cell line, BenMen-1 (figure 3.4E and F). The BenMen-1 cell line was derived from a WHO I meningioma and immortalized by manipulating telomerase activity (Püttmann *et al.*, 2005). High telomerase activity correlates with higher grade meningiomas allowing unlimited growth (Boldrini *et al.*, 2003). Therefore BenMen-1 cells may represent a higher grade now they have been immortalized and could explain the inconsistencies between BenMen-1 and primary cells used in this study. In addition, Mei *et al.* identified chromosome 5 amplification in BenMen-1 cells which may not be present in all primary tumours (Mei *et al.*, 2017). Accordingly, KSR1 expression was not increased in the WHO III cell line, KT21-MG1-Luc5D.

7.3 CRL4-DCAF1 does not regulate KSR1 expression or localization

We previously reported that CRL4-DCAF1 does not regulate KSR1 expression in Merlin-deficient schwannoma (Zhou *et al.*, 2016a). We confirmed this result in meningioma and BenMen-1 by knocking down DCAF1 and observing changes in KSR1 expression (figure 3.5). KSR1 was unchanged suggesting that CRL4-DCAF1 does not target KSR1 for degradation in meningioma. Poly-ubiquitination of substrates by E3 ubiquitin ligase complexes, such as CRL4-DCAF1, often leads to proteasome-dependent degradation. We found that DCAF1 knockdown did not affect the poly-ubiquitination of KSR1 confirming that KSR1 poly-ubiquitination is not CRL4-DCAF1-dependent (figure 4.7). Indeed, Rinaldi *et al.* identified PRAJA2 as the E3 ubiquitin ligase responsible for KSR1 poly-ubiquitination and subsequent degradation (Rinaldi *et al.*, 2016). The mechanism of KSR1 upregulation in Merlin-deficient cells has not yet been determined; therefore, PRAJA2 protein expression and activity should be further investigated.

Although KSR1 was predominantly nuclear in Schwann cells and schwannoma, we identified an increase in cytoplasmic KSR1 in schwannoma compared with Schwann cells (figure 3.6). Therefore, we hypothesised that nuclear export of KSR1 was mediated by CRL4-DCAF1. However, there was no difference in KSR1 localization between HMC and BenMen-1 (figure 3.8). Furthermore, DCAF1 knockdown did not lead to KSR1 redistribution in schwannoma or meningioma (figure 3.7 and 3.9). Accordingly, the evidence suggests that CRL4-DCAF1 does not regulate KSR1 nuclear export. We did not explore whether CRL4-DCAF1 regulates KSR1 membrane localization, which could also affect KSR1 activity.

7.4 CRL4-DCAF1 regulates KSR1-dependent RAF/MEK/ERK activity

DCAF1 knockdown in Merlin-deficient schwannoma led to a significant reduction in pERK1/2 expression suggesting that CRL4-DCAF1 regulates RAF/MEK/ERK activity (figure 3.10). Unfortunately, we were unable to show this in Merlin-deficient meningioma or BenMen-1 (figure 3.11 and 3.12). However, DCAF1 knockdown was around 20% less efficient in meningioma than in schwannoma. Therefore, remaining DCAF1 expression in meningioma may be sufficient to maintain RAF/MEK/ERK activity. To test this theory, an alternative DCAF1 lentivirus with increased efficiency should be utilized. Another important consideration is that there may be alternative mechanisms regulating RAF/MEK/ERK activity in meningioma that are absent in schwannoma. Indeed, Bassiri *et al.* reported that there were 15 commonly upregulated or downregulated phospho-proteins between schwannoma and BenMen-1 cells compared with hundreds of phospho-proteins identified in the separate datasets, highlighting the substantial differences between schwannoma and meningioma signalling (Bassiri *et al.*, 2017). In addition, *Nf2* mutant meningiomas tend to be more heterogenous than other mutant meningiomas with increased chromosomal instability (Clark *et al.*, 2013; Clark *et al.*, 2016).

Unfortunately, DCAF1 knockdown was not sufficient to downregulate CYCLIN D1 expression in schwannoma or meningioma, downstream of the RAF/MEK/ERK pathway (figure 3.10–12). Therefore, RAF/MEK/ERK signalling is only partly-dependent on DCAF1. We hypothesised that targeting DCAF1 and KSR1 together would inhibit RAF/MEK/ERK signalling more effectively in schwannoma and lead to downregulation of CYCLIN D1. In figure 3.13, DCAF1 or KSR1 knockdown alone did not significantly reduce pMEK1/2 or pERK1/2 expression in contrast to our previous experiment and

published data by Zhou *et al.* (Zhou *et al.*, 2016a). This is probably because our sample size was small compared with the previous experiment and the KSR1 shRNA construct was less effective than the construct used by Zhou *et al.* However, we observed a significant decrease in pMEK1/2 activity in schwannoma after DCAF1 and KSR1 knockdown compared with the scramble control suggesting that DCAF1 and KSR1 function together to regulate RAF/MEK/ERK activity in schwannoma (figure 3.13). CYCLIN D1 expression was not reduced in schwannoma after DCAF1 and KSR1 knockdown suggesting that more complete inhibition of DCAF1 and KSR1 expression is necessary or that CYCLIN D1 expression is not completely dependent on DCAF1 or KSR1 signalling. Similarly, pERK1/2 and CYCLIN D1 expression were not reduced in BenMen-1 following DCAF1 and KSR1 knockdown (figure 3.14).

We showed that DCAF1 and KSR1 interact in a Merlin-deficient model; therefore, we wanted to determine if DCAF1 regulation of RAF/MEK/ERK activity was dependent on KSR1. We knocked down DCAF1 expression, overexpressed human KSR1 and immunoprecipitated the KSR1 complex in a HEK293T model (figure 4.8). DCAF1 knockdown led to a significant reduction of pMEK1/2, MEK1/2, pERK1/2 and ERK1/2 in the KSR1 complex providing evidence that DCAF1 facilitates KSR1's interaction with the RAF/MEK/ERK pathway. Therefore, DCAF1 enhances RAF/MEK/ERK activity in a KSR1-dependent manner. We also showed, for the first time, that endogenous DCAF1 and KSR1 interact in a Merlin-deficient model suggesting that DCAF1-mediated regulation of KSR1 activity is important in Merlin-deficient cells (figure 4.1).

We identified a mechanism by which DCAF1 facilitates RAF/MEK/ERK activity by enhancing KSR1 association with MEK1/2 and ERK1/2. To understand more about the nature of this regulation we used truncated DCAF1 and KSR1 constructs to identify

potential binding sites between DCAF1 and KSR1 (figure 4.2 and 4.3). DCAF1 binds to the N-terminal KSR1 complex that contain domains responsible for Raf phosphorylation and, ERK1/2 and 14-3-3 protein binding (Morrison, 2001; Müller *et al.*, 2001; Ritt *et al.*, 2007). DCAF1 knockdown reduced both MEK1/2 and ERK1/2 association with KSR1 but C-RAF was unchanged (figure 4.8). Therefore, DCAF1 is unlikely to specifically modulate C-RAF or ERK1/2 binding to KSR1 and possibly inhibits KSR1 binding to 14-3-3 proteins to activate KSR1 activity. In support of this theory, the DCAF1/KSR1 interaction occurred predominantly in the cytoplasm of HEK293T cells rather than the nucleus (figure 4.5). Further investigation is required to determine the specific mechanism of CRL4-DCAF1 regulation of KSR1 activity.

We identified DDB1 as well as DCAF1 in the wild-type KSR1 and N-terminal KSR1 complexes suggesting that CRL4-DCAF1 ubiquitin activity enhances KSR1's kinase/scaffolding function rather than DCAF1 kinase activity (figure 4.3). Interestingly overexpression of the S518A Merlin mutant, which inhibits CRL4-DCAF1, also reduced pMEK1/2 in the KSR1 complex further suggesting that CRL4-DCAF1 ubiquitin activity is responsible (Zhou *et al.*, 2016a). Indeed, KSR1 binds to the C-terminal DCAF1 complex containing the CRL4-DCAF1 substrate recruitment domain for ubiquitination (Angers *et al.*, 2006) (figure 4.2).

The experimental setup we used to investigate KSR1 ubiquitination was not sensitive enough to identify mono-ubiquitination in the presence of poly-ubiquitination and therefore it is possible that KSR1 is a CRL4-DCAF1 substrate for mono-ubiquitination (figure 4.6). Sagar *et al.* reported that ubiquitination of Thyroid hormone-activating type 2 deiodinase can modify its conformation and therefore inhibit its enzymatic activity (Sagar *et al.*, 2007). Similarly, CRL4-DCAF1-mediated monoubiquitylation of

LATS2 inhibited its kinase activity (Li *et al.*, 2014). Furthermore, mono-ubiquitination of K476 on Zeta-chain-associated protein kinase 70 (ZAP-70) can stabilize its active conformation (Ball *et al.*, 2016). Indeed, DCAF1 could ubiquitinate KSR1, changing its conformation and interfering with KSR1 binding to 14-3-3 proteins leading to enhanced KSR1 activity and plasma membrane accumulation (Jagemann *et al.*, 2008). CRL4-DCAF1 mediated KSR1 mono-ubiquitination could be explored utilizing an *in vitro* ubiquitylation assay as reported by Li *et al.* to test CRL4-DCAF1 ubiquitination of LATS1 (Li *et al.*, 2014). In addition, mass spectrometry of purified KSR1 could be performed to identify the ubiquitination sites and further evaluate the role of ubiquitination.

7.5 DCAF1 and KSR1 as therapeutic targets

DCAF1 knockdown significantly reduced proliferation in schwannoma cells and we have shown that this is consistent in both meningioma and BenMen-1 cells (figure 3.11 and 3.12) (Li *et al.*, 2010; Zhou *et al.*, 2016a). We showed that DCAF1 regulates RAF/MEK/ERK activity in schwannoma and therefore targeting DCAF1 and KSR1 may lead to a greater inhibition of the RAF/MEK/ERK pathway than targeting either protein alone (figure 3.10). Although RAF/MEK/ERK inhibition was not achieved by DCAF1 knockdown in meningioma, we stipulated that DCAF1 and KSR1 knockdown would still be beneficial as it would target multiple pathways that are required for Merlin-deficient tumourigenesis (figure 3.11). For example, Li *et al.* demonstrated that changes in gene transcription following DCAF1 knockdown or Merlin overexpression significantly overlap, suggesting DCAF1 is a master regulator in Merlin-deficient cells (Li *et al.*, 2010). Furthermore, loss of DCAF1 inhibited integrin and Hippo pathway target genes suggesting that the reduction in proliferation observed after DCAF1 knockdown

in meningioma and BenMen-1 cells may also involve inhibition of these pathways (Li *et al.*, 2010).

We identified a KSR1 inhibitor (APS_2_79) that disrupts the phosphorylation of MEK1/2 bound to KSR1 whereby preventing KSR1-mediated RAF/MEK/ERK activation (Dhawan, Scopton & Dar, 2016). We tested the therapeutic potential of APS_2_79 as a monotherapy in Merlin-deficient cells because KSR1 and the RAF/MEK/ERK pathway were overexpressed. Dhawan *et al.* showed that APS_2_79 bound to the KSR2 active site with an IC50 of 120 nM and activity against KSR1-MEK binding in HEK293T cells. Dhawan *et al.* reported that 3 µM was required to reduce the viability of the K-RAS mutant cell line A549: K-RAS G12S, by half (Dhawan, Scopton & Dar, 2016). However, APS_2_79 treatment did not reduce RAF/MEK/ERK activity or proliferation of Merlin-deficient schwannoma or meningioma at concentrations up to 10 µM (data not shown). Therefore, we tested the potential of targeting RAF/MEK/ERK activity with AZD6244 in combination with MLN3651.

7.6 MLN3651 inhibits CRL4-DCAF1 activity in Merlin-deficient cells and has potential as a therapeutic

In the absence of a specific CRL4-DCAF1 inhibitor we utilized the NAE inhibitor MLN3651, an oral successor of MLN4924. MLN4924 inhibited neddylation-mediated activation of E3 ubiquitin ligases including CRL4-DCAF1 (Cooper *et al.*, 2017; Wei *et al.*, 2014; Yu *et al.*, 2015). We showed that MLN3651 treatment in schwannoma, meningioma and BenMen-1 successfully inhibited neddylation (figure 5.1). We also showed that MLN3651 activated the Hippo pathway and therefore inhibited Hippo-mediated gene transcription in Merlin-deficient schwannoma and meningioma (figure 5.2–4). The Hippo pathway components LATS1/2 are direct targets of CRL4-DCAF1 and

these proteins are increased in MLN3651-treated cells suggesting that MLN3651 inhibits neddylation and activation of CRL4-DCAF1. However, Zou *et al*. also implicated Cullin 7-containing E3 ubiquitin ligase complexes in Hippo pathway regulation and showed that MLN4924 Hippo pathway activation is dependent on inhibition of Cullin 7 neddylation (Zou *et al.*, 2018). Therefore, further evidence is needed to determine if CRL4-DCAF1 is effectively inhibited with MLN3651 treatment and if MLN3651's anti-tumourigenic effects are CRL4-DCAF1-dependent.

MLN3651 treatment of Merlin-deficient schwannoma cells for 144 hours significantly decreased cell viability (figure 5.7). In addition, proliferation was significantly reduced and apoptosis activation was significantly increased after 72 hours of MLN3651 treatment, demonstrating that MLN3651 is a potent, anti-tumourigenic therapeutic for Merlin-deficient schwannoma (figure 5.7 and 5.8). In contrast, Merlin-positive schwannoma cells were much less sensitive to MLN3651; therefore, MLN3651 sensitivity could be CRL4-DCAF1-dependent (figure 5.14). Furthermore, primary human Schwann cells were also less sensitive to MLN3651 than Merlin-deficient schwannoma suggesting that MLN3651 is less toxic to normal cells (figure 5.15). However, there was considerable variation in human Schwann cell response to MLN3651.

We treated Merlin-deficient meningioma cells with MLN3651 for 72 hours and observed considerable variation in sensitivity between individual tumours (figure 5.9A and 5.9B). We were able to separate these tumours based on their IC50 to produce two different sub-groups; those that responded and those that did not. The responder sub-group had an average IC50 of 1.31 μM whilst the non-responder sub-group had an average IC50 of 12.81 μM. We did not explore the reason for the differences in MLN3651 sensitivity. However, Milhollen *et al.* reported that NAE mutations can

confer resistance to MLN4924 (Milhollen *et al.*, 2012). In addition, Cooper *et al.* demonstrate that MLN4924 does not inhibit the mTOR pathway (Cooper *et al.*, 2017). Indeed, it has been shown that mTOR signalling is dysregulated in Merlin-deficient meningioma; therefore, this could be a potential resistance mechanism (James *et al.*, 2009). Interestingly, when we treated meningioma cells for 144 hours with MLN3651, there was no difference in response between those that had previously been grouped as responders and non-responders suggesting that non-responders can overcome resistance mechanisms (figure 5.9C). We also confirmed that after 72 hours of MLN3651 treatment, proliferation was significantly reduced and apoptosis was significantly increased (figure 5.9D and 5.10. There were no differences in proliferation and apoptosis following MLN3651 treatment between responder and non-responder sub-groups suggesting another mechanism confers resistance at this time point. We did not monitor alternative cell death mechanisms such as autophagy which have been shown to be important in the cellular response to MLN4924 (Lan *et al.*, 2016; Luo *et al.*, 2012; Zhao *et al.*, 2012).

Merlin-positive meningioma cells were also much less sensitive to MLN3651 than Merlin-deficient meningioma responders after 72 hours of MLN3651 treatment (figure 5.14). Although Merlin-positive meningioma responded to MLN3651 after 144 hours, the IC50 was much higher than Merlin-deficient meningiomas at the same time point, suggesting that Merlin-deficient tumours are more sensitive to MLN3651. This sensitivity could be mediated by increased CRL4-DCAF1 activity in primary Merlin-deficient meningioma.

HMC were less sensitive to MLN3651 at 72 hours and 144 hours compared with Merlin-deficient ‘responders’ at 72 hours and all Merlin-deficient meningiomas at 144

hours (figure 5.15). However, this resistance was mediated by a component of the HMC medium as when we repeated this experiment in meningioma medium (without added growth factors), HMC were more sensitive to MLN3651 than Merlin-deficient meningioma after 72 hours (figure 5.15). Indeed, when we cultured Merlin-deficient meningiomas in HMC medium, they were much more resistant than those culture in meningioma medium (figure 5.16). The constituents of the commercially available HMC medium are not disclosed; however Kuhn *et al.* reported that increased exogenous Insulin-like growth factor 1 (IGF-1) reduced multiple myeloma cell sensitivity to proteasome inhibition providing a possible rationale for HMC medium-mediated resistance to MLN3651 (Kuhn *et al.*, 2012). Unfortunately, specialized HMC medium is required for the optimal growth of HMC; therefore, we cannot accurately assess MLN3651 sensitivity in this model and *in vivo* toxicity studies are required.

In BenMen-1 cells, the Hippo pathway was not significantly activated after MLN3651 treatment (figure 5.4). However, 72 hours of MLN3651 treatment significantly reduced viability (IC50 - 0.29 μM) and proliferation (figure 5.11A and 5.12). In addition, 24 hours of MLN3651 treatment significantly increased apoptosis; therefore, MLN3651 activity in BenMen-1 is independent of Hippo pathway activation and presumably CRL4-DCAF1 inhibition (figure 5.11B). The viability of WHO II and WHO III tumours was also significantly reduced by MLN3651, suggesting it has potential in higher grade Merlin-deficient tumours (figure 5.13).

7.7 MLN3651 increases RAF/MEK/ERK activity in Merlin-deficient cells

We reported that CRL4-DCAF1 increased KSR1-mediated RAF/MEK/ERK activity in Merlin-deficient cells (figure 3.10 and 4.7). As MLN3651 successfully inhibited CRL4-DCAF1 in Merlin-deficient cells leading to Hippo pathway activation, we monitored

pERK1/2 expression after MLN3651 treatment in schwannoma, meningioma and BenMen-1 (figure 5.5 and 5.6). We were surprised that RAF/MEK/ERK activity was significantly increased after MLN3651 treatment presumably in a CRL4-DCAF1-independent manner. Indeed, Zheng *et al.* reported that MLN4924 activated RAF/MEK/ERK activity in acute lymphoblastic leukaemia (ALL) which was induced by protein kinase C β2 in MLN4924-treated cells (Zheng *et al.*, 2018). Interestingly, RAF/MEK/ERK activity was protective in acute lymphoblastic leukaemia cells by preventing apoptotic cell death and indeed, RAF/MEK/ERK inhibition (with AZD6244) sensitized cells to MLN4924 (Zheng *et al.*, 2018). Therefore, we postulated that combination therapy of MLN3651 and RAF/MEK/ERK inhibition would further sensitize Merlin-deficient schwannoma and meningioma.

In addition, Zhou *et al.* discovered that low doses of MLN4924 increased cancer cell proliferation mediated by enhanced EGFR activation and enhanced PI3K/AKT/MTOR and RAF/MEK/ERK signalling (Zhou *et al.*, 2016b). We also observed increases in cell viability at low doses of MLN3651 (100 nM), particularly in meningioma (figure 5.9). Indeed, EGFR is overexpressed and activated in meningiomas; therefore, increased viability may be due to increased EGFR signalling mediated by MLN3651 (Arnli *et al.*, 2017). Possible EGFR activation with low doses of MLN3651 provides an additional rationale for combination therapy of MLN3651 and RAF/MEK/ERK inhibition in meningioma.

7.8 Combination of MLN3651 and AZD6244

We chose AZD6244 to target RAF/MEK/ERK activity for two reasons. Firstly, APS_2_79 targeting KSR1-mediated RAF/MEK/ERK activity was ineffective as a monotherapy and secondly Ammoun *et al.* reported anti-proliferative effects of AZD6244 at

therapeutically relevant concentrations in schwannoma (Ammoun *et al.*, 2010b). Indeed, 0.1 µM and 1 µM AZD6244 significantly decreased pERK1/2 expression in schwannoma after 72 hours, in agreement with Ammoun *et al.* (figure 6.1). However, we did not identify any benefit of combining MLN3651 and AZD6244 in schwannoma (figure 6.1 and 6.2). There was a trend of reduced pERK1/2 activity with the combination of AZD6244 and MLN3651 compared with MLN3651 alone; however, this was not statistically significant. AZD6244 alone did not supress schwannoma proliferation, in contrast to Ammoun *et al.*, and combination of MLN3651 and AZD6244 did not change proliferation compared with MLN3651 alone (Ammoun *et al.*, 2010b). Therefore, AZD6244 has little potential as a therapeutic for the treatment of schwannoma and more potent RAF/MEK/ERK inhibitors should be assessed in combination with MLN3651 to determine synergistic or additive effects.

In primary Merlin-deficient meningioma, combination of MLN3651 and AZD6244 unexpectedly activated the Hippo pathway by increasing LATS2 expression after 72 hours whereas MLN3651 alone did not lead to a significant increase in LATS2 (figure 6.3). This suggests that RAF/MEK/ERK has a role in regulating LATS2 expression and therefore the Hippo pathway in meningioma. Indeed, You *et al.* reported that ERK1/2 inhibition led to a decrease in YAP protein in NSCLC cells which could be mediated by LATS1/2 (You *et al.*, 2015). In meningioma, a 72 hour 0.1 µM AZD6244 treatment period was not sufficient to reduce pERK1/2 expression and 1 µM was required to significantly reduce RAF/MEK/ERK activity (figure 6.3). Interestingly, the combination of MLN3651 and 0.1 µM or 1 µM AZD6244 led to a significant reduction in pERK1/2 activity compared with MLN3651 alone in contrast to combination therapy in schwannoma. We were able to show that these effects were consistent in BenMen-1

demonstrating that robust Hippo pathway activation can be achieved in these cells (figure 6.5). Whilst MLN3651 and AZD6244 had no significant effect on the proliferation of primary meningioma cells, the combination of MLN3651 and AZD6244 in BenMen-1 significantly reduced proliferation compared with either treatment alone (figure 6.4 and 6.6). Therefore, the combination of MLN3651 and AZD6244 is a potential therapy for meningioma.

7.9 Experimental limitations

This study is limited to data derived from experiments in primary schwannoma and meningioma cell cultures and relevant cell lines. Whilst this data reflects human tumours, there is no *in vivo* data to support the results. Both HMC and Schwann cells were less sensitive to MLN3651; however, this sensitivity was mediated by the cell culture medium in the case of HMC. In addition *in vitro* Schwann cells and HMC cells proliferate at a much higher rate than those *in vivo*, in the absence of injury (Decimo *et al.*, 2012; Kim *et al.*, 2000; Webster, Martin & O'Connell, 1973). Therefore, further *in vivo* efficacy and toxicity studies are needed to fully assess the potential of MLN3651 as a therapeutic for NF2-associated tumours. Previously, our human cell model has been used to support the translation of Sorafenib into the treatment of NF2-related tumours (Ammoun *et al.*, 2008) (EudraCT: 2011-001789-16). However, MLN3651, APS_2_79 and B32B3 have not yet been approved for the treatment of any cancers making a fast-track translation into clinic more difficult.

As we primarily used primary samples, the amount of material available for experiments was often limited. Primary tumours proliferate for a small number of passages before they undergo senescence and eventually die. This was a particular problem for primary schwannoma tumours as these samples were often much smaller

and tended to proliferate for a smaller number of passages compared with meningioma tumours. Therefore, we were unable to complete the required number of repeats to detect statistical significance for some experiments. In addition, we were unable to acquire enough schwannoma tissue for successful DCAF1 immunoprecipitation.

Protein expression and MLN3651 drug response in primary tumours were variable in this study confounding our results. This variability could be attributable to variation of mutations, epigenetic differences, histopathological subtype and culture passage of primary tumours. Unfortunately, we did not stratify the primary tumours into mutation type, epigenetic group or histopathological subtype in this study. We confirmed loss of Merlin protein expression which correlates well with an *Nf2* gene mutation but we did not definitively confirm the presence of a *Nf2* gene mutation by sequencing. Indeed, we recognised some instances where a *Traf7* mutation correlated with a loss of Merlin protein expression and these tumours were removed from analysis.

An additional limitation is the lack of a specific CRL4-DCAF1 inhibitor. MLN3651 targets NAE to prevent neddylation of Cullins as well as p53 and MDM2 (Brownell *et al.*, 2010; Dohmesen, Koeppel & Dobbelstein, 2008; Xirodimas *et al.*, 2004). We were able to confirm that Merlin-deficient tumour cells have additional sensitivity to MLN3651 compared with Merlin-positive cells which may be mediated by enhanced CRL4-DCAF1 activity. However, we have no conclusive evidence that inhibition of CRL4-DCAF1 mediates the effects of MLN3651 on Merlin-deficient cells. Indeed, it is probably a combination of factors that leads to MLN3651's anti-proliferative and apoptotic effects.

7.10 Translational potential

We investigated DCAF1 and KSR1 expression in Merlin-deficient tumours and demonstrated that CRL4-DCAF1 enhanced KSR1-mediated RAF/MEK/ERK activation in HEK293T and schwannoma. CRL4-DCAF1 is also hyper-active in hepatocellular carcinoma and DCAF1 in NSCLC is associated with poor prognosis (Ni *et al.*, 2017; Wang *et al.*, 2013). Therefore, investigation of CRL4-DCAF1 regulation of KSR1 activity may be important in these cancers as well as Merlin-deficient tumours. We also demonstrated that targeting DCAF1 and KSR1 expression had additive effects on the proliferation of meningioma. KSR1 is upregulated in colorectal cancer, endometrial carcinoma and breast cancer whereas DCAF1 expression has not been investigated in these tumours (Fisher *et al.*, 2015; Llobet *et al.*, 2011; Stebbing *et al.*, 2015). Whether DCAF1 and KSR1 knockdown in these tumours has additive effects on proliferation remains to be determined.

Merlin-deficient schwannoma and meningioma are more sensitive to MLN3651 than Merlin-positive tumours. In addition, MLN4924 has potential as a therapeutic for mesothelioma which are often Merlin-deficient (Cooper *et al.*, 2017). Therefore, MLN3651 should be tested in other tumours in which the *nf2* gene is mutated and/or Merlin protein expression is reduced such as glioma and hepatocellular carcinoma. In addition, we have shown the additive potential of MLN3651 and AZD6244 in meningioma which may also have potential in other tumours in which the Hippo pathway and RAF/MEK/ERK pathway are dysregulated.

7.11 Conclusions

We explored several lines of evidence to demonstrate the potential of targeting CRL4-DCAF1 and KSR1 in Merlin-deficient tumours both alone and in combination. We

discovered that DCAF1 protein is overexpressed in schwannoma and meningioma which probably enhances CRL4-DCAF1 and DCAF1 kinase activity. We showed that DCAF1 expression is important in Merlin-deficient meningioma and regulates proliferation. We also report that KSR1 protein is overexpressed in Merlin-deficient meningioma. However, KSR1 expression was not increased in the benign meningioma cell line, BenMen-1. In spite of this, KSR1 knockdown significantly decreased proliferation in BenMen-1 demonstrating the potential of KSR1 as a target in meningioma. Interestingly, combination of DCAF1 and KSR1 knockdown significantly reduced proliferation in BenMen-1 compared with DCAF1 or KSR1 knockdown alone. Therefore suggesting these proteins have potential to be targeted together. Future studies should investigate the mechanisms by which DCAF1 and KSR1 reduce proliferation and determine if it is dependent on CRL4-DCAF1 and RAF/MEK/ERK activity or independent protein functions.

We also showed that CRL4-DCAF1 enhanced KSR1-mediated RAF/MEK/ERK signalling in schwannoma. Unfortunately, we were not able to show that CRL4-DCAF1 regulation of KSR1 was relevant in meningioma cells as DCAF1 knockdown did not result in any changes to RAF/MEK/ERK signalling. Future work should elucidate if DCAF1 pro-tumourigenic functions are partly dependent on RAF/MEK/ERK regulation via KSR1 as well as regulation of the Hippo pathway. Furthermore, the mechanism of CRL4-DCAF1 regulation of KSR1 should also be investigated to determine if it is dependent on CRL4-DCAF1 ubiquitin ligase activity.

We showed that MLN3651 was able to inhibit neddylation and activate the Hippo pathway. MLN3651 displayed anti-tumourigenic activity in schwannoma and meningioma; therefore, has potential as a therapeutic target in Merlin-deficient

tumours. MLN3651 also showed significant activity in higher grade meningiomas suggesting its use is not limited to low-grade tumours. We were unable to determine if MLN3651 activity was dependent on CRL4-DCAF1 inhibition as MLN3651 targets many E3 ubiquitin ligases and neddylated substrates. However, we were able to show that Merlin-positive schwannoma and meningioma cells were more resistant to MLN3651 suggesting that Merlin-deficiency sensitizes cells to MLN3651, which could be due to activated CRL4-DCAF1. A specific CRL4-DCAF1 inhibitor is required to fully assess the potential of targeting CRL4-DCAF1 in Merlin-deficient cells.

The KSR1 inhibitor APS_2_79 was not able to inhibit RAF/MEK/ERK signalling in schwannoma and meningioma and did not affect proliferation. Dhawan *et al.* show that APS_2_79 can sensitize cells to MEK1/2 inhibition; therefore, this combination should also be tested in Merlin-deficient cells. Furthermore, whilst APS_2_79 can interact with KSR2 at nanomolar concentrations, the APS_2_79 interaction with KSR1 was not specifically investigated. Therefore, a much higher concentration of APS_2_79 may be required to inhibit KSR1-mediated RAF/MEK/ERK signalling and a more potent and specific therapeutic is necessary to fully evaluate KSR1 as a therapeutic target.

We combined MLN3651 and AZD6244 because they target Hippo pathway activation and RAF/MEK/ERK activity, downstream of CRL4-DCAF1 and KSR1, respectively. DCAF1 and KSR1 knockdown had an additive effect on proliferation and we hypothesised that it was dependent on inhibition of Hippo and RAF/MEK/ERK pathways. We chose AZD6244 as APS_2_79 had no therapeutic effect in Merlin-deficient tumours. Furthermore, we noticed that MLN3651 led to an increase in RAF/MEK/ERK activity providing an additional rationale for combination therapy. Combination therapy of MLN3651 and AZD6244 had no additive effect in schwannoma at the concentrations

tested. Conversely, combination therapy in meningioma and BenMen-1 led to sustained Hippo pathway activation, reduced RAF/MEK/ERK activity and significantly reduced proliferation compared with either treatment alone demonstrating that MLN3651 and AZD6244 have additive therapeutic potential. Whether MLN3651 and AZD6244's therapeutic potential is dependent on the inhibition of CRL4-DCAF1 and KSR1 activity remains to be determined.

Appendix - Supplementary figures

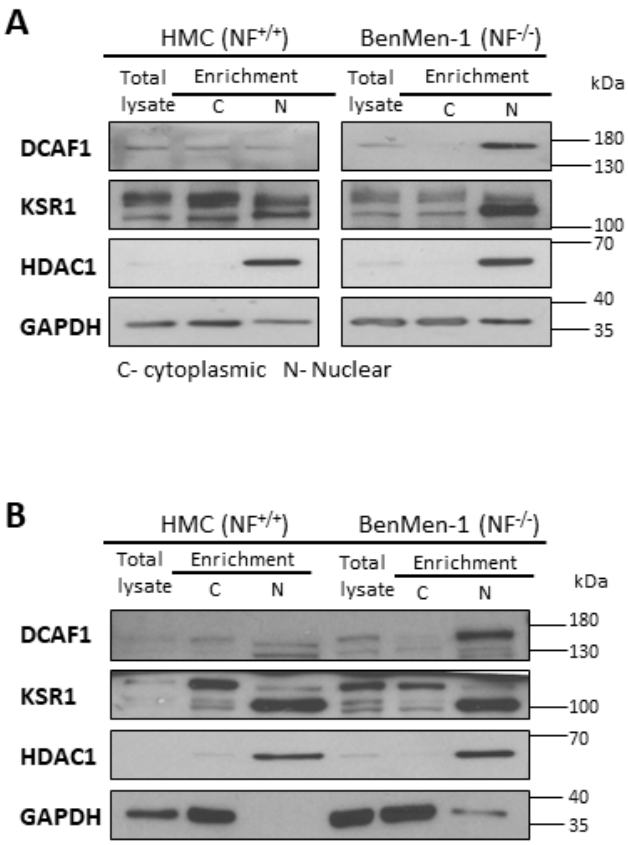

Supplementary figure 1 - Additional HMC and BenMen-1 repeats for DCAF1 and KSR1 localization. A, B: Additional Western blots of DCAF1 and KSR1 in total, cytoplasmic (C) and nuclear (N) lysate of human meningeal cells (HMC) and Benign meningioma 1 (BenMen-1) cells. Nuclear DCAF1 was increased in BenMen-1 compared with HMC whilst KSR1 localization was unchanged. GAPDH-cytoplasmic control, HDAC1-nuclear control.

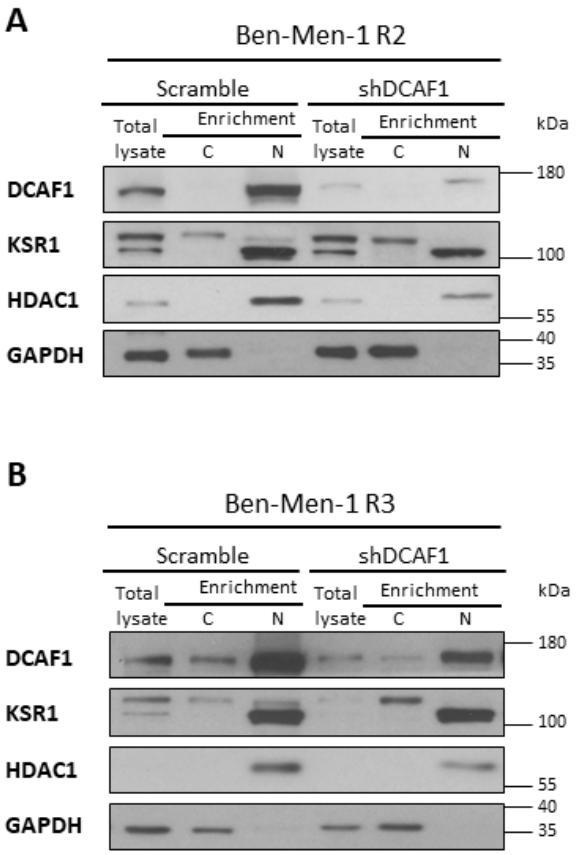

Supplementary figure 2 - Additional BenMen-1 DCAF1 knockdown repeats for KSR1 localization. A: Additional Western blots to show KSR1 localization after DCAF1 knockdown in Benign meningioma 1 (BenMen-1) cells. Scramble or DCAF1 lentivirus (shDCAF1) was added for 24 hours followed by a 24 hour recovery period and then 7 days of puromycin selection before cytoplasmic (C) and nuclear (N) enrichment. KSR1 localization did not change after DCAF1 knockdown, GAPDH-cytoplasmic control, HDAC1-nuclear control.

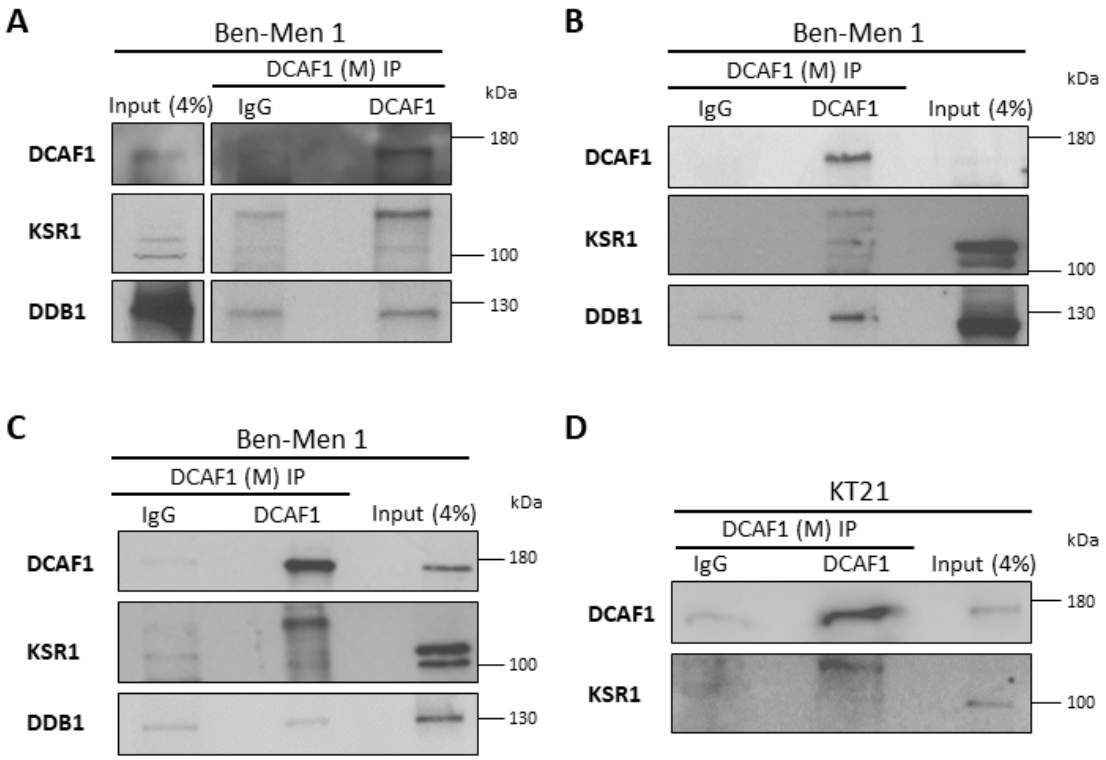

Supplementary figure 3 - Additional repeats for endogenous DCAF1 and KSR1 interaction in BenMen-1 and KT21-MG1-Luc5D. A, B, C: Additional Western blots of DCAF1, KSR1 and DDB1 in Benign meningioma 1 (BenMen-1) lysate (input), immunoprecipitated IgG (control) and immunoprecipitated DCAF1. DCAF1 was immunoprecipitated from 3 mg BenMen-1 lysates using a mouse (M) DCAF1 antibody (Proteintech). KSR1 and DDB1 were present in the DCAF1 complex. Input samples represent protein lysate prior to the immunoprecipitation and 4% of the total protein used for the immunoprecipitation was ran in the Western blot. **D:** Western blot of DCAF1 and KSR1 in WHO III meningioma cell line (KT21-MG1-Luc5D) (KT21) (input), immunoprecipitated IgG (control) and immunoprecipitated DCAF1. DCAF1 was immunoprecipitated from 2 mg KT21 lysates using a mouse (M) DCAF1 antibody (Proteintech). KSR1 was present in the DCAF1 complex. Input samples represent protein lysate prior to the immunoprecipitation and 4% of the total protein used for the immunoprecipitation was ran in the Western blot.

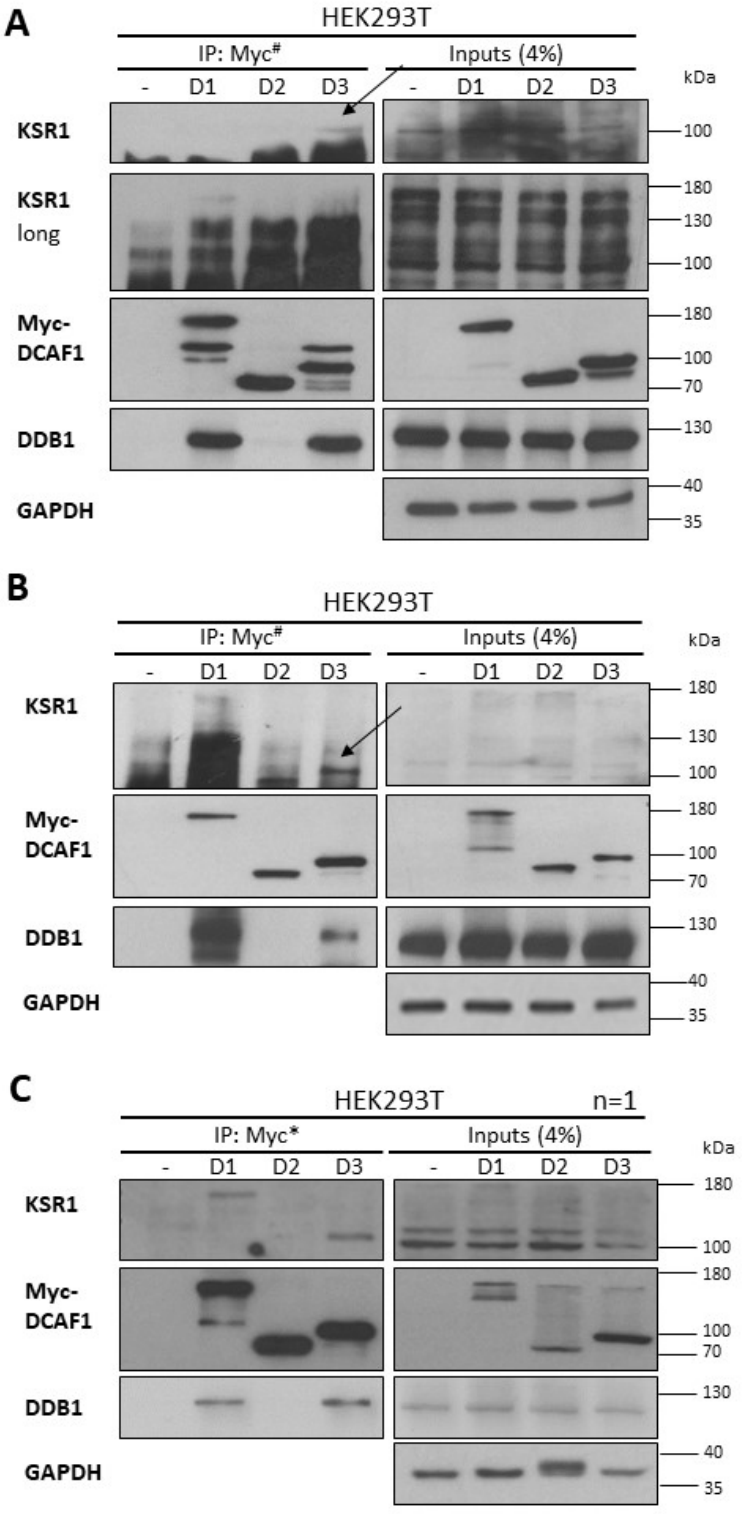

Supplementary figure 4 – Additional overexpressed DCAF1 immunoprecipitation experiments. A, B: Additional Western blots of DCAF1 sequences D1, D2 and D3, with a Myc-tag, overexpressed in HEK293T and immunoprecipitated from 1 mg HEK293T using a Myc-tag antibody. The Western blot shows KSR1, Myc, DDB1 and GAPDH. KSR1 was present in the C-terminal DCAF1 complex (indicated by the arrow) and a high molecular weight KSR1-reactive band is present in the wild-type DCAF1 complex. DDB1 is the positive control and is present in the D1 and D3 immunoprecipitated complexes. Immunoprecipitated Myc-tag in non-transfected HEK293T (-) was used as a negative control. Input lysates show protein levels prior to immunoprecipitation. 4% of protein amount used in immunoprecipitation was ran as input samples. **C:** An alternative protocol (protocol 2- *) for Myc immunoprecipitation was used to isolate the D1, D2 and D3 complexes. KSR1 was present in the C-terminal DCAF1 complex and a high molecular weight KSR1-reactive band was present in the wild-type DCAF1 complex.

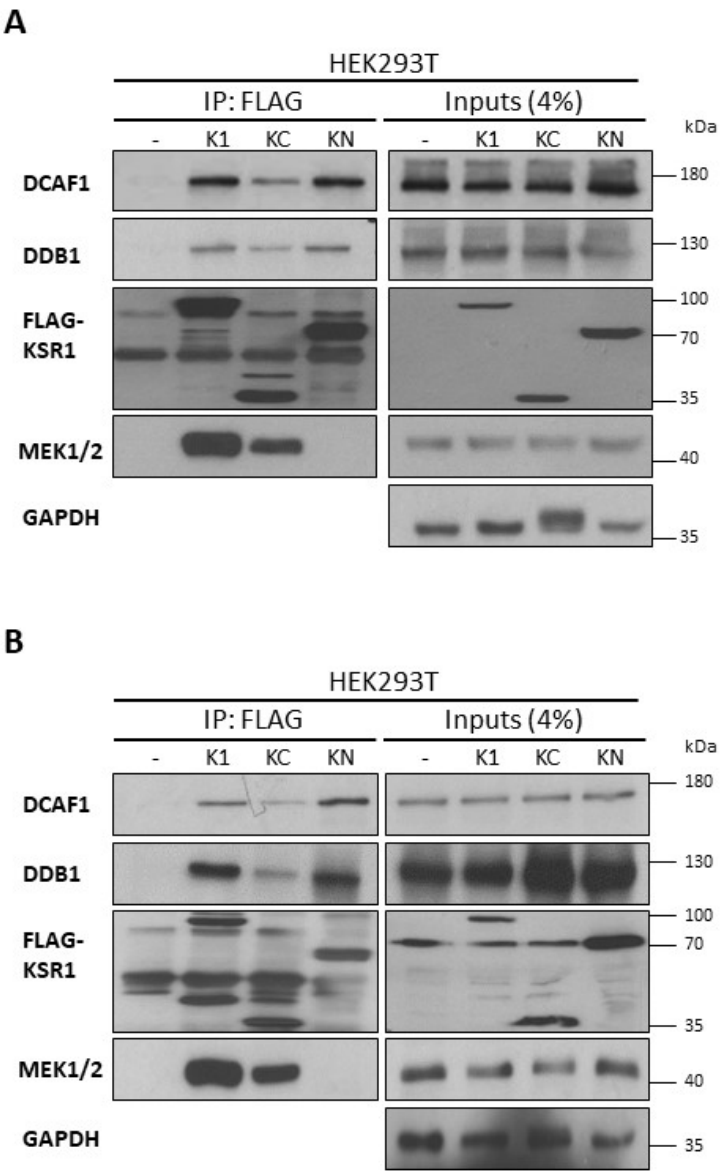

Supplementary figure 5 - Additional overexpressed KSR1 immunoprecipitation experiments. A, B: Additional Western blots of KSR1 sequences K1, KC and KN, with a FLAG-tag, overexpressed in HEK293T and immunoprecipitated from 1 mg HEK293T using a FLAG-tag antibody. The Western blot shows DCAF1, DDB1, FLAG, MEK1/2 and GAPDH. DCAF1 and DDB1 were present in the K1 and KN complexes and a smaller amount in the KC complex. MEK1/2 was used as a positive control and is present in the K1 and KC complexes. FLAG-tagged proteins were immunoprecipitated from non-transfected HEK293T (-) and used as a negative control. Input lysates show protein levels prior to immunoprecipitation. 4% of the total protein used for immunoprecipitation was used as input lysates.

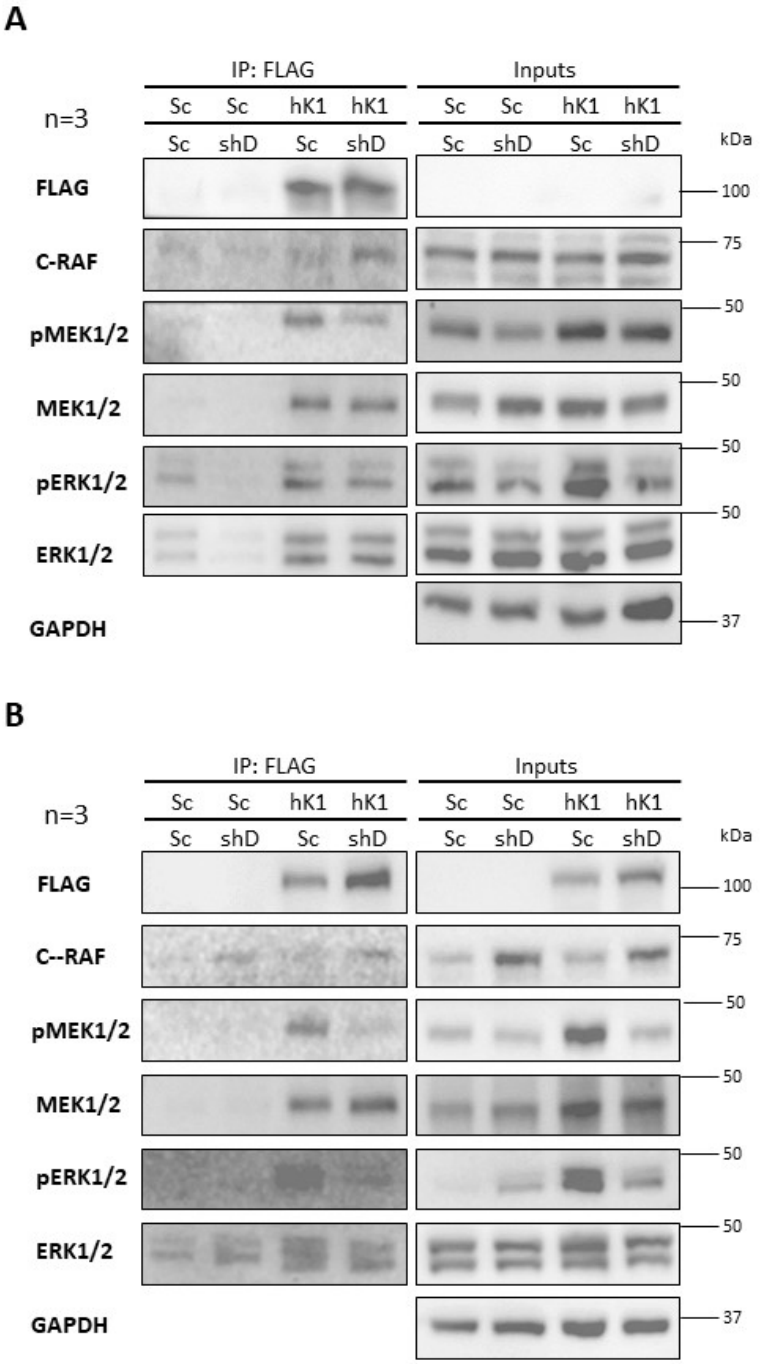

Supplementary figure 6 - Additional human KSR1 immunoprecipitation experiments showing RAF/MEK/ERK proteins after DCAF1 knockdown. A, B: DCAF1 expression was targeted with a shRNA lentiviral plasmid in HEK293T cells and then human KSR1 (hK1) with a FLAG-tag was overexpressed. DCAF1 lentivirus was added for 24 hours and then fresh medium was added for 24 hours followed by four days of puromycin selection. Cells were then split and 24 hours later hK1 lentivirus was added for 48 hours followed by cell lysis. hK1 complexes were immunoprecipitated using FLAG-tag antibody from 1 mg of HEK293T lysate. Western blots show immunoprecipitated FLAG complexes and input lysates probed with FLAG, C-RAF, pMEK1/2, MEK1/2, pERK1/2. ERK1/2 and GAPDH. The amount of pMEK1/2, and pERK1/2 in the hK1 complex was reduced when DCAF1 was knocked down. Sc- scramble, shD- DCAF1 knockdown. FLAG immunoprecipitated Sc/Sc and Sc/shD lysates represent negative controls and input samples show endogenous levels of proteins prior to immunoprecipitation.

References

Ahmad, Z., Brown, C. M., Patel, A. K., Ryan, A. F., Ongkeko, R. & Doherty, J. K. (2010) 'Merlin knockdown in human Schwann cells: clues to vestibular schwannoma tumorigenesis'. *Otol Neurotol*, 31 (3), pp. 460-466.

Ahn, J., Novince, Z., Concel, J., Byeon, C. H., Makhov, A. M., Byeon, I. J., Zhang, P. & Gronenborn, A. M. (2011) 'The Cullin-RING E3 ubiquitin ligase CRL4-DCAF1 complex dimerizes via a short helical region in DCAF1'. *Biochemistry*, 50 (8), pp. 1359-1367.

Ahn, J., Vu, T., Novince, Z., Guerrero-Santoro, J., Rapic-Otrin, V. & Gronenborn, A. M. (2010) 'HIV-1 Vpr loads uracil DNA glycosylase-2 onto DCAF1, a substrate recognition subunit of a cullin 4A-ring E3 ubiquitin ligase for proteasome-dependent degradation'. *J Biol Chem*, 285 (48), pp. 37333-37341.

Akbarnia, B. A., Gabriel, K. R., Beckman, E. & Chalk, D. (1992) 'Prevalence of scoliosis in neurofibromatosis'. *Spine (Phila Pa 1976)*, 17 (8 Suppl), pp. S244-248.

Alanin, M. C., Klausen, C., Caye-Thomasen, P., Thomsen, C., Fugleholm, K., Poulsgaard, L., Lassen, U., Mau-Sorensen, M. & Hofland, K. F. (2015) 'The effect of bevacizumab on vestibular schwannoma tumour size and hearing in patients with neurofibromatosis type 2'. *Eur Arch Otorhinolaryngol*, 272 (12), pp. 3627-3633.

Alfthan, K., Heiska, L., Grönholm, M., Renkema, G. H. & Carpén, O. (2004) 'Cyclic AMP-dependent protein kinase phosphorylates Merlin at serine 518 independently of p21-activated kinase and promotes Merlin-ezrin heterodimerization'. *J Biol Chem*, 279 (18), pp. 18559-18566.

Altuna, X., Lopez, J. P., Yu, M. A., Arandazi, M. J., Harris, J. P., Wang-Rodriguez, J., An, Y., Dobrow, R., Doherty, J. K. & Ongkeko, W. M. (2011) 'Potential role of imatinib

mesylate (Gleevec, STI-571) in the treatment of vestibular schwannoma'. *Otol Neurotol*, 32 (1), pp. 163-170.

Ammoun, S., Cunliffe, C. H., Allen, J. C., Chiriboga, L., Giancotti, F. G., Zagzag, D., Hanemann, C. O. & Karajannis, M. A. (2010a) 'ErbB/HER receptor activation and preclinical efficacy of lapatinib in vestibular schwannoma'. *Neuro Oncol*, 12 (8), pp. 834-843.

Ammoun, S., Flaiz, C., Ristic, N., Schuldt, J. & Hanemann, C. O. (2008) 'Dissecting and targeting the growth factor-dependent and growth factor-independent extracellular signal-regulated kinase pathway in human schwannoma'. *Cancer Res*, 68 (13), pp. 5236-5245.

Ammoun, S., Ristic, N., Matthies, C., Hilton, D. A. & Hanemann, C. O. (2010b) 'Targeting ERK1/2 activation and proliferation in human primary schwannoma cells with MEK1/2 inhibitor AZD6244'. *Neurobiol Dis*, 37 (1), pp. 141-146.

Ammoun, S., Schmid, M. C., Ristic, N., Zhou, L., Hilton, D., Ercolano, E., Carroll, C. & Hanemann, C. O. (2012) 'The role of insulin-like growth factors signaling in Merlin-deficient human schwannomas'. *Glia*, 60 (11), pp. 1721-1733.

Ammoun, S., Schmid, M. C., Triner, J., Manley, P. & Hanemann, C. O. (2011) 'Nilotinib alone or in combination with selumetinib is a drug candidate for neurofibromatosis type 2'. *Neuro Oncol*, 13 (7), pp. 759-766.

Angers, S., Li, T., Yi, X., MacCoss, M. J., Moon, R. T. & Zheng, N. (2006) 'Molecular architecture and assembly of the DDB1-CUL4A ubiquitin ligase machinery'. *Nature*, 443 (7111), pp. 590-593.

Apicella, G., Paolini, M., Deantonio, L., Masini, L. & Krengli, M. (2016) 'Radiotherapy for vestibular schwannoma: Review of recent literature results'. *Rep Pract Oncol Radiother*, 21 (4), pp. 399-406.

Arnli, M. B., Backer-Grøndahl, T., Ytterhus, B., Granli, U. S., Lydersen, S., Gulati, S. & Torp, S. H. (2017) 'Expression and clinical value of EGFR in human meningiomas'. *PeerJ*, 5 pp. e3140.

Balasenthil, S., Sahin, A. A., Barnes, C. J., Wang, R. A., Pestell, R. G., Vadlamudi, R. K. & Kumar, R. (2004) 'p21-activated kinase-1 signaling mediates CYCLIN D1 expression in mammary epithelial and cancer cells'. *J Biol Chem*, 279 (2), pp. 1422-1428.

Ball, K. A., Johnson, J. R., Lewinski, M. K., Guatelli, J., Verschueren, E., Krogan, N. J. & Jacobson, M. P. (2016) 'Non-degradative Ubiquitination of Protein Kinases'. *PLoS Comput Biol*, 12 (6), pp. e1004898.

Baser, M. E., Friedman, J. M., Aeschliman, D., Joe, H., Wallace, A. J., Ramsden, R. T. & Evans, D. G. (2002a) 'Predictors of the risk of mortality in neurofibromatosis 2'. *Am J Hum Genet*, 71 (4), pp. 715-723.

Baser, M. E., Friedman, J. M., Joe, H., Shenton, A., Wallace, A. J., Ramsden, R. T. & Evans, D. G. (2011) 'Empirical development of improved diagnostic criteria for neurofibromatosis 2'. *Genet Med*, 13 (6), pp. 576-581.

Baser, M. E., Friedman, J. M., Wallace, A. J., Ramsden, R. T., Joe, H. & Evans, D. G. (2002b) 'Evaluation of clinical diagnostic criteria for neurofibromatosis 2'. *Neurology*, 59 (11), pp. 1759-1765.

Bassiri, K., Ferluga, S., Sharma, V., Syed, N., Adams, C. L., Lasonder, E. & Hanemann, C. O. (2017) 'Global Proteome and Phospho-proteome Analysis of Merlin-deficient

Meningioma and Schwannoma Identifies PDLIM2 as a Novel Therapeutic Target'. *EBioMedicine*, 16 pp. 76-86 (Accessed- 26th April 2018).

Battaglia, A., Mastrodimos, B. & Cueva, R. (2006) 'Comparison of growth patterns of acoustic neuromas with and without radiosurgery'. *Otol Neurotol*, 27 (5), pp. 705-712.

Benhamouche, S., Curto, M., Saotome, I., Gladden, A. B., Liu, C. H., Giovannini, M. & McClatchey, A. I. (2010) 'NF2/Merlin controls progenitor homeostasis and tumorigenesis in the liver'. *Genes Dev*, 24 (16), pp. 1718-1730.

Bernards, A. & Gusella, J. F. (1994) 'The importance of genetic mosaicism in human disease'. *N Engl J Med*, 331 (21), pp. 1447-1449.

Bianchi, A. B., Hara, T., Ramesh, V., Gao, J., Klein-Szanto, A. J., Morin, F., Menon, A. G., Trofatter, J. A., Gusella, J. F. & Seizinger, B. R. (1994) 'Mutations in transcript isoforms of the neurofibromatosis 2 gene in multiple human tumour types'. *Nat Genet*, 6 (2), pp. 185-192.

Bianchi, A. B., Mitsunaga, S. I., Cheng, J. Q., Klein, W. M., Jhanwar, S. C., Seizinger, B., Kley, N., Klein-Szanto, A. J. & Testa, J. R. (1995) 'High frequency of inactivating mutations in the neurofibromatosis type 2 gene (NF2) in primary malignant mesotheliomas'. *Proc Natl Acad Sci U S A*, 92 (24), pp. 10854-10858.

Boldrini, L., Pistolesi, S., Gisfredi, S., Ursino, S., Lupi, G., Caniglia, M., Pingitore, R., Basolo, F., Parenti, G. & Fontanini, G. (2003) 'Telomerase in intracranial meningiomas'. *Int J Mol Med*, 12 (6), pp. 943-947.

Bott, M., Brevet, M., Taylor, B. S., Shimizu, S., Ito, T., Wang, L., Creaney, J., Lake, R. A., Zakowski, M. F., Reva, B., Sander, C., Delsite, R., Powell, S., Zhou, Q., Shen, R., Olshen, A., Rusch, V. & Ladanyi, M. (2011) 'The nuclear deubiquitinase BAP1 is commonly

inactivated by somatic mutations and 3p21.1 losses in malignant pleural mesothelioma'. *Nat Genet*, 43 (7), pp. 668-672.

Boutet, N., Bignon, Y. J., Drouin-Garraud, V., Sarda, P., Longy, M., Lacombe, D. & Gorry, P. (2003) 'Spectrum of PTCH1 mutations in French patients with Gorlin syndrome'. *J Invest Dermatol*, 121 (3), pp. 478-481.

Breivik, C. N., Nilsen, R. M., Myrseth, E., Pedersen, P. H., Varughese, J. K., Chaudhry, A. A. & Lund-Johansen, M. (2013) 'Conservative management or gamma knife radiosurgery for vestibular schwannoma: tumor growth, symptoms, and quality of life'. *Neurosurgery*, 73 (1), pp. 48-56; discussion 56-47.

Brennan, D. F., Dar, A. C., Hertz, N. T., Chao, W. C., Burlingame, A. L., Shokat, K. M. & Barford, D. (2011) 'A Raf-induced allosteric transition of KSR stimulates phosphorylation of MEK'. *Nature*, 472 (7343), pp. 366-369.

Brennan, J. A., Volle, D. J., Chaika, O. V. & Lewis, R. E. (2002) 'Phosphorylation regulates the nucleocytoplasmic distribution of kinase suppressor of Ras'. *J Biol Chem*, 277 (7), pp. 5369-5377.

Bretscher, A., Edwards, K. & Fehon, R. G. (2002) 'ERM proteins and Merlin: integrators at the cell cortex'. *Nat Rev Mol Cell Biol*, 3 (8), pp. 586-599.

Brown, D. N., Caffa, I., Cirmena, G., Piras, D., Garuti, A., Gallo, M., Alberti, S., Nencioni, A., Ballestrero, A. & Zoppoli, G. (2016) 'Squalene epoxidase is a bona fide oncogene by amplification with clinical relevance in breast cancer'. *Sci Rep*, 6 pp. 19435.

Brownell, J. E., Sintchak, M. D., Gavin, J. M., Liao, H., Bruzzese, F. J., Bump, N. J., Soucy, T. A., Milhollen, M. A., Yang, X., Burkhardt, A. L., Ma, J., Loke, H. K., Lingaraj, T., Wu, D., Hamman, K. B., Spelman, J. J., Cullis, C. A., Langston, S. P., Vyskocil, S., Sells, T. B.,

Mallender, W. D., Visiers, I., Li, P., Claiborne, C. F., Rolfe, M., Bolen, J. B. & Dick, L. R. (2010) 'Substrate-assisted inhibition of ubiquitin-like protein-activating enzymes: the NEDD8 E1 inhibitor MLN4924 forms a NEDD8-AMP mimetic in situ'. *Mol Cell*, 37 (1), pp. 102-111.

Buccoliero, A. M., Castiglione, F., Rossi Degl'Innocenti, D., Sardi, I., Genitori, L. & Taddei, G. L. (2010) 'Merlin expression in pediatric anaplastic ependymomas real time PCR study'. *Fetal Pediatr Pathol*, 29 (4), pp. 245-254.

Cargnello, M., Tcherkezian, J., Dorn, J. F., Huttlin, E. L., Maddox, P. S., Gygi, S. P. & Roux, P. P. (2012) 'Phosphorylation of the eukaryotic translation initiation factor 4E-transporter (4E-T) by c-Jun N-terminal kinase promotes stress-dependent P-body assembly'. *Mol Cell Biol*, 32 (22), pp. 4572-4584.

Cayé-Thomasen, P., Baandrup, L., Jacobsen, G. K., Thomsen, J. & Stangerup, S. E. (2003) 'Immunohistochemical demonstration of vascular endothelial growth factor in vestibular schwannomas correlates to tumor growth rate'. *Laryngoscope*, 113 (12), pp. 2129-2134.

Cayé-Thomasen, P., Werther, K., Nalla, A., Bøg-Hansen, T. C., Nielsen, H. J., Stangerup, S. E. & Thomsen, J. (2005) 'VEGF and VEGF receptor-1 concentration in vestibular schwannoma homogenates correlates to tumor growth rate'. *Otol Neurotol*, 26 (1), pp. 98-101.

Channavajhala, P. L., Wu, L., Cuozzo, J. W., Hall, J. P., Liu, W., Lin, L. L. & Zhang, Y. (2003) 'Identification of a novel human kinase supporter of Ras (hKSR-2) that functions as a negative regulator of Cot (Tpl2) signaling'. *J Biol Chem*, 278 (47), pp. 47089-47097.

Chen, H., Xue, L., Wang, H., Wang, Z. & Wu, H. (2017) 'Differential NF2 Gene Status in Sporadic Vestibular Schwannomas and its Prognostic Impact on Tumour Growth Patterns'. *Sci Rep*, 7 (1), pp. 5470.

Chen, Z. J. (2005) 'Ubiquitin signalling in the NF-kappaB pathway'. *Nat Cell Biol*, 7 (8), pp. 758-765.

Chinthalapudi, K., Mandati, V., Zheng, J., Sharff, A. J., Bricogne, G., Griffin, P. R., Kissil, J. & Izard, T. (2018) 'Lipid binding promotes the open conformation and tumor-suppressive activity of neurofibromin 2'. *Nat Commun*, 9 (1), pp. 1338.

Chow, H. Y., Dong, B., Duron, S. G., Campbell, D. A., Ong, C. C., Hoeflich, K. P., Chang, L. S., Welling, D. B., Yang, Z. J. & Chernoff, J. (2015) 'Group I Paks as therapeutic targets in NF2-deficient meningioma'. *Oncotarget*, 6 (4), pp. 1981-1994.

Clapéron, A. & Therrien, M. (2007) 'KSR and CNK: two scaffolds regulating RAS-mediated RAF activation'. *Oncogene*, 26 (22), pp. 3143-3158.

Clark, V. E., Erson-Omay, E. Z., Serin, A., Yin, J., Cotney, J., Ozduman, K., Avşar, T., Li, J., Murray, P. B., Henegariu, O., Yilmaz, S., Günel, J. M., Carrión-Grant, G., Yilmaz, B., Grady, C., Tanrikulu, B., Bakircioğlu, M., Kaymakçalan, H., Caglayan, A. O., Sencar, L., Ceyhun, E., Atik, A. F., Bayri, Y., Bai, H., Kolb, L. E., Hebert, R. M., Omay, S. B., Mishra-Gorur, K., Choi, M., Overton, J. D., Holland, E. C., Mane, S., State, M. W., Bilgüvar, K., Baehring, J. M., Gutin, P. H., Piepmeier, J. M., Vortmeyer, A., Brennan, C. W., Pamir, M. N., Kiliç, T., Lifton, R. P., Noonan, J. P., Yasuno, K. & Günel, M. (2013) 'Genomic analysis of non-NF2 meningiomas reveals mutations in TRAF7, KLF4, AKT1, and SMO'. *Science*, 339 (6123), pp. 1077-1080.

Clark, V. E., Harmancı, A. S., Bai, H., Youngblood, M. W., Lee, T. I., Baranoski, J. F., Ercan-Sencicek, A. G., Abraham, B. J., Weintraub, A. S., Hnisz, D., Simon, M., Krischek, B., Erson-Omay, E. Z., Henegariu, O., Carrión-Grant, G., Mishra-Gorur, K., Durán, D., Goldmann, J. E., Schramm, J., Goldbrunner, R., Piepmeier, J. M., Vortmeyer, A. O., Günel, J. M., Bilgüvar, K., Yasuno, K., Young, R. A. & Günel, M. (2016) 'Recurrent somatic mutations in POLR2A define a distinct subset of meningiomas'. *Nat Genet*, 48 (10), pp. 1253-1259.

ClinicalTrials.gov[Internet]. [Online]. Available at: https://clinicaltrials.gov/ct2/results?cond=nf2&term=&cntry=&state=&city=&dist= (Accessed: 26th April 2018).

Clinicaltrialsregister.eu[Internet]. [Online]. Available at: https://www.clinicaltrialsregister.eu/ctr-search/search?query=nf2 (Accessed: 26th April 2018).

Conference-statement (1988) 'Neurofibromatosis. Conference statement. National Institutes of Health Consensus Development Conference'. *Arch Neurol*, 45 (5), pp. 575-578.

Cooper, J. & Giancotti, F. G. (2014) 'Molecular insights into NF2/Merlin tumor suppressor function'. *FEBS Lett*, 588 (16), pp. 2743-2752.

Cooper, J., Xu, Q., Zhou, L., Pavlovic, M., Ojeda, V., Moulick, K., de Stanchina, E., Poirier, J. T., Zauderer, M., Rudin, C. M., Karajannis, M. A., Hanemann, C. O. & Giancotti, F. G. (2017) 'Combined Inhibition of NEDD8-Activating Enzyme and mTOR Suppresses'. *Mol Cancer Ther*, 16 (8), pp. 1693-1704.

Costanzo-Garvey, D. L., Pfluger, P. T., Dougherty, M. K., Stock, J. L., Boehm, M., Chaika, O., Fernandez, M. R., Fisher, K., Kortum, R. L., Hong, E. G., Jun, J. Y., Ko, H. J., Schreiner, A., Volle, D. J., Treece, T., Swift, A. L., Winer, M., Chen, D., Wu, M., Leon, L. R., Shaw, A. S., McNeish, J., Kim, J. K., Morrison, D. K., Tschöp, M. H. & Lewis, R. E. (2009) 'KSR2 is an essential regulator of AMP kinase, energy expenditure, and insulin sensitivity'. *Cell Metab*, 10 (5), pp. 366-378.

Decimo, I., Fumagalli, G., Berton, V., Krampera, M. & Bifari, F. (2012) 'Meninges: from protective membrane to stem cell niche'. *Am J Stem Cells*, 1 (2), pp. 92-105.

Deguen, B., Goutebroze, L., Giovannini, M., Boisson, C., van der Neut, R., Jaurand, M. C. & Thomas, G. (1998) 'Heterogeneity of mesothelioma cell lines as defined by altered genomic structure and expression of the NF2 gene'. *Int J Cancer*, 77 (4), pp. 554-560.

Deremer, D. L., Ustun, C. & Natarajan, K. (2008) 'Nilotinib: a second-generation tyrosine kinase inhibitor for the treatment of chronic myelogenous leukemia'. *Clin Ther*, 30 (11), pp. 1956-1975.

Deshaies, R. J., Emberley, E. D. & Saha, A. (2010) 'Control of Cullin-ring ubiquitin ligase activity by NEDD8'. *Subcell Biochem*, 54 pp. 41-56.

Dewan, R., Pemov, A., Kim, H. J., Morgan, K. L., Vasquez, R. A., Chittiboina, P., Wang, X., Chandrasekharappa, S. C., Ray-Chaudhury, A., Butman, J. A., Stewart, D. R. & Asthagiri, A. R. (2015) 'Evidence of polyclonality in neurofibromatosis type 2-associated multilobulated vestibular schwannomas'. *Neuro Oncol*, 17 (4), pp. 566-573.

DeWire, M., Fouladi, M., Turner, D. C., Wetmore, C., Hawkins, C., Jacobs, C., Yuan, Y., Liu, D., Goldman, S., Fisher, P., Rytting, M., Bouffet, E., Khakoo, Y., Hwang, E. I., Foreman, N., Stewart, C. F., Gilbert, M. R., Gilbertson, R. & Gajjar, A. (2015) 'An open-

label, two-stage, phase II study of bevacizumab and lapatinib in children with recurrent or refractory ependymoma: a collaborative ependymoma research network study (CERN)'. *J Neurooncol*, 123 (1), pp. 85-91.

Dhawan, N. S., Scopton, A. P. & Dar, A. C. (2016) 'Small molecule stabilization of the KSR inactive state antagonizes oncogenic Ras signalling'. *Nature*, 537 (7618), pp. 112-116.

Dohmesen, C., Koeppel, M. & Dobbelstein, M. (2008) 'Specific inhibition of Mdm2-mediated neddylation by Tip60'. *Cell Cycle*, 7 (2), pp. 222-231.

Dombi, E., Baldwin, A., Marcus, L. J., Fisher, M. J., Weiss, B., Kim, A., Whitcomb, P., Martin, S., Aschbacher-Smith, L. E., Rizvi, T. A., Wu, J., Ershler, R., Wolters, P., Therrien, J., Glod, J., Belasco, J. B., Schorry, E., Brofferio, A., Starosta, A. J., Gillespie, A., Doyle, A. L., Ratner, N. & Widemann, B. C. (2016) 'Activity of Selumetinib in Neurofibromatosis Type 1-Related Plexiform Neurofibromas'. *N Engl J Med*, 375 (26), pp. 2550-2560.

Dow, G., Biggs, N., Evans, G., Gillespie, J., Ramsden, R. & King, A. (2005) 'Spinal tumors in neurofibromatosis type 2. Is emerging knowledge of genotype predictive of natural history?'. *J Neurosurg Spine*, 2 (5), pp. 574-579.

Duda, D. M., Borg, L. A., Scott, D. C., Hunt, H. W., Hammel, M. & Schulman, B. A. (2008) 'Structural insights into NEDD8 activation of cullin-RING ligases: conformational control of conjugation'. *Cell*, 134 (6), pp. 995-1006.

Dupont, S., Zacchigna, L., Cordenonsi, M., Soligo, S., Adorno, M., Rugge, M. & Piccolo, S. (2005) 'Germ-layer specification and control of cell growth by Ectodermin, a Smad4 ubiquitin ligase'. *Cell*, 121 (1), pp. 87-99.

Durand, A., Labrousse, F., Jouvet, A., Bauchet, L., Kalamaridès, M., Menei, P., Deruty, R., Moreau, J. J., Fèvre-Montange, M. & Guyotat, J. (2009) 'WHO grade II and III meningiomas: a study of prognostic factors'. *J Neurooncol*, 95 (3), pp. 367-375.

Dziuk, T. W., Woo, S., Butler, E. B., Thornby, J., Grossman, R., Dennis, W. S., Lu, H., Carpenter, L. S. & Chiu, J. K. (1998) 'Malignant meningioma: an indication for initial aggressive surgery and adjuvant radiotherapy'. *J Neurooncol*, 37 (2), pp. 177-188.

Ebert, C., von Haken, M., Meyer-Puttlitz, B., Wiestler, O. D., Reifenberger, G., Pietsch, T. & von Deimling, A. (1999) 'Molecular genetic analysis of ependymal tumors. NF2 mutations and chromosome 22q loss occur preferentially in intramedullary spinal ependymomas'. *Am J Pathol*, 155 (2), pp. 627-632.

Egelhoff, J. C., Bates, D. J., Ross, J. S., Rothner, A. D. & Cohen, B. H. (1992) 'Spinal MR findings in neurofibromatosis types 1 and 2'. *AJNR Am J Neuroradiol*, 13 (4), pp. 1071-1077.

Evans, D. G. (2009) 'Neurofibromatosis type 2 (NF2): a clinical and molecular review'. *Orphanet J Rare Dis*, 4 pp. 16.

Evans, D. G., Baser, M. E., McGaughran, J., Sharif, S., Howard, E. & Moran, A. (2002) 'Malignant peripheral nerve sheath tumours in neurofibromatosis 1'. *J Med Genet*, 39 (5), pp. 311-314.

Evans, D. G., Freeman, S., Gokhale, C., Wallace, A., Lloyd, S. K., Axon, P., Ward, C. L., Rutherford, S., King, A., Huson, S. M., Ramsden, R. T. & service, M. N. (2015) 'Bilateral vestibular schwannomas in older patients: NF2 or chance?'. *J Med Genet*, 52 (6), pp. 422-424.

Evans, D. G., Huson, S. M., Donnai, D., Neary, W., Blair, V., Newton, V. & Harris, R. (1992) 'A clinical study of type 2 neurofibromatosis'. *Q J Med*, 84 (304), pp. 603-618.

Evans, D. G., Moran, A., King, A., Saeed, S., Gurusinghe, N. & Ramsden, R. (2005) 'Incidence of vestibular schwannoma and neurofibromatosis 2 in the North West of England over a 10-year period: higher incidence than previously thought'. *Otol Neurotol*, 26 (1), pp. 93-97.

Evans, D. G., Ramsden, R. T., Shenton, A., Gokhale, C., Bowers, N. L., Huson, S. M., Pichert, G. & Wallace, A. (2007) 'Mosaicism in neurofibromatosis type 2: an update of risk based on uni/bilaterality of vestibular schwannoma at presentation and sensitive mutation analysis including multiple ligation-dependent probe amplification'. *J Med Genet*, 44 (7), pp. 424-428.

Evans, D. G., Sainio, M. & Baser, M. E. (2000) 'Neurofibromatosis type 2'. *J Med Genet*, 37 (12), pp. 897-904.

Evans, D. G., Trueman, L., Wallace, A., Collins, S. & Strachan, T. (1998) 'Genotype/phenotype correlations in type 2 neurofibromatosis (NF2): evidence for more severe disease associated with truncating mutations'. *J Med Genet*, 35 (6), pp. 450-455.

Fernandez, M. R., Henry, M. D. & Lewis, R. E. (2012) 'Kinase suppressor of Ras 2 (KSR2) regulates tumor cell transformation via AMPK'. *Mol Cell Biol*, 32 (18), pp. 3718-3731.

Ferner, R. E. & Gutmann, D. H. (2002) 'International consensus statement on malignant peripheral nerve sheath tumors in neurofibromatosis'. *Cancer Res*, 62 (5), pp. 1573-1577.

Ferner, R. E., Hughes, R. A. & Weinman, J. (1996) 'Intellectual impairment in neurofibromatosis 1'. *J Neurol Sci*, 138 (1-2), pp. 125-133.

Ferner, R. E., Huson, S. M., Thomas, N., Moss, C., Willshaw, H., Evans, D. G., Upadhyaya, M., Towers, R., Gleeson, M., Steiger, C. & Kirby, A. (2007) 'Guidelines for the diagnosis and management of individuals with neurofibromatosis 1'. *J Med Genet*, 44 (2), pp. 81-88.

Fisher, K. W., Das, B., Kim, H. S., Clymer, B. K., Gehring, D., Smith, D. R., Costanzo-Garvey, D. L., Fernandez, M. R., Brattain, M. G., Kelly, D. L., MacMillan, J., White, M. A. & Lewis, R. E. (2015) 'AMPK Promotes Aberrant PGC1β Expression To Support Human Colon Tumor Cell Survival'. *Mol Cell Biol*, 35 (22), pp. 3866-3879.

Flaiz, C., Chernoff, J., Ammoun, S., Peterson, J. R. & Hanemann, C. O. (2009) 'PAK kinase regulates Rac GTPase and is a potential target in human schwannomas'. *Exp Neurol*, 218 (1), pp. 137-144.

Fouladi, M., Stewart, C. F., Blaney, S. M., Onar-Thomas, A., Schaiquevich, P., Packer, R. J., Goldman, S., Geyer, J. R., Gajjar, A., Kun, L. E., Boyett, J. M. & Gilbertson, R. J. (2013) 'A molecular biology and phase II trial of lapatinib in children with refractory CNS malignancies: a pediatric brain tumor consortium study'. *J Neurooncol*, 114 (2), pp. 173-179.

Fraenzer, J. T., Pan, H., Minimo, L., Smith, G. M., Knauer, D. & Hung, G. (2003) 'Overexpression of the NF2 gene inhibits schwannoma cell proliferation through promoting PDGFR degradation'. *Int J Oncol*, 23 (6), pp. 1493-1500.

Friedman, J. M., Arbiser, J., Epstein, J. A., Gutmann, D. H., Huot, S. J., Lin, A. E., McManus, B. & Korf, B. R. (2002) 'Cardiovascular disease in neurofibromatosis 1: report of the NF1 Cardiovascular Task Force'. *Genet Med*, 4 (3), pp. 105-111.

Germino, E. A., Miller, J. P., Diehl, L., Swanson, C. J., Durinck, S., Modrusan, Z., Miner, J. H. & Shaw, A. S. (2018) 'Homozygous KSR1 deletion attenuates morbidity but does not prevent tumor development in a mouse model of RAS-driven pancreatic cancer'. *PLoS One*, 13 (3), pp. e0194998.

Giblett, S. M., Lloyd, D. J., Light, Y., Marais, R. & Pritchard, C. A. (2002) 'Expression of kinase suppressor of Ras in the normal adult and embryonic mouse'. *Cell Growth Differ*, 13 (7), pp. 307-313.

Gilbert, M. R., Ruda, R. & Soffietti, R. (2010) 'Ependymomas in adults'. *Curr Neurol Neurosci Rep*, 10 (3), pp. 240-247.

Giovannini, M., Bonne, N. X., Vitte, J., Chareyre, F., Tanaka, K., Adams, R., Fisher, L. M., Valeyrie-Allanore, L., Wolkenstein, P., Goutagny, S. & Kalamarides, M. (2014) 'mTORC1 inhibition delays growth of neurofibromatosis type 2 schwannoma'. *Neuro Oncol*, 16 (4), pp. 493-504.

Golovnina, K., Blinov, A., Akhmametyeva, E. M., Omelyanchuk, L. V. & Chang, L. S. (2005) 'Evolution and origin of Merlin, the product of the Neurofibromatosis type 2 (NF2) tumor-suppressor gene'. *BMC Evol Biol*, 5 pp. 69.

Gousias, K., Schramm, J. & Simon, M. (2016) 'The Simpson grading revisited: aggressive surgery and its place in modern meningioma management'. *J Neurosurg*, 125 (3), pp. 551-560.

Goutagny, S., Raymond, E., Esposito-Farese, M., Trunet, S., Mawrin, C., Bernardeschi, D., Larroque, B., Sterkers, O., Giovannini, M. & Kalamarides, M. (2015) 'Phase II study of mTORC1 inhibition by everolimus in neurofibromatosis type 2 patients with growing vestibular schwannomas'. *J Neurooncol*, 122 (2), pp. 313-320.

Goutebroze, L., Brault, E., Muchardt, C., Camonis, J. & Thomas, G. (2000) 'Cloning and characterization of SCHIP-1, a novel protein interacting specifically with spliced isoforms and naturally occurring mutant NF2 proteins'. *Mol Cell Biol*, 20 (5), pp. 1699-1712.

Green, R. M., Cloughesy, T. F., Stupp, R., DeAngelis, L. M., Woyshner, E. A., Ney, D. E. & Lassman, A. B. (2009) 'Bevacizumab for recurrent ependymoma'. *Neurology*, 73 (20), pp. 1677-1680.

Hadfield, K. D., Smith, M. J., Urquhart, J. E., Wallace, A. J., Bowers, N. L., King, A. T., Rutherford, S. A., Trump, D., Newman, W. G. & Evans, D. G. (2010) 'Rates of loss of heterozygosity and mitotic recombination in NF2 schwannomas, sporadic vestibular schwannomas and schwannomatosis schwannomas'. *Oncogene*, 29 (47), pp. 6216-6221.

Hamilton, R. L. & Pollack, I. F. (1997) 'The molecular biology of ependymomas'. *Brain Pathol*, 7 (2), pp. 807-822.

Hanemann, C. O. (2008) 'Magic but treatable? Tumours due to loss of Merlin'. *Brain*, 131 (Pt 3), pp. 606-615.

Hanemann, C. O. & Evans, D. G. (2006) 'News on the genetics, epidemiology, medical care and translational research of Schwannomas'. *J Neurol*, 253 (12), pp. 1533-1541.

Hansasuta, A., Choi, C. Y., Gibbs, I. C., Soltys, S. G., Tse, V. C., Lieberson, R. E., Hayden, M. G., Sakamoto, G. T., Harsh, G. R., Adler, J. R. & Chang, S. D. (2011) 'Multisession stereotactic radiosurgery for vestibular schwannomas: single-institution experience with 383 cases'. *Neurosurgery*, 69 (6), pp. 1200-1209.

Hawasli, A. H., Rubin, J. B., Tran, D. D., Adkins, D. R., Waheed, S., Hullar, T. E., Gutmann, D. H., Evans, J., Leonard, J. R., Zipfel, G. J. & Chicoine, M. R. (2013) 'Antiangiogenic agents for nonmalignant brain tumors'. *J Neurol Surg B Skull Base*, 74 (3), pp. 136-141.

He, Y. J., McCall, C. M., Hu, J., Zeng, Y. & Xiong, Y. (2006) 'DDB1 functions as a linker to recruit receptor WD40 proteins to CUL4-ROC1 ubiquitin ligases'. *Genes Dev*, 20 (21), pp. 2949-2954.

Hershko, A. & Ciechanover, A. (1998) 'The ubiquitin system'. *Annu Rev Biochem*, 67 pp. 425-479.

Hexter, A., Jones, A., Joe, H., Heap, L., Smith, M. J., Wallace, A. J., Halliday, D., Parry, A., Taylor, A., Raymond, L., Shaw, A., Afridi, S., Obholzer, R., Axon, P., King, A. T., Friedman, J. M., Evans, D. G. & Group, E. S. N. R. (2015) 'Clinical and molecular predictors of mortality in neurofibromatosis 2: a UK national analysis of 1192 patients'. *J Med Genet*, 52 (10), pp. 699-705.

Hilton, D. A., Ristic, N. & Hanemann, C. O. (2009) 'Activation of ERK, AKT and JNK signalling pathways in human schwannomas in situ'. *Histopathology*, 55 (6), pp. 744-749.

Hochart, A., Gaillard, V., Baroncini, M., André, N., Vannier, J. P., Vinchon, M., Dubrulle, F., Lejeune, J. P., Vincent, C., Nève, V., Sudour Bonnange, H., Bonne, N. X. & Leblond, P.

(2015) 'Bevacizumab decreases vestibular schwannomas growth rate in children and teenagers with neurofibromatosis type 2'. *J Neurooncol*, 124 (2), pp. 229-236.

Hochstrasser, M. (1998) 'There's the rub: a novel ubiquitin-like modification linked to cell cycle regulation'. *Genes Dev*, 12 (7), pp. 901-907.

Hrecka, K., Gierszewska, M., Srivastava, S., Kozaczkiewicz, L., Swanson, S. K., Florens, L., Washburn, M. P. & Skowronski, J. (2007) 'Lentiviral Vpr usurps Cul4-DDB1[VprBP] E3 ubiquitin ligase to modulate cell cycle'. *Proc Natl Acad Sci U S A*, 104 (28), pp. 11778-11783.

Håvik, A. L., Bruland, O., Myrseth, E., Miletic, H., Aarhus, M., Knappskog, P. M. & Lund-Johansen, M. (2018) 'Genetic landscape of sporadic vestibular schwannoma'. *J Neurosurg*, 128 (3), pp. 911-922.

Jackson, S. & Xiong, Y. (2009) 'CRL4s: the CUL4-RING E3 ubiquitin ligases'. *Trends Biochem Sci*, 34 (11), pp. 562-570.

Jacob, A., Lee, T. X., Neff, B. A., Miller, S., Welling, B. & Chang, L. S. (2008) 'Phosphatidylinositol 3-kinase/AKT pathway activation in human vestibular schwannoma'. *Otol Neurotol*, 29 (1), pp. 58-68.

Jagemann, L. R., Pérez-Rivas, L. G., Ruiz, E. J., Ranea, J. A., Sánchez-Jiménez, F., Nebreda, A. R., Alba, E. & Lozano, J. (2008) 'The functional interaction of 14-3-3 proteins with the ERK1/2 scaffold KSR1 occurs in an isoform-specific manner'. *J Biol Chem*, 283 (25), pp. 17450-17462.

Jain, S. & Sehgal, V. N. (2000) 'Terbinafine, a unique oral antifungal: current perceptions'. *Int J Dermatol*, 39 (6), pp. 412-423.

James, M. F., Han, S., Polizzano, C., Plotkin, S. R., Manning, B. D., Stemmer-Rachamimov, A. O., Gusella, J. F. & Ramesh, V. (2009) 'NF2/Merlin is a novel negative regulator of mTOR complex 1, and activation of mTORC1 is associated with meningioma and schwannoma growth'. *Mol Cell Biol*, 29 (15), pp. 4250-4261.

Jessen, W. J., Miller, S. J., Jousma, E., Wu, J., Rizvi, T. A., Brundage, M. E., Eaves, D., Widemann, B., Kim, M. O., Dombi, E., Sabo, J., Hardiman Dudley, A., Niwa-Kawakita, M., Page, G. P., Giovannini, M., Aronow, B. J., Cripe, T. P. & Ratner, N. (2013) 'MEK inhibition exhibits efficacy in human and mouse neurofibromatosis tumors'. *J Clin Invest*, 123 (1), pp. 340-347.

Jia, L., Li, H. & Sun, Y. (2011) 'Induction of p21-dependent senescence by an NAE inhibitor, MLN4924, as a mechanism of growth suppression'. *Neoplasia*, 13 (6), pp. 561-569.

Jin, J., Arias, E. E., Chen, J., Harper, J. W. & Walter, J. C. (2006) 'A family of diverse Cul4-Ddb1-interacting proteins includes Cdt2, which is required for S phase destruction of the replication factor Cdt1'. *Mol Cell*, 23 (5), pp. 709-721.

Johansson, G., Mahller, Y. Y., Collins, M. H., Kim, M. O., Nobukuni, T., Perentesis, J., Cripe, T. P., Lane, H. A., Kozma, S. C., Thomas, G. & Ratner, N. (2008) 'Effective in vivo targeting of the mammalian target of rapamycin pathway in malignant peripheral nerve sheath tumors'. *Mol Cancer Ther*, 7 (5), pp. 1237-1245.

Johnson, M. D., Okedli, E., Woodard, A., Toms, S. A. & Allen, G. S. (2002) 'Evidence for phosphatidylinositol 3-kinase-Akt-p7S6K pathway activation and transduction of mitogenic signals by platelet-derived growth factor in meningioma cells'. *J Neurosurg*, 97 (3), pp. 668-675.

Jones, J., Wu, K., Yang, Y., Guerrero, C., Nillegoda, N., Pan, Z. Q. & Huang, L. (2008) 'A targeted proteomic analysis of the ubiquitin-like modifier NEDD8 and associated proteins'. *J Proteome Res*, 7 (3), pp. 1274-1287.

Kaempchen, K., Mielke, K., Utermark, T., Langmesser, S. & Hanemann, C. O. (2003) 'Upregulation of the Rac1/JNK signaling pathway in primary human schwannoma cells'. *Hum Mol Genet*, 12 (11), pp. 1211-1221.

Kalamarides, M., Niwa-Kawakita, M., Leblois, H., Abramowski, V., Perricaudet, M., Janin, A., Thomas, G., Gutmann, D. H. & Giovannini, M. (2002) 'Nf2 gene inactivation in arachnoidal cells is rate-limiting for meningioma development in the mouse'. *Genes Dev*, 16 (9), pp. 1060-1065.

Karajannis, M. A., Legault, G., Hagiwara, M., Ballas, M. S., Brown, K., Nusbaum, A. O., Hochman, T., Goldberg, J. D., Koch, K. M., Golfinos, J. G., Roland, J. T. & Allen, J. C. (2012) 'Phase II trial of lapatinib in adult and pediatric patients with neurofibromatosis type 2 and progressive vestibular schwannomas'. *Neuro Oncol*, 14 (9), pp. 1163-1170.

Karajannis, M. A., Legault, G., Hagiwara, M., Giancotti, F. G., Filatov, A., Derman, A., Hochman, T., Goldberg, J. D., Vega, E., Wisoff, J. H., Golfinos, J. G., Merkelson, A., Roland, J. T. & Allen, J. C. (2014) 'Phase II study of everolimus in children and adults with neurofibromatosis type 2 and progressive vestibular schwannomas'. *Neuro Oncol*, 16 (2), pp. 292-297.

Kaur, M., Khan, M. M., Kar, A., Sharma, A. & Saxena, S. (2012) 'CRL4-DDB1-VPRBP ubiquitin ligase mediates the stress triggered proteolysis of Mcm10'. *Nucleic Acids Res*, 40 (15), pp. 7332-7346.

Kawabata, Y., Takahashi, J. A., Arakawa, Y. & Hashimoto, N. (2005) 'Long-term outcome in patients harboring intracranial ependymoma'. *J Neurosurg*, 103 (1), pp. 31-37.

Kim, H. A., Pomeroy, S. L., Whoriskey, W., Pawlitzky, I., Benowitz, L. I., Sicinski, P., Stiles, C. D. & Roberts, T. M. (2000) 'A developmentally regulated switch directs regenerative growth of Schwann cells through CYCLIN D1'. *Neuron*, 26 (2), pp. 405-416.

Kim, K., Kim, J. M., Kim, J. S., Choi, J., Lee, Y. S., Neamati, N., Song, J. S., Heo, K. & An, W. (2013) 'VprBP has intrinsic kinase activity targeting histone H2A and represses gene transcription'. *Mol Cell*, 52 (3), pp. 459-467.

Kim, S. & Jho, E. H. (2016) 'Merlin, a regulator of Hippo signaling, regulates Wnt/β-catenin signaling'. *BMB Rep*, 49 (7), pp. 357-358.

Kissil, J. L., Wilker, E. W., Johnson, K. C., Eckman, M. S., Yaffe, M. B. & Jacks, T. (2003) 'Merlin, the product of the *Nf2* tumor suppressor gene, is an inhibitor of the p21-activated kinase, Pak1'. *Mol Cell*, 12 (4), pp. 841-849.

Klaeboe, L., Lonn, S., Scheie, D., Auvinen, A., Christensen, H. C., Feychting, M., Johansen, C., Salminen, T. & Tynes, T. (2005) 'Incidence of intracranial meningiomas in Denmark, Finland, Norway and Sweden, 1968-1997'. *Int J Cancer*, 117 (6), pp. 996-1001.

Kluwe, L. & Mautner, V. F. (1998) 'Mosaicism in sporadic neurofibromatosis 2 patients'. *Hum Mol Genet*, 7 (13), pp. 2051-2055.

Komander, D. & Rape, M. (2012) 'The ubiquitin code'. *Annu Rev Biochem*, 81 pp. 203-229.

Kortum, R. L., Costanzo, D. L., Haferbier, J., Schreiner, S. J., Razidlo, G. L., Wu, M. H., Volle, D. J., Mori, T., Sakaue, H., Chaika, N. V., Chaika, O. V. & Lewis, R. E. (2005) 'The molecular scaffold kinase suppressor of Ras 1 (KSR1) regulates adipogenesis'. *Mol Cell Biol*, 25 (17), pp. 7592-7604.

Kortum, R. L. & Lewis, R. E. (2004) 'The molecular scaffold KSR1 regulates the proliferative and oncogenic potential of cells'. *Mol Cell Biol*, 24 (10), pp. 4407-4416.

Kuhn, D. J., Berkova, Z., Jones, R. J., Woessner, R., Bjorklund, C. C., Ma, W., Davis, R. E., Lin, P., Wang, H., Madden, T. L., Wei, C., Baladandayuthapani, V., Wang, M., Thomas, S. K., Shah, J. J., Weber, D. M. & Orlowski, R. Z. (2012) 'Targeting the insulin-like growth factor-1 receptor to overcome bortezomib resistance in preclinical models of multiple myeloma'. *Blood*, 120 (16), pp. 3260-3270.

Lallemand, D., Manent, J., Couvelard, A., Watilliaux, A., Siena, M., Chareyre, F., Lampin, A., Niwa-Kawakita, M., Kalamarides, M. & Giovannini, M. (2009) 'Merlin regulates transmembrane receptor accumulation and signaling at the plasma membrane in primary mouse Schwann cells and in human schwannomas'. *Oncogene*, 28 (6), pp. 854-865.

Lamszus, K., Lachenmayer, L., Heinemann, U., Kluwe, L., Finckh, U., Höppner, W., Stavrou, D., Fillbrandt, R. & Westphal, M. (2001) 'Molecular genetic alterations on chromosomes 11 and 22 in ependymomas'. *Int J Cancer*, 91 (6), pp. 803-808.

Lan, H., Tang, Z., Jin, H. & Sun, Y. (2016) 'Neddylation inhibitor MLN4924 suppresses growth and migration of human gastric cancer cells'. *Sci Rep*, 6 pp. 24218.

Lassaletta, L., Torres-Martín, M., Peña-Granero, C., Roda, J. M., Santa-Cruz-Ruiz, S., Castresana, J. S., Gavilan, J. & Rey, J. A. (2013) 'NF2 genetic alterations in sporadic vestibular schwannomas: clinical implications'. *Otol Neurotol*, 34 (7), pp. 1355-1361.

Lau, Y. K., Murray, L. B., Houshmandi, S. S., Xu, Y., Gutmann, D. H. & Yu, Q. (2008) 'Merlin is a potent inhibitor of glioma growth'. *Cancer Res*, 68 (14), pp. 5733-5742.

Laulajainen, M., Muranen, T., Carpén, O. & Grönholm, M. (2008) 'Protein kinase A-mediated phosphorylation of the NF2 tumor suppressor protein Merlin at serine 10 affects the actin cytoskeleton'. *Oncogene*, 27 (23), pp. 3233-3243.

Lee, W. S., Chen, R. J., Wang, Y. J., Tseng, H., Jeng, J. H., Lin, S. Y., Liang, Y. C., Chen, C. H., Lin, C. H., Lin, J. K., Ho, P. Y., Chu, J. S., Ho, W. L., Chen, L. C. & Ho, Y. S. (2003) 'In vitro and in vivo studies of the anticancer action of terbinafine in human cancer cell lines: G0/G1 p53-associated cell cycle arrest'. *Int J Cancer*, 106 (1), pp. 125-137.

Li, B., Lu, L., Zhong, M., Tan, X. X., Liu, C. Y., Guo, Y. & Yi, X. (2013) 'Terbinafine inhibits KSR1 and suppresses Raf-MEK-ERK signaling in oral squamous cell carcinoma cells'. *Neoplasma*, 60 (4), pp. 406-412.

Li, W., Cooper, J., Zhou, L., Yang, C., Erdjument-Bromage, H., Zagzag, D., Snuderl, M., Ladanyi, M., Hanemann, C. O., Zhou, P., Karajannis, M. A. & Giancotti, F. G. (2014) 'Merlin/NF2 loss-driven tumorigenesis linked to CRL4(DCAF1)-mediated inhibition of the hippo pathway kinases LATS1 and 2 in the nucleus'. *Cancer Cell*, 26 (1), pp. 48-60.

Li, W., You, L., Cooper, J., Schiavon, G., Pepe-Caprio, A., Zhou, L., Ishii, R., Giovannini, M., Hanemann, C. O., Long, S. B., Erdjument-Bromage, H., Zhou, P., Tempst, P. & Giancotti, F. G. (2010) 'Merlin/NF2 suppresses tumorigenesis by inhibiting the E3 ubiquitin ligase CRL4(DCAF1) in the nucleus'. *Cell*, 140 (4), pp. 477-490.

Lim, S. & de Souza, P. (2013) 'Imatinib in neurofibromatosis type 2'. *BMJ Case Rep*, 2013

Lin, D., Hegarty, J. L., Fischbein, N. J. & Jackler, R. K. (2005) 'The prevalence of "incidental" acoustic neuroma'. *Arch Otolaryngol Head Neck Surg*, 131 (3), pp. 241-244.

Lin, J. J., Milhollen, M. A., Smith, P. G., Narayanan, U. & Dutta, A. (2010) 'NEDD8-targeting drug MLN4924 elicits DNA rereplication by stabilizing Cdt1 in S phase, triggering checkpoint activation, apoptosis, and senescence in cancer cells'. *Cancer Res*, 70 (24), pp. 10310-10320.

Lin, S., Shang, Z., Li, S., Gao, P., Zhang, Y., Hou, S., Qin, P., Dong, Z., Hu, T. & Chen, P. (2018) 'Neddylation inhibitor MLN4924 induces G'. *Oncol Lett*, 15 (2), pp. 2583-2589.

Liu, L., Channavajhala, P. L., Rao, V. R., Moutsatsos, I., Wu, L., Zhang, Y., Lin, L. L. & Qiu, Y. (2009) 'Proteomic characterization of the dynamic KSR-2 interactome, a signaling scaffold complex in MAPK pathway'. *Biochim Biophys Acta*, 1794 (10), pp. 1485-1495.

Llobet, D., Eritja, N., Domingo, M., Bergada, L., Mirantes, C., Santacana, M., Pallares, J., Macià, A., Yeramian, A., Encinas, M., Moreno-Bueno, G., Palacios, J., Lewis, R. E., Matias-Guiu, X. & Dolcet, X. (2011) 'KSR1 is overexpressed in endometrial carcinoma and regulates proliferation and TRAIL-induced apoptosis by modulating FLIP levels'. *Am J Pathol*, 178 (4), pp. 1529-1543.

Lomas, J., Bello, M. J., Arjona, D., Alonso, M. E., Martinez-Glez, V., Lopez-Marin, I., Amiñoso, C., de Campos, J. M., Isla, A., Vaquero, J. & Rey, J. A. (2005) 'Genetic and epigenetic alteration of the NF2 gene in sporadic meningiomas'. *Genes Chromosomes Cancer*, 42 (3), pp. 314-319.

Lozano, J., Xing, R., Cai, Z., Jensen, H. L., Trempus, C., Mark, W., Cannon, R. & Kolesnick, R. (2003) 'Deficiency of kinase suppressor of Ras1 prevents oncogenic ras signaling in mice'. *Cancer Res*, 63 (14), pp. 4232-4238.

Lu-Emerson, C. & Plotkin, S. R. (2009) 'The Neurofibromatoses. Part 1: NF1'. *Rev Neurol Dis*, 6 (2), pp. E47-53.

Luo, Z., Yu, G., Lee, H. W., Li, L., Wang, L., Yang, D., Pan, Y., Ding, C., Qian, J., Wu, L., Chu, Y., Yi, J., Wang, X., Sun, Y., Jeong, L. S., Liu, J. & Jia, L. (2012) 'The NEDD8-activating enzyme inhibitor MLN4924 induces autophagy and apoptosis to suppress liver cancer cell growth'. *Cancer Res*, 72 (13), pp. 3360-3371.

López-Lago, M. A., Okada, T., Murillo, M. M., Socci, N. & Giancotti, F. G. (2009) 'Loss of the tumor suppressor gene NF2, encoding Merlin, constitutively activates integrin-dependent mTORC1 signaling'. *Mol Cell Biol*, 29 (15), pp. 4235-4249.

Maniakas, A. & Saliba, I. (2012) 'Microsurgery versus stereotactic radiation for small vestibular schwannomas: a meta-analysis of patients with more than 5 years' follow-up'. *Otol Neurotol*, 33 (9), pp. 1611-1620.

Matallanas, D., Birtwistle, M., Romano, D., Zebisch, A., Rauch, J., von Kriegsheim, A. & Kolch, W. (2011) 'Raf family kinases: old dogs have learned new tricks'. *Genes Cancer*, 2 (3), pp. 232-260.

Mautner, V. F., Lindenau, M., Baser, M. E., Kluwe, L. & Gottschalk, J. (1997) 'Skin abnormalities in neurofibromatosis 2'. *Arch Dermatol*, 133 (12), pp. 1539-1543.

Mautner, V. F., Nguyen, R., Kutta, H., Fuensterer, C., Bokemeyer, C., Hagel, C., Friedrich, R. E. & Panse, J. (2010) 'Bevacizumab induces regression of vestibular

schwannomas in patients with neurofibromatosis type 2'. *Neuro Oncol*, 12 (1), pp. 14-18.

Mautner, V. F., Tatagiba, M., Lindenau, M., Fünsterer, C., Pulst, S. M., Baser, M. E., Kluwe, L. & Zanella, F. E. (1995) 'Spinal tumors in patients with neurofibromatosis type 2: MR imaging study of frequency, multiplicity, and variety'. *AJR Am J Roentgenol*, 165 (4), pp. 951-955.

Mawrin, C., Chung, C. & Preusser, M. (2015) 'Biology and clinical management challenges in meningioma'. *Am Soc Clin Oncol Educ Book*, pp. e106-115.

McClatchey, A. I., Saotome, I., Mercer, K., Crowley, D., Gusella, J. F., Bronson, R. T. & Jacks, T. (1998) 'Mice heterozygous for a mutation at the Nf2 tumor suppressor locus develop a range of highly metastatic tumors'. *Genes Dev*, 12 (8), pp. 1121-1133.

Meerang, M., Bérard, K., Friess, M., Bitanihirwe, B. K., Soltermann, A., Vrugt, B., Felley-Bosco, E., Bueno, R., Richards, W. G., Seifert, B., Stahel, R., Weder, W. & Opitz, I. (2016) 'Low Merlin expression and high Survivin labeling index are indicators for poor prognosis in patients with malignant pleural mesothelioma'. *Mol Oncol*, 10 (8), pp. 1255-1265.

Mei, Y., Bi, W. L., Greenwald, N. F., Agar, N. Y., Beroukhim, R., Dunn, G. P. & Dunn, I. F. (2017) 'Genomic profile of human meningioma cell lines'. *PLoS One*, 12 (5), pp. e0178322.

Merchant, T. E. & Fouladi, M. (2005) 'Ependymoma: new therapeutic approaches including radiation and chemotherapy'. *J Neurooncol*, 75 (3), pp. 287-299.

Merker, V. L., Esparza, S., Smith, M. J., Stemmer-Rachamimov, A. & Plotkin, S. R. (2012) 'Clinical features of schwannomatosis: a retrospective analysis of 87 patients'. *Oncologist*, 17 (10), pp. 1317-1322.

Milhollen, M. A., Thomas, M. P., Narayanan, U., Traore, T., Riceberg, J., Amidon, B. S., Bence, N. F., Bolen, J. B., Brownell, J., Dick, L. R., Loke, H. K., McDonald, A. A., Ma, J., Manfredi, M. G., Sells, T. B., Sintchak, M. D., Yang, X., Xu, Q., Koenig, E. M., Gavin, J. M. & Smith, P. G. (2012) 'Treatment-emergent mutations in NAEβ confer resistance to the NEDD8-activating enzyme inhibitor MLN4924'. *Cancer Cell*, 21 (3), pp. 388-401.

Milhollen, M. A., Traore, T., Adams-Duffy, J., Thomas, M. P., Berger, A. J., Dang, L., Dick, L. R., Garnsey, J. J., Koenig, E., Langston, S. P., Manfredi, M., Narayanan, U., Rolfe, M., Staudt, L. M., Soucy, T. A., Yu, J., Zhang, J., Bolen, J. B. & Smith, P. G. (2010) 'MLN4924, a NEDD8-activating enzyme inhibitor, is active in diffuse large B-cell lymphoma models: rationale for treatment of NF-{kappa}B-dependent lymphoma'. *Blood*, 116 (9), pp. 1515-1523.

Mindos, T., Dun, X. P., North, K., Doddrell, R. D., Schulz, A., Edwards, P., Russell, J., Gray, B., Roberts, S. L., Shivane, A., Mortimer, G., Pirie, M., Zhang, N., Pan, D., Morrison, H. & Parkinson, D. B. (2017) 'Merlin controls the repair capacity of Schwann cells after injury by regulating Hippo/YAP activity'. *J Cell Biol*, 216 (2), pp. 495-510.

Mori, T., Gotoh, S., Shirakawa, M. & Hakoshima, T. (2014) 'Structural basis of DDB1-and-Cullin 4-associated Factor 1 (DCAF1) recognition by Merlin/NF2 and its implication in tumorigenesis by CD44-mediated inhibition of Merlin suppression of DCAF1 function'. *Genes Cells*, 19 (8), pp. 603-619.

Morrison, D. K. (2001) 'KSR: a MAPK scaffold of the Ras pathway?'. *J Cell Sci*, 114 (Pt 9), pp. 1609-1612.

Morrison, H., Sherman, L. S., Legg, J., Banine, F., Isacke, C., Haipek, C. A., Gutmann, D. H., Ponta, H. & Herrlich, P. (2001) 'The NF2 tumor suppressor gene product, Merlin, mediates contact inhibition of growth through interactions with CD44'. *Genes Dev*, 15 (8), pp. 968-980.

Morrison, H., Sperka, T., Manent, J., Giovannini, M., Ponta, H. & Herrlich, P. (2007) 'Merlin/neurofibromatosis type 2 suppresses growth by inhibiting the activation of Ras and Rac'. *Cancer Res*, 67 (2), pp. 520-527.

Mukherjee, J., Kamnasaran, D., Balasubramaniam, A., Radovanovic, I., Zadeh, G., Kiehl, T. R. & Guha, A. (2009) 'Human schwannomas express activated platelet-derived growth factor receptors and c-kit and are growth inhibited by Gleevec (Imatinib Mesylate)'. *Cancer Res*, 69 (12), pp. 5099-5107.

Muranen, T., Grönholm, M., Renkema, G. H. & Carpén, O. (2005) 'Cell cycle-dependent nucleocytoplasmic shuttling of the neurofibromatosis 2 tumour suppressor Merlin'. *Oncogene*, 24 (7), pp. 1150-1158.

Muzevic, D., Legcevic, J., Splavski, B. & Cayé-Thomasen, P. (2014) 'Stereotactic radiotherapy for vestibular schwannoma'. *Cochrane Database Syst Rev*, (12), pp. CD009897.

Müller, J., Cacace, A. M., Lyons, W. E., McGill, C. B. & Morrison, D. K. (2000) 'Identification of B-KSR1, a novel brain-specific isoform of KSR1 that functions in neuronal signaling'. *Mol Cell Biol*, 20 (15), pp. 5529-5539.

Müller, J., Ory, S., Copeland, T., Piwnica-Worms, H. & Morrison, D. K. (2001) 'C-TAK1 regulates Ras signaling by phosphorylating the MAPK scaffold, KSR1'. *Mol Cell*, 8 (5), pp. 983-993.

Nakagawa, T., Mondal, K. & Swanson, P. C. (2013) 'VprBP (DCAF1): a promiscuous substrate recognition subunit that incorporates into both RING-family CRL4 and HECT-family EDD/UBR5 E3 ubiquitin ligases'. *BMC Mol Biol*, 14 pp. 22.

Ni, W., Zhang, Y., Zhan, Z., Ye, F., Liang, Y., Huang, J., Chen, K., Chen, L. & Ding, Y. (2017) 'A novel lncRNA uc.134 represses hepatocellular carcinoma progression by inhibiting CUL4A-mediated ubiquitination of LATS1'. *J Hematol Oncol*, 10 (1), pp. 91.

Niault, T. S. & Baccarini, M. (2010) 'Targets of Raf in tumorigenesis'. *Carcinogenesis*, 31 (7), pp. 1165-1174.

Nowak, A., Dziedzic, T., Czernicki, T., Kunert, P. & Marchel, A. (2016) 'Management of spinal tumors in neurofibromatosis type 2 patients'. *Neurol Neurochir Pol*, 50 (1), pp. 31-35.

Nowosielski, M., Hoffmann, M., Wyrwicz, L. S., Stepniak, P., Plewczynski, D. M., Lazniewski, M., Ginalski, K. & Rychlewski, L. (2011) 'Detailed mechanism of squalene epoxidase inhibition by terbinafine'. *J Chem Inf Model*, 51 (2), pp. 455-462.

Nunes, F., Shen, Y., Niida, Y., Beauchamp, R., Stemmer-Rachamimov, A. O., Ramesh, V., Gusella, J. & MacCollin, M. (2005) 'Inactivation patterns of NF2 and DAL-1/4.1B (EPB41L3) in sporadic meningioma'. *Cancer Genet Cytogenet*, 162 (2), pp. 135-139.

Nunes, F. P., Merker, V. L., Jennings, D., Caruso, P. A., di Tomaso, E., Muzikansky, A., Barker, F. G., Stemmer-Rachamimov, A. & Plotkin, S. R. (2013) 'Bevacizumab treatment

for meningiomas in NF2: a retrospective analysis of 15 patients'. *PLoS One*, 8 (3), pp. e59941.

Office-for-National-Statistics (2016) 'Past and projected data from the period and cohort life tables, 2016-based, UK: 1981 to 2066'. [Online]. Available at: https://www.ons.gov.uk/peoplepopulationandcommunity/birthsdeathsandmarriages/lifeexpectancies/bulletins/pastandprojecteddatafromtheperiodandcohortlifetables/2016baseduk1981to2066#links-to-related-statistics (Accessed: 26th April 2018).

Okada, T., Lopez-Lago, M. & Giancotti, F. G. (2005) 'Merlin/NF-2 mediates contact inhibition of growth by suppressing recruitment of Rac to the plasma membrane'. *J Cell Biol*, 171 (2), pp. 361-371.

Ory, S., Zhou, M., Conrads, T. P., Veenstra, T. D. & Morrison, D. K. (2003) 'Protein phosphatase 2A positively regulates Ras signaling by dephosphorylating KSR1 and Raf-1 on critical 14-3-3 binding sites'. *Curr Biol*, 13 (16), pp. 1356-1364.

Ostrom, Q. T., Gittleman, H., Farah, P., Ondracek, A., Chen, Y., Wolinsky, Y., Stroup, N. E., Kruchko, C. & Barnholtz-Sloan, J. S. (2013) 'CBTRUS statistical report: Primary brain and central nervous system tumors diagnosed in the United States in 2006-2010'. *Neuro Oncol*, 15 Suppl 2 pp. ii1-56.

Ostrom, Q. T., Gittleman, H., Fulop, J., Liu, M., Blanda, R., Kromer, C., Wolinsky, Y., Kruchko, C. & Barnholtz-Sloan, J. S. (2015) 'CBTRUS Statistical Report: Primary Brain and Central Nervous System Tumors Diagnosed in the United States in 2008-2012'. *Neuro Oncol*, 17 Suppl 4 pp. iv1-iv62.

Pajtler, K. W., Witt, H., Sill, M., Jones, D. T., Hovestadt, V., Kratochwil, F., Wani, K., Tatevossian, R., Punchihewa, C., Johann, P., Reimand, J., Warnatz, H. J., Ryzhova, M.,

Mack, S., Ramaswamy, V., Capper, D., Schweizer, L., Sieber, L., Wittmann, A., Huang, Z., van Sluis, P., Volckmann, R., Koster, J., Versteeg, R., Fults, D., Toledano, H., Avigad, S., Hoffman, L. M., Donson, A. M., Foreman, N., Hewer, E., Zitterbart, K., Gilbert, M., Armstrong, T. S., Gupta, N., Allen, J. C., Karajannis, M. A., Zagzag, D., Hasselblatt, M., Kulozik, A. E., Witt, O., Collins, V. P., von Hoff, K., Rutkowski, S., Pietsch, T., Bader, G., Yaspo, M. L., von Deimling, A., Lichter, P., Taylor, M. D., Gilbertson, R., Ellison, D. W., Aldape, K., Korshunov, A., Kool, M. & Pfister, S. M. (2015) 'Molecular Classification of Ependymal Tumors across All CNS Compartments, Histopathological Grades, and Age Groups'. *Cancer Cell*, 27 (5), pp. 728-743.

Paldor, I., Abbadi, S., Bonne, N., Ye, X., Rodriguez, F. J., Rowshanshad, D., Itzoe, M., Vigilar, V., Giovannini, M., Brem, H., Blakeley, J. O. & Tyler, B. M. (2017) 'The efficacy of lapatinib and nilotinib in combination with radiation therapy in a model of NF2 associated peripheral schwannoma'. *J Neurooncol*, 135 (1), pp. 47-56.

Patel, M. R., Sadiq, A. A., Jay-Dixon, J., Jirakulaporn, T., Jacobson, B. A., Farassati, F., Bitterman, P. B. & Kratzke, R. A. (2012) 'Novel role of c-jun N-terminal kinase in regulating the initiation of cap-dependent translation'. *Int J Oncol*, 40 (2), pp. 577-582.

Pearson, B. E., Markert, J. M., Fisher, W. S., Guthrie, B. L., Fiveash, J. B., Palmer, C. A. & Riley, K. (2008) 'Hitting a moving target: evolution of a treatment paradigm for atypical meningiomas amid changing diagnostic criteria'. *Neurosurg Focus*, 24 (5), pp. E3.

Pemov, A., Li, H., Patidar, R., Hansen, N. F., Sindiri, S., Hartley, S. W., Wei, J. S., Elkahloun, A., Chandrasekharappa, S. C., Boland, J. F., Bass, S., Mullikin, J. C., Khan, J., Widemann, B. C., Wallace, M. R., Stewart, D. R., Program, N. C. S. & Laboratory, N. D. C. G. R. (2017) 'The primacy of NF1 loss as the driver of tumorigenesis in

neurofibromatosis type 1-associated plexiform neurofibromas'. *Oncogene*, 36 (22), pp. 3168-3177.

Perry, A., Cai, D. X., Scheithauer, B. W., Swanson, P. E., Lohse, C. M., Newsham, I. F., Weaver, A. & Gutmann, D. H. (2000) 'Merlin, DAL-1, and progesterone receptor expression in clinicopathologic subsets of meningioma: a correlative immunohistochemical study of 175 cases'. *J Neuropathol Exp Neurol*, 59 (10), pp. 872-879.

Perry, A., Giannini, C., Raghavan, R., Scheithauer, B. W., Banerjee, R., Margraf, L., Bowers, D. C., Lytle, R. A., Newsham, I. F. & Gutmann, D. H. (2001) 'Aggressive phenotypic and genotypic features in pediatric and NF2-associated meningiomas: a clinicopathologic study of 53 cases'. *J Neuropathol Exp Neurol*, 60 (10), pp. 994-1003.

Petrilli, A. M. & Fernández-Valle, C. (2016) 'Role of Merlin/NF2 inactivation in tumor biology'. *Oncogene*, 35 (5), pp. 537-548.

Plotkin, S. R., Merker, V. L., Halpin, C., Jennings, D., McKenna, M. J., Harris, G. J. & Barker, F. G. (2012) 'Bevacizumab for progressive vestibular schwannoma in neurofibromatosis type 2: a retrospective review of 31 patients'. *Otol Neurotol*, 33 (6), pp. 1046-1052.

Poulikakos, P. I., Xiao, G. H., Gallagher, R., Jablonski, S., Jhanwar, S. C. & Testa, J. R. (2006) 'Re-expression of the tumor suppressor NF2/Merlin inhibits invasiveness in mesothelioma cells and negatively regulates FAK'. *Oncogene*, 25 (44), pp. 5960-5968.

Preusser, M., Brastianos, P. K. & Mawrin, C. (2018) 'Advances in meningioma genetics: novel therapeutic opportunities'. *Nat Rev Neurol*, 14 (2), pp. 106-115.

Püttmann, S., Senner, V., Braune, S., Hillmann, B., Exeler, R., Rickert, C. H. & Paulus, W. (2005) 'Establishment of a benign meningioma cell line by hTERT-mediated immortalization'. *Lab Invest*, 85 (9), pp. 1163-1171.

Ragge, N. K., Baser, M. E., Riccardi, V. M. & Falk, R. E. (1997) 'The ocular presentation of neurofibromatosis 2'. *Eye (Lond)*, 11 (Pt 1) pp. 12-18.

Razidlo, G. L., Kortum, R. L., Haferbier, J. L. & Lewis, R. E. (2004) 'Phosphorylation regulates KSR1 stability, ERK activation, and cell proliferation'. *J Biol Chem*, 279 (46), pp. 47808-47814.

Rimkus, T. K., Carpenter, R. L., Qasem, S., Chan, M. & Lo, H. W. (2016) 'Targeting the Sonic Hedgehog Signaling Pathway: Review of Smoothened and GLI Inhibitors'. *Cancers (Basel)*, 8 (2),

Rinaldi, L., Delle Donne, R., Sepe, M., Porpora, M., Garbi, C., Chiuso, F., Gallo, A., Parisi, S., Russo, L., Bachmann, V., Huber, R. G., Stefan, E., Russo, T. & Feliciello, A. (2016) 'praja2 regulates KSR1 stability and mitogenic signaling'. *Cell Death Dis*, 7 pp. e2230.

Ritt, D. A., Zhou, M., Conrads, T. P., Veenstra, T. D., Copeland, T. D. & Morrison, D. K. (2007) 'CK2 Is a component of the KSR1 scaffold complex that contributes to Raf kinase activation'. *Curr Biol*, 17 (2), pp. 179-184.

Rockwell, P., O'Connor, W. J., King, K., Goldstein, N. I., Zhang, L. M. & Stein, C. A. (1997) 'Cell-surface perturbations of the epidermal growth factor and vascular endothelial growth factor receptors by phosphorothioate oligodeoxynucleotides'. *Proc Natl Acad Sci U S A*, 94 (12), pp. 6523-6528.

Rong, R., Surace, E. I., Haipek, C. A., Gutmann, D. H. & Ye, K. (2004a) 'Serine 518 phosphorylation modulates Merlin intramolecular association and binding to critical effectors important for NF2 growth suppression'. *Oncogene*, 23 (52), pp. 8447-8454.

Rong, R., Tang, X., Gutmann, D. H. & Ye, K. (2004b) 'Neurofibromatosis 2 (NF2) tumor suppressor Merlin inhibits phosphatidylinositol 3-kinase through binding to PIKE-L'. *Proc Natl Acad Sci U S A*, 101 (52), pp. 18200-18205.

Rosenbaum, C., Kluwe, L., Mautner, V. F., Friedrich, R. E., Müller, H. W. & Hanemann, C. O. (1998) 'Isolation and characterization of Schwann cells from neurofibromatosis type 2 patients'. *Neurobiol Dis*, 5 (1), pp. 55-64.

Roy, F., Laberge, G., Douziech, M., Ferland-McCollough, D. & Therrien, M. (2002) 'KSR is a scaffold required for activation of the ERK/MAPK module'. *Genes Dev*, 16 (4), pp. 427-438.

Rubio, M. P., Correa, K. M., Ramesh, V., MacCollin, M. M., Jacoby, L. B., von Deimling, A., Gusella, J. F. & Louis, D. N. (1994) 'Analysis of the neurofibromatosis 2 gene in human ependymomas and astrocytomas'. *Cancer Res*, 54 (1), pp. 45-47.

Ruf, W., Disse, J., Carneiro-Lobo, T. C., Yokota, N. & Schaffner, F. (2011) 'Tissue factor and cell signalling in cancer progression and thrombosis'. *J Thromb Haemost*, 9 Suppl 1 pp. 306-315.

Ruggieri, M., Praticò, A. D., Serra, A., Maiolino, L., Cocuzza, S., Di Mauro, P., Licciardello, L., Milone, P., Privitera, G., Belfiore, G., Di Pietro, M., Di Raimondo, F., Romano, A., Chiarenza, A., Muglia, M., Polizzi, A. & Evans, D. G. (2016) 'Childhood neurofibromatosis type 2 (NF2) and related disorders: from bench to bedside and biologically targeted therapies'. *Acta Otorhinolaryngol Ital*, 36 (5), pp. 345-367.

Ruttledge, M. H., Sarrazin, J., Rangaratnam, S., Phelan, C. M., Twist, E., Merel, P., Delattre, O., Thomas, G., Nordenskjöld, M. & Collins, V. P. (1994) 'Evidence for the complete inactivation of the NF2 gene in the majority of sporadic meningiomas'. *Nat Genet*, 6 (2), pp. 180-184.

Ryder, N. S. & Dupont, M. C. (1985) 'Inhibition of squalene epoxidase by allylamine antimycotic compounds. A comparative study of the fungal and mammalian enzymes'. *Biochem J*, 230 (3), pp. 765-770.

Sabha, N., Au, K., Agnihotri, S., Singh, S., Mangat, R., Guha, A. & Zadeh, G. (2012) 'Investigation of the in vitro therapeutic efficacy of nilotinib in immortalized human NF2-null vestibular schwannoma cells'. *PLoS One*, 7 (6), pp. e39412.

Sagar, G. D., Gereben, B., Callebaut, I., Mornon, J. P., Zeöld, A., da Silva, W. S., Luongo, C., Dentice, M., Tente, S. M., Freitas, B. C., Harney, J. W., Zavacki, A. M. & Bianco, A. C. (2007) 'Ubiquitination-induced conformational change within the deiodinase dimer is a switch regulating enzyme activity'. *Mol Cell Biol*, 27 (13), pp. 4774-4783.

Saha, A. & Deshaies, R. J. (2008) 'Multimodal activation of the ubiquitin ligase SCF by NEDD8 conjugation'. *Mol Cell*, 32 (1), pp. 21-31.

Santos, D. C., Zaphiropoulos, P. G., Neto, C. F., Pimentel, E. R., Sanches, J. A. & Ruiz, I. R. (2011) 'PTCH1 gene mutations in exon 17 and loss of heterozygosity on D9S180 microsatellite in sporadic and inherited human basal cell carcinomas'. *Int J Dermatol*, 50 (7), pp. 838-843.

Sayedyahossein, S., Li, Z., Hedman, A. C., Morgan, C. J. & Sacks, D. B. (2016) 'IQGAP1 Binds to Yes-associated Protein (YAP) and Modulates Its Transcriptional Activity'. *J Biol Chem*, 291 (37), pp. 19261-19273.

Sekido, Y., Pass, H. I., Bader, S., Mew, D. J., Christman, M. F., Gazdar, A. F. & Minna, J. D. (1995) 'Neurofibromatosis type 2 (NF2) gene is somatically mutated in mesothelioma but not in lung cancer'. *Cancer Res*, 55 (6), pp. 1227-1231.

Selvanathan, S. K., Shenton, A., Ferner, R., Wallace, A. J., Huson, S. M., Ramsden, R. T. & Evans, D. G. (2010) 'Further genotype--phenotype correlations in neurofibromatosis 2'. *Clin Genet*, 77 (2), pp. 163-170.

Serrano, I., McDonald, P. C., Lock, F., Muller, W. J. & Dedhar, S. (2013) 'Inactivation of the Hippo tumour suppressor pathway by integrin-linked kinase'. *Nat Commun*, 4 pp. 2976.

Shaw, R. J., Paez, J. G., Curto, M., Yaktine, A., Pruitt, W. M., Saotome, I., O'Bryan, J. P., Gupta, V., Ratner, N., Der, C. J., Jacks, T. & McClatchey, A. I. (2001) 'The Nf2 tumor suppressor, Merlin, functions in Rac-dependent signaling'. *Dev Cell*, 1 (1), pp. 63-72.

Sher, I., Hanemann, C. O., Karplus, P. A. & Bretscher, A. (2012) 'The tumor suppressor Merlin controls growth in its open state, and phosphorylation converts it to a less-active more-closed state'. *Dev Cell*, 22 (4), pp. 703-705.

Shih, K. C., Chowdhary, S., Rosenblatt, P., Weir, A. B., Shepard, G. C., Williams, J. T., Shastry, M., Burris, H. A. & Hainsworth, J. D. (2016) 'A phase II trial of bevacizumab and everolimus as treatment for patients with refractory, progressive intracranial meningioma'. *J Neurooncol*, 129 (2), pp. 281-288.

Smith, M. J., Bowers, N. L., Bulman, M., Gokhale, C., Wallace, A. J., King, A. T., Lloyd, S. K., Rutherford, S. A., Hammerbeck-Ward, C. L., Freeman, S. R. & Evans, D. G. (2017) 'Revisiting neurofibromatosis type 2 diagnostic criteria to exclude LZTR1-related schwannomatosis'. *Neurology*, 88 (1), pp. 87-92.

Soucy, T. A., Smith, P. G., Milhollen, M. A., Berger, A. J., Gavin, J. M., Adhikari, S., Brownell, J. E., Burke, K. E., Cardin, D. P., Critchley, S., Cullis, C. A., Doucette, A., Garnsey, J. J., Gaulin, J. L., Gershman, R. E., Lublinsky, A. R., McDonald, A., Mizutani, H., Narayanan, U., Olhava, E. J., Peluso, S., Rezaei, M., Sintchak, M. D., Talreja, T., Thomas, M. P., Traore, T., Vyskocil, S., Weatherhead, G. S., Yu, J., Zhang, J., Dick, L. R., Claiborne, C. F., Rolfe, M., Bolen, J. B. & Langston, S. P. (2009) 'An inhibitor of NEDD8-activating enzyme as a new approach to treat cancer'. *Nature*, 458 (7239), pp. 732-736.

Stangerup, S. E. & Caye-Thomasen, P. (2012) 'Epidemiology and natural history of vestibular schwannomas'. *Otolaryngol Clin North Am*, 45 (2), pp. 257-268, vii.

Stebbing, J., Zhang, H., Xu, Y., Lit, L. C., Green, A. R., Grothey, A., Lombardo, Y., Periyasamy, M., Blighe, K., Zhang, W., Shaw, J. A., Ellis, I. O., Lenz, H. J. & Giamas, G. (2015) 'KSR1 regulates BRCA1 degradation and inhibits breast cancer growth'. *Oncogene*, 34 (16), pp. 2103-2114.

Stewart, S., Sundaram, M., Zhang, Y., Lee, J., Han, M. & Guan, K. L. (1999) 'Kinase suppressor of Ras forms a multiprotein signaling complex and modulates MEK localization'. *Mol Cell Biol*, 19 (8), pp. 5523-5534.

Striedinger, K., VandenBerg, S. R., Baia, G. S., McDermott, M. W., Gutmann, D. H. & Lal, A. (2008) 'The neurofibromatosis 2 tumor suppressor gene product, Merlin, regulates

human meningioma cell growth by signaling through YAP'. *Neoplasia*, 10 (11), pp. 1204-1212.

Suarez-Merino, B., Hubank, M., Revesz, T., Harkness, W., Hayward, R., Thompson, D., Darling, J. L., Thomas, D. G. & Warr, T. J. (2005) 'Microarray analysis of pediatric ependymoma identifies a cluster of 112 candidate genes including four transcripts at 22q12.1-q13.3'. *Neuro Oncol*, 7 (1), pp. 20-31.

Sugiura, A., McLelland, G. L., Fon, E. A. & McBride, H. M. (2014) 'A new pathway for mitochondrial quality control: mitochondrial-derived vesicles'. *EMBO J*, 33 (19), pp. 2142-2156.

Sun, C. X., Haipek, C., Scoles, D. R., Pulst, S. M., Giovannini, M., Komada, M. & Gutmann, D. H. (2002) 'Functional analysis of the relationship between the neurofibromatosis 2 tumor suppressor and its binding partner, hepatocyte growth factor-regulated tyrosine kinase substrate'. *Hum Mol Genet*, 11 (25), pp. 3167-3178.

Swords, R. T., Erba, H. P., DeAngelo, D. J., Bixby, D. L., Altman, J. K., Maris, M., Hua, Z., Blakemore, S. J., Faessel, H., Sedarati, F., Dezube, B. J., Giles, F. J. & Medeiros, B. C. (2015) 'Pevonedistat (MLN4924), a First-in-Class NEDD8-activating enzyme inhibitor, in patients with acute myeloid leukaemia and myelodysplastic syndromes: a phase 1 study'. *Br J Haematol*, 169 (4), pp. 534-543.

Swords, R. T., Kelly, K. R., Smith, P. G., Garnsey, J. J., Mahalingam, D., Medina, E., Oberheu, K., Padmanabhan, S., O'Dwyer, M., Nawrocki, S. T., Giles, F. J. & Carew, J. S. (2010) 'Inhibition of NEDD8-activating enzyme: a novel approach for the treatment of acute myeloid leukemia'. *Blood*, 115 (18), pp. 3796-3800.

Tang, X., Jang, S. W., Wang, X., Liu, Z., Bahr, S. M., Sun, S. Y., Brat, D., Gutmann, D. H. & Ye, K. (2007) 'Akt phosphorylation regulates the tumour-suppressor Merlin through ubiquitination and degradation'. *Nat Cell Biol*, 9 (10), pp. 1199-1207.

Terrell, J., Shih, S., Dunn, R. & Hicke, L. (1998) 'A function for monoubiquitination in the internalization of a G protein-coupled receptor'. *Mol Cell*, 1 (2), pp. 193-202.

Therrien, M., Chang, H. C., Solomon, N. M., Karim, F. D., Wassarman, D. A. & Rubin, G. M. (1995) 'KSR, a novel protein kinase required for RAS signal transduction'. *Cell*, 83 (6), pp. 879-888.

Thurneysen, C., Opitz, I., Kurtz, S., Weder, W., Stahel, R. A. & Felley-Bosco, E. (2009) 'Functional inactivation of NF2/Merlin in human mesothelioma'. *Lung Cancer*, 64 (2), pp. 140-147.

Trofatter, J. A., MacCollin, M. M., Rutter, J. L., Murrell, J. R., Duyao, M. P., Parry, D. M., Eldridge, R., Kley, N., Menon, A. G. & Pulaski, K. (1993) 'A novel moesin-, ezrin-, radixin-like gene is a candidate for the neurofibromatosis 2 tumor suppressor'. *Cell*, 72 (5), pp. 791-800.

Trotman, L. C., Wang, X., Alimonti, A., Chen, Z., Teruya-Feldstein, J., Yang, H., Pavletich, N. P., Carver, B. S., Cordon-Cardo, C., Erdjument-Bromage, H., Tempst, P., Chi, S. G., Kim, H. J., Misteli, T., Jiang, X. & Pandolfi, P. P. (2007) 'Ubiquitination regulates PTEN nuclear import and tumor suppression'. *Cell*, 128 (1), pp. 141-156.

True, L. D. (2008) 'Quality control in molecular immunohistochemistry'. *Histochem Cell Biol*, 130 (3), pp. 473-480.

Tsuda, Y., Kanje, M. & Dahlin, L. B. (2011) 'Axonal outgrowth is associated with increased ERK 1/2 activation but decreased caspase 3 linked cell death in Schwann cells after immediate nerve repair in rats'. *BMC Neurosci*, 12 pp. 12.

Twist, E. C., Ruttledge, M. H., Rousseau, M., Sanson, M., Papi, L., Merel, P., Delattre, O., Thomas, G. & Rouleau, G. A. (1994) 'The neurofibromatosis type 2 gene is inactivated in schwannomas'. *Hum Mol Genet*, 3 (1), pp. 147-151.

von Haken, M. S., White, E. C., Daneshvar-Shyesther, L., Sih, S., Choi, E., Kalra, R. & Cogen, P. H. (1996) 'Molecular genetic analysis of chromosome arm 17p and chromosome arm 22q DNA sequences in sporadic pediatric ependymomas'. *Genes Chmomosomes Cancer*, 17 (1), pp. 37-44.

Walcott, B. P., Nahed, B. V., Brastianos, P. K. & Loeffler, J. S. (2013) 'Radiation Treatment for WHO Grade II and III Meningiomas'. *Front Oncol*, 3 pp. 227.

Wang, B. S., Liu, Y. Z., Yang, Y., Zhang, Y., Hao, J. J., Yang, H., Wang, X. M., Zhang, Z. Q., Zhan, Q. M. & Wang, M. R. (2013) 'Autophagy negatively regulates cancer cell proliferation via selectively targeting VPRBP'. *Clin Sci (Lond)*, 124 (3), pp. 203-214.

Wang, L., Jiang, C. F., Li, D. M., Ge, X., Shi, Z. M., Li, C. Y., Liu, X., Yin, Y., Zhen, L., Liu, L. Z. & Jiang, B. H. (2016) 'MicroRNA-497 inhibits tumor growth and increases chemosensitivity to 5-fluorouracil treatment by targeting KSR1'. *Oncotarget*, 7 (3), pp. 2660-2671.

Wang, X., Arceci, A., Bird, K., Mills, C. A., Choudhury, R., Kernan, J. L., Zhou, C., Bae-Jump, V., Bowers, A. & Emanuele, M. J. (2017) 'VprBP/DCAF1 Regulates the Degradation and Nonproteolytic Activation of the Cell Cycle Transcription Factor FoxM1'. *Mol Cell Biol*, 37 (13),

Webster, H. D., Martin, R. & O'Connell, M. F. (1973) 'The relationships between interphase Schwann cells and axons before myelination: a quantitative electron microscopic study'. *Dev Biol*, 32 (2), pp. 401-416.

Wei, D., Li, H., Yu, J., Sebolt, J. T., Zhao, L., Lawrence, T. S., Smith, P. G., Morgan, M. A. & Sun, Y. (2012) 'Radiosensitization of human pancreatic cancer cells by MLN4924, an investigational NEDD8-activating enzyme inhibitor'. *Cancer Res*, 72 (1), pp. 282-293.

Wei, W., Guo, H., Liu, X., Zhang, H., Qian, L., Luo, K., Markham, R. B. & Yu, X. F. (2014) 'A first-in-class NAE inhibitor, MLN4924, blocks lentiviral infection in myeloid cells by disrupting neddylation-dependent Vpx-mediated SAMHD1 degradation'. *J Virol*, 88 (1), pp. 745-751.

Wellenreuther, R., Kraus, J. A., Lenartz, D., Menon, A. G., Schramm, J., Louis, D. N., Ramesh, V., Gusella, J. F., Wiestler, O. D. & von Deimling, A. (1995) 'Analysis of the neurofibromatosis 2 gene reveals molecular variants of meningioma'. *Am J Pathol*, 146 (4), pp. 827-832.

Wen, P. Y., Yung, W. K., Lamborn, K. R., Norden, A. D., Cloughesy, T. F., Abrey, L. E., Fine, H. A., Chang, S. M., Robins, H. I., Fink, K., Deangelis, L. M., Mehta, M., Di Tomaso, E., Drappatz, J., Kesari, S., Ligon, K. L., Aldape, K., Jain, R. K., Stiles, C. D., Egorin, M. J. & Prados, M. D. (2009) 'Phase II study of imatinib mesylate for recurrent meningiomas (North American Brain Tumor Consortium study 01-08)'. *Neuro Oncol*, 11 (6), pp. 853-860.

Wicking, C., Gillies, S., Smyth, I., Shanley, S., Fowles, L., Ratcliffe, J., Wainwright, B. & Chenevix-Trench, G. (1997) 'De novo mutations of the Patched gene in nevoid basal

cell carcinoma syndrome help to define the clinical phenotype'. *Am J Med Genet*, 73 (3), pp. 304-307.

Wiemels, J., Wrensch, M. & Claus, E. B. (2010) 'Epidemiology and etiology of meningioma'. *J Neurooncol*, 99 (3), pp. 307-314.

Windheim, M., Peggie, M. & Cohen, P. (2008) 'Two different classes of E2 ubiquitin-conjugating enzymes are required for the mono-ubiquitination of proteins and elongation by polyubiquitin chains with a specific topology'. *Biochem J*, 409 (3), pp. 723-729.

Wu, A., Garcia, M. A., Magill, S. T., Chen, W., Vasudevan, H. N., Perry, A., Theodosopoulos, P. V., McDermott, M. W., Braunstein, S. E. & Raleigh, D. R. (2018) 'Presenting Symptoms and Prognostic Factors for Symptomatic Outcomes Following Resection of Meningioma'. *World Neurosurg*, 111 pp. e149-e159.

Wu, K., Yan, H., Fang, L., Wang, X., Pfleger, C., Jiang, X., Huang, L. & Pan, Z. Q. (2011) 'Mono-ubiquitination drives nuclear export of the human DCN1-like protein hDCNL1'. *J Biol Chem*, 286 (39), pp. 34060-34070.

Xia, W., Mullin, R. J., Keith, B. R., Liu, L. H., Ma, H., Rusnak, D. W., Owens, G., Alligood, K. J. & Spector, N. L. (2002) 'Anti-tumor activity of GW572016: a dual tyrosine kinase inhibitor blocks EGF activation of EGFR/erbB2 and downstream Erk1/2 and AKT pathways'. *Oncogene*, 21 (41), pp. 6255-6263.

Xiao, G. H., Beeser, A., Chernoff, J. & Testa, J. R. (2002) 'p21-activated kinase links Rac/Cdc42 signaling to Merlin'. *J Biol Chem*, 277 (2), pp. 883-886.

Xing, H. R., Cordon-Cardo, C., Deng, X., Tong, W., Campodonico, L., Fuks, Z. & Kolesnick, R. (2003) 'Pharmacologic inactivation of kinase suppressor of ras-1 abrogates Ras-mediated pancreatic cancer'. *Nat Med*, 9 (10), pp. 1266-1268.

Xirodimas, D. P., Saville, M. K., Bourdon, J. C., Hay, R. T. & Lane, D. P. (2004) 'Mdm2-mediated NEDD8 conjugation of p53 inhibits its transcriptional activity'. *Cell*, 118 (1), pp. 83-97.

Xu, H. M. & Gutmann, D. H. (1998) 'Merlin differentially associates with the microtubule and actin cytoskeleton'. *J Neurosci Res*, 51 (3), pp. 403-415.

Yamakami, I., Uchino, Y., Kobayashi, E. & Yamaura, A. (2003) 'Conservative management, gamma-knife radiosurgery, and microsurgery for acoustic neurinomas: a systematic review of outcome and risk of three therapeutic options'. *Neurol Res*, 25 (7), pp. 682-690.

Yang, C., Asthagiri, A. R., Iyer, R. R., Lu, J., Xu, D. S., Ksendzovsky, A., Brady, R. O., Zhuang, Z. & Lonser, R. R. (2011) 'Missense mutations in the NF2 gene result in the quantitative loss of Merlin protein and minimally affect protein intrinsic function'. *Proc Natl Acad Sci U S A*, 108 (12), pp. 4980-4985.

Yang, D., Tan, M., Wang, G. & Sun, Y. (2012) 'The p21-dependent radiosensitization of human breast cancer cells by MLN4924, an investigational inhibitor of NEDD8 activating enzyme'. *PLoS One*, 7 (3), pp. e34079.

Yang, I., Sughrue, M. E., Han, S. J., Aranda, D., Pitts, L. H., Cheung, S. W. & Parsa, A. T. (2010) 'A comprehensive analysis of hearing preservation after radiosurgery for vestibular schwannoma'. *J Neurosurg*, 112 (4), pp. 851-859.

Yang, K. C., Wu, C. C., Wu, C. H., Chen, J. H., Chu, C. H., Chen, C. H., Chou, Y. H., Wang, Y. J., Lee, W. S., Tseng, H., Lin, S. Y., Lee, C. H. & Ho, Y. S. (2006) 'Involvement of proapoptotic Bcl-2 family members in terbinafine-induced mitochondrial dysfunction and apoptosis in HL60 cells'. *Food Chem Toxicol*, 44 (2), pp. 214-226.

Yi, C., Troutman, S., Fera, D., Stemmer-Rachamimov, A., Avila, J. L., Christian, N., Persson, N. L., Shimono, A., Speicher, D. W., Marmorstein, R., Holmgren, L. & Kissil, J. L. (2011) 'A tight junction-associated Merlin-angiomotin complex mediates Merlin's regulation of mitogenic signaling and tumor suppressive functions'. *Cancer Cell*, 19 (4), pp. 527-540.

Yin, F., Yu, J., Zheng, Y., Chen, Q., Zhang, N. & Pan, D. (2013) 'Spatial organization of Hippo signaling at the plasma membrane mediated by the tumor suppressor Merlin/NF2'. *Cell*, 154 (6), pp. 1342-1355.

You, B., Yang, Y. L., Xu, Z., Dai, Y., Liu, S., Mao, J. H., Tetsu, O., Li, H., Jablons, D. M. & You, L. (2015) 'Inhibition of ERK1/2 down-regulates the Hippo/YAP signaling pathway in human NSCLC cells'. *Oncotarget*, 6 (6), pp. 4357-4368.

Yu, C., Ji, S. Y., Sha, Q. Q., Sun, Q. Y. & Fan, H. Y. (2015) 'CRL4-DCAF1 ubiquitin E3 ligase directs protein phosphatase 2A degradation to control oocyte meiotic maturation'. *Nat Commun*, 6 pp. 8017.

Yu, J. L., Xing, R., Milsom, C. & Rak, J. (2010) 'Modulation of the oncogene-dependent tissue factor expression by kinase suppressor of ras 1'. *Thromb Res*, 126 (1), pp. e6-10.

Yu, W., Fantl, W. J., Harrowe, G. & Williams, L. T. (1998) 'Regulation of the MAP kinase pathway by mammalian Ksr through direct interaction with MEK and ERK'. *Curr Biol*, 8 (1), pp. 56-64.

Zehou, O., Fabre, E., Zelek, L., Sbidian, E., Ortonne, N., Banu, E., Wolkenstein, P. & Valeyrie-Allanore, L. (2013) 'Chemotherapy for the treatment of malignant peripheral nerve sheath tumors in neurofibromatosis 1: a 10-year institutional review'. *Orphanet J Rare Dis*, 8 pp. 127.

Zhang, H., Photiou, A., Grothey, A., Stebbing, J. & Giamas, G. (2012) 'The role of pseudokinases in cancer'. *Cell Signal*, 24 (6), pp. 1173-1184.

Zhang, H., Xu, Y., Filipovic, A., Lit, L. C., Koo, C. Y., Stebbing, J. & Giamas, G. (2013) 'SILAC-based phosphoproteomics reveals an inhibitory role of KSR1 in p53 transcriptional activity via modulation of DBC1'. *Br J Cancer*, 109 (10), pp. 2675-2684.

Zhang, N., Bai, H., David, K. K., Dong, J., Zheng, Y., Cai, J., Giovannini, M., Liu, P., Anders, R. A. & Pan, D. (2010) 'The Merlin/NF2 tumor suppressor functions through the YAP oncoprotein to regulate tissue homeostasis in mammals'. *Dev Cell*, 19 (1), pp. 27-38.

Zhang, N., Zhao, Z., Long, J., Li, H., Zhang, B., Chen, G., Li, X., Lv, T., Zhang, W., Ou, X., Xu, A. & Huang, J. (2017) 'Molecular alterations of the NF2 gene in hepatocellular carcinoma and intrahepatic cholangiocarcinoma'. *Oncol Rep*, 38 (6), pp. 3650-3658.

Zhang, Y., Shi, C. C., Zhang, H. P., Li, G. Q. & Li, S. S. (2016) 'MLN4924 suppresses neddylation and induces cell cycle arrest, senescence, and apoptosis in human osteosarcoma'. *Oncotarget*, 7 (29), pp. 45263-45274.

Zhao, B., Li, L., Tumaneng, K., Wang, C. Y. & Guan, K. L. (2010) 'A coordinated phosphorylation by Lats and CK1 regulates YAP stability through SCF(beta-TRCP)'. *Genes Dev*, 24 (1), pp. 72-85.

Zhao, B., Wei, X., Li, W., Udan, R. S., Yang, Q., Kim, J., Xie, J., Ikenoue, T., Yu, J., Li, L., Zheng, P., Ye, K., Chinnaiyan, A., Halder, G., Lai, Z. C. & Guan, K. L. (2007) 'Inactivation of YAP oncoprotein by the Hippo pathway is involved in cell contact inhibition and tissue growth control'. *Genes Dev*, 21 (21), pp. 2747-2761.

Zhao, Y., Xiong, X., Jia, L. & Sun, Y. (2012) 'Targeting CULLIN-RING ligases by MLN4924 induces autophagy via modulating the HIF1-REDD1-TSC1-mTORC1-DEPTOR axis'. *Cell Death Dis*, 3 pp. e386.

Zheng, N., Schulman, B. A., Song, L., Miller, J. J., Jeffrey, P. D., Wang, P., Chu, C., Koepp, D. M., Elledge, S. J., Pagano, M., Conaway, R. C., Conaway, J. W., Harper, J. W. & Pavletich, N. P. (2002) 'Structure of the Cul1-Rbx1-Skp1-F boxSkp2 SCF ubiquitin ligase complex'. *Nature*, 416 (6882), pp. 703-709.

Zheng, S., Leclerc, G. M., Li, B., Swords, R. T. & Barredo, J. C. (2018) 'Inhibition of the NEDD8 conjugation pathway induces calcium-dependent compensatory activation of the pro-survival MEK/ERK pathway in acute lymphoblastic leukemia'. *Oncotarget*, 9 (5), pp. 5529-5544.

Zhou, L., Ercolano, E., Ammoun, S., Schmid, M. C., Barczyk, M. A. & Hanemann, C. O. (2011) 'Merlin-deficient human tumors show loss of contact inhibition and activation of Wnt/β-catenin signaling linked to the PDGFR/Src and Rac/PAK pathways'. *Neoplasia*, 13 (12), pp. 1101-1112.

Zhou, L. & Hanemann, C. O. (2012) 'Merlin, a multi-suppressor from cell membrane to the nucleus'. *FEBS Lett*, 586 (10), pp. 1403-1408.

Zhou, L., Lyons-Rimmer, J., Ammoun, S., Müller, J., Lasonder, E., Sharma, V., Ercolano, E., Hilton, D., Taiwo, I., Barczyk, M. & Hanemann, C. O. (2016a) 'The scaffold protein

KSR1, a novel therapeutic target for the treatment of Merlin-deficient tumors'. *Oncogene*, 35 (26), pp. 3443-3453.

Zhou, L., Zhang, W., Sun, Y. & Jia, L. (2018) 'Protein neddylation and its alterations in human cancers for targeted therapy'. *Cell Signal*, 44 pp. 92-102.

Zhou, X., Tan, M., Nyati, M. K., Zhao, Y., Wang, G. & Sun, Y. (2016b) 'Blockage of neddylation modification stimulates tumor sphere formation in vitro and stem cell differentiation and wound healing in vivo'. *Proc Natl Acad Sci U S A*, 113 (21), pp. E2935-2944.

Zotti, T., Scudiero, I., Vito, P. & Stilo, R. (2017) 'The Emerging Role of TRAF7 in Tumor Development'. *J Cell Physiol*, 232 (6), pp. 1233-1238.

Zou, J., Ma, W., Li, J., Littlejohn, R., Zhou, H., Kim, I. M., Fulton, D. J. R., Chen, W., Weintraub, N. L., Zhou, J. & Su, H. (2018) 'Neddylation mediates ventricular chamber maturation through repression of Hippo signaling'. *Proc Natl Acad Sci U S A*,

Zöller, M., Rembeck, B., Akesson, H. O. & Angervall, L. (1995) 'Life expectancy, mortality and prognostic factors in neurofibromatosis type 1. A twelve-year follow-up of an epidemiological study in Göteborg, Sweden'. *Acta Derm Venereol*, 75 (2), pp. 136-140.